Abrogation of CD4 driven autoimmunity associated with tumour immunotherapy while preserving anti-tumour CD8 mediated immunity

By

MAHER GHANEIM NAWAF

A thesis submitted to the University of Birmingham for the degree of

DOCTOR OF PHILOSOPHY

In

Immunology

Department of infection and immunity

School of Medicine

College of Medical and Dental Sciences

University of Birmingham

February 2016

Abstract

In human, cancer immunotherapeutic strategies using blocking antibodies to target FoxP3^{+} regulatory T cells using anti-CTLA-4 blockade and to inhibit PD-1 signalling have achieved significant clinical responses, with in some instances cancer free survival among patients, especially when they are used in combination. However, this has been associated with significant off target toxic autoimmune side effects that have restricted dose escalation efficacy of these therapeutic strategies. Previous work in our lab generated a FoxP3 knock out mouse model without FoxP3^{+} dependent CD4 driven autoimmunity when the TNFRSF receptors OX40 and CD30 signals are abrogated simultaneously. This suggests a novel approach which can be applied to abrogate off target CD4 driven side effects in cancer immunotherapy, without compromising CD8 anti-tumour immune responses. Here we showed that the CD30^{KO}OX40^{KO}FoxP3^{KO} (tKO) mice are resistant to tumour progression in a mouse model of melanoma where anti-tumour immunity is CD8 dependent, particularly when combined with anti-PD-1 blockade. This was mimicked in CD30^{KO}OX40^{KO} (dKO) mice and WT mice treated respectively with anti-CTLA-4, anti-PD-1, or anti-CTLA-4, anti-PD-1 and anti-OX40L and anti-CD30L blocking mAbs. Interestingly, the CD4 driven autoimmunity has been abrogated using the fourfold combination: anti-(CTLA-4, PD-1, OX40L and CD30L) mAbs, while an excellent CD8 anti-tumour response is preserved in C57Bl/6 mice harbouring melanoma tumours.

In the second part of this thesis, I have investigated the effects of overexpression of IFNγ in our mouse model of melanoma, using *sanroque* mice. Work in our lab has shown that overexpression of IFNγ renders T cells resistant to being regulated by

Tregs. IFNγ activates M1 macrophages, and in human tumours, an M1 phenotype is associated with a favourable prognosis. I have shown that tumours do grow more slowly in *sanroque* mice, although the effects are not as striking as with abrogation of Treg function in combination with PD-1 blockade. A striking finding in *sanroque* mice was that PD-1 expression on tumour infiltrating CD4 and CD8 T cells was virtually completely abrogated which was independent on Tregs, indicating that this might explain the delayed tumour growth. In keeping with this observation, whereas PD-1 blockade inhibits tumour growth in normal mice, there was no additional effect of PD-1 blockade in *sanroque* mice on tumour growth. Studies in the lab have shown that resistance to regulation is conferred by nitric oxide induced expression on T cells of OX40L, which signals through OX40 on T cells. Previous studies have also suggested that this effect can be mimicked by agonistic OX40 mAbs *in vivo*. I found that agonistic OX40 mAbs in WT mice also downregulated PD-1 expression on tumour infiltrating CD4 and CD8 T cells. This suggests that the effect of M1 macrophages on anti-tumour immune responses is to modulate PD-1 expression via OX40 signals. The direct role of IFNγ in this modulation is to be tested using blocking mAbs to IFNγ

In conclusion, blocking OX40 and CD30 signals is a novel approach to dissociate anti-tumour immune response and autoimmune pathology, which will potentiate cancer immunotherapy for cancer patients. Agonistic OX40 mAbs combined with anti-PD-1 may be not an ideal approach for cancer immunotherapy.

Dedication

This work is dedicated to Basema, Allen, Ava, my family and the victims of genocide conducted on 3rd August 2014 against Iraqi minorities (Yazidis and Christians).

Acknowledgments

I am enormously grateful to my lead supervisor, Prof. Dr. Peter J. Lane, who has been professional, motivating, patient and helpful. His guidance in achieving this research has had a profound impact on my science and on my life. Special thanks go to my co-supervisor Dr. David Withers, for his unfailing support and wide knowledge. I also acknowledge Dr. Fiona M. McConnell and Dr. Fabrina M. Gaspal for the willing assistance in laboratory and research methods they offered me from the first day I joined Prof. Lane's group. I thank the members of Prof. Antal Rot's lab especially Dr. Maria Ulvmar and Li Chan who taught me everything I needed to know about handling tumours. Thanks also go to Prof. James Allison, University of Texas, USA, Hido Yagita, University of Juntendo, Japan and Dr. Nick Jones, University of Birmingham, for providing us with blocking antibodies and mice. For their insightful attention and advice, I would also like to thank my PhD progress committee Prof. Adam Cunningham and Dr. Simon Afford. I'm grateful to my lab colleagues Emily Halford, Gwilym Web, Clare Marriot, Emma Mackley, Emma Dutton, and Poonam Jakhu, for making the lab active, enjoyable and social. Many thanks are due to [redacted] staff for looking after our animals and providing training opportunities. Special thanks also to Prof. Graham Anderson, Prof. Adam Cunningham, Dr. Jorge Caamano and Dr. Kai Toellner and their groups, who were supportive and helped with the use of lab equipment and materials. Finally, I am profoundly thankful to the UK government and British people who have supported and secured me and my family life.

Table of Contents

Chapter One 1
General introduction 2
1.1 Introduction to the pathogenesis of tumours 2
1.1.1 The development of cancer 2
1.1.2 Malignant melanoma 4
1.1.3 Pathogenesis of melanoma 4
1.1.4 Immunosurveillance and immunoediting of cancer 9
1.1.5 Melanoma associated antigens 14
1.2 General overview of the immune system 16
1.2.1 Development of T lymphocytes in the thymus 17
1.2.2 Mechanisms of T cell immune tolerance 20
1.2.3 Evidence that OX40 supresses Treg function 36
1.2.4 Treg infiltration of tumours 45
1.3 Cancer immunotherapy 47
1.3.1 Tumour immunotherapy: targeting CTLA-4 48
1.3.2 Tumour immunotherapy: targeting the PD-1/PD-L1 pathway 54
1.3.3 CTLA-4 and PD-1 combined immunotherapy 58
1.3.4 Other TNFRSF members as costimulators and targets for cancer immunotherapy 60
1.4 Roquin regulates posttranscriptional mRNA expression 65
1.5 Aims of the study 67
Chapter Two 69
Materials and methods 70
2.1 Mice used in experiments 70
2.2 Murine cell culture and preservation 70
2.3 Subcutaneous injection of mice 73
2.4 Intravital imaging of tumours 73
2.5 Preparation of cell suspensions for flow cytometry 74
2.6 Flow cytometric analysis 75
2.7 Immunofluorescence histology 78
2.8 Confocal imaging 80
2.9 Adoptive cell transfer 80
2.10 Immunomodulatory agents used *in vivo* 80

2.11 Circulating serum autoantibody screening and titration 81
2.12 Liver function tests 82
2.13 Liver histology 82
2.14 Analysis of gene expression 83
2.14.1 Primers used for gene analysis 83
2.14.2 mRNA isolation and cDNA synthesis 83
2.14.3 Real time quantitative polymerase chain reaction (qPCR) 84
2.15 Statistical analysis 85
Chapter Three Results 86
Tumour immune responses in WT, dKO and tKO mouse models and the effect of anti-PD-1 on tumour growth 87
3.1 Introduction 87
3.2 Results 88
3.2.1 Tumour immune responses in dKO and tKO compared with WT mice 88
3.2.2 The anti-tumour response in tKO mice depleted of CD8-T cells 103
3.2.3 The effect of anti PD-1 blockade on tumours in $FoxP3^{KO}$ mice 105
3.3 Discussion 119
3.3.1 Mice deficient in Foxp3 Tregs (tKO mice) are resistant to B16-F10-luc^{+} melanoma tumours and are highly infiltrated with CD8 T cells that express abundantly the inhibitor PD-1. 119
3.3.2 Inhibition of melanoma growth in tKO mice is CD8 T cell dependent 122
3.3.3 PD-1 blockade in Foxp3 Treg deficient (tKO) mice mimics the blockade combinations (CTLA-4,PD-1) in dKO mice and (CTLA-4,PD-1,OX40L,CD30L) in WT mice, to abrogate B16 melanoma growth 122
3.3.4 Conclusion 123
Chapter Four Results 125
Concurrent administration of OX40L and CD30L blocking antibodies eliminates the CD4 driven autoimmune toxicity related to CTLA-4 and PD-1 blockades 126
4.1 Introduction 126
4.2 Results 127
4.2.1 The efficacy of combining OX40L and CD30L blocking antibodies with CTLA-4 and PD-1 treatments on tumour growth and CTLA-4 and PD-1 associated autoimmunity 127
4.2.2 The efficacy of monoclonal antibody immunotherapy for treating B16-F10 melanoma in CTLA-4 heterozygous mice 143
4.3 Discussion 149

4.3.1 Simultaneous blockade of OX40L and CD30L does not interfere with the anti-tumour effect of CTLA-4 and PD-1 blocking antibodies used for the treatment of B16 melanoma in C57Bl/6 mice 149
4.3.2 Concurrent injection of antibodies to OX40L and CD30L abrogates the CD4 driven autoimmunity associated with CTLA-4 and PD-1 blocking antibodies.. 150
4.3.3 Partial impairment of CTLA-4 combined with anti-PD-1 is not as effective as double blockade of CTLA-4 and PD-1 in the treatment of B16 melanoma but the efficacy is improved with CD30 and OX40 blockade 153
4.4 Conclusion 154
Chapter Five Results 156
Tumour immune response in a mouse model where T effectors are resistant to regulation 157
5.1 Introduction 157
5.2 Results 158
5.2.1 Tumour immune response in Roq$^{san/san}$ and Roq$^{san/san}$dKO mice compared with WT and dKO mice 158
5.2.2 The effect of αPD-1 immunotherapy on melanoma growth in Roq$^{san/san}$ and Roq$^{san/san}$ dKO mice compared to WT mice 165
5.2.3 Experiment to test whether the lack of expression of PD-1 and increased CD8 infiltrate in Roq$^{san/san}$ mice was cell intrinsic or due to the environment in Roq$^{san/san}$ mice. 169
5.2.4 The effect of anti-OX40 agonistic mAbs on PD-1 expression on T cells and melanoma response 173
5.3 Discussion 178
5.3.1 Tumours grow in Roq$^{san/san}$ and Roq $^{san/san}$dKO mice, but grow more slowly than in WT mice 178
5.3.2 Impaired PD-1 expression is intrinsic to Roquin mutant mice but the phenotype is partial in Roq$^{san/san}$dKO 179
5.3.3 Anti-PD-1 slows tumour growth and increases survival rate in WT and Roq$^{san/san}$dKO mice but not in Roq$^{san/san}$ mice as a result of lack expression of PD-1 on Roq$^{san/san}$ T cells 180
5.3.4 The suppressive expression of PD-1 is T cell intrinsic..... 181
5.3.5 Anti-OX40 agonists downregulate PD-1 expression on CD4^{+} and CD8^{+} T cells 182
5.3.6 Conclusion 183
5.3.7 Future work 183

Chapter Six 185
General Discussion 186
Papers 198
References 199

List of Figures

Figure 1.1: Pathogenesis progression of malignant melanoma 8

Figure 1.2: Thymus anatomy and T cell developmental stages 19

Figure 1.3: T subsets of $CD4^+$ regulatory T cells 29

Figure 3.1: Tumour volumes and weights in B16-F10-luc^+ transfected WT, dKO and tKO mice 90

Figure 3.2: The dynamics of *in vivo* B16-F10-luc^+ tumour growth in WT, dKO and tKO mice 91

Figure 3.3: Flow cytometric analysis of tumour infiltrates in WT, dKO and tKO mice 95

Figure 3.4: Flow cytometric analysis of lymphocytes from the draining (inguinal) lymph node of melanoma transfected WT, dKO and tKO mice. 97

Figure 3.5: $CD4^+$ T cells and Tregs are the predominant lymphocyte subsets in melanoma transfected WT tumours. 100

Figure 3.6: Treg infiltration into melanoma transfected is reduced in dKO tumours compared to wildtype. 101

Figure 3.7: CD8 T cells are predominant in melanoma transfected tKO tumours 102

Figure 3.8: CD8 T cell depleteion abrogates the B16 melanoma resistance shown by tKO mice 104

Figure 3.9: B16-F10 melanoma cell line gene expression of PD-L1, PDL-2, CD30L and OX40L. 107

Figure 3.10: The effect of monoclonal antibodies on B16 melanoma growth in WT, dKO and tKO mice. 110

Figure 3.11: Flow cytometric analysis of the effect of monoclonal antibodies on tumour infiltrating cell populations in WT, dKO and tKO mice. 113

Figure 3.12: The effect of monoclonal antibodies on IFNγ production by $CD8^+$ T cells in WT, dKO and tKO mice. 117

Figure 4.1: The experimental design of studying the efficacy of blocking antibodies on cancer immunotherapy and antibody associated toxicity. 128

Figure 4.2: Tumour volumes for B16-F10 transfected C57BL/6 mice groups treated with monoclonal blocking antibodies. 130

Figure 4.3: Tumour weights for B16-F10 transfected C57BL/6 mice groups treated with monoclonal blocking antibodies. 131

Figure 4.4: Kaplan Meier survival curves for B16-F10-luc^+ transfected C57BL/6 mice groups treated with monoclonal blocking antibodies. 134

Figure 4.5: Number of lymphocyte aggregates per mm^2 of liver tissue x100..... 135

Figure 4.6: Liver function tests after injecting combinations of mAbs against CTLA-4, PD-1, OX40L and CD30L in B16-F10 injected C57Bl6 mice 137

Figure 4.7: Depigmentation in B16-F10 injected C57Bl/6 mice treated with CTLA-4 mAbs. 140

Figure 4.8: Fluorescence micrographs and serum autoantibody titres for anti-(CTLA-4,PD-1) and anti-(CTLA-4,PD-1,CD30L,OX40L) treatment groups on stomach, liver and kidney sections 141

Figure 4.9: Experimental design to test the efficacy of immunotherapy in CTLA-4 heterozygous mice..... 144

Figure 4.10: Tumour volumes and weights in CTLA-4 heterozygous mice treated with anti-PD-1 mAbs 147

Figure 4.11: The effect of PD-1 blockade on $FoxP3^+$ Treg recruitment into WT and CTLA-4 heterozygous mice with established B16-F10 melanoma..... 148

Figure 5.1: Pattern of tumour growth in WT, dKO, $Roq^{san/san}$, $Roq^{san/san}$dKO mice. 159

Figure 5.2: Flow cytometric analysis of tumours and tumour draining lymph nodes in WT, dKO, $Roq^{san/san}$, $Roq^{san/san}$dKO mice 161

Figure 5.3: Expression of PD-1 on $CD8^+$ T cells in tumour infiltrates. 164

Figure 5.4: αPD-1 immunotherapy of melanoma in WT, $Roq^{san/san}$ and $Roq^{san/san}$ dKO mice 167

Figure 5.5: Experimental design to investigate whether the lack of expression of PD-1 on CD8 infiltrates in $Roq^{san/san}$ mice is cell intrinsic or cell extrinsic..... 170

Figure 5.6: Adoptive transfer of WT ($CD45.1^+$) and $Roq^{san/san}$ ($CD45.2^+$) splenocytes mixtures into T cell deficient hosts transfected with B16 melanoma 171

Figure 5.7: The effect of anti-OX40 agonistic mAbs on melanoma response 175

Figure 5.8: OX40 agonistic mAbs downregulate PD-1 expression on $CD4^+$ and $CD8^+$ T cell tumour infiltrates. 177

Figure 6.1: The balance between tumour associated Tregs and tumour specific effector cells. 190

Figure 6.2: The beneficial effects of the gene deficiencies in $CD30^{KO}OX40^{KO}FoxP3^{KO}$ mice on tumour immune responses can be mimicked by the use of antibody blockade in WT and $CD30^{KO}OX40^{KO}$ mice. 191

Figure 6.3: Strategy to dissociate tumour immunity from autoimmunity..... 194

Figure 6.4: Blocking of OX40 in the presence of tumour-associated macrophages, type MØ1 or MØ2 197

List of Tables

Table 1:1: The tumour necrosis factor receptors superfamilies' (TNFRSF) and their ligands (Wu and Hymowitz 2009, Magis *et al.* 2012)..... 44

Table 2:1: Mouse strains (Wild type and Genetically modified) used in the research 71

Table 2:2: Antibodies used for fluorescence activated cell sorting 77

Table 2:3: Primary antibodies used for immunofluorescence 79

Table 2:4: Secondary and tertiary antibodies used for immunofluorescence..... 79

Table 2:5: Monoclonal antibodies used in the study..... 81

Table 2:6: The sequences of primers for the genes of interest..... 83

List of Abbreviations

ADP	Adenosine Di-Phosphate
AICD	Activation Induced Cell Death
AIRE	Autoimmune Regulator
AMP	Adenosine Mono Phosphate
ATP	Adenosine Tri-Phosphate
BAK	Bcl-2 Homologous Antagonist Killer
BAX	Bcl-2-Associated X Protein
Bcl-2	B-Cell Lymphoma 2
BCR	B Cells Receptor
BIM	BCL-2 Interacting Mediator of Cell Death
BRAF	B-Raf
CTA	Cancer Testis Antigens
CCND-1	Cyclin D-1
CDK4	Cyclin D Dependent Kinase 4
CDKN2A	Cyclin Dependent Kinase Inhibitor 2A
cTEC	Cortical Thymic Epithelial Cells
CTLA-4	Cytotoxic T Lymphocytes Associate Protein 4
DC	Dendritic Cells
DN	Double Negative
DP	Double Positive
EAE	Experimental Autoimmune Encephalomyelitis

E-cadherin	Epithelial Cadherin
ERK	Extracellular-Signal-Regulated Kinases
FasR	Fas Receptor
FDC	Follicular Dendritic Cells
FoxP3	Forkhead Box P3
GITR	Glucocorticoid-Induced TNFR Family Related Gene
GM-CSF	Granulocytes Macrophages Colony Stimulating Factor
gp100	Glycoprotein 100
GVHD	Graft Versus Host Disease
HSC	Haematopoietic Stem Cells
IBD	Inflammatory Bowel Disease
IDO	Indoleamine 2,3-Deoxygenase
IFNγ	Interferon γ
IgSF	Immunoglobulin Super Family
IL-10	Interleukin 10
IPEX	Immunodysregulation Polyendocrinopathy, and Enteropathy, X-linked
ITIM	Immunoreceptor Tyrosine-Based Inhibitory Motif
iTregs	*In Vitro* Induced Tregs
ITSM	Immunoreceptor Tyrosine-Based Switch Motif
JUN	c-Jun N-Terminal Kinases
KNG2D	Natural Killer Group2 Member D
LAG-3	Lymphocyte-Activation Protein 3

Lck	Lymphocyte-Specific Protein Tyrosine Kinase
LTi	Lymphoid Tissue Inducer Cells
MAPK	Mitogen Activated Protein Kinase
MART-1	Melanoma Antigen Recognised by T cells 1
MCA	Methylcholanthrene
MDSCs	Myeloid Derived Suppressor Cells
MFS	Median Free Survival
MHCI	Major Histocompatibility Class I
MHCII	Major Histocompatibility Class II
MITF	Microphthalmia Associated Transcription Factor
MMP-2	Matrix Metalloproteinase-2
MØ	Macrophages
MOS	Median Overall Survival
MT1-MMP	Membrane-Type Matrix Metalloproteinase-1
mTEC	Medullary Thymic Epithelial Cells
NK	Natural Killer Cells
NKT	Natural Killer T cells
NRAS	N-Ras
NSCLC	Non-Small Cell Lung Cancer
nTregs	Thymus Derived Natural Regulatory T cells
Nur77	Nerve Growth Factor IB
OR	Objective Response
pDCs	Plasmacytoid DCs

PD-L1	Programmed Death Ligand 1
PI3K	Phosphoinositide 3-Kinase
PIP3	Phosphatidylinositol (3,4,5)-Trisphosphate
PKB	Protein Kinase B
PMEL	Premelanosome Protein
PREX2	Phosphatidyl Inositol-3,4,5-Trisphosphate-Dependent Rac Exchange Factor 2
PTEN	Phosphatase and Tensin Homologue
pTregs	*In Vivo* Peripheral Induced Tregs
RAG	Recombination Activating Gene
RAG-2	Recombination Activating Gene-2
RANK	Receptor Activator of Nuclear Factor κB
ROS	Reactive Oxygen Species
SCLC	Small Cell Lung Cancer
SH-2	Src Homology 2
STAT	Signal Transducer and Activator of Transcription
T cells	T Lymphocytes
TAA	Tumour Associated Antigens
TAP	Peptide Transporter Associated with Antigen Processing
Tc	Conventional T cells
TCR	T Cells Receptor
TNFRSF	Tumour Necrosis Factor Receptor Super Family
TNFSFR	Tumour Necrosis Factor Super Family Receptor

TRA	Tissue Restricted Antigens
TRAILR	Tumour Necrosis Factor-Related Apoptosis-Inducing Receptor
TRAMP	Transgenic Adenocarcinoma of the Mouse Prostate
TSA	Tissues Specific Antigens
TYRP-1	Tyrosinase Related Protein 1
UV	Ultra Violet
VEGF	Vascular Endothelial Growth Factor
Wnt	Wingless-Type Mammary Tumour Virus Integration Site Family
γδ T	Gamma Delta T cells

Chapter One

General introduction

1.1 Introduction to the pathogenesis of tumours

1.1.1 The development of cancer

Malignant tumours develop after a progressive series of molecular changes happen in a genetically altered cell that acquires mutations which confer the advantages of selective clone growth, analogous to the Darwinian concept of evolution. According to UK Cancer Research, in 2012, more than 338,000 individuals were diagnosed with cancer, approximately 920 per day, and more than 162,000 deaths, approximately 440 per day, were attributed to cancer in the UK. Hereditary genes and environmental carcinogens are believed to contribute to cancer development. Cancer is generally a genetic syndrome and recent molecular sequencing methods have identified approximately 140 tumour driving genes involved in twelve tumorigenesis pathways (Vogelstein *et al.* 2013). About 5% of familial colorectal cancer cases are due to the inheritance of a mutation in the adenomatous polyposis coli (APC) gene (Nishisho *et al.* 1991). However, random mutations happening during normal cell division can also lead to the emergence of cancerous cells and tumorigenesis (Vogelstein and Kinzler 2004). The contribution of risk factors to the frequency of cancer types among tissues is still ambiguous.

In human, the incidence of colorectal, small cell lung cancer (SCLC), non-small cell lung cancer (NSCLC) and melanoma are reported to be the outliers, having hundreds to thousands of asynchronous mutations per tumour compared to other types of tumours (Vogelstein *et al.* 2013). This reflects the impact of carcinogens,

particularly ultra violet (UV) light and smoking, on genetics in the development of those types of tumours. However, variation in the incidence of cancer among tissues can be correlated with the total number of accumulated mutations during tissue stem cell division and with age. Tomasetti and Vogelstain, (2015) used a mathematical and statistical approach for the data available about tissue stem cell division and estimated the total number of stem cell divisions in each human tissue during its life time. The total number of tissue replications was then correlated with the incidence of various tumours (excluding prostate and breast cancer for which there were insufficient data). This approach showed that two thirds of the risk of cancer incidence is contributed by the total number of divisions of tissue stem cells during the tissue lifetime while the other third is correlated to heredity and environmental risk factors, explaining the increased frequency of mutation in tumours of replicating tissues such as colorectal cancer and melanoma, relative to those of non-renewable tissues such as the brain, as well as the lower frequency of paediatric cancers than those in elderly patients. Accordingly, Wodarz and Zauber, (2015) suggest the use of cancer evolution modulators such as Aspirin to determine the growth of cancerous cells that possess high somatic mutation rates (Wodarz and Zauber 2015).

Hanahan and Weinberg, (2011) reviewed a number of cell intrinsic and cell extrinsic properties that are prerequisite for normal cells to overcome normal growth and biological checkpoints and develop into cancer. These hallmarks include mechanisms that support angiogenesis, genome instability and mutation, immortality replication, proliferation signalling, tumour promoting inflammation, and invasion and metastases; and the mechanisms that evade cell death, growth suppression and

immune system destruction (Hanahan and Weinberg 2011). This study will address melanoma as a model of tumours.

1.1.2 Malignant melanoma

Melanoma is an aggressive malignant growth of melanin producing cells for which there are both intrinsic (genetic) and extrinsic (environmental) risk factors. Melanoma global epidemiology studies reported high incidence rates among Caucasian populations; it seems that natural ultraviolet exposure is the greatest extrinsic melanoma risk factor, in spite of the fact that mutations in the melanoma suppressor genes Cyclin Dependent Kinase inhibitor 2A (CDKN2A) and Cyclin D dependent Kinase 4 (CDK4) have been implicated in familial melanoma progression (MacKie *et al.* 2009). Melanoma represents only 4% of all cancer cases but its metastatic form is a potentially fatal disease with 80% mortality rate and only 14% survival rate for 5 years (MacKie *et al.* 2009). In 2011, approximately 13,300 people were diagnosed with malignant melanoma and there were 2,148 deaths in 2012 in the UK (CancerResearchUK 2014).

1.1.3 Pathogenesis of melanoma

Many models describe the pathogenesis progression of dermatological melanoma. One that is widely used is the Clark model (Miller and Mihm 2006), which depends on a description of histological changes observable as melanocytes transform into malignant melanoma. It includes abnormal melanocytes proliferating in benign nevi along the basal epidermis layer. As a result of genetic mutations, cells acquire atypical phenotypes which may occur within the pre-nevi or from a new nevus site. Cells of atypical phenotype may then undergo unlimited hyperplasia, gain invasive

properties and lose differentiation. Then progressive intra-epidermal growth leads to radial malignancy followed by vertical spreading into the basement membrane of the dermis layer and finally becomes metastatic melanoma (Figure 1.1) (Clark Jr *et al.* 1984). Miller and Mihm, (2006) correlated the histological changes of the Clark model with genetic mutations to understand the molecular signalling pathways leading to melanoma progression.

1.1.3.1 Radial growth phase of melanoma in epidermis

Usually as a consequence of UV exposure, a high mutational load on melanocyte DNA and the resulting DNA damage stimulate the Mitogen Activated Protein Kinase (MAPK) pathway, leading to hyperplastic growth and the development of a benign nevus. NRAS-BRAF-MEK1/2-ERK1/2 proteins make up the downstream MAPK signalling cascade which govern cell proliferation, differentiation and survival (Lopez-Bergami 2011). Somatic mutations in BRAF and NRAS, which are responsible for more than 75% of melanomas, are found in melanocytes in benign nevi (Kumar *et al.* 2004, Miller and Mihm 2006) and malignant melanoma (Hodis *et al.* 2012). The mutated forms $BRAF^{V600E}$ and NRAS cause phosphorylation of serine threonine kinases and constitutive overexpression of transcription factors leading to uncontrollable growth and survival of melanocytes (Lopez-Bergami 2011).

Aside from the mutations leading to MAPK involvement, mutations in tumour suppressor genes contribute to approximately 25-50% of non-familial or familial melanoma cases. (Chin *et al.* 2006, MacKie *et al.* 2009). Under normal conditions, Phosphatase and Tensin Homologue (PTEN) regulates PI3K/PKB pathway by inhibiting Phosphatidylinositol (3,4,5)-trisphosphate (PIP3) phosphorylation. In non-

familial forms, mutation in the PTEN gene (Guldberg *et al.* 1997) or its regulator protein encoding gene PREX2 (Berger *et al.* 2012) results in overproduction of PIP3, activation of PKB and inactivation of anti-apoptotic molecules such as BCL-2, and up-regulation of cell cycle and cell survival transcription factors such as forkhead (FKHR) (Miller and Mihm 2006). However, PTEN mutations may also occur concurrently with BRAF mutations (Flaherty *et al.* 2012), and the combination leads to atypical melanocyte phenotypes and an aggressive dysplastic predisposition to form malignant lesions (Figure 1.1).

1.1.3.2 Melanoma vertical growth and metastasis

The Clark model describes melanoma as progressing from radial growth in the epidermis to vertical expansion and invasion of the dermis, where invasive melanocytes dissociate from the primary lesion and migrate via the blood stream or lymphatics to develop metastases in various organs (Figure 1.1) (Clark Jr *et al.* 1984). The Breslow Scale is a clinically validated index linking depth of melanoma determined histopathologically to prognostic outcomes. According to this index, melanoma stages are: Stage I less or equal to 0.75mm, Stage II 0.76mm - 1.50mm, Stage III 1.51mm - 2.25mm, Stage IV 2.26mm - 3.0mm and Stage V greater than 3.0mm (Balch *et al.* 2001). The ominous signs of melanoma mortality are in the last two stages especially when accompanied by metastasis.

There is a debate about the mechanisms of melanoma progression and metastasis; however, transformations in the cell adhesion molecules, cadherins, integrins and β-catenin, are the major players in this transformation (Miller and Mihm 2006). Extracellular Epithelial cadherin (E-cadherin) with its intercellular tail forms a complex

with β-catenin and cytoskeletal actin. This complex functions in cell-cell communication at cells junctions. Melanocytes and keratinocytes in the epidermis express E-cadherin while mesenchymal cells in the dermal layer express Neural-cadherin (N-cadherin) (Miller and Mihm 2006). In a co-cultured system, melanoma cells showed shifting in expression of E-cadherin into N-cadherin and lost gap-junction mediated communication with cultured keratinocytes. Instead melanoma cells communicated with each other and with fibroblasts while normal melanocytes preserved their communication with keratinocytes (Hsu *et al.* 2000). This suggests how melanoma progresses from epidermis, where keratinocytes are found, into dermis, where fibroblasts exist. Moreover, expression of αVβ3 integrin enhances vertical growth of melanoma. It activates basement membrane collagen degradation enzymes MT1-MMP and MMP-2 (Hofmann *et al.* 2000), mediates interaction with extracellular matrix components, induces anti-apoptotic genes and stimulates motility (Miller and Mihm 2006).

Some types of melanoma do not fit the Clark linear melanoma progression. Therefore, a nonlinear model has been proposed by (Damsky *et al.* 2014) which hypothesises that mutations in melanocytes may produce early disseminator metastatic melanocytes while in a primary phase of dysplasia. Each day thousands of pre-cancerous cells generated in our body are recognised and eliminated by the immune system, so to progress, a tumour must bypass the immune system. This is the seventh hallmark of cancer reviewed in Hanahan and Weinberg, (2011) and is discussed next in this study.

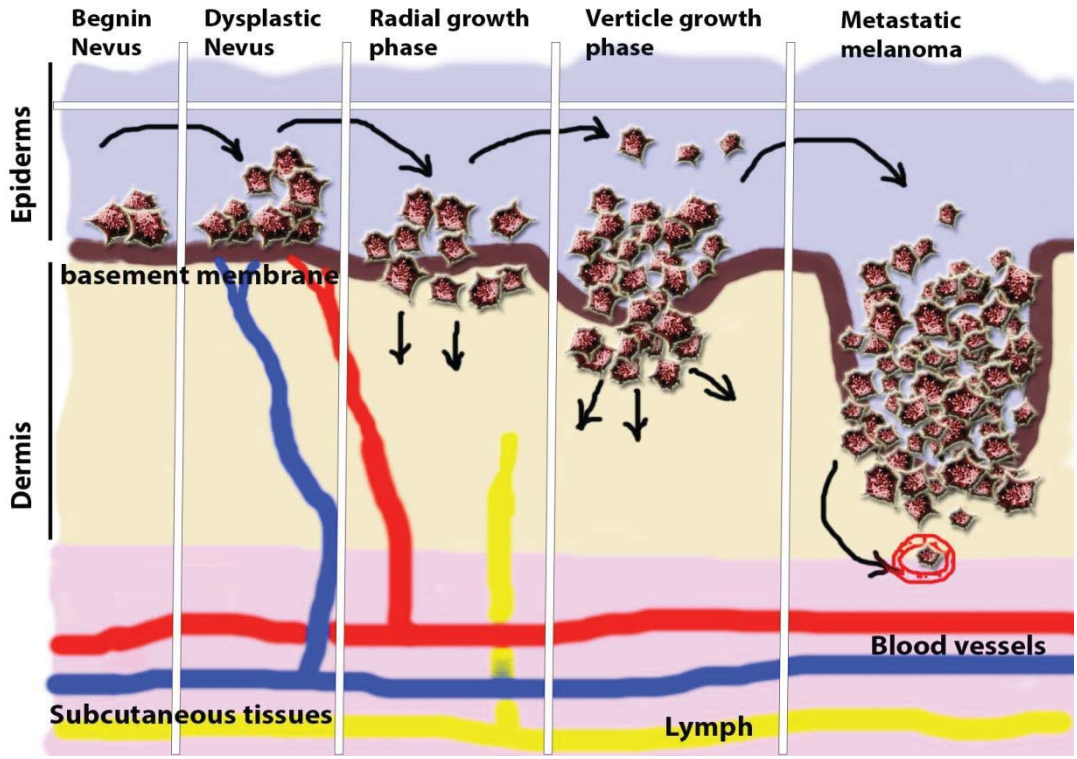

Figure 1.1: Pathogenesis progression of malignant melanoma

Melanoma starts when melanocytes acquire atypical phenotype as a result of mutations in melanocytes in the epidermis. Melanocytes proliferate in benign nevi then cells undergo unlimited hyperplasia, gain invasive properties and lose differentiation. Then a progressive intra-epidermal growth occurs that leads to radial malignancy. This is followed by vertical growth into the basement membrane of the dermis layer and finally reaches the subcutaneous tissues, where the blood supply and lymphatic system are found; subsequent migration to distant organs causes metastatic melanoma.

1.1.4 Immunosurveillance and immunoediting of cancer

Paul Ehrlich was the pioneer who suggested a role of the immune system in controlling tumour growth a hundred years ago and this opened a debate over the intervening decades. In 1957, Burnet and Thomas hypothesised that the early spontaneous cancerous cells appearing in long lived animals can be recognised and eliminated by the natural immune system components before developing into a clinically apparent disease. This concept, known as the immunosurveillance hypothesis, remained controversial for many years, because of lack of direct evidence (Dunn *et al.* 2004). Murine models of natural immunity to tumorigenesis via spontaneous and carcinogen-induced pathways emerged at the end of the 1990s after successful investigations in mice deficient in perforins, interferon γ ($IFN\gamma^{-/-}$) and recombination activation genes ($RAG^{-/-}$), re-establishing the immunosurveillance theory and expanding it to include innate and adaptive immunity to cancers (Dunn *et al.* 2004, Vesely *et al.* 2011).

The Schreiber group showed significant susceptibility to Methylcholanthrene (MCA)-induced sarcoma in IFNγ insensitive $STAT1^{-/-}$ mice, lymphocyte-deficient $RAG2^{-/-}$ mice [T, B and NKT cells] and $STAT1^{-/-}$ $RAG2^{-/-}$ deficient mice compared with WT mice. Similarly, over 15 months, the immunodeficient mice were more prone to spontaneous neoplasia than WT mice and those neoplastic tumours progressed when transplanted into naïve immunodeficient mice. Moreover, in the neoplasia transplantation approach, it was found that the immunogenicity of tumours derived from MCA-induced sarcoma in $RAG2^{-/-}$ mice was greater than similarly induced tumours derived from WT mice. Transplantation of MCA-induced sarcomas from WT

and RAG2$^{-/-}$ mice into syngeneic immunocompetent WT hosts showed progressive growth of all WT derived sarcoma, whereas spontaneous rejection of 40% of RAG2$^{-/-}$ derived sarcoma was found (Shankaran *et al.* 2001).

It has been proposed that the extrinsic suppressor pressure of the intact immune system on tumours leads to the evolution in immunocompetent hosts of tumour cells with reduced immunogenicity; this idea would predict not a one step process, but continuous sculpting by the immune system and development of escape mechanisms in tumour cells. An immunosurveillance theory based on the elimination by the immune system of cancerous cells at early stages was clearly inadequate to describe such a scenario, leading Schreiber in 2001 to introduce an immunoediting hypothesis encompassing three phases: elimination, equilibrium and escape (Shankaran *et al.* 2001, Dunn *et al.* 2002).

1.1.4.1 Tumour elimination phase

In the elimination (immunosurveillance) phase of tumorigenesis, neoplastically transformed cells generated after the failure of tumour suppressor pathways such as p53 are recognised and destroyed by innate and adaptive immune cells. Transformed cells express tumour antigens in the context of MHCI, stress induced molecules such as NKG2D ligands and calreticulin, and death receptors FasR and TRAILR. CD8^{+} T cells, γδ T cells and NK cells express NKG2D receptor which recognise stress ligands and calreticulin on transformed cells and destroy them via perforins, granzymes and IFNγ (Mittal *et al.* 2014). CD8 T cells not only inhibit tumour proliferation and angiogenesis mediated by IFNγ, but also stimulate tumour apoptosis through FasL and TRAIL receptors. DC and MØ also take up tumour antigens and

present them in the context of MHC or Cd1d to $CD4^+$ and $CD8^+$ T cells or NKT respectively, and produce IL-12 which induces cellular cytotoxicity effector functions and costimulatory survival molecules such as TNFSFR4 and TNFSFR18. Moreover, MØ and neutrophils produce anti-tumour cytokines TNF-α, IL-1, IL-12 and ROS (Dunn *et al.* 2004, Mittal *et al.* 2014). At this stage, high tumour immunogenicity engages immune effector mechanisms and the balance between tumour and immune response shifts in the favour of anti-tumour immunity, and tumorigenic cells can be eliminated.

1.1.4.2 Tumour equilibrium phase

Equilibrium is the next phase of immunoediting in which the tumours are functionally dormant; at this stage the adaptive arm of the immune system restrains tumour growth and the innate arm is redundant. Due to immune pressure and genetic instability of tumour variants some clones resist elimination by downregulation of antigen presentation and promotion of immune suppression mechanisms particularly IL-10 and IL-23 cytokines and PD-L1 molecules (Vesely *et al.* 2011). There is currently no model to explain the events of interaction between the immune system and tumour cells in this phase, but it seems that an equilibrium state between the immune suppression cytokines, IL-10, TGF-β and immune promoting cytokines, IFNγ and IL-12, maintains dormancy in immunocompetent hosts (Mittal *et al.* 2014). MacKie *et al.,* (2003) published a report supporting dormancy: a man and a woman transplanted with allogenic kidney shown development of metastatic melanoma within 24 months of organ implant. The transplant registry revealed that the recipients received kidneys from the same donor who recovered from primary melanoma 16 years before death (MacKie *et al.* 2003). This suggests that the immunosuppressed

condition of the recipients enabled melanoma to escape to a clinically apparent disease whereas the immunocompetent donor immune system had kept the disease at a sub-clinical level for a decade and a half.

1.1.4.3 Tumour escape phase

The constant pressure of anti-tumour adaptive immunity against tumour growth combines with the accumulation of somatic mutations in tumour variants to produce tumour cell clones with genetic and epigenetic modifications that evade immunity and escape to develop to clinically detectable tumours. The evolved clones evade adaptive immunity in a number of ways. Since tumours arise from self-tissues, tolerance mechanisms that eliminate self-reactive T cells in the thymus can render the tumour invisible to the adaptive immune system due to the presence of specific tumour neoantigens (Vesely *et al.* 2011). Tumours exhibit intrinsic modifications resulting in the downregulation of tumour antigens, MHCI and danger signal ligands NKG2D, and defects in intracellular antigen-processing machinery such as transporter associated with antigen processing 1 (TAP1) loss. In this regard, recurrence of metastatic melanoma in patients after successful therapy with melanoma-derived peptides was associated with selective or complete loss of HLA class I and antigen expression on melanoma cells, pointing to the adaptive immune response as a significant selective pressure (Khong *et al.* 2004). In cases of low antigen and MHC expression, tumours resist immunity either by overexpression of death receptors PD-L1, Fas and TRAILR for cytotoxic T cells or by upregulating of tumour survival molecules Bcl-XL (Dunn *et al.* 2004).

Tumours also secrete soluble mediators and cytokines that not only impair lymphocyte and DC function but also recruit the immunosuppressive cells such as myeloid derived suppressed cells (MDSCs), plasmacytoid DCs (pDCs) and Tregs into the tumour mass. The ability of DC to home to lymphoid tissues and then trigger anti-cancer immunity is $CCR7^{+}$ mediated, however, human and mouse tumours are reported to produce cholesterol metabolites, liver X receptor ligands (LXRL), which interfere with DC migration by inhibition of CCR7 expression on DC (Villablanca *et al.* 2010). Tumours also secrete enzymes that arrest lymphocyte proliferation or kill them. Indoleamine 2,3 deoxygenase (IDO) is an enzyme that catalyses the conversion of the essential amino acid tryptophan to the toxic product kynurenines. IDO is expressed by the majority of human tumours and in mice (Uyttenhove *et al.* 2003), rejection of tumours expressing IDO failed due to the inhibition of recruitment of alloreactive T cells to the tumour microenvironment; injection of anti-IDO reversed this failure to some degree. It seems that IDO has dual action on lymphocytes, initially arresting their proliferation by starvation (shortage of tryptophan), and then inhibiting their function with toxic metabolites, kynurenines.

The production of VEGF, IL1-β, GM-CSF, TGF-β, IL-10, IL-4 and IL-13 cytokines by tumours play various parts in tumour progression. Whereas VEGF is critical for tumour angiogenesis because it supplies it with oxygen and nutrients and suppresses DC function, (Neufeld *et al.* 1999, Hanahan and Weinberg 2011), IL-1 and GM-CSF are necessary for MDSCs expansion and accumulation into tumour sites, where they exert their immunosuppressive effect through secretion of TGF-β, arginase1 and iNOS (Gabrilovich and Nagaraj 2009). In addition, tumours have the capacity either to recruit mainly thymus derived Tregs to the tumour mass through

the CCL-22 chemokine or to accumulate induced Tregs dependent on TGF-β conversion of effector $CD4^+$ T cells; the two regulatory cell types exert a wide range of suppressive mechanisms (Liyanage *et al.* 2002, Zou 2006) that will be discussed further in this chapter.

Furthermore, tumours may generate tolerogenic architecture similar to lymph nodes, enabling a suppressive environment and facilitating their progression. $CCR7^+$ Lymphoid Tissue Inducer cells (LTi) (responsible for embryonic lymphoid neogenesis) have been shown to be recruited into the melanoma milieu of CCL-21 expressing tumours, generating a lymphoid like network which results in infiltration of MDSCs, Tregs and monocytic M2 macrophages (Shields *et al.* 2010). This infiltration was accompanied by faster tumour growth compared with the same melanoma cell line not expressing the chemokine CCL-21 (Shields *et al.* 2010). Although not shown to be essential, the presence of LTi correlated positively with both promotion of tolerogenic response and tumour progression.

1.1.5 Melanoma associated antigens

The mammalian immune system typically discriminates between self and foreign antigens; however, unresponsiveness to self, which is established through tolerance mechanisms, represents a major challenge for cancer immunotherapists because tumours typically express native tissues antigens. Combined serological and molecular approaches have identified numerous antigens associated with tumour tissues that can be recognised by T lymphocytes. Accordingly, tumour associated antigens (TAA) have been categorised into: (1) tissue differentiation antigens (2) overexpressed antigens (3) cancer testis antigens (CTA) or germline antigens, the

expression of which is restricted to gametogenesis during embryogenesis but may be expressed by some tumours in adulthood (4) tumour specific antigens generated from mutated genes (5) tumour viral antigens resulting from oncogenic viral infections such as Hepatitis B virus (Restifo *et al.* 2012, Coulie *et al.* 2014).

A body of evidence shows that just as normal melanocytes express tissue differentiation antigens such as PMEL (gp100), tyrosinase, TYRP-1, TYRP-2, and MART1, which participate in melanogenesis, so too do malignant melanocytes, and often to excess. Adoptive transfer of tumour infiltrating T lymphocytes reactive for gp100 and MART1 into metastatic melanoma patients led to complete tumour regression but was also associated with autoimmunity, indicating that toxic side effects need to be considered when using either effector T cell transfer or antigen based peptide vaccination (Castelli *et al.* 2000, Yeh *et al.* 2009, Restifo *et al.* 2012).

Cancer testis antigens (CTA) are commonly expressed on malignant melanomas, lung cancer and some other types of cancer. These antigens are expressed only during embryonic stages and normally on male gametes; however, immunity is not induced against gametes because they do not express MHC molecules. Due to epigenetic changes in tumours these antigens specifically re-emerge on tumours, e.g. MAGE, BAGE, GAGE and NY-ESO-1 families (Simpson *et al.* 2005). In a clinical trial, 17 patients with metastatic melanoma and 8 with synovial sarcoma, treated previously with traditional cancer medicines, were given autologous engineered NY-ESO specific TCR lymphocytes, resulting in tumour regression without toxicity to normal tissues in 47% and 80% of the patients, respectively (Robbins *et al.* 2011). The specific of expression of cancer testis antigens on a wide range of tumours

qualifies them as therapeutic targets with minimum toxicity sequels (Restifo *et al.* 2012).

Melanoma is considered to be an immunogenic syndrome and it has been widely used as a tumour model in experimental and human clinical studies to dissect tumour immunology (Maio 2012). These are supported by documented cases of spontaneous healing of melanoma (Speeckaert *et al.* 2011); responses to immune-modulating agents such as IFNs and IL-2 (Atkins *et al.* 1999, Gogas *et al.* 2006); recognition of melanoma specific and functional lymphocytes in melanoma patients (Dudley *et al.* 2002); identification of several melanoma-specific antigens (Castelli *et al.* 2000, Simpson *et al.* 2005, Jacobs *et al.* 2012). In addition to immunological reasons, practical reasons also contributed to the use of melanoma as a primary model for the investigation of cancer immunity. It has been suggested that melanoma is more easily adaptable to cell culture than other human cancer types, so many lines were generated and used for the testing of antibodies and lymphocyte reactivity (Houghton *et al.* 2001).

As mentioned before, tumours arise from self-tissues and the promiscuous expression of self-tissue antigens by thymic stromal cells that establishes self-tolerance to protect the body from autoimmunity represents a major hurdle for cancer immunotherapy.

1.2 General overview of the immune system

The remarkable evolution of the adaptive immune system started in jawed vertebrates around 500 million years ago. This system has developed to include a complex array of cells and molecules that protects the mammalian body against

infectious agents and disorders. Before that, innate immunity provided general or first line of defence protection against foreign invasion in multicellular invertebrates. Whilst innate immunity recognises conserved pathogen associated molecular patterns (PAMPs), adaptive immunity coordinates with innate immunity to identify foreign antigens specifically using a highly diverse and extensive repertoire of B and T lymphocytes, resulting in a delayed response and the generation of memory for rapid elimination of any repeated invasion (Cooper and Alder 2006). The diverse repertoire of T cells is generated in the thymus through a complex series of developmental stages and pathways that preserve T cell functionality and self-tolerance, which will be dissected in (1.2.1) and (1.2.2). This study will focus only on immunity and tolerance in T lymphocytes.

1.2.1 Development of T lymphocytes in the thymus

The thymus is the primary lymphoid organ whose molecular and cellular microenvironment provides the milieu for T lymphocyte development (Klein *et al.* 2014). Anatomically, it consists of an outer region called the cortex, which is dominated by immature T lymphocytes and cortical thymic epithelial cell (cTEC) populations, and the inner region, the medulla, which is mainly populated with mature T lymphocytes, medullary thymic epithelial cells (mTEC) and DCs (Pearse 2006, Klein *et al.* 2009). The two areas are linked by the cortico-medullary junctional (CMJ) area where blood vessels are continuously seeding immature thymocytes derived from differentiated multipotent precursors that are generated from haematopoietic stem cell (HSC) progenitors in the bone marrow and that migrate to the thymus for maturation (Figure 1.2) (Benz and Bleul 2005).

The early immature thymocytes, denoted double negative (DN) because of the absence of either of the T cell co-receptors CD4 and CD8, entering the thymus at CMJ area, undergo subsequent functional and phenotypical changes characterised by changes in expression of CD25 and CD44 through four distinct developmental stages (Godfrey *et al.* 1993). According to the expression of the markers in each stage and their location within the thymus, four distinct developmental subsets have been identified. During the first developmental stage DN1 ($CD4^-$ $CD8^-$ $CD44^{high}$ $CD25^-$), cells migrate outward from the CMJ zone towards the mid-cortex and upregulate CD25 to become DN2 ($CD4^-$ $CD8^-$ $CD44^+$ $CD25^+$). This stage is followed by movement into the subcapsular area and downregulation of CD44, accompanied by differentiation into a mature T cell lineage stage DN3 ($CD4^-$ $CD8^-$ $CD44^-$ $CD25^+$). Further maturation results in the loss of CD25 and CD44 and transition into the final stage DN4 ($CD4^+$ $CD8^+$ $CD44^-$ $CD25^-$) which is able to upregulate $CD4^+$ $CD8^+$ and become a so-called double positive (DP) thymocytes; the DP cells return to the medullary area (Godfrey *et al.* 1993, Lind *et al.* 2001, Klein *et al.* 2009).

During the transition from DN2 to DN3, thymocyte division is decreased and the genes encoding RAG1 and RAG2 are expressed to initiate the formation of pre-TCR complex. The RAG1 and RAG2 enzymes stimulate *VDJ* gene rearrangement at *TCRβ* position that encodes for a heterodimeric β chain. The TCRβ chain then combines with an invariant α chain leading to the formation of either a functional pre-TCR receptor ($TCR\beta^+$pre-TCRα), which associates with intracellular CD3 proteins for downstream signalling and for proceeding to DN4 and DP phases (Dudley *et al.* 1994, Saint-Ruf *et al.* 1994), or a non-functional pre-TCR receptor on thymocytes

which are then eliminated through the β selection process (Dudley *et al.* 1994, Fehling *et al.* 1995). Expression of a functional TCR induces TCRβ allelic exclusion

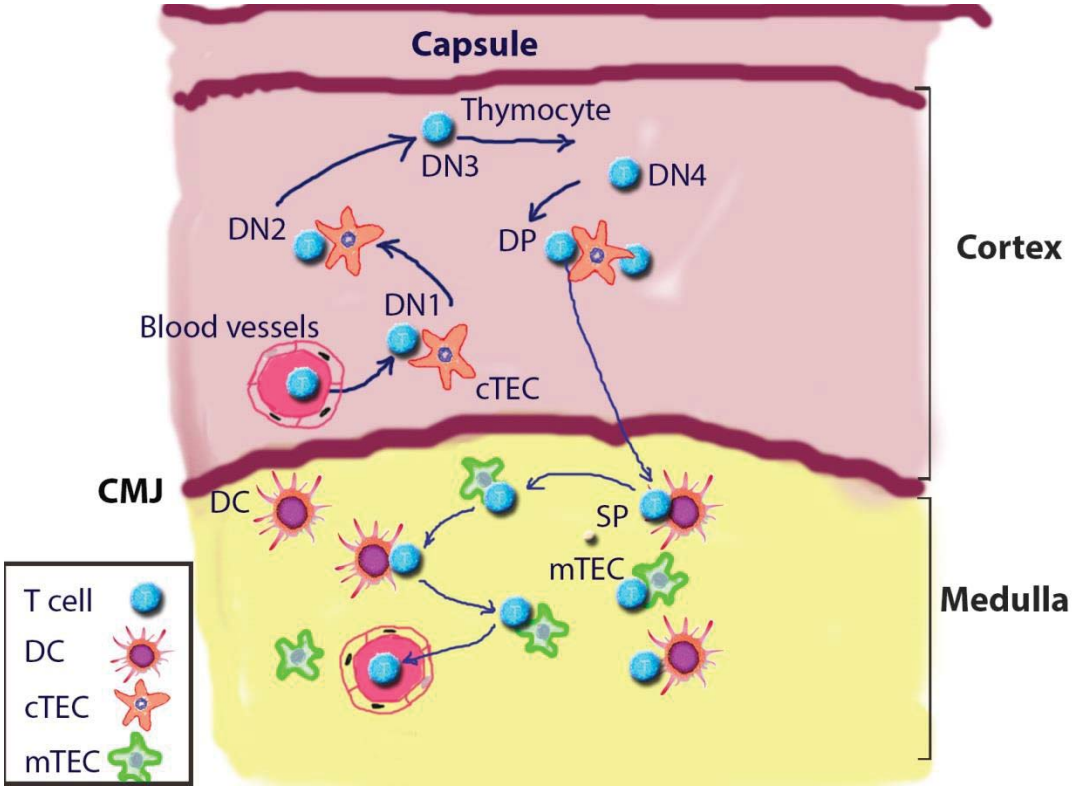

Figure 1.2: Thymus anatomy and T cell developmental stages

Histologically, the thymus is divided into cortex and medulla and each is constituted with various phenotypes of thymic epithelial cells. T cells enter the thymus at the cortico medullary junction (CMJ). Then, the cells move through the cortex where they undergo phenotypical and functional changes through four stages, called double negative (DN). (DN1) $CD4^{-}CD8^{-}$ uncommitted progenitors differentiate into (DN2) thymocytes which undergo proliferation and lose the B cell and NK cell lineage phenotypes. Then, cells commit to the T cell lineage and start the rearrangement of T cell receptor β-chain (DN3) followed by transition into (DN4) which ends as the double positive (DP) $CD4^{+}CD8^{+}$ phenotype. The DP cells migrate back into medulla where they differentiate into single positive cells (SP), either $CD4^{+}$ or $CD8^{+}$. During this journey, T cells undergo positive selection in the cortex, which is mediated by cortical epithelial cells (cTEC) while negative selection occurs in the medulla and is mediated by medullary epithelial cells (mTEC) and dendritic cells (DC).

and DN3 differentiation into the DN4 stage. This excludes rearrangement of the other TCRβ allele, preserving expression of a single copy of the TCR on each cell (Khor and Sleckman 2002). It also initiates survival and proliferation of thymocytes and differentiation into DN4 and immature DP stages by induction of Tcrα loci gene rearrangement, inactivation of RAG1 and RAG2, expression of CD4 and CD8, and formation of complete TCR from TCRβ and TCRα chains binding (Dudley *et al.* 1994, Petrie and Zúñiga-Pflücker 2007, Janas and Turner 2010). At this stage, the T cells exhibit mature DP phenotype and start their migration deep into the thymic medulla for selection.

1.2.2 Mechanisms of T cell immune tolerance

Central tolerance in the thymus encompasses crucial mechanisms through which the body can deplete autoreactive T cells to avoid their pathology. The fate of αβ DP T cells is determined by their ability to recognise self-antigens presented by thymic stromal APCs. Only 5% of the 50 $x10^6$ αβ DP T cells that are produced daily in the mouse thymus survive after the stringent positive and negative selection processes of central tolerance (Kyewski and Klein 2006). The developmental fate of the T cell has been conceptualised in an affinity model based on the strength of binding between TCR and peptide/MHC molecules (Klein *et al.* 2014).

In this model, αβTCR cells which, due to the expression of non-functional TCRs, fail to engage to self-ligands embedded in MHC molecules expressed on cortical thymic epithelial cells (cTEC) and die in a type of apoptosis called neglect; 90% of thymocytes die at this stage (Klein *et al.* 2009, Klein *et al.* 2014). Although this step enriches the autoreactive T cell population, it also ensures that useful αβ T cells with

low to intermediate affinity to self-ligands are positively selected and can commit to SP lineages and differentiate into $CD4^+$ or $C8^+$ T cells, depending on their membrane expression of MHCII and MHCI respectively (Klein *et al.* 2014). αβ T cells with high affinity to self-ligands are eliminated through the negative selection mechanism (clonal deletion), but self-reactive TCR clones with an affinity situated between the threshold of positive and negative selections are proposed to differentiate by clonal diversion into nTregs, a subset of T cells that plays a vital role in immune system regulation called regulatory T cells (Josefowicz *et al.* 2012, Klein *et al.* 2014). During the life of a healthy mammal, dominant central and recessive peripheral tolerance mechanisms - clonal deletion, clonal diversion and anergy - preserve the body from pathogenic T cells that are self-reactive (Xing and Hogquist 2012).

1.2.2.1 Central T lymphocyte tolerance

The thymic medullary cellular components, mTECs and mDCs, form the niche where negative selection of central tolerance dominantly depletes high affinity self-antigen reactive T cells through induction of intrinsic apoptosis in those thymocytes. A robust TCR signal induces expression of the BCL-2 family member BIM (BH3) which activates the production of the proapoptotic mediators BAX and BAK that antagonise survival molecules activity such as BCL-2 and BCL-X (Goodnow *et al.* 2005). $BIM^{-/-}$ mice were reported to be refractory to clonal deletion of self-specific T cells (Bouillet *et al.* 2002) as were mice deficient in another apoptotic mediator nerve growth factor IB (Nur77) (Zhou *et al.* 1996), which suggests that both BIM and Nur77 may collaborate for proper negative selection. Vigorous activation of ERK and Jun Kinase (JUN), molecules of the MAPK pathway, after interaction with high affinity TCR instructs the pathway in favour of cell death; however this pathway may divert in

favour of positive selection if the affinity is low (Xing and Hogquist 2012). The thymic cortex is specified for positive selection but may also contribute to clonal deletion. McCaughtry *et al*., (2008) demonstrated that cTECs activate and imprint autoreactive thymocytes, but a subset of DCs is subsequently responsible for their negative selection. The relative inefficacy of cTECs in inducing deletion may be due to the lack of expression of costimulatory molecules that augment the TCR signal and induce apoptosis (McCaughtry *et al.* 2008).

Diverse tissue restricted antigens are expressed within the thymus to ensure deletion of self-reactive T cells. mTECs professionally exhibit promiscuous gene expression (pGE) of self-tissue restricted antigens (TRA) that mirror peripheral organ epitopes and contribute to self-tolerance either directly by presentation of auto-tissue epitopes to T cells (Derbinski *et al.* 2001) or indirectly by cross presentation of TRA into DCs (Gallegos and Bevan 2004, Kyewski and Klein 2006). The nuclear transcriptional factor AIRE, encoded by the autoimmune regulator gene *AIRE,* controls pGE of TRA on mTECs which promotes clonal deletion of organ-specific reactive T cells or guides their development into nTregs (Metzger and Anderson 2011, Cowan *et al.* 2013, Malchow *et al.* 2013). A key role for AIRE in self-tolerance is evident in both humans and mice. Individuals that harbour a mutated AIRE suffer from a multiorgan systemic autoimmune syndrome known as autoimmune polyendocrinopathy-candidiasis-ectodermal dystrophy (APECED) (Aaltonen *et al.* 1997). Similarly, a systemic autoimmune phenotype is observed in AIRE deficient mice as a result of defective TRA expression on the mTECs required for the induction of tolerance, and was reported as a possible mouse model of APECED (Anderson *et al.* 2002). A serious impediment to cancer immunotherapy is self-tolerance (Kyewski and Klein 2006).

The majority of tumours arise from self-tissues and expression of their epitopes results in the elimination of tumour-specific cytotoxic T cells in the thymus. Compared to their *AIRE* WT counterparts, *AIRE* deficient mice showed resistance to B16 melanoma growth and rejection of the tumours after challenging with irradiated melanoma cells (Träger *et al.* 2012). Immune response to and increased frequency of CD8 T cells specific for the melanoma gp100 antigen, normally expressed on mTECs, was found only in the $AIRE^{-/-}$ group, but specificity to the melanoma TRP-2 antigen, not expressed on mTECs, was detected in both $AIRE^{-/-}$ and $AIRE^{+/+}$ groups (Träger *et al.* 2012). These results confirm that AIRE controls gp100 expression and creates tolerance to it, while TRP-2 is out of AIRE control. Therefore self-antigen derived vaccines should be modified; otherwise negative selection will generate a population of tolerant T cells that would limit cancer vaccination.

In spite of these considerations, approaches that manipulate central tolerance by targeting AIRE mTECs may nonetheless provide for the generation of high affinity tumour-specific T cells. The TNF receptor activator of nuclear factor κ-B (RANK) is expressed on mTECs and interaction with its ligand RANKL on T cells and other thymic cells plays an important role in the development of $AIRE^{+}$ mTECs (Hikosaka *et al.* 2008). A recent study demonstrated that blockade of RANKL in mice resulted in a transient and selective defect in $AIRE^{+}$ mTECs and TSA processing that subsequently caused imperfect central tolerance and thymic clonal deletion of B16 specific lymphocytes, which extended the survival time of mice inoculated with melanoma compared to its isotype controls (Khan *et al.* 2014). $AIRE^{+}$ mTECs also contribute to clonal deletion indirectly by introducing TSA into thymic DCs which cross-present TSA to autoreactive T cells, combining mTEC and DC function for TSA

presentation and making central tolerance more efficient (Gallegos and Bevan 2004, Hubert *et al.* 2011).

1.2.2.2 Peripheral T lymphocyte tolerance

In healthy individuals, despite the stringent mechanisms of central tolerance, a repertoire of self-reactive T cells manages to escape and migrate into the periphery, providing potential for anti-cancer responses but causing autoimmunity, where they are restrained by peripheral tolerance strategies. Moreover, some self-antigens, such as those derived from developmental proteins, are absent from the thymus and T cells recognising these self-antigens need to be controlled (Xing and Hogquist 2012).

One of the mechanisms of peripheral tolerance to tumours is ignorance, which induces a state of inactivation in T cells due to insufficient cognate antigen presentation by APCs to trigger stimulation. Assuming that only high affinity self T cells are deleted during central tolerance, the T cells carrying lower affinity TCRs that exit to the periphery are likely to be relatively insensitive to tumour antigen and to need strong stimulus to force activation. Failure of immunogenic viral sarcoma antigens to reach lymph nodes and prime cytotoxic T cells permitted tumour growth in mice, but repetitive vaccination with sarcoma cells led to tumour rejection in a manner mediated by sarcoma specific T cells (Ochsenbein *et al.* 1999). Although those sarcomas were immunogenic, the immune system ignored them until sufficient antigen was supplied; furthermore, tumours may escape immunity by downregulation of antigens that have been targeted by the immune system (Khong *et al.* 2004).

There is clear evidence that T cells demand two signals for optimum activation. The first signal comes from affinity/avidity binding of TCR-peptide-/MHC cells complexes

while the second is provided by APC co-signalling molecules from the IgF and the TNFRF super families interacting with their receptors on T cells (Chen and Flies 2013). Any problem in those two signals drives peripheral T cells either to an unresponsive/suppressive state (anergy) or to activation induced cell death (AICD apoptosis). The role of IgSF and TNFRSF members in immunity will be discussed further in this chapter.

Anergy or suppression is a state of arrested T cell growth, proliferation and cytokine production as a consequence of TCR ligation with its epitope on APCs without costimulation or ligation but with a second inhibitory signal provided by inhibitory molecules, mainly CTLA-4 and PD-1, and by neutralizing autoreactive T cells it mediates peripheral tolerance and prevents autoimmunity (Tivol *et al.* 1995, Nishimura *et al.* 1999, Schwartz 2003). Maturation of DCs is required for immunity; immature DCs fail to express costimulatory molecules, so inhibit the NF-κB pathway, which is required for T cell activation, and thus force T cells into a tolerogenic rather than a responsive state (Hawiger *et al.* 2001) whilst adoptive transfer into mice of mature splenic DCs plus antigen has been shown to prime CD4 T cells into Th1 and Th2 functional cells (de Heusch *et al.* 2004). Moreover, the key co-inhibitor, CTLA-4, mediates peripheral anergy in activated T cells through competition with CD28 costimulatory receptors of B7 family on APCs, CD80 and CD86 (Greenwald *et al.* 2005). The high avidity of CTLA-4 for CD80 and CD86 enables it to exclude CD28 from the T cell surface and provide inhibitory signals that arrest T cell cycle and induce tolerance anergy. Blocking of CTLA-4 prevents anergy whereas blocking of CD28 does not (Perez *et al.* 1997). The apparent role of CTLA-4 in tolerance has

been confirmed in CTLA-4$^{-/-}$ mice which undergo fatal massive lymphoproliferation and multiorgan tissue destruction within three weeks (Tivol *et al.* 1995).

PD-1 ligation with its ligands PD-L1 and PD-L2 constitutes a second coinhibitor pathway that attenuates intercellular TCR signals and induces peripheral tolerance (Nishimura *et al.* 1999). After PD-L1 ligation, the PD-1 intercellular tail immunoreceptor tyrosine-based inhibitory motif (ITIM) is phosphorylated, recruiting tyrosine phosphatases SH-2 and SH-1 which dephosphorylate Zap70 and limit PI3K/PKB axis activation, so that early T cell activation, proliferation and cytokine production are constrained (Sheppard *et al.* 2004, Yokosuka *et al.* 2012). The role of PD-1 in tolerance is evident in B6-*PD-1*$^{-/-}$ mutant mice which show spontaneous chronic lupus-like autoimmune disease (Nishimura *et al.* 1999). Evidence suggests that PD-1 acts exclusively in an antigen specific manner to inhibit effector functions of autoreactive T cells and infiltration into organs (Salama *et al.* 2003) or synergistically with CTLA-4 to induce tolerance (Probst *et al.* 2005). In a model using antigen presentation by resting DC, concomitant inhibition of PD-1 and CTLA-4 enhanced expansion of the primed autoreactive CD8 T cell subset more than that primed by PD-1 blockade alone (Probst *et al.* 2005).

The function ascribed to lymph node stromal cells (LNSCs), including fibroblasts, FDC and endothelial cells, as parenchyma supporting T cells, has recently been broadened to include regulation of CD8 peripheral tolerance (Fletcher *et al.* 2011). These cells constitutively express TSAs, and repetitive cognate interaction with self-reactive T cells induces death receptor (Fas, CD95) expression on T cells in the presence of IL-2, whereas FasL (CD95L) upregulated on stromal cells leads to the

activation-induced cell death (AICD) pathway and its distal caspases, and ultimately T cell apoptosis (Green *et al.* 2003, Fletcher *et al.* 2011). Human autoimmune lymphoproliferative syndrome (ALPS) (Fisher *et al.* 1995) and mouse systemic lupus erythematosus-like autoimmune disease (Watanabe-Fukunaga *et al.* 1992) result from defects in Fas mediated apoptosis, and confirm the role of Fas mediated peripheral tolerance. Not only does Fas induce apoptosis in naïve T cells but also in tumour specific effector T cells. It was found that Fas mediated AICD of melanoma specific CD8 T cells in the peripheral blood of melanoma patients and in *in vitro* expanded melanoma reactive T cells for adoptive transfer, even if the melanoma did not express FasL, suggesting that continuous engagement of tumour specific T cells with tumour antigen induces Fas in T cells and leads them to spontaneous suicide. Therefore, interfering with Fas death using vaccination or caspase blockers could rescue T cells from apoptosis (Zaks *et al.* 1999, Saito *et al.* 2000).

1.2.2.3 Regulatory T cell mediated peripheral tolerance

1.2.2.3.1 Regulatory T cell phenotypes

Regulatory T cells represent another crucial aspect of peripheral tolerance that protects the body against pathogenic self-reactive T cells and non-self-exacerbated immune responses. Thymus derived Tregs (nTregs) are generated before birth in humans and soon after birth in mice, and account for up to 5-10% of peripheral $CD4^+$ T cells. Peripheral Tregs (pTregs) can also be induced (iTreg) from conventional peripheral $CD4^+$ T cells *in vivo*, or *in vitro* under certain conditions, such as using TGF-β and IL-10 (Figure 1.3) (Sakaguchi *et al.* 2008, Abbas *et al.* 2013). Suppressor T cells were proposed as early as 1970 by Gershon (Gershon and Kondo 1970) but

their existence was regarded with scepticism due to the lack of identifying markers. This uncertainty was ended when Sakaguchi group identified the IL-2Rα chain (CD25) as a phenotypic marker for a subset of naïve $CD4^+$ T cells, which inhibits autoimmunity in athymic nude mice and maintains allogenic skin transplants, suggesting that it mediates peripheral tolerance (Sakaguchi *et al.* 1995). Whereas in humans Tregs could be distinguished by their $CD4^+CD25^{high}$ phenotype, in mice Tregs express various levels of CD25, and $CD4^+CD25^{inter}$ are activated T cells, making complete molecular characterisation of Tregs elusive (Sakaguchi *et al.* 1995, Baecher-Allan *et al.* 2001).

Using genetic mapping of the DNA of scurfy mice, the Ramsdell group demonstrated a defect in the translated product of a gene they designated Foxp3, scurfin, to be responsible for progression of the scurfy disease while its normal product preserved immune homeostasis (Brunkow *et al.* 2001). Later, in mice, Foxp3 was revealed to be the lineage differentiator and master regulator for the development of both nTreg and pTreg subsets of $CD4^+CD25^+$ T cells (Fontenot *et al.* 2003, Khattri *et al.* 2003). The human *FOXP3* mutation analogue to the scurfy mouse defect predisposes humans to a similar syndrome described by the onset of fatal X-linked neonatal diabetes mellitus, enteropathy and endocrinopathy (IPEX) (Wildin *et al.* 2001). In contrast to mice where Tregs permanently express Foxp3, human conventional

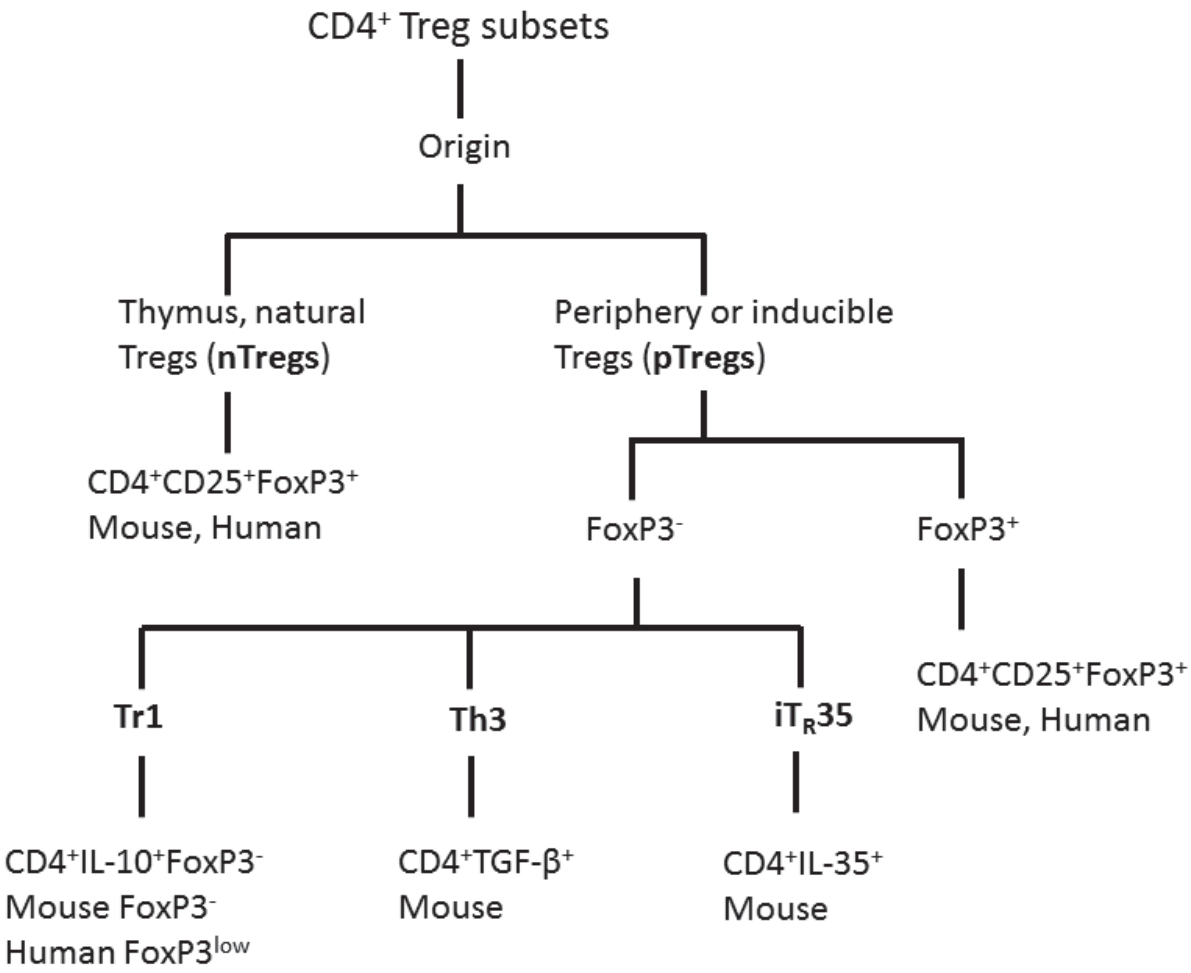

Figure 1.3: T subsets of $CD4^+$ regulatory T cells

Multiple subsets of $CD4^+$ regulatory T cells have been identified according to their suggested origin and suppressive action. Natural Tregs (nTregs) or thymic derived Tregs are generated *in vivo* in the thymus which express $CD25^+$ and $FoxP3^+$ and exert multiple inhibitory mechanisms including cell-cell contact and suppressive cytokines (Sakaguchi *et al.* 1995, Hori *et al.* 2003). pTregs, generated *in vivo* from conventional $CD4^+$ T cells under certain conditions, are either $FoxP3^+$, [so having the same phenotype as nTregs, or $FoxP3^-$, with different phenotypes] dependent on suppressive cytokine production: Tr1 produce IL-10 (Schmitt *et al.* 2012) and in human express low levels of FoxP3; Th3 produce TGF-β (Weiner 2001); and iT_R35 produce IL-35 (Collison *et al.* 2010).

activated T cells also express FOXP3 transiently, making Foxp3 not so reliable as an intercellular specific marker for Tregs (Gavin *et al.* 2006, Pillai *et al.* 2007).

Other Treg markers; CTLA-4, GITR, LAG-3, OX40, CD39, CD73, ICOS, PD-1, CCR4, CCR6, CCR7, have been identified in many human and murine studies but are not unique identifiers because they are also expressed on activated effector T cells (Sakaguchi *et al.* 2008, Josefowicz *et al.* 2012, Whiteside 2012). CD127 (IL-7Rα) can be used to distinguish between Tregs and effector T cells, as its downregulation on resting human Tregs ($CD25^+CD45RA^+$) has been associated with Foxp3 expression and *in vitro* suppression, compared with effector/memory ($CD25^+CD45RO^+$) T cells which showed upregulation of CD127 and no inhibitory characteristics (Liu *et al.* 2006, Seddiki *et al.* 2006). The difficulty in distinguishing thymus derived $Foxp3^+$ Tregs from peripherally generated $Foxp3^+$ Tregs and transiently $Foxp3^+$ effector cells created a controversial debate about the extent to which each Treg subset contributes to tolerance and anti-tumour immunity.

The extracellular glycoprotein receptor neuropilin-1 (Nrp-1) not only normally acts with its ligands, semaphorins, to guide neurone development (Gu *et al.* 2003) and abnormally mediates tumour angiogenesis and metastasis as a receptor for VEGF (Miao *et al.* 2000) and TGF-β (Glinka *et al.* 2011), but also acts as a Treg activator via TGF-β-1 (Glinka and Prud'homme 2008), which enhances stimulus by prolonging their interaction with DCs (Sarris *et al.* 2008), and can be used as a marker for nTregs (Bruder *et al.* 2004). Two recent papers reported high levels of Nrp-1 expression on murine $Foxp3^+$ nTregs, in contrast to *in vivo* generated $Foxp3^+$ pTregs of two different antigen specificities which lacked surface Nrp-1 expression; in

addition, Nrp-1 upregulation in nTregs and in *in vitro* cultured pTregs but not in conventional $CD4^+$ T cells was boosted in the presence of TGF-β (Weiss *et al.* 2012, Yadav *et al.* 2012). This raises the possibility that Nrp-1 can be used to discriminate between thymic and peripheral Tregs populations in mice, but this has not been reported in human.

Other studies suggested the use of the intracellular Helios transcription factor, a lymphocyte developmental factor that is a member of the Ikaros family, to distinguish nTregs (Thornton *et al.* 2010), but this was precluded after James Allison's group demonstrated that Helios was robustly expressed on peripherally induced moth peptide specific Tregs in an APC dependent manner, differently and faster than Foxp3 but unstable in the absence of subsequent antigen stimulation (Gottschalk *et al.* 2012).

1.2.2.3.2 Treg suppressive mechanisms

Whether nTregs or pTregs, there is a number of suppression mechanisms used to maintain immune homeostasis. Tregs modulate responder T lymphocytes and APCs through a cell-cell contact suppression mechanism. Tregs activated by TCR in an IL-2 dependent manner can suppress directly naïve T cell activation, effector T cell proliferation and IL-2 production. Treg mediated cell contact suppression of APCs is either by cytolytic granzyme and perforin release or by cell inhibition delivered by signalling molecules (Sakaguchi *et al.* 2008). Protease granzyme B formed by Tregs induces apoptosis in cocultured cells, and, along with tumour reactive NK cells and $CD8^+$ cells and their pore forming perforins, mediates cell death in a contact dependent manner. G*zmb*$^{-/-}$ (granzyme deficient) and *Prf1*$^{-/-}$ (perforin deficient)

mice were shown to be resistant to RMAS lymphoma and B16 melanoma growth compared to WT mice, but this resistance was abrogated after adoptive transfer of WT $Gz^{+}Pr^{+}$ Tregs but not $Gz^{-}Pr^{+}$ Tregs or $Gz^{+}Pr^{-}$ Tregs (Gondek *et al.* 2005, Cao *et al.* 2007).

Tregs express the ectoenzymes CD39 and CD73, which collaborate to digest pericellular adenosine triphosphate (ATP) into ADP and subsequently the suppressive product adenosine (Deaglio *et al.* 2007). Under such conditions, Tregs firstly deprive responding T cells and APCs of ATP as an energy source and secondly enhance adenosine binding to its A2A receptor on T cells and APCs, which results in cAMP elevation in those cells and consequently inhibition of T cell responses and modulation of APC function (Deaglio *et al.* 2007, Ernst *et al.* 2010, Schmidt *et al.* 2012).

Another crucial surface molecule for Treg suppressive function is CTLA-4. It is constitutively expressed on Tregs and is under Foxp3 control. Blocking of CTLA-4 on Tregs revokes their suppressive ability (Sakaguchi *et al.* 2008, Sakaguchi *et al.* 2009). Studies of bone marrow transplantation and adoptive T cell transfers have proved the ability of CTLA-$4^{+/+}$ T cells to regulate CTLA-$4^{-/-}$ T cell responses and this regulation is dominated by Tregs (Friedline *et al.* 2009). Moreover, selective depletion of CTLA-4 on Tregs produces mice that develop fatal spontaneous lymphoproliferative T cell mediated autoimmune disease and robust anti-tumour responses (Wing *et al.* 2008). These manifestations confirm the necessity of CTLA-4 for Treg function and tolerance induction, which operates mainly by downregulation of CD80 and CD86 costimulatory molecules on APCs in a process called

transendocytosis, thereby suppressing T cell priming by APCs (Wing *et al.* 2008, Friedline *et al.* 2009, Qureshi *et al.* 2011). Prolonged and close interactions between Tregs and DCs mediated by Nrp-1 and LFA-1 respectively can enhance inhibitory CTLA-4 signals from Tregs to DCs and also may reduce contact between DCs and conventional T cells (Tadokoro *et al.* 2006, Sarris *et al.* 2008, Schmidt *et al.* 2012). Another immunosuppressive action of CTLA-4 Tregs is stimulation of intracellular IDO synthesis in DCs, which degrades the amino acid tryptophan, essential for activated T cell maintenance, leading to either effector T cell death or generation of iTregs (Fallarino *et al.* 2003, Schmidt *et al.* 2012).

LAG-3, a CD4-related molecule that binds MHCII, was shown (Huang *et al.* 2004) to maximise activated Treg regulatory function in *in vitro* and *in vivo* studies while this suppressive capacity was reduced in Tregs deficient in the expression of LAG-3. This suppression capacity is reported to be due to the engagement of LAG-3 on Tregs to MHCII on DCs and delivery of inhibitory signals that modulate DC maturation and expression of stimulatory molecules, suggesting that Tregs are indirectly controlling the activation of responding cells via DCs (Liang *et al.* 2008, Josefowicz *et al.* 2012). DC function can also be modulated by the immunoglobulin family member TIGIT, upregulated on Tregs and effector/memory T cells, which, following cognition with the poliovirus receptor on DCs, supports the generation of immunosuppressive IL-10 producing DCs. Blocking of TIGIT showed inhibition of delayed hypersensitivity in WT mice whereas no effect was found in IL-$10^{-/-}$ mice (Yu *et al.* 2009).

Receptors belonging to TNFR family, in particular OX40, GITR, 4-1BB, and TNFRII are also essential for controlling Treg function. They are constitutively expressed on

Tregs but also upregulated on activated and memory T cells and function as costimulatory and survival molecules (Croft 2009, Josefowicz *et al.* 2012).

Production of the potent suppressive cytokines TGF-β, IL-10 and IL-35 is also implicated in Treg regulatory function (Figure 1.3). Deficiency of TGF-β generally in mice and specifically in T cells contributes to the progression of autoimmunity (von Boehmer 2005, Josefowicz *et al.* 2012, Schmidt *et al.* 2012). Tregs express persistent membrane bound TGF-β1 which supresses $CD4^+CD25^-$ cells and dampens immunoglobulin production by B cells in a cell-cell contact dependent manner, and blocking of TGF-β abolishes such repression (Nakamura *et al.* 2001). Soluble TGF-β is also found to be secreted by human and mouse $CD4^+CD25^+$ Tregs, which limits conventional $CD4^+$ T cell expansion *in vitro* and has been demonstrated to be involved in Treg suppressive function and protection from inflammatory colitis in a severe combined immunodeficiency (SCID) mouse model (Nakamura *et al.* 2004). Nonetheless, such a TGF-β contribution to Treg suppressive function is questioned by other research groups. Shevach and co-workers showed that *in vitro* blocking of neither TGF-β1 nor its receptor reversed the suppression activity of $CD4^+CD25^+$ Tregs and found no differences in susceptibility to suppression by Tregs between conventional CD4 T cells from WT mice and the same cell type from $Smad^{-/-}$ and DNRII Tg mice, which are unresponsive to TGF-β, suggesting that Treg suppressive ability is independent of TGF-β (Piccirillo *et al.* 2002). Contrasting results stated that specific murine colon cancer $CD8^+$ reactive cytotoxic T cells can be inhibited by Tregs in a TGF-β dependent manner because transgenic CD8 cells for dominant-negative TGF-β receptor rejected the tumour (Chen *et al.* 2005). Other work showed

that TGF-β released by DCs mediated the induction of tissue Tregs that leads to the suppression of intestinal inflammation (Travis *et al.* 2007).

IL-10 is an anti-inflammatory cytokine produced by nTregs and Foxp3^{-} induced Tregs (Tr1); although some early *in vitro* studies reported Treg regulation to be independent of IL-10 and TGF-β, *in vivo* experiments have shown that IL-10^{+} Tregs mediate both peripheral tolerance and suppression of inflammation in epithelial surfaces such as colon, lungs and skin (Vieira *et al.* 2004, von Boehmer 2005, Schmidt *et al.* 2012). IL-10 may not regulate autoimmunity but it is crucial for limiting inflammatory reactions at tissue interfaces. In a system where a Cre construct was used to block IL-10 specifically on Tregs, those Tregs failed to control colitis, respiratory inflammations and skin hypersensitivity in spite of normal production of IL-4, INF-γ, IL-2 and TNF-α cytokines (Rubtsov *et al.* 2008). Similarly, cell transfer of IL-10 deficient nTregs failed to prevent Foxp3 induced disease in RAG$^{-/-}$ recipient, whereas the disease was controlled after cell transfer of IL-10^{+} iTregs (Schmitt *et al.* 2012). IL-10 producing Tregs supress pathogenic Th17 cell dependent inflammation by amplifying negative signals that destabilise the Th17 differentiation transcription factor STAT3, (Chaudhry *et al.* 2011); it also inhibits tumour associated pathogenic Th17 cells via type 1 interferons which recruit Tregs into the tumour microenvironment (Stewart *et al.* 2013). Interference with those Tregs may promote tumour growth associated with Th17 proinflammation.

A subset of Tregs not expressing Foxp3, called iT$_R$35, has been observed to accumulate in B16 melanoma and colorectal adenocarcinoma tumours with potent suppression activity dependent on neither TGF-β nor IL-10 but on IL-35. Intestinal

parasitic inflammation also induced generation of iT_R35, which contributed to high production of IL-35 by nTregs and led to the generation of iT_R35 cells (Collison *et al.* 2010). IL-35 is composed of two proteins p35 and EBI3; any defect in either protein results in an imbalance in mucosal immunity and progression to severe colitis, confirming the role of IL-35 in Treg suppressive function (Josefowicz *et al.* 2012, Schmidt *et al.* 2012).

Although mechanisms are still unclear, results from many studies suggest that Tregs express transcription factors that induce homing chemokines resemble to that in effector T cells, enabling them to migrate to the same site as the $CD4^+$ responder population of T effectors to apply appropriate regulation (Schmidt *et al.* 2012). In this regard, interferon gamma has been shown to induce overexpression of the Th1 transcription factor T-bet in Tregs, leading to their upregulation of the Th1 homing chemokine CXCR3 and facilitating homeostatic regulation of Th1 anti *Mycobacterium tuberculosis* immunity in lung granulomas. Absence of T-bet on Tregs caused severe inflammation characterised by splenomegaly and lymphadenopathy (Koch *et al.* 2009).

1.2.3 Evidence that OX40 supresses Treg function

1.2.3.1 Expression and signalling

30 members of TNFRSF have been identified (Table 1:1), of which most importantly OX40, CD30, GITR, 4-1BB, CD27, DR3 and HVEM provide costimulatory signals that synergize with that of the TCR and CD3 for optimal T cell activation and facilitation of the progression of the T cell life cycle, production of cytokines and promotion of T cell survival and formation of memory lymphocytes (Croft 2009, Chen and Flies 2013).

Three membranes bound receptor molecules, each composed of three to four extracellular cysteine rich domains expressed on T cells, combine with one membrane bound or soluble trimer ligand on APCs to form a receptor-ligand complex. This combination phosphorylates the TNF intracellular receptor tail motif which recruits either the adaptor proteins for T cell activation, TNF receptor associated factors (TRAFs) or the adaptors for T cell inhibition, TNFR associated death domain (TRADD) (Croft 2003, Watts 2005, Chen and Flies 2013).

In both human, chromosome 1, and mouse, chromosome 4, OX40 (TNFRSF4, CD134) and CD30 (TNFRSF8, Ki-1) genes locate closely within the TNF cluster, suggesting shared T cell functionality (Tan *et al.* 1997, Locksley *et al.* 2001, Withers *et al.* 2011). OX40 and CD30 members of TNFR family are expressed on various cell types including T cells, B cells, NK cells, neutrophils, eosinophils, Hodgkin's lymphoma cells. In contrast to other TNFRs such as CD28 and HVEM, which are constitutively expressed on T cells, both OX40 and CD30 are not present on resting naïve/memory cells, but only appear on *in vitro* and *in vivo* activated T cells in an antigen and TCR dependent manner, their upregulation peaking two-five days after stimulation (Croft 2003, Toennies *et al.* 2004, Watts 2005). Stimulated APCs, mast cells, NK cells, CD4 effector T cells and endothelial cells overexpress the glycoprotein membrane bound or soluble OX40L (TNFSF4, CD252) and CD30L (TNFSF8, CD153) but they are also expressed constitutively on LTi (Croft 2003, Kim *et al.* 2003, Watts 2005, Croft 2009). Ligation of OX40 and CD30 receptors with OX40L and CD30L respectively phosphorylates signal adaptor proteins (TRAF1,2,3 and 5), which activate downstream signalling pathways NF-κB, PI3K/PKB and JNK and p38 MAPK (Watts 2005, Croft 2009). Activation of those pathways induces: (1)

production of the anti-apoptotic molecules Bcl-2 and Bcl-xL and hampering of pro-apoptotic activators such as BIM, thus supporting cell survival (Rogers *et al.* 2001); (2) promotion of T cell cycle progression through release of survivin and aurora B kinase that activate CDK mediated mitosis progression (Song *et al.* 2005); (3) overexpression of cytokines IL-2, IL-4, IL-5 and IFNγ, which drive T cell lineage differentiation and upregulate the cytokine receptors IL-2Rα and IL-12Rβ, which amplify sensitisation of T cells to TNFRs (Croft 2003, So *et al.* 2006, Williams *et al.* 2007).

Although several studies have shown that OX40 and CD30 preferentially drive differentiation of $CD4^+$ T cells toward the Th2 lineage (Del Prete *et al.* 1995, Ohshima *et al.* 1998, Watts 2005), a significant concomitant role of those receptors has been demonstrated in their contribution in the survival of responder CD4 T cells specific for OVA antigen when associated with LTi (Kim *et al.* 2003) and the survival of CD4 T cells in mice challenged with *Salmonella* (Gaspal *et al.* 2008*)*. However, differences in antigen presentation may influence the expanded T cell pool. CD8 T cells expanded by priming with CMV are preserved in $CD30^{-/-}OX40^{-/-}$ mice, but the same population is lost when mice are immunised with OVA peptide (Bekiaris *et al.* 2009). Double deficient ($CD30^{-/-}OX40^{-/-}$) mice were significantly less able to sustain a memory T cell population and recall antibody response than $OX40^{-/-}$, $CD30^{-/-}$, or $OX40L^{-/-}$ mice, which showed a partial defect relative to WT mice, suggesting impairment in the survival of initially expanded activated T cell pool (Gramaglia *et al.* 2000, Gaspal *et al.* 2005, Soroosh *et al.* 2006). Withers *et al.*, (2009) showed that in the intestinal lamina propria of $CD30^{-/-}OX40^{-/-}$ mice, the number of CD4 memory T cells is heavily reduced compared with WT, and this reduction is not due to lack of

homing chemokines or reduction in Bcl-2 and Bc-xL expression but due to the failure in the persistence of initially expanded CD T cells (Withers *et al.* 2009). The persistence of this memory reservoir is heavily dependent on survival signals provided by -CD30L and OX40L-expressing LTi (Withers *et al.* 2012).

It seems that, rather than being involved in Th cell polarization, OX40 and CD30 support immune responses of T cells subsets, including the promotion of effector/memory T cell survival. CD30 and OX40 receptors and their ligands are overexpressed in a wide range of inflammatory syndromes and have been implicated in Th1 and Th2 mediated autoimmune diseases; therefore, they are interesting targets for autoimmunity and cancer immunotherapy (Kennedy *et al.* 2006, Croft 2010).

1.2.3.2 OX40 supresses Treg function

The constitutive expression of OX40 on nTregs but not conventional T cells (Tc) and its significant impact on nTregs and activated T cells made it an attractive target for manipulating CD4 effector T cells and Tregs therapeutically (Takeda *et al.* 2004, Valzasina *et al.* 2004). The observation that $OX40^{-/-}$ mice show a reduction in the population of nTregs in the spleen while there is an outgrowth of nTregs in the spleens and thymi of transgenic mice that stably overexpress OX40L (OX40L-TgL) implies a requirement for OX40 for nTreg development and homeostasis (Takeda *et al.* 2004). A recent study confirmed that OX40 is permanently expressed by $CD4^{-}$ $CD25^{+}$ nTreg progenitors in the thymus of Foxp3-GFP mice, while its ligand OX40L is steadily upregulated on mTECs; ligation between the two molecules augments the TCR signal, governed by CD28 and TAK1, which leads to nTreg maturation to the

$CD4^+CD25^+Foxp3^+$ phenotype (Mahmud *et al.* 2014). Blocking OX40L impaired nTreg development, whereas injection of OX40 agonists stimulated nTreg differentiation, due to amplified sensitivity to IL-2Rα-STAT5 signalling. Similar effects on nTreg development were observed with GITR and TNFRII receptors, and in *vivo* combination blocking of GITR, OX40 and TNFRII extended the abrogation of nTreg development (Mahmud *et al.* 2014).

Definitive mechanisms for OX40's roles in nTreg homeostasis and function in naïve states and during immune responses are still unclear and controversial. *In vitro* studies showed that compared to WT Tregs, Tregs from OX40L-TgL mice could suppress WT T cells while Tregs from $OX40^{KO}$ mice could not, but sensitivity to regulation was abrogated in the presence of OX40L-expressing APCs (Takeda *et al.* 2004). Similarly, investigation of the effects of OX40 agonists on GFP reporter $Foxp3^+$ Tregs diminished their capacity to suppress responder T cells *in vitro* and T cell mediated skin graft rejection *in vivo*. Moreover, the expression of *Foxp3* and the induction of peripheral Tregs from Tc cells were inhibited, suggesting a negative impact of OX40 on Treg function (Vu *et al.* 2007). In contrast, work by Fiona Powrie's lab identified a decisive role for OX40 in the homing of naive $Foxp3^+$ Tregs into the large intestine and primed Tregs into the colon and peripheral lymphoid tissues in inflammation, which was crucial in the suppression of inflammatory T cell mediated colitis in $RAG^{-/-}$ mice (Griseri *et al.* 2010). Additionally, Tregs deficient in OX40 failed to prevent the murine induced colitis caused by pathogenic IFNγ and IL-17 producing $CD4^+$ T cells, inflammatory macrophages and neutrophils, confirming involvement of $OX40^+$ Tregs in both innate and adaptive arms of inflammatory responses (Griseri *et al.* 2010, Piconese *et al.* 2010). Griseri *et al.*, (2010) also showed that OX40

deficiency on Tregs has no effect on their proliferation and Foxp3 expression but renders them susceptible to apoptosis after activation, (Griseri *et al.* 2010) suggesting that survival signals provided by OX40 are necessary for the longevity of activated Tregs.

IL-2 is an essential cytokine for Treg homeostasis, development and function. Its intracellular signalling is regulated by the suppressor of cytokine signalling (SOCS1) protein which in turn is regulated by Foxp3 mediated microRNA155 (miR155) induction (Sakaguchi *et al.* 2008, Josefowicz *et al.* 2012). OX40 has been found to maximise Treg susceptibility to the IL-2-STAT5-Foxp3 signalling pathway which sustains Treg expansion and strengthening of their suppressive stability. Significant amounts of SOCS1, suppressor of IL-2, have been identified in $OX40^{-/-}$ Tregs showing unresponsiveness to IL-2, suggesting a mechanism for the tuning of Treg function by OX40 (Piconese *et al.* 2010).

Thus, while some research groups report that OX40 stimulation hampers Treg suppressive capability in *in vitro*, *in vivo* and tumour models (Valzasina *et al.* 2004, Vu *et al.* 2007, Piconese *et al.* 2008, Weinberg *et al.* 2011), there are many other groups convinced of the importance of OX40 in Tregs homing, proliferation and suppressive function *in vitro* and in *vivo* in GVHD, heart transplantation, colitis and chronic viral hepatitis and hepatocellular carcinoma (Takeda *et al.* 2004, Hippen *et al.* 2008, Griseri *et al.* 2010, Xiao *et al.* 2012, Piconese *et al.* 2014). Stimulation of host Tregs with OX40 agonist under naïve conditions led to Treg proliferation and potentiated suppression to prolong allo-grafted heart survival (Xiao *et al.* 2012) and reduce EAE severity (Ruby *et al.* 2009). Similarly, APC expressing OX40L expanded

Tregs 1000 fold more than anti CD3/CD28, and proliferation of the Treg population extended the survival rate associated with xenogeneic human PBMNCs GVHD in naïve irradiated mice (Hippen *et al.* 2008). In a milieu where effector T cell cytokines were absent, the Treg population was found to be augmented after OX40 stimulation, but when OX40 was introduced after disease manifestation in an EAE model the inflammatory condition was exacerbated (Ruby *et al.* 2009). Thus, involvement of OX40 after T cell polarization may compromise Treg expansion in favour of effector T cell proliferation or memory T cell generation (Xiao *et al.* 2008). A recent study revealed distinct subsets of Tregs in human chronic hepatitis virus C (CHC) at different stages of hepatitis, and even within the same tissue. CHC progressively develops into hepatic cirrhosis and/or hepatic cancer and elicits both suppressive and inflammatory behaviour from Tregs in an OX40 mediated manner (Piconese *et al.* 2014). Non-cirrhosis stage human liver tissue had a dominant population of Th1-like Tregs with an $OX40^{-}$T-$bet^{+}IFN\gamma^{+}$ phenotype and low expression of both thymus derived Treg imprinting Helios transcription factor and the Foxp3 locus stability indicator Treg specific de-methylated region (TSDR). This Treg phenotype was non-suppressive and its differentiation was IL-12 dependent. In contrast, the potent Th1-suppressing Tregs with the phenotype $OX40^{+}$T-$bet^{+}IFN\gamma^{-}$ have been identified in both hepatic cirrhosis and hepatic cancer stages. Those Tregs overexpressed $Helios^{+}$ and showed high demethylation of TSDR site and proliferated vigorously in the presence of monocytes/macrophages, which produced TNF-α and upregulated OX40L also found in the tumours (Piconese *et al.* 2014). This study suggests that OX40 mediated the adaptation of Tregs to modulate their suppressive machineries in response to the cellular microenvironment induced inside the same organ.

The adapter proteins TRAF2, 3 and 5 enable CD30 and OX40 to share the same signalling pathway; maybe CD30 compensates or augments the role of OX40 in Tregs. Our group showed that the fatal CD4 driven autoimmune disease that results from Foxp3 deficiency can be avoided when OX40 and CD30 are simultaneously nullified in mice which have no nTregs (Gaspal *et al.* 2011). Abrogation of those TNFRs abolished the capability of stimulated CD4 T cells to secrete IL-4 and IFNγ, which are crucial drivers of Th2 and Th1 responses respectively; however activated CD8 T cells retained their ability for IFNγ production (Gaspal *et al.* 2011). This triple $CD30^{KO}OX40^{KO}Foxp3^{KO}$ (tKO) depletion neither resulted in high titres of autoantibodies and infiltration of lymphocyte into nonlymphoid organs nor threatened the lives of mice or their fertility. Similar results could be obtained using OX40L and CD30L blocking antibodies after transfer of tKO thymocytes into $RAG^{-/-}$ mice. However, deficiency in either CD30 or OX40 alone in $Foxp3^{KO}$ mice was still lethal and the lethality was more related to CD30 deficiency than that of OX40 (Gaspal *et al.* 2011). The outcome of this study suggests that Tregs are dispensable when OX40 and CD30 are blocked, and this approach could be used on the one hand to disturb Treg mediated suppression of anti-tumour immunity, and on the other hand to target CD4 mediated autoimmune pathology.

Table 1:1: The tumour necrosis factor receptors superfamilies' (TNFRSF) and their ligands adapted from (Wu and Hymowitz 2009, Magis *et al.* 2012)

Standard nomenclature (Receptor)	Other terminology	Associated with apoptosis (Death Domain)	Standard nomenclature (Ligand)	Other terminology
TNFRSF1A	TNFRI, CD18, CD120a, P55-R, TNFR60, FPF, MS5, TBP1, TNF-R	DD	TNFSF1	LT-α, LT, TNF-β
TNFRSF1B	TNFRII, CD120b, P75-R, TNFR80, TBPII		TNFSF2	TNF-α, TNF, Cachectin
TNFRSF3	LTβR, CD18, D12S370, TNF-R-III		TNFSF3 TNFSF14	LT-αβ2 LIGHT
TNFRSF4	OX40, CD134, ACT35, IMD16, TXGP1L		TNFSF4	OX40L, CD252
TNFRSF5	CD40, Bp50, CDW40, TNFRSF5, p50		TNFSF5	CD40L, CD154
TNFRSF6	Fas, CD95, Apo-1, ALPS1A	DD	TNFSF2	FasL, CD95L
TNFRSF6B	DcR3, DJ583P15.1.1, M68, M68E, TR6		TNFSF2 TNFSF14 TNFSF15	FasL, CD95L LIGHT TNF-like molecule 1A/TL1A
TNFRSF7	CD27, T14, S152, Tp55, S152, L		TNFSF7	CD27L, CD70
TNFRSF8	CD30, Ki-1, D1S166E		TNFSF8	CD30L
TNFRSF9	4-1BB, CD137, ILA		TNFSF9	4-1BBL
TNFRSF10A	DR4,Apo-2, TRAIL-R1	DD	TNFSF10	TRAIL, Apo-2L, TL2
TNFRSF10B	DR5, TRAIL-R2	DD		
TNFRSF10C	DcR1, TRAIL-R3, TRID			
TNFRSF10D	DcR2, TRAIL-R4			
TNFRSF11A	RANK, TRANCE-R, CD26, OFE, OSTS		TNFSF11	RANKL, TRANCE, OPGL
TNFRSF11B	OPG, osteoprotegerin, TR1, OCIF			
TNFRSF12A	CD266, Fn14, TWEAK-R		TNFSF12	TWEAK, Apo-3L
TNFRSF13B	TACI, CAML interactor, CD267		TNFSF13	APRIL, B cells activator of the TNF Family/ BAFF
TNFRSF13C	BAFF-R, BR3		TNFSF13B	BAFF, TNSF13B
TNFRSF14	HVEM, HveA, ATAR, LIGHT-R		TNFSF14	LIGHT, HVEM-L, LT-α, BTLA
TNFRSF16	Nerve growth factor receptor/ NGFR, p75 neutrophin R, CD271	DD	NGF, BDNF	
TNFRSF17	BCMA, BCM, CD269		TNFSF13	APRIL, BAFF
TNFRSF18	GITR, AITR, CD357,		TNFSF18	GITRL, AITRL, TL6

	GITR-D			
TNFRSF19	TROY, TAJ, TRADE		NGR1/LINGO1	
TNFRSF19L	RELT		Not known	
TNFRSF21	CD358, DR6	DD	Not known	
TNFRSF25	DR3, Apo-3, TRAMP, TNFRSF12	DD	TNFSF15	TL1A, VEGI, DcR3
EDAR	DL, ED3, ED5, ED1R, EDA1R	DD	Ed, Ectodysplasin EDA1	
EDA2R	XEDAR, EDA-A2R, TNFRSF27		EDA2	

1.2.4 Treg infiltration of tumours

Superabundant accumulation of Tregs in various types of tumours, including melanoma, has been recognised and solidly correlated with tumour progression (Curiel *et al.* 2004, Viguier *et al.* 2004, Zou 2006, Nishikawa and Sakaguchi 2010); and can be used in combination with the presence of other immune cells as an indicator for the prediction of survival (Curiel *et al.* 2004, Galon *et al.* 2006, deLeeuw *et al.* 2012). Dysfunctional Treg-mediated tumour immunity was described in two pioneer studies. The first research identified Tregs in early and late stages of human NSLC and ovarian cancer, respectively (Woo *et al.* 2001); and the other study showed that using blocking antibodies for CD25 enhanced sarcoma and melanoma rejection in a murine model (Tanaka *et al.* 2002). Treg migration into tumour microenvironments has been attributed to many chemokines, but the receptor, ligand interaction between CCR4 (on Tregs) and CCL22 (in tumour cells) is the most widely accepted (Curiel *et al.* 2004, Gobert *et al.* 2009), and this axis has recently become the target for immunotherapy. Selective inhibition of CCR4 expressed on a population of Tregs named effector Tregs ($CD45A^{-}Foxp3^{high}CCR4^{+}$) resulted in the reduction of this population and the induction of $CD8^{+}$ immune responses specific for

NY-ESO-1 antigen on *in vitro* human melanoma and *in vivo* human leukaemia-lymphoma (Sugiyama *et al.* 2013).

The source of tumour infiltrating Tregs is still ambiguous. While some studies reported that they derive from the conversion of naïve peripheral conventional T cells (pTregs) persisting in tumours *de novo* (Valzasina *et al.* 2006, Bilate and Lafaille 2012), others stated that they either arise from the thymus (nTregs) (Malchow *et al.* 2013) or are a mixture of both (Zhou and Levitsky 2007). nTreg development in the thymus is a sophisticated process under the regulation of AIRE, generating nTregs with high affinity TCRs specific for self-tissues antigens including TAAs (Kyewski and Klein 2006, Cowan *et al.* 2013, Malchow *et al.* 2013). On the other hand, pTreg induction, from naïve Tc cells previously emerged from negative selection and having TCRs with low affinity to self-antigens, is dependent on chronic cognition to antigen, suggesting it is a stochastic process, producing Tregs that are unstable and less suppressive than nTregs (Sakaguchi *et al.* 2008). In the TRAMP mouse model, which develops spontaneous prostate adenocarcinoma, Malchow *et al*, (2013) identified a predominant prostate antigen, SV40T, for which there are specific Tregs (designated MJ23). MJ23 Treg presence was enriched relative to other tissues only in the prostate tissue of tumour free male but not in female mice, confirming their reactivity to self-prostate (Malchow *et al.* 2013). Moreover, transplantation into irradiated 12-16 week B6 tumour free or TRAMP mice of MJ23tg RAG1$^{-/-}$ bone marrow, expressing the TCRβ sequence recognizing prostate specific antigen, resulted in the development of MJ23 precursors into Foxp3^{+} Tregs in the thymus (Malchow *et al.* 2013). The specific thymic development of MJ23 Tregs has been confirmed to be *AIRE* dependent by its failure to occur in *AIRE* deficient recipients, and strikingly was

also observed in *AIRE* sufficient males and even females without prostate glands. This set of results confirms the concept that tumours are predominantly enriched with Tregs of thymus origin and that those nTregs are specific for self-tissue antigens that are promiscuously expressed by mTECs rather than recognizing tumour antigens (Kyewski and Klein 2006, Cowan *et al.* 2013, Malchow *et al.* 2013, Savage *et al.* 2014).

During pregnancy, fetal antigen specific Foxp3^{+} Tregs accumulate in the maternal murine body to sustain tolerance to the foetus, and such selective accumulation does not occur in non-pregnant mice. The frequency of fetal antigen specific Tregs was found to decrease somewhat post-partum, but to undergo rapid re-expansion in subsequent pregnancies, showing that tolerance can be tuned by the maintenance of a minor population of memory Tregs (Rowe *et al.* 2012). The parallel development of self-specific nTregs and tumour specific cytotoxic T cells which are self-reactive is one of the hurdles to be overcome for successful cancer therapy.

1.3 Cancer immunotherapy

Paul Ehrlich was one of the pioneers who suggested a hundred years ago that the immune system might have a role in repressing tumours. William Coley made an early and fruitful attempt at immunotherapy at the end of 19th century when he observed a beneficial response in cancer patients injected with a dead bacterial mixture at tumour sites (Lesokhin *et al.* 2015). After decades of stumbling in the battle with cancer using various strategies such as surgery, irradiation and vaccination, it is envisaged that the targeting of immune costimulatory checkpoints

with the particular aim of overcoming tolerance heralds new successes in the treatment of cancer (Pardoll 2012).

1.3.1 Tumour immunotherapy: targeting CTLA-4

1.3.1.1 The biological function of CTLA-4

Upon activation, T cells begin to express the IgSF member type1 transmembrane glycoprotein CTLA-4, a CD28 homolog and a homodimer with a distal interface structure enabling it to bind to two molecules of its ligands, CD80 and CD86, which are expressed on APCs. CTLA-4 expression, the majority of which is intracellular, peaks 24-48 hours after activation, and then acts as an autonomous and nonautonomous negative regulator for T cell immune responses (Schwartz *et al.* 2001, Greenwald *et al.* 2005, Wing *et al.* 2011). Tregs express CTLA-4 constitutively and, as already mentioned, it is crucial for $Foxp3^+$ Treg suppressive function and prevention of multi-organ CD4 driven fatal autoimmunity syndrome (Tivol *et al.* 1995, Chambers *et al.* 1997, Wing *et al.* 2008). CTLA-4 functions in a number of ways to inhibit effector T cell responses and influence APC function and maturation:

(1) competition with CD28 for CD80 and CD86 ligation due to its higher affinity for the ligands (Rudd *et al.* 2009, Qureshi *et al.* 2011, Wing *et al.* 2011);

(2) activation of SHP1 and SHP2 phosphatases and in particular protein phosphatase 2A PP2A via its cytoplasmic tail motif YVKM, which not only dephosphorylates TCR-CD3 activated Lck protein kinase leading to downregulation of PI3K but also inhibits PKB activation for further T cells suppression;

(3) removal of CD80 and CD86 from APC surfaces in a trans-endocytotic process and inhibition of IL-6 transcription, which regulates DC differentiation;

(4) induction of the tryptophan degradation enzyme IDO in DCs to produce kynurenine, a cell death enhancer and an immunosupressor.

1.3.1.2 Therapeutic applications of CTLA-4

The preclinical work of the team of James Allison proved for the first time that intraperitoneal injection of αCTLA-4 mAbs boosts eradication of partly immunogenic colon carcinoma (expressing B7), $B7^+$ 51Blim10 melanoma and $MHCII^+$ fibrosarcoma Sal N before and after the establishment of the tumours in BALB/c mice (Leach *et al.* 1996). This work was followed by testing of anti-CTLA-4 therapeutic effect on aggressive and poorly immunogenic tumours. Subcutaneous B16-BL6 melanoma and lung metastatic B16-F10 melanoma do not respond to anti-CTLA-4 single treatment; however when the mice were injected with irradiated tumour cells that stimulate DCs to express GM-CSF in combination with CTLA-4 blocking, the mice showed resistance to the tumours (van Elsas *et al.* 1999). Tumour rejection was CD8 and NK1.1 but not CD4-dependent and in long term therapy of lung metastasis the skin of treated mice exhibited depigmentation at the site of αCTLA-4 injection (van Elsas *et al.* 1999). An interpretation of these results is that when there is a partial endogenous immune response, blocking of CTLA-4 induces anti-tumour immunity. In cases where tumour immunogenicity is poor, or the immune system is in some way compromised, however, this approach may require combination with other treatments such as vaccination to trigger an anti-tumour response.

The promise of these experimental observations inspired the production of human anti-CTLA-4 and translation of the methods to clinical situations. Initial human clinical trials conducted, using human αCTLA-4 alone, reported regression of tumours in pre-treated metastatic melanoma and ovarian carcinoma and in combination with gp100 TAA vaccine was able to eradicate melanoma in approximately 20% cases, but with adverse autoimmunity, including particularly severe colitis (Beck *et al.* 2006), in approximately 45% cases (Hodi *et al.* 2003, Phan *et al.* 2003, Beck *et al.* 2006). The progression of fatal autoimmune disease in mice with conditional CTLA-4 deficiency in Tregs (Wing *et al.* 2008), along with tumour evasion of immune rejection via supernumerary infiltration of Tregs (Facciabene *et al.* 2012) would suggest that the αCTLA-4 therapeutic effect works mainly by limiting Treg activity. The upregulation of CTLA-4 on activated T cells, however, would also make them targets for the cellular activity of αCTLA-4. To dissect this, lymphopenic mice were reconstituted for 10 weeks with a mixture of Tregs and T effector cells from both mice expressing human in place of mouse CTLA-4 and WT mice, enabling blockade of different subsets with species specific αCTLA-4, in mice transplanted subcutaneously with B16 melanoma and treated with αCTLA-4 and GM-CSF stimulating tumour vaccine (Gvax) (Peggs *et al.* 2009). Tumour growth showed no significant effect of the treatment when either Tregs or T effector cells alone were specifically targeted. Synchronous targeting of both populations, however, significantly reduced tumour growth compared to controls, interpreted by the authors to show that the anti-tumour effect of αCTLA-4 depends on synergy of its action on the two target populations (Peggs *et al.* 2009, Riley 2013). Others found that the efficacy of the αCTLA-4 was dependent on antibody isotype; an IgG2a αCTLA-4 dramatically reduced numbers of Tregs

associated with murine intra-colon adenocarcinoma, and this was accompanied by tumour rejection and increased proliferation of cytotoxic CD8 T cells, whereas an IgG1 αCTLA-4, or form of it mutated to prevent binding to Fc receptors, failed to exert such effects (Selby *et al.* 2013). In a treatment using αCTLA-4 and Gvax, Simpson *et al.*, (2013) demonstrated that intra-B16 melanoma CTLA-4^{high} Tregs diminished after αCTLA-4 treatment, and this reduction was mediated by the activation of antibody dependent cell mediated phagocytosis in intra-melanoma CD11b^{+}FcγIVR^{high} macrophages (Selby *et al.* 2013, Simpson *et al.* 2013).

It was not until 2011 that the αCTLA-4 drug ipilimumab was approved by the USA FDA for clinical use. It has been used for targeting prostate cancer (Kwon *et al.* 2014), NSC lung cancer (Tomasini *et al.* 2012), pancreatic cancer (Royal *et al.* 2010), kidney cancer (Yang *et al.* 2007), blood malignancies (Bashey *et al.* 2008, Ansell *et al.* 2009) and melanoma (Hodi *et al.* 2010); here I will focus on melanoma only. 440 patients with stages III/ IV melanoma were enrolled into a phase III clinical study and were treated with four doses of 3mg/kg body weight of ipilimumab with and without gp100 vaccine. The median overall survival (MOS) of patients given the full treatment was found to be ten months compared with approximately six months in 136 patients treated with the vaccine only. The highest objective response was recorded by the group receiving ipilimumab alone, in which 60% survived for more than 2 years; this was followed by ipilimumab/gp100 group with a 2-year survival of 17.4%. Set against the improved MOS, 10-15% of the ipilimumab groups demonstrated immune related adverse events (IRAEs) of grades three/four, (needs hospitalisation/life threatening), which was a fourfold increase over the vaccine alone group, 3%. The IRAEs include a collection of toxic side effects related to the

administration of the therapy which will be discussed next. In spite of the survival advantages of ipilimumab, fourteen patients died due to the antibody treatment related toxicity (Hodi *et al.* 2010).

Another human IgG2-αCTLA-4 named tremelimumab was used in phase I/II trails for targeting melanoma (Camacho *et al.* 2009), but in a cohort phase III study, treatment of patients with advanced metastatic melanoma with a dose of 15mg/kg tremelimumab for 3 months showed no significant objective response (approximately 10% increase in survival) compared with chemotherapies (dacarbazine or temozolomide), regardless of its extension of the response duration: about 36 months versus approximately 14 months for the chemotherapies (Ribas *et al.* 2013). Similar to ipilimumab IRAEs attributable to tremelimumab were enterocolitis, dermatitis and hypophysitis (Hodi *et al.* 2010, Ribas *et al.* 2013). In phase II trials, clinical responses and IRAEs for both ipilimumab and tremelimumab are comparable but the profile of ipilimumab regarding dosages, scheduling and toxicity management is considered to be more favourable. An escalation of ipilimumab dose to 10mg/kg body weight combined with dacarbazine for four doses followed by dacarbazine alone every 21 days until about 6 months in phase III trial was accompanied with an improvement in overall survival of approximately 21% for three years in naïve metastatic melanoma patients compared with dacarbazine alone approximately 12%. The increase in dose was accompanied by an increase in treatment related toxicity, in particular hepatitis (Robert *et al.* 2011) and dermatitis, in the maintenance phase of treatment when ipilimumab was injected every twelve weeks (Maio *et al.* 2015).

Ipilimumab therapeutic efficiency in the long term has been assessed in a survey of the available data from twelve phase II/III ipilimumab trials. Data analysis describes a steady state beyond 3 years in the overall survival curve of about 21% of advanced melanoma patients who had an objective response, that may persist for more than 10 years, motivating clinicians to consider ipilimumab as a long term therapeutic option (Schadendorf *et al.* 2015). However, the survey did not consider the balance between ipilimumab therapy and its IRAEs, or price.

The IRAEs accompanying ipilimumab therapy are attributable in large part to the mechanisms that cause the fatal autoimmunity observed in CTLA-$4^{-/-}$ mice. Although there are different ways of rating the severity of treatment side-effects, a generally accepted set of criteria grades adversity from 1-5, where grade 1 and 2 refer to mild-moderate toxicity, and grades 3, 4 and 5 denote severe, grievous and fatal respectively (Camacho 2015). Ipilimumab efficacy is dose-dependent but paralleled by the frequency of IRAEs. In a double blind phase II trial for pre-treated melanoma patients, Wolchok *et al.*, (2010) found that the rate of occurrence of IRAEs of any grade was 70%, 64% and 26% in treatment groups receiving 10mg/kg, 3mg/kg and 0.3mg/kg doses of ipilimumab respectively, and the highest dose was associated with the greatest frequency of adverse outcomes grades 3 and 4 (Wolchok *et al.* 2010). The most frequently occurring IRAE associated with ipilimumab is skin toxicity, characterised by rashes, prurity and vitiligo, which appear after about three weeks of treatment in approximately 70% of patients. After 1.5-2 months of treatment approximately 40% of melanoma patients suffered from gastrointestinal (GI) IRAEs, most frequently diarrhoea and colitis (Weber *et al.* 2012). GI symptoms are also accompanied by elevation of liver function enzymes ALT and AST as a consequence

of liver toxicity in approximately 7% of the patients. Within 3-4 months of starting ipilimumab treatment approximately 6% of melanoma patients experience hypophysitis and its related symptoms such as headache, diplopia and nausea. Ocular, neurological, lymphoid gland, muscular and hormone disturbances, kidney dysfunction, and infectious diseases may also correlate with ipilimumab treatment. Due to this toxicity, ipilimumab treated patients need to be monitored by a team of specialists and may require the administration of corticosteroids or TNF inhibitors to counteract the IRAEs (Weber *et al.* 2012, Camacho 2015). In a phase III melanoma trial, grade 3-4 IRAEs associated with ipilimumab treatment alone or in combination with gp100 vaccine were reversed by injection of antidiarrheal and analgesic agents and steroids (Weber *et al.* 2013).

1.3.2 Tumour immunotherapy: targeting the PD-1/PD-L1 pathway

1.3.2.1 The biological function of PD-1

Several studies have identified PD-1 as contributing to tolerance and failure to reject cancer (Dong *et al.* 2002, Keir *et al.* 2008, Francisco *et al.* 2010). Unlike CTLA-4 which is expressed early on activated T cells, the Ig monomer PD-1 upregulates on CD4 and CD8 T cells in their effector phase, and may also be induced on other leukocytes including Tregs (Greenwald *et al.* 2005, Francisco *et al.* 2009). PD-1 ligands PD-L1 and PD-L2 are ubiquitously expressed on tumour cells and cells such as TAM, MDSCs and fibroblasts which associate with tumours and contribute to the dampening of the tumour reactive T cell response (Dong *et al.* 2002, Jin *et al.* 2011). Interaction of PD-1 with its ligands PD-L1/2 triggers signalling that leads to the phosphorylation of the PD-1 intracellular tail associated immunoreceptor tyrosine

based switch motif (ITSM). Phosphatase SHP-2 binds to ITSM, leading to the deactivation of the Zap70 and PI3K enzymes downstream of TCR-CD28 signalling, and resulting in the induction of T cell apoptosis or exhaustion (Greenwald *et al.* 2005, Jin *et al.* 2011, Pauken and Wherry 2015). It has been found that some Treg subsets, also expressing PD-1, can inhibit both anti-tumour T cells and DC maturation, since these two populations can express PD-1 ligands (Francisco *et al.* 2009, Chen *et al.* 2014). A viral model study has reported that persistent exposure to chronic lymphocytic choriomeningitis (LCMV) viral infection leads to a state of anergy or exhaustion in virus specific $CD8^+$ T cells. The genetic profile of the impaired $CD8^+$ T cells showed overexpression of PD-1, and injection of αPD-1 mAbs restored the cells' functionality and reduced LCMV infection, whereas treating with αCTLA-4 mAbs made no difference (Barber *et al.* 2006). Such results encouraged the targeting of PD-1 in tumour therapy.

1.3.2.2 Therapeutic applications of PD-1

Preclinical studies confirmed the importance of PD-1 and its ligands expression on tumours and the stromal cells around them in tumour resistance to immune rejection and the efficacy of adaptive $CD8^+$ T cell immunity in promoting tumour regression in mice in which PD-1 was either deficient or blocked (Iwai *et al.* 2002, Strome *et al.* 2003, Flies *et al.* 2011). Successful targeting of CTLA-4 as therapy for human tumours encouraged the targeting of other molecules, including PD-1, to enhance the action of tumour specific effector T cells (Pentcheva-Hoang *et al.* 2009, Pardoll 2012). Two phase I clinical trials included large numbers of pre-treated patients with various tumour types: NSCLC, melanoma, renal cell carcinoma (RCC), colorectal carcinoma (CRC), breast cancer (BC), ovarian cancer (OC) and gastric cancer (GC).

The first used αPD-1 mAb (BMS-936558) in a range of doses (1-10) mg/14 days for 12 cycles (Topalian *et al.* 2012) while the second administered αPD-L1 mAb, using a similar treatment regime, but for 16 cycles (Brahmer *et al.* 2012). The objective response (OR) related to αPD-1 was 18% NSCLC, 28% melanoma and 27% RCC but the OR correlated to αPD-L1 was 10.2% NSCLC, 17.3% melanoma, 11.7% RCC and 5.8% OC. The respective overall objective response and durable response for more than 1 year were 36% and 64% respectively for αPD-1, compared to αPD-L1 where it was (6-17) % and 50% respectively (Brahmer *et al.* 2012, Topalian *et al.* 2012).

Generally the therapeutic effect related to αPD-1 seems better than that of αPD-L1, possibly because PD-L2 compensates for the blockade of PD-L1. Grade 3 and 4 αPD-1 related adverse events were evident in 14% of the treated patients and three deaths resulted from pulmonary toxicity, whilst the same grades of adverse outcome were found in only 9% of αPD-L1 treated patients indicating a safer profile than αPD-1 (Brahmer *et al.* 2012, Topalian *et al.* 2012). Rash and arthralgia are the most prevalent sequelae of αPD-1 administration. IRAE toxic effects associated with αPD-1 are generally similar to those appearing with αCTLA-4 treatment, but the αPD-1 safety profile is better (Robert *et al.* 2015b). In this regard, CTLA-$4^{-/-}$ mice manifest fatal autoimmune phenotype within (21-28) days (Tivol *et al.* 1995, Chambers *et al.* 1997) whereas PD-$1^{-/-}$ mice develop lupus like autoimmunity 9 months after birth, and otherwise have no apparent autoimmunity unless challenged with an infectious agent; there is no autoimmunity attached to the phenotype of PD-$L1^{-/-}$ mice (Nishimura *et al.* 1999, Dong *et al.* 2004, Quezada and Peggs 2013).

Several studies considered a number of biomarkers for predicting an objective tumour response when targeted with αPD-1 or αPD-L1 therapies. Histological tumour biopsies were used to evaluate tissues from patients pre- and post-αPD-1 (pembrolizumab) and αPD-L1 (MPDL3280A) administration. A superior response and better tumour shrinkage was found in many cancer types - melanoma, bladder cancer, NSCLC, RCC, ocular, and squamous and non-squamous cancers - which demonstrated high levels of expression of PD-L1 on tumour cells and TILs, and of PD-1 expression on pre-existing adaptive $CD8^+$ T effector cells, both at the margin of and infiltrated into tumour tissues (Herbst *et al.* 2014, Powles *et al.* 2014, Tumeh *et al.* 2014). Some tumours unresponsive to PD-1 blockade were found to be negative for PD-L1, so screening patients and selecting them for treatment on the basis of PD-L1 expression of their tumours would be beneficial (Ribas 2012, Topalian *et al.* 2012).

In 2014, the αPD-1 agent nivolumab was approved by the FDA for melanoma treatment on the basis of clinical data documenting and its therapeutic benefits. A long term phase I study enrolled 107 pre-treated advanced melanoma patients resistant to traditional therapies for 12 cycles of treatment with 1.3 or 10m/kg nivolumab at 14 day intervals. The objective response was reported as 31% with a median duration 16.8 months and an overall survival rate of 62% at one year and 43% at two. 22% of the patients displayed grade 3 and 4 adverse events, mostly dermatitis (36%), colitis (18%) and endocrinopathy (13%) (Topalian *et al.* 2014). In spite of its increased toxicity relative to conventional treatments (22% vs 14%), the persistence of clinical improvement after discontinuation of treatment makes nivolumab a therapeutically viable option (Topalian *et al.* 2012). Moreover, it has

been found recently that in naïve metastatic melanoma patients who are negative for *BRAF* mutation, nivolumab therapy confers a significantly better survival rate (approximately 73% at one year and objective response 40%) compared to the respective statistics of dacarbazine chemotherapy (approximately 42% and 14%) (Robert *et al.* 2015a). The potential therapeutic effect of nivolumab (Bristol-Mayers Squibb) and its FDA approved homologue pembrolizumab (Merck) has been extended to include incurable solid tumours and refractory haematopoietic malignancies such as metastatic NSCsLC and Hodgkin's lymphoma (Ansell *et al.* 2015, Garon *et al.* 2015).

1.3.3 CTLA-4 and PD-1 combined immunotherapy

Cancer immunotherapy has been revolutionized by the use of CTLA-4 and PD-1 inhibitors, since the two agents have discrete mechanisms which can act synergistically on the inhibitors of T effector responses (Parry *et al.* 2005). In a murine model of B16 melanoma it has been shown that adding CTLA-4 and PD-1 blockades to a vaccine, Gvax or Fvax, not only increases the ratio of B16 infiltrated specific T cells to Tregs and MDSCs but also doubles melanoma rejection activity to 50% compared to either antibodies or vaccine alone. The triple combination, antibodies to CTLA-4, PD-1 and PD-L1, increased tumour rejection activity and tumour-free survival by a further 15%, but toxicities related to the combined therapies have not been reported (Curran *et al.* 2010).

Resistance to one of the PD-1 or CTLA-4 blockers did not preclude tumour response to another blocker. In a phase I clinical trial, ipilimumab treated patients with relapsed metastatic melanoma were treated with lambrolizumab (αPD-1), 10mg/kg every 2-3

weeks or 2mg/kg every 3 weeks, and tumour responses were assessed every 12 weeks. There was a 50% objective response in the 2 weeks regimen and 21% OR in the 3 week regimen, with a response duration of more than 8 months (Hamid *et al.* 2013). Wolchok *et al*, (2013) used sequential (n=33) and concurrent (n=53) regimens of nivolumab and ipilimumab for the treatment of metastatic melanoma cases. In the concurrent arm the OR was 53% with more than 80% tumour size shrinkage, but was associated with 53% grade 3 and 4 adverse events. The sequential arm gave much lower OR (20%) and toxicity (18%) (Wolchok *et al.* 2013). The outcomes of this study demonstrate a very significant anti-tumour effect from combined CTLA-4 and PD-1 targeting, but the consequences of their toxicity constrain their therapeutic use.Two recent phase I and phase III studies compared the immunotherapeutic efficacy and safety of nivolumab and ipilimumab alone and in combination in the treatment of unmedicated metastatic melanoma. Nivolumab plus ipilimumab showed the highest treatment OR (57-61)%, and median progression free survival (MPFS) (11.5 months) this was followed by nivolumab - OR 43%, MPFS 6.9 months - while ipilimumab was the least effective therapy - OR 11-19% and MPFS 2.9 months. The therapy-related adverse events of grades 3 and 4 were 55%, 16.3 and 26% respectively (Larkin *et al.* 2015, Postow *et al.* 2015). Most of the IRAEs were colitis, diarrhoea, escalated ALT, dermatologic syndrome and irreversible endocrinopathy, which required hormones replacement. Moreover, discontinuation of treatment due to adverse effects was the highest in the combined nivolumab and ipilimumab regimen (approximately 40%) and there were 3 IRAE deaths; side-effect related discontinuations were 14.8% for ipilimumab and 7.7% for nivolumab (Larkin *et al.* 2015, Postow *et al.* 2015).

1.3.4 Other TNFRSF members as costimulatory molecules and targets for cancer immunotherapy

The unique features of TNFR members in T cells biology and their functions in immune responses have made them prominent targets for cancer immunotherapy (Table 1:1). In sections 1.2.3 and 1.2.2.2 we focused on OX40, CD30 and Fas, here we will focus on other most important TNFRSF members.

1.3.4.1 GITR (TNFRSF18)

Glucocorticoid-induced TNF receptor family-related protein (GITR) (TNFRSF18) is constitutively expressed on $Foxp3^+$ Tregs; its expression on non-Tregs peaked within 24-72 hrs of priming, while its ligand, GITRL, was upregulated on APCs (DCs, B-cells and macrophages) and vascular endothelial cells (Tone et al. 2003). Interaction between GITRT and GITRL stimulates intracellular signals that combine with TCR signals to augment T cell expansion and function (Shevach and Stephens 2006). Simulating GITR signals using anti-GITR agonists can on one hand lead to autoimmunity by breaking tolerance through the inhibition of the suppressive function of Tregs, and on the other hand enhance anti-tumour immunity by boosting effector T cells (McHugh et al. 2002, Valzasina et al. 2004, Ko et al. 2005, Shevach and Stephens 2006). In addition to suppressing Treg function, anti-GITR agonists have been shown to deplete intra-colorectal tumour Tregs through activation of FcγRs expressed by colorectal associated leukocytes, resulting in tumour rejection (Bulliard et al. 2013).

1.3.4.2 CD40 (TNFRSF5)

Another essential TNFR in immunity is CD40, which is a transmembrane costimulatory molecule expressed on haematopoietic immune cells such as B cells, DCs, and macrophages and non-hematopoietic cells such as fibroblasts (Banchereau *et al.* 1995). The CD40 receptor interacts with the three protein molecules that make up its ligand CD40L, transmembrane or soluble, which is upregulated on primed T cells following presentation by CD40 expressing cells of many types of antigen (van Kooten and Banchereau 2000). The outcomes of DC:T cells and B cell:T cells interactions are vital for both adaptive and humoral immunity. In DCs, CD40-CD40L ligation leads to their maturation: inducing the expression of the costimulatory molecules, CD80 and CD86; promoting antigen presentation on MHC; inducing the secretion of the cytokines TNF-α, IL-8 and MIP-1. Collectively, this licences DCs for triggering the activation and differentiation of T cells (Caux *et al.* 1994, Ma and Clark 2009). The importance of CD40 for B cells is obvious in CD40 knock out mice. Kawabe *et al.* (1994) showed that mice deficient in the CD40 gene had reduced numbers of B cells of the $CD23^+$, IgM^+ and IgD^+ phenotype. There was also failure of germinal centre formation, absence of T cell-dependent immunoglobulin isotype class switching, and hyper IgM concentration in the serum (Kawabe *et al.* 1994), suggesting a significant role of CD40 in humoral immunity. It has further been reported that deregulation of CD40/CD40L pathway under pathogenic conditions may contribute to the development of multiple autoimmune diseases such as inflammatory bowel disease, rheumatoid arthritis, Type 1 diabetes and systemic lupus erythematosus (Peters *et al.* 2009, Borcherding *et al.* 2010). This CD40 dependent T-cell driven autoimmunity may be due to the potential role of CD40

in augmenting TCR threshold during T cell selection, or in coordinating with other TNFRs such as RANK in the establishment of the environment required for negative selection and generation of tolerance in the thymus (Akiyama *et al.* 2008).

Tumours and their microenvironment supress cancer immunity by inhibiting the maturation of DCs and permitting the generation of tolerogenic T cells, processes which can be overcome using CD40 agonistic antibodies. A preclinical study showed complete rejection of three B-cell lymphoma models (A20, A31, BCL_1) of $CD40^+$ phenotype in Balb/c mice and SCID mice, reconstituted with lymphocytes, treated with anti-CD40 agonistic antibodies compared to their the same lymphomas treated with isotype-matched control IgG (French *et al.* 1999). The rejections were dependent on CD8 T cells, which expanded tenfold after the administration of the CD40 agonist. Moreover, the mice were subsequently resistant to re-challenge with the lymphoma cell lines (French *et al.* 1999). Unlike anti-CTLA-4 and anti-PD-1 which block negative checkpoints, anti-CD40 agonistic antibodies activate APCs and stimulate antibody-dependent cytotoxicity/phagocytosis via FcγRs (Li and Ravetch 2011, Vonderheide and Glennie 2013). Vonderheide *et al*., (2001) conducted the first phase I clinical trial for CD40 using recombinant human anti-CD40L agonistic antibodies to treat 32 non-Hodgkin's lymphoma patients in an escalating dose approach, 0.05, 0.10, and 0.15 mg/kg/day. The treatment led to long-term complete remission, but grade 3 and 4 toxicity increased from 14%-57% with the increase in dose (Vonderheide *et al.* 2001).

To test the feasibility of expanding anti-CD40 therapeutic efficacy by combination with other cancer therapy approaches, incurable surgical pancreatic ductal

adenocarcinoma patients were recruited into a small clinical trial (NCT00711191)(Beatty *et al.* 2011). The patients were treated with anti-CD40 agonistic Abs, CP-870893, combined with the chemotherapy Gemcitabine. The regimen showed adenocarcinoma regression in a number of patients and this anti-tumour effect was not T cell- or DC-dependent, but was dependent on the infiltration of macrophages into tumours, where they demonstrated tumour stroma catalytic activity, suggesting the necessity of both innate and adaptive immunity for an objective cancer response (Beatty *et al.* 2011). Another recent phase I clinical trial was performed on patients with advanced melanoma to improve anti-CD40 therapeutic effect by combining it with immune checkpoint blocker anti-CTLA-4 (Bajor *et al.* 2015). Twenty-four patients received four different doses of human IgG2 anti-CD40 agonistic Abs, CP-870,893, combined with human IgG2 anti-CTLA-4 Abs, Tremelimumab. The overall O.R was approximately 27% and median overall survival was approximately two years; however this treatment approach was associated with a high frequency of cytokine release syndrome among patients (79%), occurring one day after antibody administration and necessitating intensive care (Bajor et al. 2015).

1.3.4.3 4-1BB or CD137 (TNFRSF9)

4-1BB or CD137 was the first known TNFR targeted for the treatment of established tumours in mice (Melero *et al.* 1997). Ligation of 4-1BB overexpressed on primed T cells with its ligand 4-1BBL, expressed on APCs, delivers stimulatory signals necessary for T cell activation, proliferation and survival. It was shown that treating mice with agonistic anti-4-1BB mAbs induced $CD4^+$ and $CD8^+$ T cell activation and augmented- Ag104A sarcoma and P815 mastocytoma- specific cytotoxicity, which subsequently eradicated the tumours (Melero *et al.* 1997, Tan *et al.* 1997). The

therapeutic effect of anti-4-1BB agonists can be magnified when combined with other inhibitory blockades. Concurrent injection of anti-4-1BB plus anti-PD-1 significantly reduced murine B16-F10 melanoma compared with a combination of anti-PD-1 and anti-LAG3,which was less effective in B16 inhibition (Chen *et al.* 2015). However, toxicity associated with anti-4-1BB limits its therapeutic applications; several phase I and phase 2 clinical trials were terminated due to fatal hepatic toxicity associated with administration of humanised anti-CD137 antibodies (Sznol *et al.* 2008, Li and Liu 2013).

1.3.4.4 RANK (TNFRSF11A)

The TNF receptor activator of nuclear factor κ-B (RANK) is expressed on mTECs and interaction with its ligand RANKL, produced by positively selected thymocytes and other thymic cells, plays an important role in the development of $AIRE^+$ mTECs (Hikosaka *et al.* 2008, Roberts *et al.* 2012). It has been shown that RANK signals and CD40 signals are essential for the development of mTECs and together they foster the establishment of the thymic microenvironment required for self-tolerance (Akiyama *et al.* 2008). Because RANK plays a valuable role in central tolerance, which represents a stumbling block for anti-tumour immunity, it becomes an attractive target for immunotherapists. A recent study demonstrated that blockade of RANKL in mice resulted in a transient and selective defect in $AIRE^+$ mTECs and TSA processing that subsequently caused imperfect central tolerance and thymic clonal deletion of B16 specific lymphocytes; this extended the survival time of mice inoculated with melanoma compared to its isotype controls (Khan *et al.* 2014). RANK is also expressed on osteoclasts, cells that cause bone resorption; RANK-RANKL interaction activates osteoclasts while the TNFR osteoprotegerin OPG, secreted by

osteoblasts, protects bones from resorption by binding to RANKL, thus regulating osteoclast maturation and balancing bone homeostasis; imbalance in these pathways can affect bone restoration and may cause disease (Kwan Tat *et al.* 2009, Pérez-Sayáns *et al.* 2010).

1.4 Roquin regulates posttranscriptional mRNA expression

Posttranscriptional control of gene expression maintains immune homeostasis at several transitional points and this is stabilised by RNA-binding proteins. The mRNA binding protein Roquin has been identified as a down regulator for the posttranscriptional mRNA expression of many genes, including ICOS, a CD28 paralogue that regulates T cell activation, as well as IFNγ, OX40 and TNF (Di *et al.* 2007, Leppek *et al.* 2013, Vogel *et al.* 2013). Roquin degrades mRNA by binding to the 3' untranslated region (3'UTR) of the mRNA and interacting with helicase and decapping enhancer proteins, conferring mRNA regression, although the precise mechanism has not yet been elucidated (Glasmacher *et al.* 2010). The gene *Rc3h1* encodes for Roquin1 and a single point mutation has been found to result in impaired ICOS regulation and progressive development of severe lupus like autoimmune disease in the homozygous mutant mice strain, sanroque (Vinuesa *et al.* 2005). The pathogenic phenotype of the Roquin$^{san/san}$ strain is characterised by its dominant frequency of activated and memory CD4 T cells (CD44^{high}ICOS^{high}) and accelerated differentiation of follicular T helper cells (Tfh). Moreover, in this strain, the overproduction of IFNγ by T cells drives accumulation of Tfh and spontaneous generation of germinal centres, which in combination lead to lethal autoimmune disease characterized by elevated titres of autoantibodies and infiltration by lymphocytes of non-lymphoid organs (Vinuesa *et al.* 2005, Lee *et al.* 2012). Roquin2

is a paralog of Roquin1, which is encoded by the *Rc3h2* gene, and has been found to share Roquin1 action, resulting in an mRNA decoy action and prevention of autoimmunity (Pratama *et al.* 2013). Unlike sanroque mice, which succumb to lethal autoimmunity, deficiency of Roquin2 on T cells, using the *Rc3h2*$^{fl/fl}$; Cd4-cre mouse model, yields mice with normal immune systems, in comparison to the Roquin1 deficient mice which have mild immune dysregulation (Vinuesa *et al.* 2005, Vogel *et al.* 2013). Combined depletion of Roquin1-2 resulted in the development of sanroque like autoimmunity in the *Rc3h1-2*$^{fl/fl}$; Cd4-cre mice, characterised by high frequency of the CD62L^{low}CD44^{high} phenotype for both CD4 and CD8 T cells, leading to lymphadenopathy and splenomegaly (Vogel *et al.* 2013). This study has also defined OX40 mRNA as a decoy target for both Roquin proteins, which regulate its posttranscriptional expression by binding to the 3'UTR locus of OX40 mRNA. Additionally, the ablation of both Roquin1 and Roquin2 in T cells resulted in overexpression of OX40 and activation of the NF-κB pathway and consequently prolific generation of CD4 and CD8 effector and memory T cells along with massive Tfh (Vogel *et al.* 2013). The pathogenic phenotype of Roquin$^{san/san}$ resembles that of the OX40L-Tg strain which constitutively expresses OX40L on T lymphocytes and results in CD4 driven autoimmune lethality (Murata *et al.* 2002, Gaspal *et al.* 2011). This suggests that Roquin works as an intrinsic cellular regulator for maintaining OX40 mRNA and prevention of autoimmunity.

1.5 Aims of the study

Immunotherapy for cancer that targets immune costimulatory checkpoints by blockade has revealed excellent potential, but is accompanied by strong autoimmune side-effects. Novel tumour treatments use blockade by αCTLA-4 to target the suppression of tumour rejection by Tregs whereas αPD-1 restores the responsiveness of $CD8^+$ T cells to tumours. Our group has generated a mouse model that survives and reproduces normally without $Foxp3^+$ Tregs and unaccompanied by autoimmunity due to the absence of the TNFRs CD30 and OX40 in the genome. Hence, we proposed that CD30 and OX40 have a role in the functionality of $Foxp3^+$ Tregs and in the support of CD4 driven autoimmunity. The major hurdle for successful cancer therapy is the suppression by thymic Tregs (nTregs) of tumour reactive cytotoxic T cells; elevated numbers of those nTregs have been identified in cancer patients' blood and tumour tissues. Therefore, the mouse model we have can be used to dissect antitumor immunity and autoimmunity.

In the first stage of the study we will investigate:

(1) The dynamics of tumour growth, using the B16-F10 melanoma cell line as a tumour model in $CD30^{KO}OX40^{KO}Foxp^{KO}$ and $CD30^{KO}OX40^{KO}$ mice compared to WT mice, addressing the role of OX40 and CD30 in the tumour immune response.

(2) The immunotherapeutic effects of αCTLA-4, αPD-1, αOX40L and αCD30L blockades in the same mouse models.

(3) The effects of the various blocking antibody combinations on tumour therapy, and the autoimmunity associated with CTLA-4 and PD-1 blockade, in C57BL/6 mice with pre-established B16-F10 melanoma.

Studies showed that a mutant mouse strain (Roquin) bearing a point mutation in Roquin protein leads to overexpression of IFNγ which confers resistance to T regulation (Vinuesa *et al.* 2005, Di *et al.* 2007, Vogel *et al.* 2013). Work in our lab has shown that IFNγ activates macrophages that in turn elicit strong expression of OX40L on effector T cells rendering them resistance to T regulation. Therefore we hypothesised that the immune response in the Roquin mouse model may be same as the effect of OX40 agonists which have been used to treated tumours (Weinberg *et al.* 2000).

In the second stage of the study, we will examine:

(1) The tumour immune response in sanroque mutant ($Roquin^{san/san}$) mice and the effect of CD30 and OX40 on the mutant condition using $Roquin^{san/san}CD30^{KO}OX40^{KO}$ mice generated in our lab.
(2) The effect of anti-PD-1 and of agonistic OX40 on tumour immune responses as revealed by comparison of sanroque with WT mice.

Chapter Two

Materials and methods

2.1 Mice used in experiments

All mouse procedures were performed under Home Office approved project and personal licenses. UK laws and the University of Birmingham ethics committee approval guidelines were followed. The mice were bred and maintained in [redacted] For tumour experiments, mice from the wild type (C57BL/6-Ly5.1,BoyJ) colony supplied by the [redacted] or (if otherwise stated by commercial supplier) were used as normal controls for comparison to genetically modified strains selected to investigate the precise role of particular genes in T cell functions, tumour growth and autoimmunity. The mice mainly used in this project were female mice 6-8 weeks old but some experiments used age and sex matched male mice. All mice were of C57BL/6 background. The $CD30^{KO}OX40^{KO}$ (dKO, C57BL/6), $CD30^{KO}OX40^{KO}Foxp3^{KO}$ (tKO, C57BL/6), $Roquin^{san/san}CD30^{KO}OX40^{KO}$ and $CTLA\text{-}4^{het}CD30^{KO}OX40^{KO}$ mice were generated in the BMSU for our lab (Table 2:1) (Gaspal *et al.* 2005, Gaspal *et al.* 2011).

2.2 Murine cell culture and preservation

The murine melanoma B16-F10 and B16-F10-luc^{+} cell line (Fidler 1974) was kindly provided by Dr. Maria Helena Ulvmar (University of Birmingham, Institute of Biomedical Research, Prof. Antal Rot's group), and was originally acquired from ATCC. The B16-F10-luc^{+} cell line was retrovirally transduced with a pMSCV-luc puro vector made in the lab of Sam Hwang (Fang *et al.* 2008, Moran *et al.* 2013) to express Firefly luciferase.

Table 2:1: Mouse strains (Wild type and Genetically modified) used in the research

Mouse strain	Phenotype and isotype	Supplier
C57BL/6 (WT)	Wild type mice of black 6 background and CD45 isotype	BMSU or Harlan Labs
B6.SJL-*Ptprc*^{a} *Pepc*^{b}/BoyJ (WT BoyJ)	C57BL/6, congenic and CD45.1	BMSU
CD30^{KO}OX40^{KO} (dKO, C57BL/6)	CD30 and OX40 receptor deficiency; defect in CD4 survival and memory, impaired Treg function (Gaspal *et al.* 2005); CD45.2	BMSU; bred for Prof Peter J.L. Lane, Birmingham, UK
CD30^{KO}OX40^{KO}Foxp3^{KO} (tKO, C57BL/6)	Natural Treg deficiency; lack of autoimmunity and full fertility (Gaspal *et al.* 2011); CD45.2 and CD45.1	BMSU; bred for Prof Peter J.L. Lane, Birmingham, UK
Roquin$^{san/san}$	Point mutation in Rc3H1 gene; dysregulation of the mRNA degradation protein Roquin leading to IFNγ driven SLE like autoimmunity; CD45.2	BMSU (via Harlan Labs); Carola di-Vinuesa, John Curtin Med. Sch., Australia.
Roquin$^{san/san}$CD30^{KO}OX40^{KO}	Deficiency in CD30 and OX40 receptors; Mutation in Rc3H1 gene; CD45.2	BMSU; bred for Prof Peter J.L. Lane, Birmingham, UK
CTLA-4^{KO}	CTLA-4 deficiency; lethal autoimmunity via multi-organ failure; CD45.2	BMSU ; Prof James Alison, M.D. Anderson Cancer Centre, USA
CTLA-4^{het}	CTLA-4$^{+/-}$; non-lethal autoimmunity (Kuehn *et al.* 2014); CD45.2	BMSU ; Prof James Alison, M.D. Anderson Cancer Centre, USA
CTLA-4^{het}CD30^{KO}OX40^{KO}	CD30 and OX40 deficiency and CTLA-4 heterozygous; healthy; CD45.2	BMSU; bred for Prof Peter J.L. Lane, Birmingham, UK
ZAP70^{KO}	ZAP70 deficiency; thymocyte development arrested at double positive stage, absence of CD4 and CD8 T cells (Negishi *et al.* 1995); CD45.2	BMSU; B. Seddon, National Institute for Medical Research, USA

The cell line was activated from frozen stocks and the B16-F10-luc^{+} cell line passaged three times subsequently using 2.5µg/ml puromycin (Sigma-Aldrich, UK) as selection to ensure its Firefly luciferase expression before injection into mice. Cultivation of the cell line was carried out in class II safety tissue culture hood (Holten Lamin Air, Denmark) in T75 vent cap tissue culture flasks (Sarsted, USA), using 15ml Dulbecco's Modified Eagle Medium (1x DMEM) (Gibco, UK) supplemented with 10% heat inactivated Fetal Bovine Serum (FBS, Sigma-Aldrich, UK) and 100IU/ml Penicillin, 100µg/ml Streptomycin (Gibco, life technologies, USA). The cells were incubated in monitored humidity and 5% CO2 at 37°C (Sanyo, Japan). After incubation, the cells were harvested in log phase, at which stage their confluence is about 85%. Firstly, they were washed with 10ml Dulbecco's Phosphate Buffer Saline (without Ca^{++} and Mg^{++}) (DPBS, Sigma-Aldrich, USA) then detached with 3ml TrypLETM Express enzyme (Gibco, life technologies, USA) at 37°C for 4-5 minutes; detachment was checked by light microscope (Olympus, Japan). Enzyme activity was inhibited by adding 8ml complete DMEM medium and cells were collected and centrifuged (Eppendorf, Germany) at 250-300g for 5 minutes. Cells were collected from many flasks into one 50ml BD falcon tube and centrifuged for 10 minutes at 300g. The cell sediment was washed twice with 50ml cold DPBS and suspended in 10ml cold DPBS. 1:10 dilution from the suspension was used to calculate the total viable number of cells/ml using Trypan blue (Sigma-Aldrich, UK) and a haemocytometer (Neubauer, Germany). Finally, the cells were strained through a DB Falcon strainer to remove clumps, and their concentration was adjusted to 500,000 cell/100µl and they were preserved in DPBS on cold ice before injection.

The frozen stocks of B16 melanoma were prepared from cells in complete DMEM medium and 10% DMSO (Sigma-Aldrich, USA), and stored at -80°C.

2.3 Subcutaneous injection of mice

Female mice aged 6-8 weeks were used for the tumour melanoma model. All mice were maintained in during the study period. B16-F10-luc^{+} melanoma cell suspensions were prepared as described in section 2.2. Mice were anaesthetised, the dorsal right flank areas were shaved and treated with disinfectant, and were subcutaneously injected with properly agitated 100ul DPBS containing 5x10^{5} cells. Ear tagging was carried out for mouse identification and tumour growth development was measured twice weekly using callipers and *in vivo* imaging. The mouse body weight was monitored and tumour volumes calculated using the equation V= (π/6) (l) (d^{2}), V represents the volume; l refers to the long diameter while d is the short diameter. According to the Home Office guidelines, the permissive tumour size is 12mm in diameter.

2.4 Intravital imaging of tumours

Tumours were imaged *in vivo* using detection of luciferase bioluminescence at days 6, 13, 20, 27 and 34 using IVIS Spectrum Intravital Microscope (Calliper Life Sciences, USA). Filter sterilized D-Luciferin solution was prepared at 15mg/ml in DPBS without Mg^{++} and Ca^{++}. Initially, mice were weighed and injected intraperitoneally with 10ul/g of body weight using insulin syringes. Each mouse received 150mg D-Luciferin/kg body weight. Directly after injection, mice were anesthetised in isoflurane chamber for 3 minutes and the tumour area was shaved. 10 minutes after injection, the peak bioluminescent emission signal from tumours

was measured by sub-sequential imaging using the IVIS microscope at time points 10,12,14,16,18 and 20 minutes. According to the melanoma cell line supplier, the peak bioluminescence intensity time can be recorded at approximately 20 minutes from initial Luciferin injection. IVIS® living software (Calliper Life Sciences, USA) was used to determine region of interest (ROI) and measurements were transferred to Prism Graph Pad software for further analysis.

2.5 Preparation of cell suspensions for flow cytometry

For preparation of single cell suspensions, mice were euthanized according to schedule 1 Home Office guidelines. Then, spleen, tumour inguinal draining and contra lateral lymph nodes were removed and transferred into RPMI 1640 (Sigma-Aldrich, UK). Tumours were excised, weighed and cut into two parts; one placed in 1ml digestion medium composed of RPMI, 2% Fetal Calf Serum (FCS), 100µg/ml DNase (Roche Applied Science, Germany) and 1mg/ml Collagenase D (Roche Applied Science, Germany). The second parts were frozen on dry ice and preserved at -80°C for cryostat sectioning and immunofluorescence staining. Splenocytes were prepared by physical disaggregation using a 70µm cell strainer and syringe plunger followed by lysis in Gey's solution for 5 minutes on ice and washing then resuspending in 2ml RPMI. The other tissues were snipped using fine scissors and then incubated in a thermoshaker (Eppendorf, Germany) at 37°C for 25 minutes (lymph nodes) or 35 minutes (tumours). To reduce cell clumping, 1mM/ml EDTA (Sigma Aldrich, Switzerland) was added to the digested suspension which was strained through a 70µm cell strainer. The undigested tissues were then mashed up using 2ml syringe plunger end, and washed with 5ml FACS buffer containing 0.05% sodium azide, 1mM EDTA and DPBS with 1% FBS. Centrifugation was performed for

the strained cells at 4°C, 300g for 10 minutes and the sedimented cells were resuspended in 800µl RPMI for tumours and 400µl for lymph nodes.

2.6 Flow cytometric analysis

96 well round-bottom plates (Sterilin, UK) were seeded with 200µl of the cell suspensions (approximately 10^6), centrifuged at 4°C, 1400 rpm for 3 minutes and then washed with cold PBS before staining. The washed cells were first surface stained with Live/Dead near IR dye (Molecular Probes, USA) for 20 minutes on ice to identify viable and non-viable cells. After washing twice with PBS, the cells were surface stained with the antibodies showed in Table 2:2 and incubated on ice for 30 minutes.

Intracellular staining for FoxP3 was performed using anti-FoxP3 FITC following surface staining, fixation and permeabilization of the cells with FoxP3 Fixation/Permeabilization kit (eBiosciences, UK). The cells were washed twice and resuspended in 200µl of fluorescent activating cell sorting (FACS) buffer (0.1% FBS in PBS). 10µl of counting beads, equivalent to approximately 10000 beads (Spherotech, USA), were added to each sample before analysis according to the manufacturer's protocol. Beckman Coulter CyAn^{TM}ADP was used for the acquisition of the samples and FlowJo software was used for analysis of the data.

For investigating intracellular IFNγ production, plates were coated with 200µl/well of functional grade purified anti-CD3 5µg/ml PBS in humid chamber overnight at 4°C before setting up stimulation conditions. Excess anti-CD3 was removed and wells were washed twice with sterile PBS then 800µl RPMI culture media and 0.5µg/ml anti-CD28 purified functional grade were added to each well. After that approximately

$1x10^6$ cells/ sample were added to the medium, mixed well and incubated at 37°C for 1 hour for stimulation. The stimulation was stopped by adding GolgiStop (BD) and plates were incubated for another 3 hours at 37°C. Post 4 hours stimulation, well contents and two washes with RPMI culture medium were harvested and collected into tubes. The tubes were centrifuged at 1400 rpm for 5 minutes and cells were resuspended in 200ml RPMI. Cells were surface stained as previously described, washed and fixed/permeabilised with Cytofix/Cytoperm Plus (BD) following the supplier's protocol. Direct conjugates of IFNγ antibodies were used to stain the permeabilised cells for IFNγ screening.

Table 2:2: Antibodies used for fluorescence activated cell sorting

Antibody	Clone	Dilution	Producer
anti-CD45 PerCP-Cy5.5	30-F11	1:200	(eBioscience)
anti-CD45.1 PerCP-Cy5.5	A20	1:200	(eBioscience)
anti-CD45.2 PerCPCy5.5	104	1:200	(eBioscience)
anti-CD4 PerCPCy5.5	RM4-5	1:100	(eBioscience)
anti-CD3 APC	145-2C11	1:100	(eBioscience)
anti-CD25 APC	PC61	1:100	(eBioscience)
anti-CD90.1 (Thy1.1) APC	HIS51	1:800	(eBioscience)
anti-IFNγ APC	XMG1.2	1:100	(eBioscience)
anti-CD45 APC-Cy7	30-F11	1:50	(eBioscience)
anti-TCRβ PE	H57-597	1:100	(eBioscience)
anti-CD3 PE	500A2	1:100	(eBioscience)
anti-TNFα PE	MP6-XT22	1:100	(eBioscience)
anti-CD30 PE	2SH125F-2D	1:100	(PharMingen)
anti-GM-CSF PE	MP1-22E9	1:100	(BioLegend)
anti-CD44 PE-Cy7	IM7	1:100	(eBioscience)
anti-PD-1 PE-Cy7	RMP1-30	1:100	(BioLegend)
anti-CD152 PE-Cy7	UC10-4B9	1:100	(BioLegend)
anti-CD152 PE-Cy7	UC10-4B9	1:100	(BioLegend)
anti-OX40 BV421	OX-86	1:100	(BioLegend)
anti-CD8 e-Flour450	53-6.7	1:100	(eBioscience)
anti-CD4 V500	RM4-5	1:100	(BD bioscience)
anti-FoxP3 FITC	FJK-16s	1:100	(eBioscience, UK)
anti-CD3e purified, functional	145-2C11	1:200	(eBioscience)
anti-CD28 purified, functional	37.51	1:200	(eBioscience)

2.7 Immunofluorescence histology

Tumour tissues were embedded on OCT (Tissu-Tek, The Netherlands), sectioned to 5μm thickness on a Cryostat (Bright, UK), mounted on superfrost plus slides (Hendleg-Essex, England), air dried for 60 minutes or overnight, fixed in cold acetone for 20 minutes at 4°C and air dried for 30 minutes, then either stained directly or stored at -80°C for later use. For staining, slides were hydrated for 10 minutes in PBS then blocked with 0.033% avidin and 0.0033% biotin for 15 minutes and washed for 5 minutes in PBS. This was followed by incubation with 10% horse serum (Sigma, USA) in 1% BSA/PBS for 15 minutes at room temperature (RT) in order to block non-specific binding sites. For prevention of tissues from drying and protection of sensitive reagents from light, the slides were incubated in a dark and humid environment, first with primary antibodies (except for the negative controls), for 40 minutes at RT and then washed with PBS for 10 minutes, followed by second, third and fourth step antibodies, as required for detection. For reduction of cross reactivity among secondary (tertiary, quaternary) antibodies, these were cross absorbed with 10% mouse serum (Sigma, USA) in 1% BSA/PBS for 30 minutes before applying to slides. Slides were washed between steps as previously described. Sections were soaked for 30 seconds in 600nM 4′,6-Diamidino-2-phenylindole, dihydrochloride (DAPI) (Molecular Prob, Life Science), as an antinuclear counterstain, mounted with Prolong Gold (Life Science) and finally sealed with nail varnish. The details of the primary antibodies and following amplification antibodies are listed in Table 2:3 and Table 2:4.

Table 2:3: Primary antibodies used for immunofluorescence

Antibody	Host	Producer
anti-CD8 FITC	Rat	(eBioscience)
anti-CD3 biotin	Armenian Hamster	
anti-CD4 conjugated to Alexa Flour 647	Rat IgG1	(eBioscience)
anti-CD31 FITC	Rat	(eBioscience)
anti-FoxP3-bio	Rat	(eBioscience)
anti-mouse IgG FITC	goat	(Sothern Biotech)

Table 2:4: Secondary and tertiary antibodies used for immunofluorescence

Antibody	Host	Producer
anti-FITC	Rabbit	(Life technologies)
anti- rabbit 488	Donkey	(Invitrogen, USA)
Streptavidin 555		(Invitrogen, USA)

2.8 Confocal imaging

Digital images were acquired from tissues stained with fluorochrome conjugated antibodies using an LSM 780 confocal microscope (Zeiss, Germany), with x10 and x63 objectives. Argon laser (488nm), helium laser (561nm), helium (633 nm) and diode laser were used to excite FITC conjugated Abs, Alexa Flour 555 conjugated Abs, Alexa Flour 647 conjugated Abs and DAPI stain respectively, and detection limits were set to minimise overlap between individual stains. The images were analysed using Zen software

2.9 Adoptive cell transfer

Splenocytes from BoyJ mice (CD45.1) and Roquin$^{san/san}$ (CD45.2) or Roquin$^{san/san}$CD30^{KO}OX40^{KO} (CD45.2) were prepared as in section 2.5, mixed 1:1 and stained for CD45.1, CD45.2, TCRβ, CD4 and CD8 to identify and determine the percentages of T cells before adoptive transfer. Cells were filtered at 70μm, counted and suspended in cold sterile PBS at the required number and then injected intraperitoneally into the recipient mice strain. As part of this procedure, the mice were also injected subcutaneously with 5x10^5 B16-F10 melanoma cells as described in section 2.3.

2.10 Immunomodulatory agents used *in vivo*

The following antibodies were used to block specific interactions *in vivo*: CD8 mAb (Herman Waldmann), courtesy of Dr. Nick Jones, IBR, University of Birmingham, used to *in vivo* deplete CD8 T cells (Cobbold *et al.* 1984). Table 2.5 shows the monoclonal antibodies mAbs used for tumour treatment: anti-CTLA-4, courtesy of

Table 2:5: Monoclonal antibodies used in the study

Antibody	Clone	Host	Dose	Effect
anti-CTLA-4	9H10	Hamster	200 µg	Blocking CTLA-4
anti-CTLA-4	9H9	Mice	200 µg	Blocking CTLA-4
anti-PD-1	RMP1-14	Rat	250 µg	Blocking PD-1
anti-CD30L	RM153	Rat	250 µg	Blocking CD30L
anti-OX40L	RM134L	Rat	250 µg	Blocking OX40L
anti-IgG		Rat	250 µg	Blocking IgG
Anti-CD8	YTS169.4.2	Rat	500 µg	Depleting CD8 T cells
anti-OX40	OX86	Rat	100 µg	Agonist OX40

James P. Allison, MD Anderson Cancer Centre, USA; anti-PD-1, anti-CD30L and anti-OX40L, courtesy of Hido Yagita, Juntendo University School of Medicine, Japan; and rat IgG (Sigma-Aldrich) as a control. The mAbs were prepared in sterile PBS and injected I.P twice/week post 5 days of B16-F10 injection (unless otherwise stated).

2.11 Circulating serum autoantibody screening and titration

Blood was collected from mice by cardiac puncture according to Home Office regulations. The blood samples were allowed to clot naturally then centrifuged at 13000 rpm, 4°C for 15 minutes. Isolated serum was transferred into new tubes and stored at -20°C until use. Frozen sera were thawed at RT, diluted 1:20 in 1X PBS. Commercially prepared 10 spot rat tissue slides (NOVA Lite®Rat Liver, Kidney, Stomach, USA) were removed from their bags and dried at RT for 20 minutes. The slides were blocked with 10% goat serum (Sigma) in 1% BSA/PBS (50µl/ spot) and incubated for 20 minutes at RT in a dark humidified chamber. The diluted mice sera were applied to the 10 spot slides and incubated as previously for 20 minutes. Slides

were then washed in PBS for 5-10 minutes, excess fluid was wiped from around spots and 50µl/spot of goat anti mouse IgG FITC was added and incubated for 20 minutes. The slides were washed, antifade reagent was added; they were covered and then stored in the dark at 4°C until imaging. Positive, negative and second step controls were also prepared. Tissues were imaged by fluorescence on a Leica DM6000B (Germany) microscope and data was interpreted using LAS and Fiji software.

2.12 Liver function tests

To assess liver function after potential autoimmune liver damage as a consequence of the cancer immunotherapy using monoclonal blocking antibodies, serum Alanine Aminotransferase (ALT) Beckman coulter test kit (OSR 6107) and Aspartate Aminotransferase (AST) Beckman coulter test kit (OSR 6109) were used according to the manufacturer's protocol on the sera harvested at sacrifice from experimental mice. Analysis, using a Beckman Coulter AU400 analyser, was performed by the Clinical Biochemistry Unit, Women's Hospital, Edgbaston, Birmingham.

2.13 Liver histology

Liver tissues were excised from dissected mice and collected in cold RPMI. The liver tissues were divided into two parts, one wrapped in aluminium foil and snap frozen then stored in -80°C until use for cryostat sections and immunofluorescent staining; the other fixed in 40% formalin (Adams, England), dehydrated, embedded in wax, sectioned into 5µm sections and stained for Haematoxylin Eosin stains in collaboration with Dr Souad Messahel, Human Biomaterials Resource Centre, Med School, University of Birmingham. The liver sections were imaged by bright field

microscopy on a Leica DM6000 (Germany) microscope, and areas of lymphocyte infiltration were identified and assessed at x10 and x20 magnifications.

2.14 Analysis of gene expression

Molecular genetic analysis was carried out in Prof. Graham Anderson's lab in collaboration with Sonia Parnell, MRC centre for immune regulation, University of Birmingham.

2.14.1 Primers used for gene analysis

Table 2:6: The sequences of primers for the genes of interest

Antigen	The sequence of forward 5' end	The sequence of reverse 3' end
β-actin	Commercial (Qiagen QT00095242)	Commercial (Qiagen QT00095242)
PD-L1	GACGCAGGCGTTTACTGCT	GCGGTATGGGGCATTGACTTT
PD-L2	CTGCCGATACTGAACCTGAGC	GCGGTCAAAATCGCACTCC
OX40L	ACGCTAAGGCTGGTGGTCTCT	TGCTCCTCTGAGTCTTTGGATTG
CD30L	AGGATCTCTTCTGTACCCTGAAAAGTA	GTTTGGTATTGTTGAGATGCTTTGA

2.14.2 mRNA isolation and cDNA synthesis

µMacs One-step cDNA synthesis kit was used to extract mRNA from pre-frozen samples and cDNA preparation was carried out in accordance with the manufacturer's protocols (Miltenyi Biotec). The frozen cells, lysing and binding buffer as well as washing buffer were kept for about 30 minutes in sterile cabinet to equalise their temperature with that of the lab. After that, 1ml of lysing/binding buffer was added to the cell samples which were then vortexed vigorously for (3-5) minutes

before being passed through a 21 gauge needle for complete cell lysis. LysateClear columns were used for clearing cell lysates after centrifugation at 13,000g for 3 minutes. To hybridise the PolyA tail of mRNA to oligo deoxy-thymidine (dT) microbeads, 50µl of µMACS oligo microbeads was added to the sample lysates, agitated gently and then loaded into MACSm columns prepared with lysis/binding buffer and fixed in MACS^{TM} magnet separator. Labelled mRNA on the magnetic beads attaches to the columns while proteins, DNA and ribosomal RNA are removed by washing the columns 2X with 200µl of lysis/binding buffer and additional 4X rinses with 100µl of the buffer. The retained mRNA was then washed 2X with 100µl equilibration/washing buffer and used for the synthesis of cDNA using the same separation columns. cDNA was synthesised by reverse transcription by dissolving the lyophilized mastermix in 20µl of suspension buffer and adding it to the columns, which were then incubated in a thermoblock at 42°C for 60 minutes to start the reaction. For prevention of sample evaporation, each column was sealed with 1µl of sealing buffer. After incubation, columns were washed 2X with 100µl equilibration/washing buffer and cDNA was released by applying 20µl of release agent to each sample which, then kept in the thermoblock at 42°C for another half an hour. The final step was to elute the synthesised cDNA from the columns which was carried out by adding 50µl of the elution buffer. The cDNA samples were collected in Eppendorf tubes and stored at 20°C.

2.14.3 Real time quantitative polymerase chain reaction (qPCR)

RotorGene (RG-3000, Qiagen) was used for performing real time qPCR in the presence of SYBER®green dye and the specific forward and reverse designed primers for the genes of interest: *pdl1, pdl2, ox40l,* and *cd30l* (Table 2:6). β-actin was

selected as the working control and the endogenous reference gene for standardisation of the other genes. The β-actin primers were commercially provided by QIAGEN as QuantiTect Primer Assay (QT00095242) while the oligonucleotides were supplied by Sigma-Genosys. Replicates of qPCR reactions were conducted in reaction buffer at a total volume of 15µl, containing 7.5µl of qPCR master mix (heat activated Taq polymerase, dNTPs, $MgCl_2$, Bioline Sensimix NoRox SyberGreen), 200nM forward and reverse primers, 1µl cDNA template and 6.2µl (DNAse/RNAse)-free PCR grade water (Sigma). The RotorGene appliance was programmed for 40 cycles of amplification: 95°C for 10 minutes for initial denaturation, then cycling at 95°C for 15 sec, followed by (60-62)°C for 20 sec and 72°C for 15 sec. Amplicons release fluorescent signals at the end of each cycle which are recorded and used to generate a melting curve for verification of amplicon specificity. Rotor-Gene 6.0 software (Corbett Research) was used for the calculation of amplification efficiencies and Ct (threshold cycle) values of the reaction based on standard curves produced from Mouse Universal cDNA (Biochain Institute). The relative mRNA expression levels were normalised to β-actin and described using the Pfaffle model for the quantification of gene expression.

2.15 Statistical analysis

Results from *in vitro* and *in vivo* experiments were expressed as medians, means or means ±SEM. Mann Witney non-parametric tests were used to analyse data with GraphPad Prism software and $p< 0.05$ was considered statistically significant. FACS plots were analysed using FlowJo v10 (Tree star).

Chapter Three Results

Tumour immune responses in WT, dKO and tKO mouse models and the effect of anti-PD-1 on tumour growth

3.1 Introduction

The many protein mutations in tumours may provoke immune responses from their hosts, but FoxP3 dependent nTregs have been found to be exploited by tumours to protect themselves from both CD4 and CD8 immune responses (Curiel *et al.* 2004, Watson *et al.* 2013). It has been shown that the thymic medulla is the site at which the development of nTregs is fostered, using the promiscuous expression of self-antigens as part of the selection process (Cowan *et al.* 2013). In prostate cancers, Malchow *et al*, (2013) identified prostate cancer infiltrating nTregs, which were self-prostate antigen specific but not tumour specific, and had been selected in the thymus of both males and females in an AIRE dependent manner. This observation suggests that the self-tissue specific nTregs that normally protect the body against autoimmunity are serving to inhibit the immune response against tumours. Previous work in our lab has generated mice without FoxP3^{+} nTregs whose autoimmunity is abrogated by the concomitant absence of the TNF receptors CD30 and OX40 (CD30^{KO}OX^{KO}FoxP3^{KO} mice); these mice live and breed normally (Gaspal *et al.* 2011). We aimed to investigate the tumour immune response in this mouse model as compared to mice without the CD30 and OX40 genes and wild type mice. In addition to the presence of Tregs, tumour survival is also assisted by their expression of the PD-L1 molecule, which counteracts tumour specific cytotoxic CD8^{+} T cells (Iwai *et al.* 2002). For this reason, we aimed to determine both the expression of the inhibitory receptor PD-1 on tumour infiltrating CD8 T cells, and any effect of PD-1 blockade on

tumour responses. CTLA-4 on the surface of FoxP3^{+} Tregs has been identified as the main mediator of their suppressive function (Wing *et al.* 2008), and has additionally been used successfully in human anti-tumour therapy trials, so we included CTLA-4 blockade as one of our test conditions.

3.2 Results

3.2.1 Tumour immune responses in dKO and tKO compared with WT mice

3.2.1.1 Experimental protocol

WT (BoyJ), CD30^{KO}OX40^{KO} (dKO) and CD30^{KO}OX40^{KO}Foxp3^{KO} (tKO) female mice, aged 6-8 weeks, were injected subcutaneously with 5x10^{5} B16-F10-luc^{+} melanoma cells on the right dorsal flank and the dynamics of tumour growth were monitored at least twice weekly for 3 weeks using *in vivo* imaging (IVIS) and by palpation, using callipers; all mice were then culled and tumours weighed and infiltrates analysed.

3.2.1.2 *Ex vivo* pattern of B16 melanoma tumour growth in dKO and tKO compared with WT mice

Tumour growth in WT mice was exponential, reaching an average volume of 1100mm^{3} 21 days after cell injection; at the same time point in dKO mice, tumour volumes averaged 800mm^{3}, and the Treg deficient tKO mice were markedly resistant to B16 growth, having tumour volumes in the region of 250mm^{3} (Figure 3.1A).

Final excised tumours weights from three experiments were pooled for comparison between groups; we found that tumour weights from tKO mice were significantly less

than those of WT ($p<0.005$) and dKO ($p<0.01$). A lower average tumour weight was obtained from dKO compared with WT mice, but this was not statistically significant ($p<0.1$) (Figure 3.1B).

3.2.1.3 *In vivo* kinetics of B16 melanoma tumour growth in dKO and tKO mice compared with WT mice

Ex vivo tumour sizes for WT, dKO and tKO hosts were substantiated by *in vivo* imaging using IVIS. The B16-F10-luc^{+} melanoma cell line expresses luciferase and digests injected luciferin which subsequently emits photons that can be captured and detected by cooled CCD scanning camera; the higher the intensity of light the more the viability of the cancer, and this is assumed to be proportional (Fang *et al.* 2008). The peak bioluminescence emission was captured at days 6, 13 and 20 for W, dKO and tKO mice (Figure 3.2); the region of interest (ROI) for which photon counts were recorded was marked in red (Figure 3.2A). Plots of the total fluxed photons measured show that tumour viability in WT mice was significantly greater than in tKO mice ($p<0.05$) particularly at day points 13 and 20 (Figure 3.2B). Tumour viability in dKO mice was found to be intermediate between the other two groups, but the difference was not significant statistically at all day points.

S.C injected with $5x10^5$
B16-F10-Luc+ melanoma cells

All mice culled at day 21

WT (BoyJ)
dKO ($CD30^{KO}OX40^{KO}$)
tKO ($CD30^{KO}OX40^{KO}Foxp3^{KO}$)

A

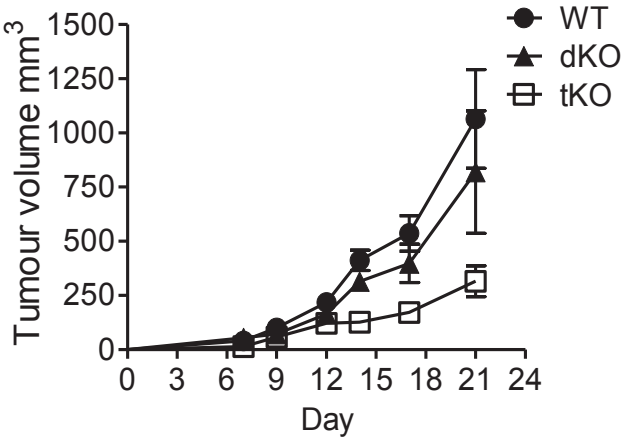

B

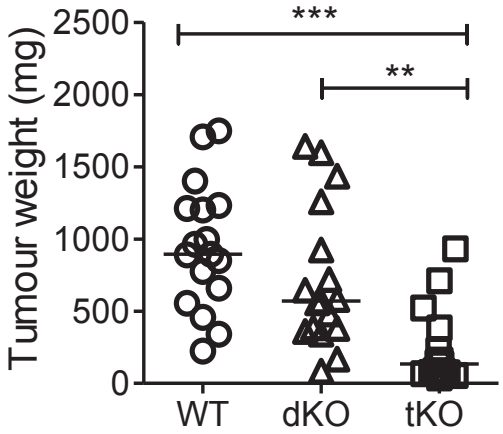

Figure 3.2: The dynamics of *in vivo* B16-F10-luc$^+$ tumour growth in WT, dKO and tKO mice

Tumour viability was recorded using intravital imaging (IVIS). The B16-F10-luc$^+$ cell line expresses luciferase, so that intra-peritoneal injection of the luciferin dye results in bioluminescence emission from the B16-F10 tumour cells. 10 minutes after injection, the peaks of bioluminescence were visualized and recorded using a dark chamber scanning microscope equipped with a CCD camera.

(A) A representative mouse from each group was selected on days 6, 13 and 20 and used to show luciferase activity of the growing tumours. IVIS® living software was used to mark a region of interest (ROI) that included the whole tumour, (red circles). The light emission intensity is plotted according to the colour-coded scale shown, the highest and lowest photon emissions represented by red and blue colours respectively.

(B) Bioluminescence emission measured as total fluxed photons per second, graph displays means ± sd. Statistical analysis was performed using IVIS® living software and the Mann Whitney non parametric test. Data are representative of three independent experiments, n=13,9,9 respective to each group in the order presented. * ,** indicate significance $p<0.05$, and $p<0.01$ respectively.

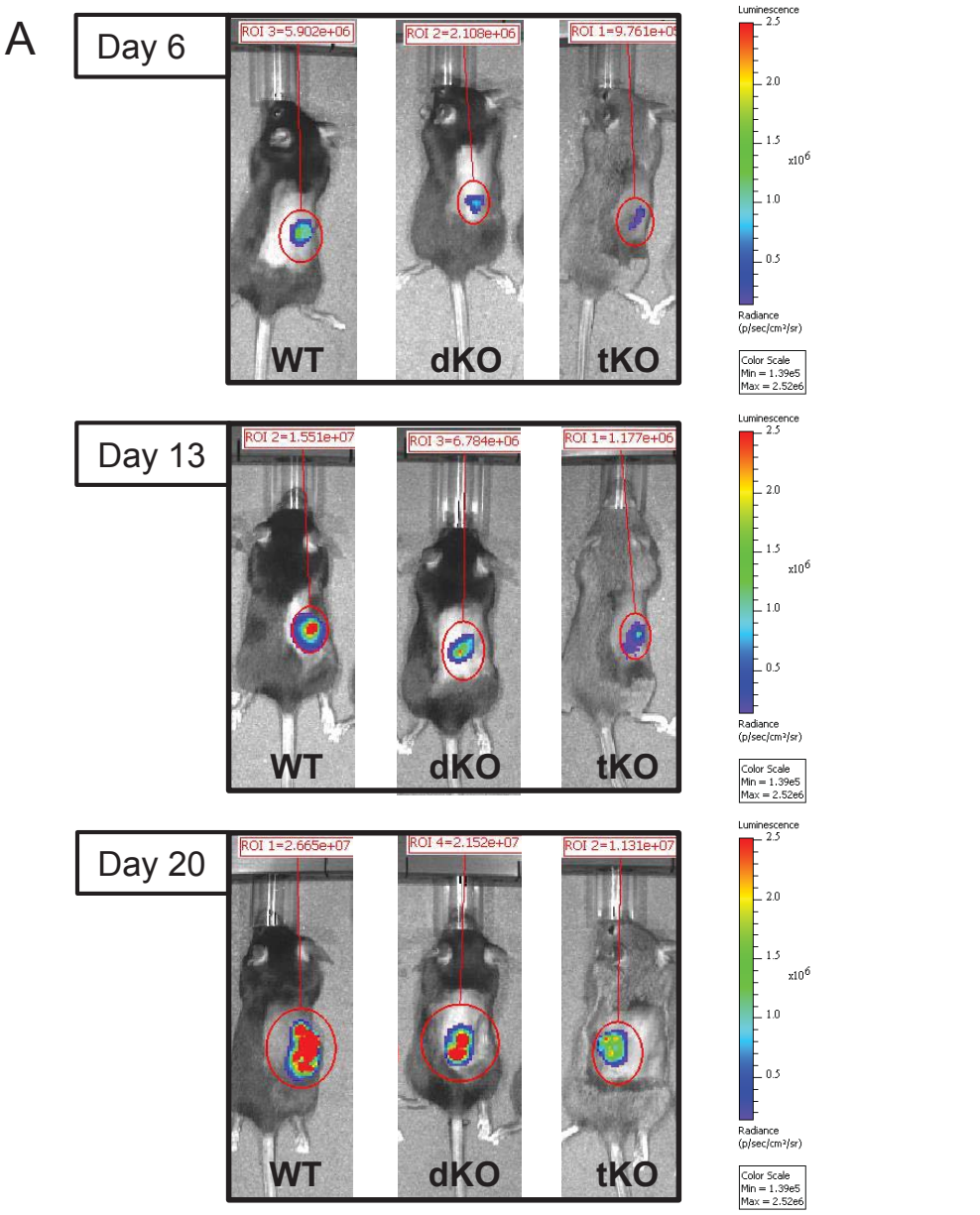
A
Day 6
ROI 3=5.902e+06
ROI 2=2.108e+06
ROI 1=9.761e+0
WT
dKO
tKO
Luminescence
2.5
2.0
1.5
x10^6
1.0
0.5
Radiance (p/sec/cm²/sr)
Color Scale Min = 1.39e5 Max = 2.52e6
Day 13
ROI 2=1.551e+07
ROI 3=6.784e+06
ROI 1=1.177e+06
Day 20
ROI 1=2.665e+07
ROI 4=2.152e+07
ROI 2=1.131e+07

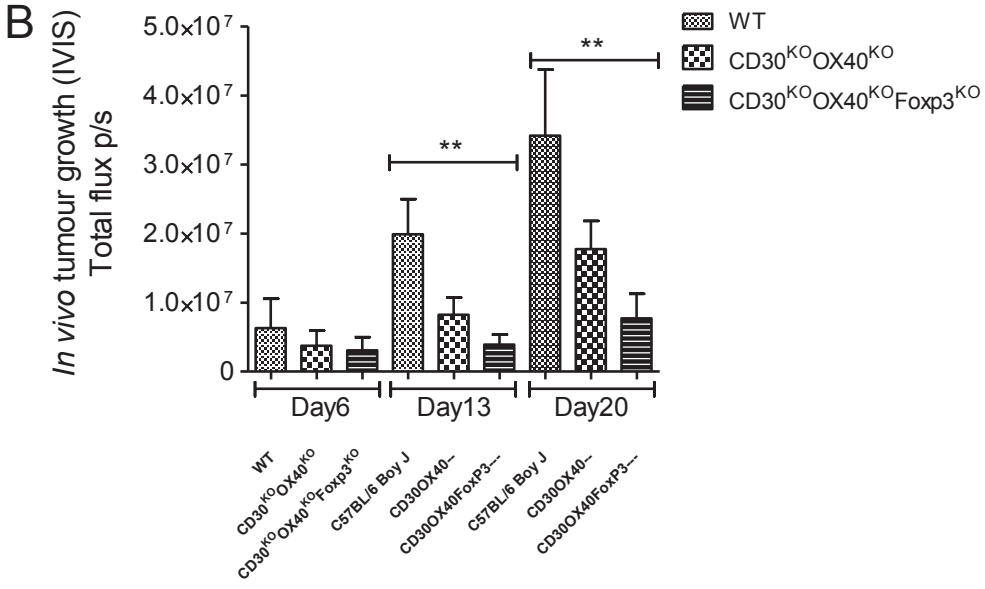
B
In vivo tumour growth (IVIS)
Total flux p/s
5.0x10^7
4.0x10^7
3.0x10^7
2.0x10^7
1.0x10^7
0
**
**
Day6
Day13
Day20
WT
CD30KOOX40KO
CD30KOOX40KOFoxp3KO
C57BL/6 Boy J
CD30OX40–
CD30OX40FoxP3–
C57BL/6 Boy J
CD30OX40–
CD30OX40FoxP3–

3.2.1.4 Flow cytometric analysis of the T cell presence in tumours and in the draining (inguinal) lymph node

To identify and phenotype the lymphocytes infiltrating the experimentally induced tumours, excised tumour tissue was prepared for flow cytometric analysis as described in section 2.5. A representative phenotypic analysis is shown in Figure 3.3A, and Figure 3.3B,C,D which show results pooled from three independent experiments. In WT tumours, the infiltrating T cells were in the ratio 2:1 of CD4:CD8 T cells; this ratio was reversed in dKO and tKO tumours, in keeping with previous results showing that OX40 and CD30 signals affect CD4 T cell effector functions synergistically, but apparently not CD8 T cells (Withers *et al.* 2011). A similar outcome has been reported in the human Kaposi sarcoma (Byun *et al.* 2013), where the infiltration of CD8 cell tumours was preserved in the absence of OX40, even though there was significant expression on infiltrating $CD8^+$ T cells of the PD-1 inhibitor, which is induced as a result of chronic exposure of tumour-reactive CD8 T cells to tumour antigens (Ahmadzadeh *et al.* 2009, Fourcade *et al.* 2012). In the current study, moreover, compared with WT, there was a significant reduction in the proportion of the total T cell infiltration contributed by Tregs, suggesting a role for CD30 and OX40 in Treg function. Quantification of T cell populations per gram of tumour showed significant reduction in CD4 infiltrates in dKO and tKO in comparison with WT ($p<0.02$) as well as in Tregs in dKO ($p<0.018$) (Figure 3.3B,D). In contrast, the enumeration of CD8 T cells showed a significant increase in their presence ($p<0.009$) in tKO mice versus WT; the intermediate increase in CD8 T cell numbers in dKO was not statistically significant (Figure 3.3C).

The analysis of the lymphocyte population in the draining (inguinal) lymph node for the tumour (Figure 3.4) mirrors the trend towards a decrease in CD4 T cells in dKO and tKO relative to WT observed in the tumour itself. Likewise, in contrast to WT, there was a tendency toward increased CD8 T cells in dKO and tKO that was not statistically significant (Figure 3.4A,B,C). Treg numbers found in dKO lymph nodes were, however, significantly lower ($p<0.03$) than those in the WT draining lymph node (Figure 3.4D).

Figure 3.3: Flow cytometric analysis of tumour infiltrates in WT, dKO and tKO mice

(A) Representative FACS contour plots of cellular infiltrates of tumours, gated on live $CD45^+CD3^+$ cells and showing expression of CD25 and FoxP3 on CD4 T cells, and PD-1 on CD8 T cells (B,C,D) numbers of T cells infiltrating tumours: (B) $CD4^+$, (C) $CD8^+$, (D) $FoxP3^+$. Each data point represents one mouse, line shows median. Statistical analysis was performed using the Mann Whitney non parametric test. Data are pooled from three independent experiments, n=16,17,15 respective to each group in the order presented. * ,**,*** indicate significance $p<0.05$, $p<0.01$ and $p<0.005$ respectively.

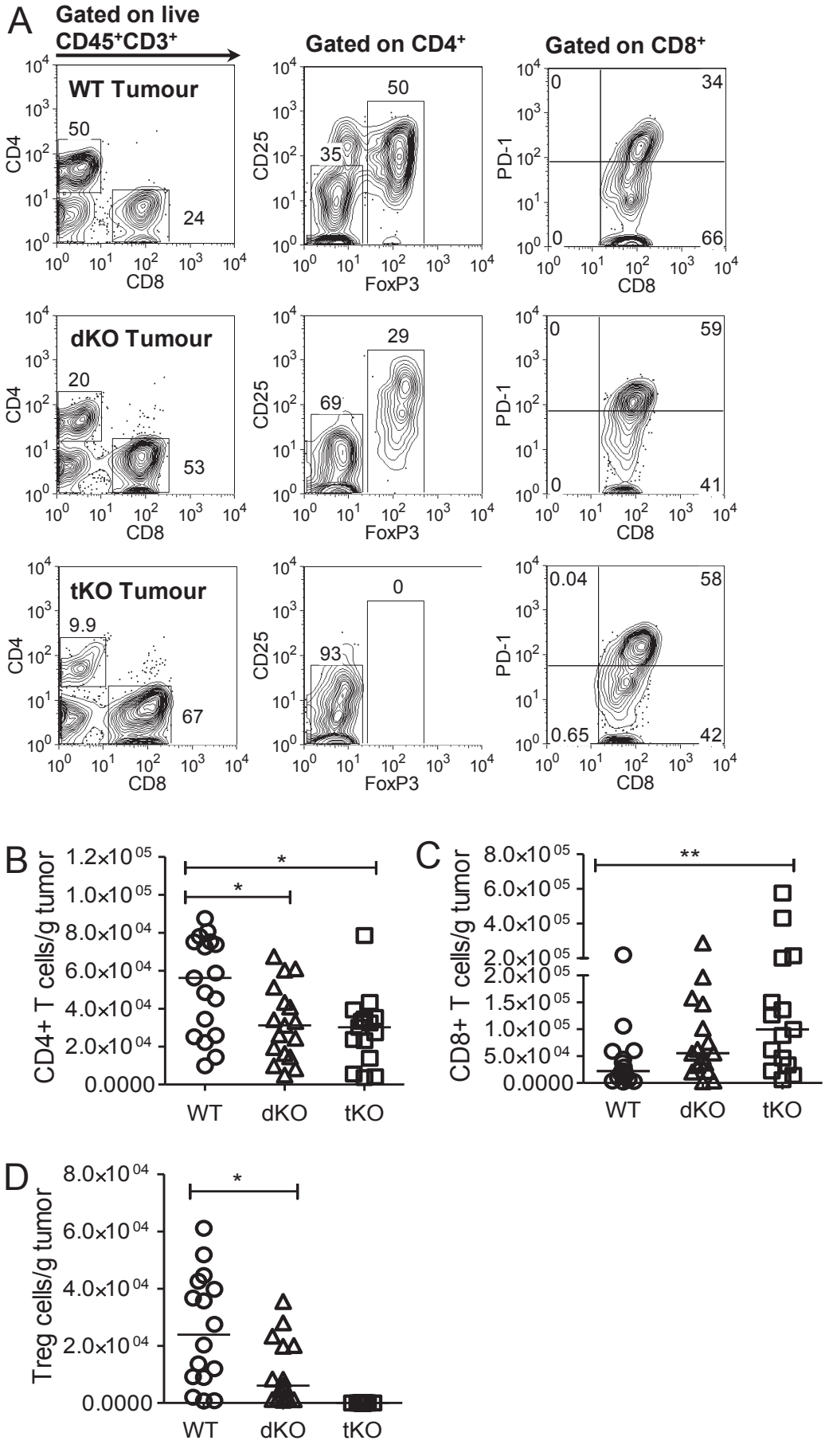
A
Gated on live CD45+CD3+
Gated on CD4+
Gated on CD8+
WT Tumour
dKO Tumour
tKO Tumour
CD4
CD8
CD25
FoxP3
PD-1
50
24
35
50
0
34
66
20
53
69
29
0
59
41
9.9
67
93
0
0.04
58
0.65
42
B
CD4+ T cells/g tumor
C
CD8+ T cells/g tumor
D
Treg cells/g tumor
WT
dKO
tKO

Figure 3.4: Flow cytometric analysis of lymphocytes from the draining (inguinal) lymph node of melanoma transfected WT, dKO and tKO mice.

(A) Representative FACS contour plots of lymphocytes from lymph nodes, gated on live $CD45^+CD3^+$ cells and showing expression of CD25 and FoxP3 on CD4 T cells, and PD-1 on CD8 T cells (B,C,D) numbers of T cells per lymph node: (B) $CD4^+$, (C) $CD8^+$, (D) $FoxP3^+$. Each data point represents one mouse, line shows median. Statistical analysis was performed using the Mann Whitney non parametric test. Data are pooled from two independent experiments, n=12,11,11 respective to each group in the order presented. * indicates significance $p<0.05$.

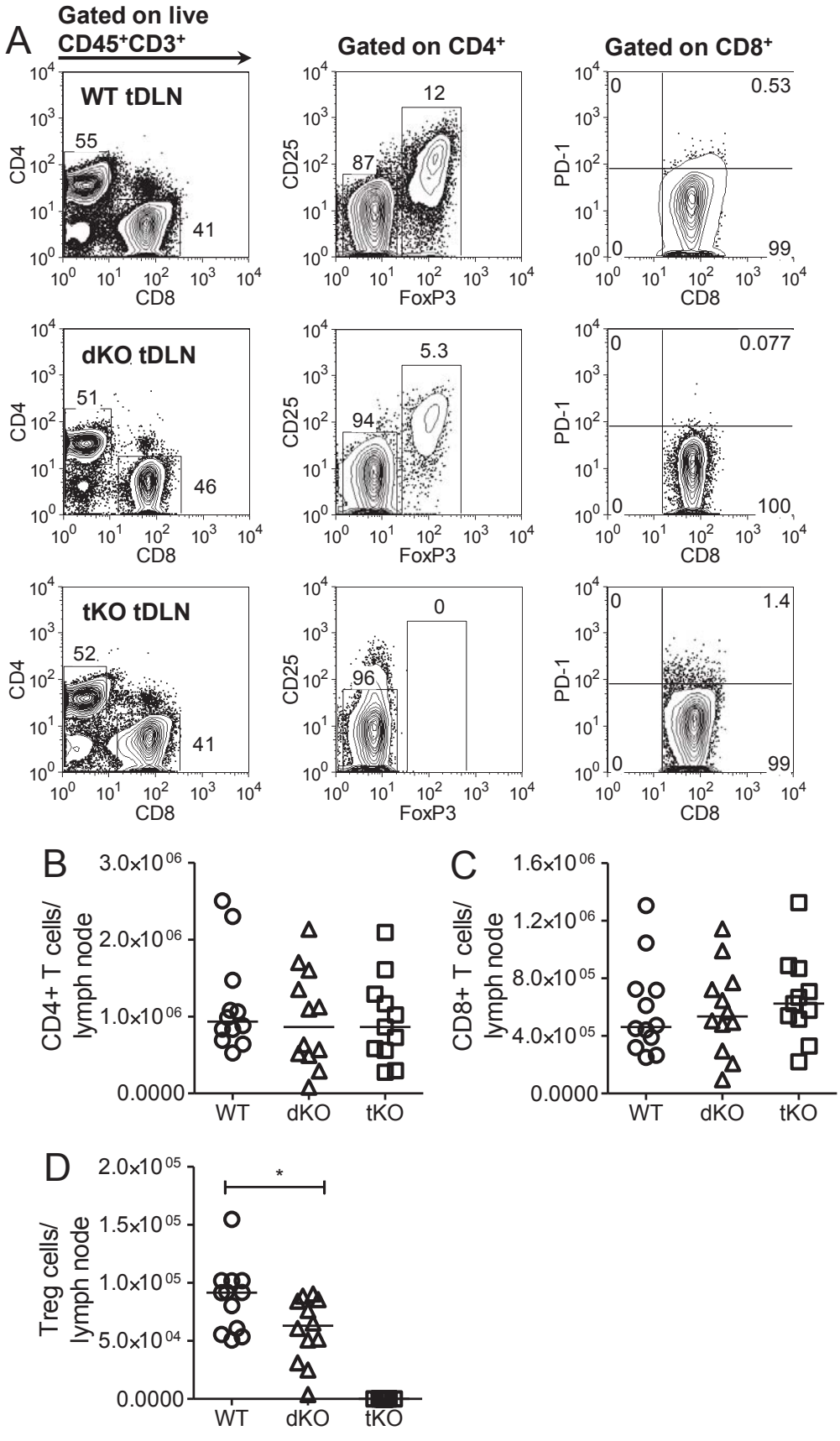
A
Gated on live
CD45+CD3+
Gated on CD4+
Gated on CD8+
WT tDLN
dKO tDLN
tKO tDLN
CD4
CD8
CD25
FoxP3
PD-1
55
41
87
12
0.53
51
46
94
5.3
0.077
52
41
96
0
1.4
99
100
B
CD4+ T cells/ lymph node
3.0x10 06
2.0x10 06
1.0x10 06
0.0000
WT
dKO
tKO
C
CD8+ T cells/ lymph node
1.6x10 06
1.2x10 06
8.0x10 05
4.0x10 05
0.0000
D
Treg cells/ lymph node
2.0x10 05
1.5x10 05
1.0x10 05
5.0x10 04
*

3.2.1.5 Density and location of infiltrating lymphocytes in tumours in dKO and tKO compared with WT mice

Immunofluorescent staining followed by confocal microscopy was used to identify lymphocyte subsets and their density and location within tumours (Figure 3.5, 3.6, 3.7). As shown by the FACS data, WT tumour sections were characterised by a high proportion of CD4 T cells and $CD4^{+}Foxp3^{+}$ Tregs (Figure 3.5B,C) and a low proportion of CD8 T cells; lymphocytes, particularly the $CD8^{+}$ T cells, were located at the margins of the tumour tissue (Figure 3.5A). By comparison, in dKO tumour sections, there were fewer CD4 T cells and Tregs, but more $CD8^{+}$ T cells (Figure 3.6). As already observed in the FACS analysis, a significant number of CD8 T cells could be identified in tumours hosted by the $Foxp3^{+}$Treg-deficient tumours (Figure 3.7B), out-numbering CD4 T cells; additionally they were distributed in deep into the tumours (Figure 3.7A), as has also been reported in murine cancers after Foxp3 depletion using diphtheria toxin (Li *et al.* 2010), and in human cancer studies, where the position and density of lymphocytes have been used as indicators for cancer prognosis (Galon *et al.* 2006).

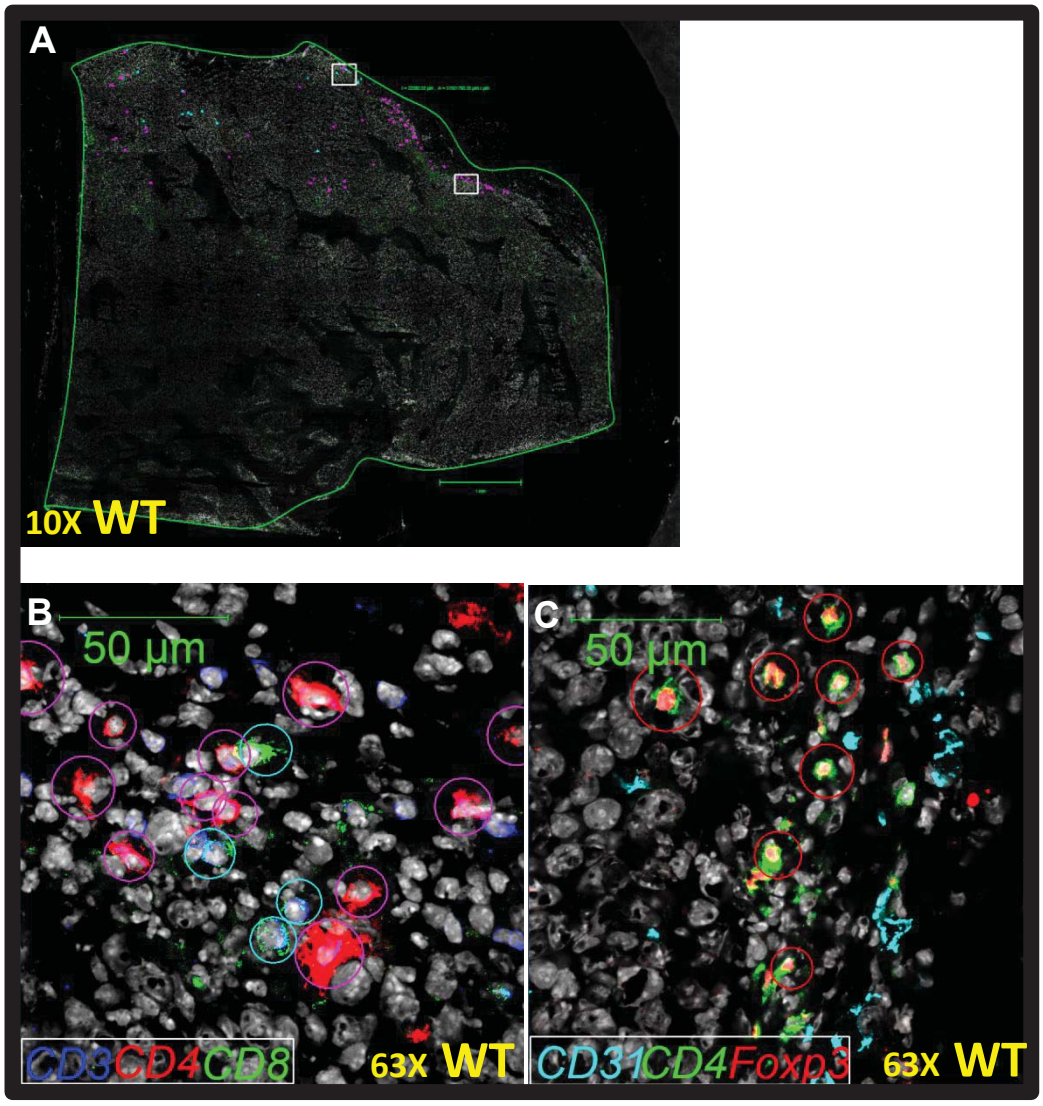

Figure 3.5: CD4+ T cells and Tregs are predominant subsets in melanoma transfected WT tumours.

Tile scan confocal pictures of representative WT (C57BL/6-Ly5.1)tumours, day 21.(A) Low power tile scan confocal picture (X10, 10X8). High power tile scan confocal pictures (X63, 2X2), (B) methanol fixed sections were stained for CD3 (blue), CD4 (red), and CD8 (green); (C) stained with CD4 (green) Foxp3 (red) and CD31 (turquoise). Schematisation of CD4 T cells in magenta circles, CD8 T cells in turquoise circles and Tregs in red circles. Data represent (n>5) of three independent experiments.

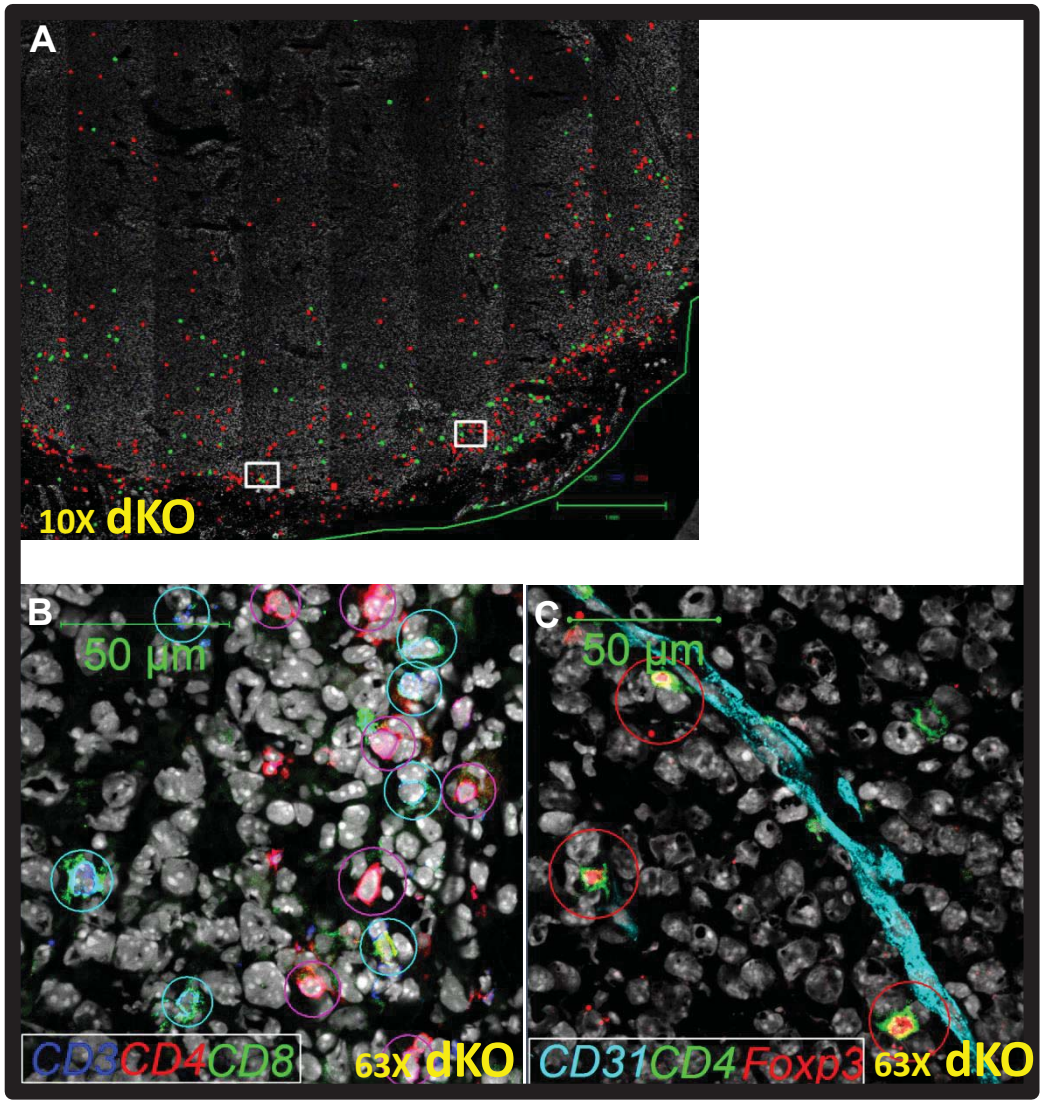

Figure 3.6: deficiency to CD30 and OX40 reduce Tregs infiltration into melanoma transfected dKO tumours.

Tile scan confocal pictures of representative dKO ($CD30^{KO}OX40^{KO}$) tumours, day 21.(A) Low power tile scan confocal picture (X10, 11X8). High power tile scan confocal pictures (X63, 2X2), (B) methanol fixed sections were stained for CD3 (blue), CD4 (red), and CD8 (green); (C) stained with CD4 (green) Foxp3 (red) and CD31 (turquoise). Schematisation of CD4 T cells in magenta circles, CD8 T cells in turquoise circles and Tregs in red circles. Data represent (n>5) of three independent experiments.

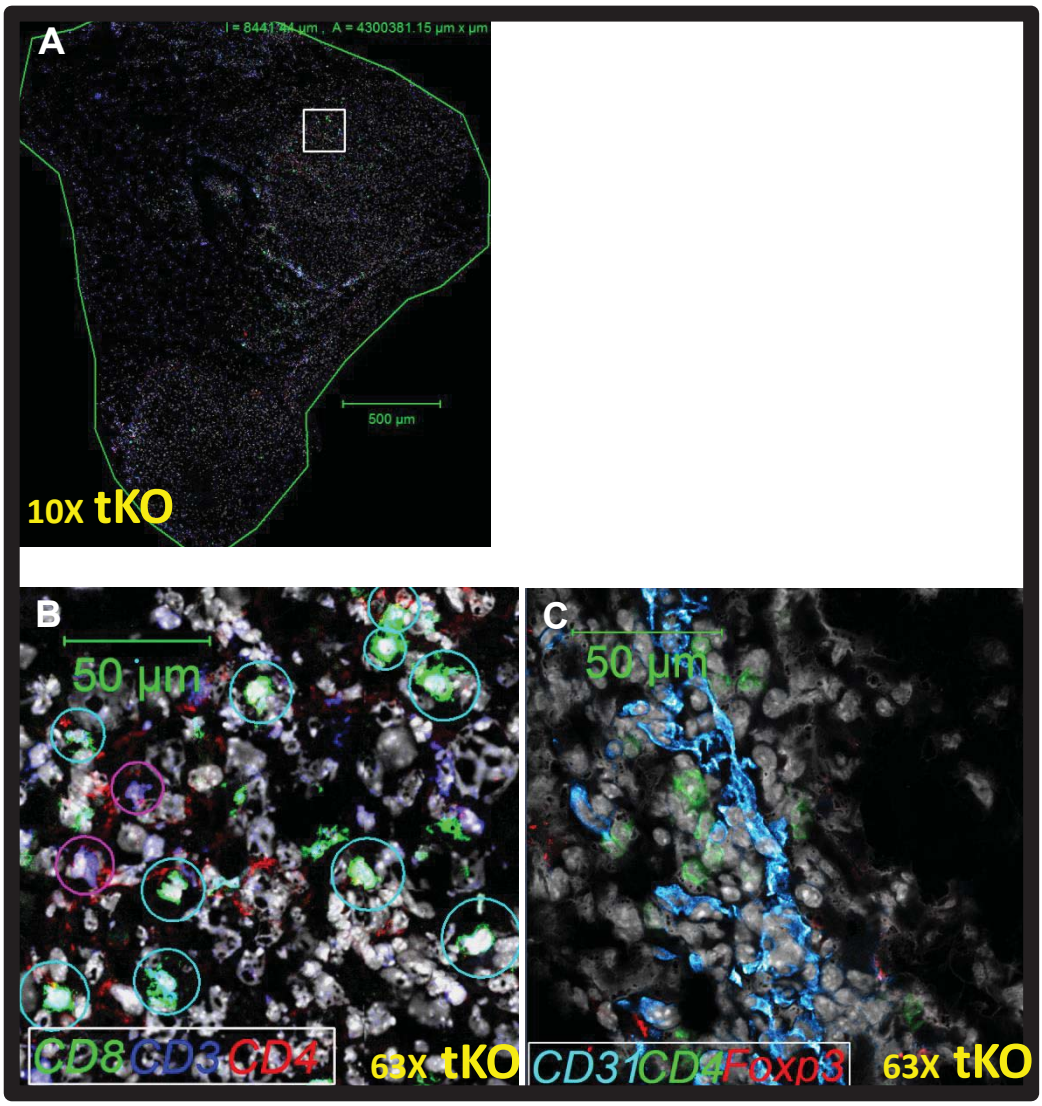

Figure 3.7: CD8+ T cells are predominant in melanoma transfected tKO tumours

Tile scan confocal pictures of representative tKO ($CD30^{KO}OX40^{KO}$ $FoxP3^{KO}$) tumours, day 21.(A) Low power tile scan confocal picture (X10, 7X5). High power tile scan confocal pictures (X63, 2X2), (B) methanol fixed sections were stained for CD3 (blue), CD4 (red), and CD8 (green); (C) stained with CD4 (green) Foxp3 (red) and CD31 (turquoise). Schematisation of CD4 T cells in magenta circles, CD8 T cells in turquoise circles and Tregs in red circles. Data represent (n>5) of three independent experiments.

3.2.2 The anti-tumour response in tKO mice depleted of CD8-T cells

3.2.2.1 Experimental protocol

In a pilot study, 5 x 10^5 B16-F10 cells were injected subcutaneously into the right dorsal flank of $CD30^{KO}OX40^{KO}Foxp3^{KO}$ (tKO) female mice aged 6-8 weeks old. Tumours were allowed to establish for two weeks; mice were then randomly assigned into two groups and injected i.p. with either control (PBS) or CD8 depleting Abs 500µg/mice (see section 2.10), once each on d14 and d18. Tumour volumes were measured before and after antibody injection. All mice were culled at day 26.

3.2.2.2 Tumour growth kinetics in tKO mice after $CD8^+$ T cell depletion

We have already shown (above) that $CD30^{KO}OX40^{KO}Foxp3^{KO}$ (tKO) mice were resistant to B16-F10 melanoma and that they exhibited significant infiltration of $CD8^+$ T cells into their tumours. The experimental protocol (section 3.2.2.1 above) was designed to test the CD8 dependence of the tumour resistance. 7 days after the first injection of depleting antibody, the tumour mean volume reached approximately 400mm^3, expanding to approximately 1000mm^3 5 days after a second mAb injection. In contrast, the tKO control tumours were approximately 100mm^3 and 250mm^3 at the respective time points (Figure 3.8A). The total pooled tumour weights, when the experiment was terminated at 4 weeks, were in the ratio 3:1 treatment: control (1250mg treated: 350mg control) (Figure 3.8B). Flow cytometric analyses of the excised tumour tissues confirmed the depletion of CD8 lymphocytes (Figure 3.8C).

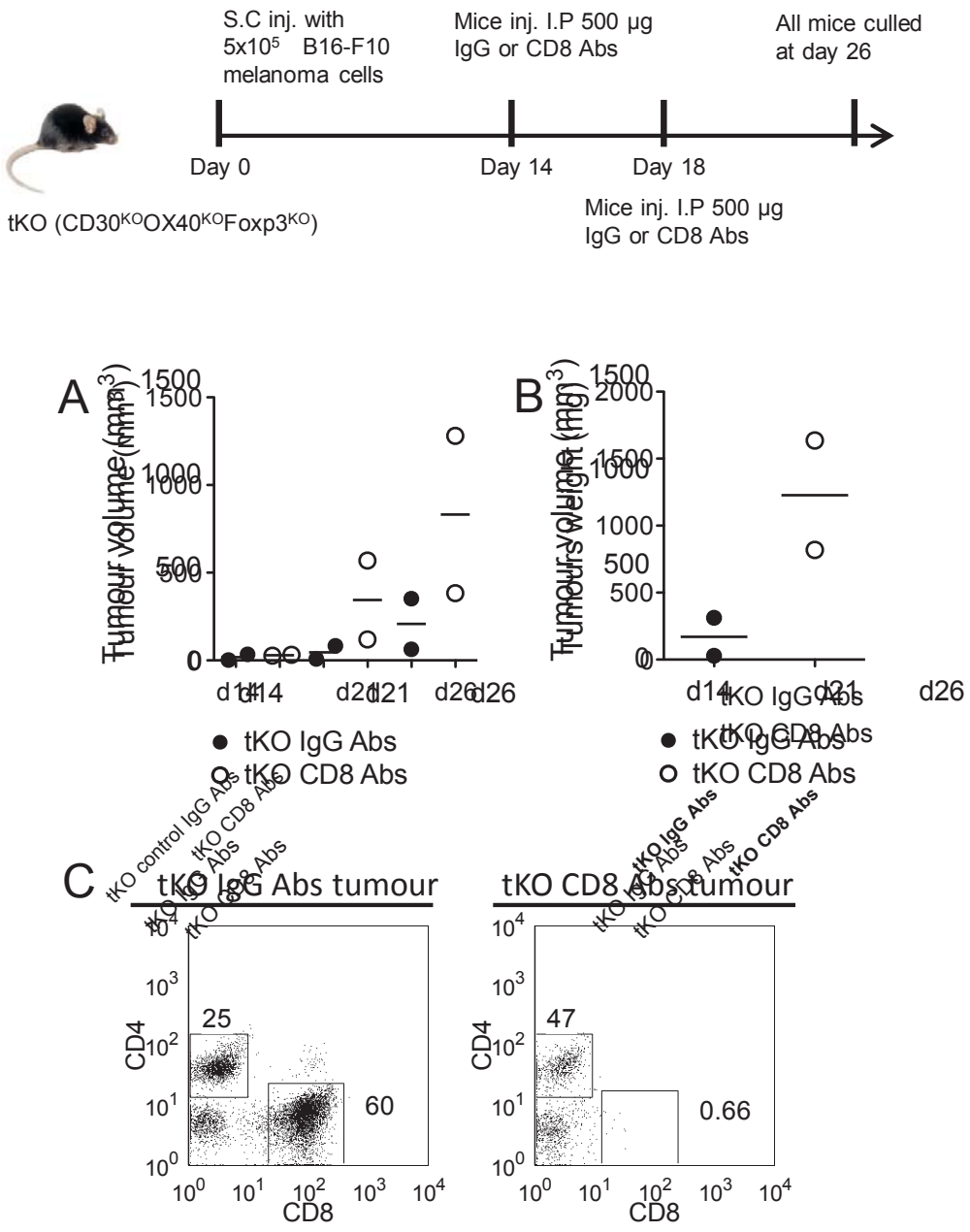

Figure 3.8: The anti-tumour response in tKO mice is CD8-dependent

5 x 10^5 B16F10 cells were injected subcutaneously into the right flank of tKO mice. At d14, mice were injected i.p. with either control or CD8 depleting Abs (A) tumour volume at d14, d21, and d26, (B) tumour weight at excision, (C) FACS analysis of tumour infiltrating T cells, gated on live $CD45^+CD3^+$ cells.

3.2.3 The effect of anti PD-1 blockade on tumours in FoxP3^{KO} mice

3.2.3.1 Experimental protocol

WT (BoyJ), CD30^{KO}OX40^{KO} (dKO) and CD30^{KO}OX40^{KO}Foxp3^{KO} (tKO) female mice, aged 6-8 weeks, were injected subcutaneously with 5x10^{5} B16-F10 melanoma cells on the right dorsal flank. 3 days later, after establishment of tumours, the mice were treated I.P. with monoclonal antibodies twice per week until the end of the experiment on day 21, WT anti-(CTLA-4, PD-1, CD30L, OX40L) mAbs, dKO anti-(CTLA-4, PD-1) mAbs, tKO anti-PD-1 mAbs and their controls with anti-IgG mAbs. The dynamics of tumour growth were monitored weekly for 3 weeks using callipers, after which all mice were culled, tumours excised and weighed, and infiltrates analysed.

3.2.3.2 B16-F10 melanoma cell line gene expression of PD-L1, PD-L2, CD30L and OX40L

B16-F10 supresses the CD8 T cell response via PD-L1 or PD-L2 (Dong *et al.* 2002, Iwai *et al.* 2002, Keir *et al.* 2008). We aimed to use PD-1 blocking antibodies to restore the CD8-dependent tumour response in tKO, so needed to determine which PDL molecules were present. Using traditional polymerase chain reaction (PCR) and real time quantitative RT-qPCR we compared mouse biochain tissue and WT splenocytes with the B16 melanoma cell line to examined its PD-L1 and PD-L2 gene expression. PCR and gel electrophoresis showed expression of *PDC1L1* gene encoding for PD-L1 (CD274) but not *PDCD1L2*, which encodes for PD-L2 (CD273)

(Figure 3.9A). Marked mRNA levels correspondent to the PD-L1 surface receptor profile were also revealed using qPCR (Dong *et al.* 2002) (Figure 3.9B).

We also investigated CD30L and OX40L genes in B16-F10 melanoma to verify that we are specifically targeting CD4 T cells but not melanoma cells. Adult lymphoid tissue inducer cells express CD30L and OX40L abundantly and can be used as a positive control with B16 melanoma (Kim *et al.* 2008, Withers *et al.* 2009). There was no expression of CD30L or OX40L genes on B16-F10 cell line whereas adult LTi and mouse universal biochain demonstrated strong expression of CD30L and OX40L in gel electrophoresis and RT-qPCR analysis (Figure 3.9C,D,E).

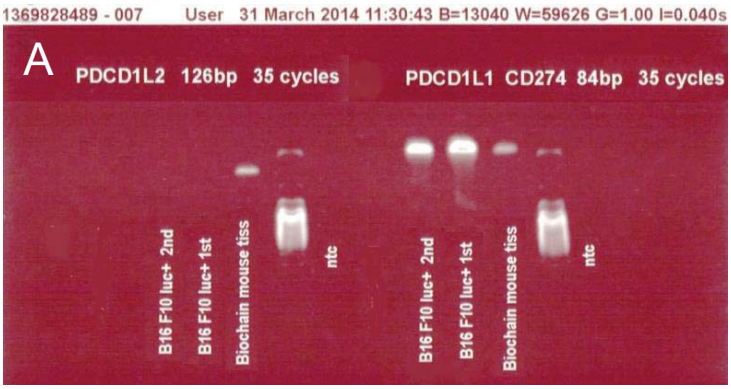
1369828489 - 007 User 31 March 2014 11:30:43 B=13040 W=59626 G=1.00 I=0.040s
A
PDCD1L2 126bp 35 cycles
PDCD1L1 CD274 84bp 35 cycles
B16 F10 luc+ 2nd
B16 F10 luc+ 1st
Biochain mouse tiss
ntc
B16 F10 luc+ 2nd
B16 F10 luc+ 1st
Biochain mouse tiss
ntc

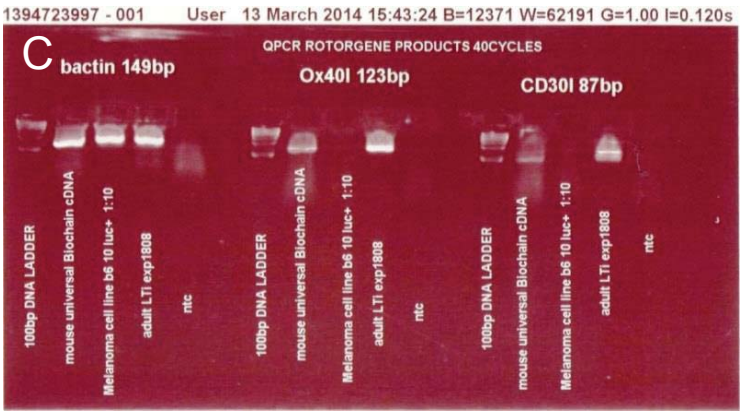
1394723997 - 001 User 13 March 2014 15:43:24 B=12371 W=62191 G=1.00 I=0.120s
C
QPCR ROTORGENE PRODUCTS 40CYCLES
bactin 149bp
Ox40l 123bp
CD30l 87bp
100bp DNA LADDER
mouse universal Biochain cDNA
Melanoma cell line b6 10 luc+ 1:10
adult LTi exp1808
ntc
100bp DNA LADDER
mouse universal Biochain cDNA
Melanoma cell line b6 10 luc+ 1:10
adult LTi exp1808
ntc
100bp DNA LADDER
mouse universal Biochain cDNA
Melanoma cell line b6 10 luc+ 1:10
adult LTi exp1808
ntc

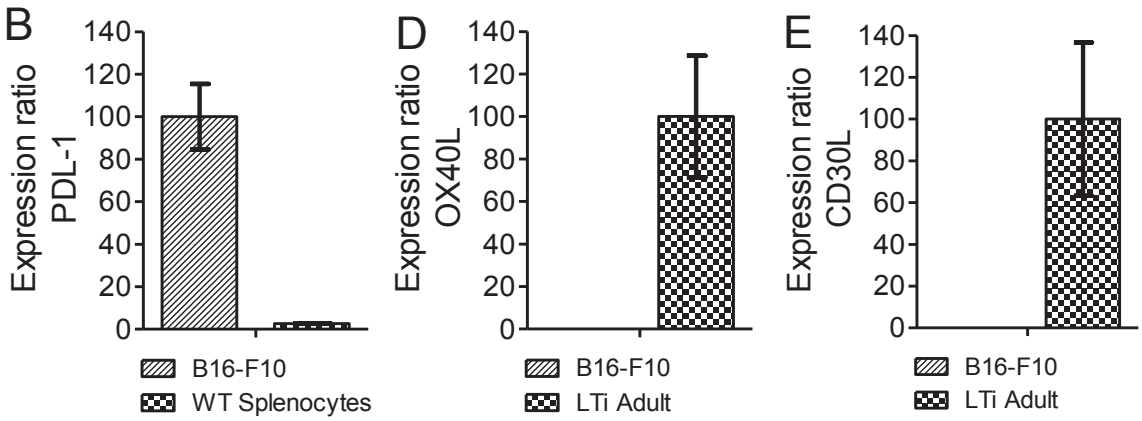
B
Expression ratio PDL-1
140
120
100
80
60
40
20
0
B16-F10
WT Splenocytes
D
Expression ratio OX40L
140
120
100
80
60
40
20
0
B16-F10
LTi Adult
E
Expression ratio CD30L
140
120
100
80
60
40
20
0
B16-F10
LTi Adult

3.2.3.3 The immunotherapeutic effect of blocking antibodies on B16 melanoma growth in WT, dKO and tKO mice.

We sought to investigate the possibility of augmenting the tKO anti-tumour response, in which tumours were significantly infiltrated with a $CD8^{+}PD\text{-}1^{+}$ T cell subset. Because tumour growth was impaired in tKO, PD-1 blockade in tKO had no marked effect. However, blocking antibody combinations anti-(CTLA-4,PD-1,CD30L, and OX40L) mAbs in WT mice and anti-(CTLA-4,PD-1) mAbs in dKO mice resulted in substantial reduction of melanoma growth compared with their controls (Figure 3.10A). A significant reduction in tumour measured volumes occurred by day 15 in WT and dKO treated mice compared with those receiving control antibodies, and continued steadily until the end of the experiment on day 21. Tumour weights pooled from WT ($p<0.009$), dKO ($p<0.004$) and tKO ($p<0.004$) treated mice showed significant reductions in comparison to WT and dKO untreated counterparts, whereas no difference was found between tKO treated and tKO untreated mice (Figure 3.10 B,C).

The effect of anti-CD30L and anti-OX40L mAbs alone or in combination has not been investigated in terms of anti-tumour response or autoimmune toxicity as controls compared to their affect when associated with anti-CTLA-4 or anti-PD-1 alone or combined due to the limited amount of antibodies we had. Therefore, we selected the combination that we thought would be most effective based on our studies in knockout mice (Gaspal et al. 2011). Data from CD30KOOX40KOFoxp3KO model suggests contribution of both OX40 and CD30 signals in the prevention of CD4 autoimmunity in Foxp3 deficient mice but the role of OX40 is dominant (Gaspal et al.

2011). The disease onset and severity was delayed in mice deficient to OX40 but sufficient of CD30 into (2.5-3) months compared to mice deficient to CD30 but sufficient to OX40 which developed earlier sever autoimmunity signs between (1.5-2) months. However, the Foxp3KO disease was abrogated when OX40 and CD30 genes depleted and this was mimicked when OX40L and CD30L blocking antibodies were used (Gaspal et al. 2011)

Figure 3.10: The effect of monoclonal antibodies on B16 melanoma growth in WT, dKO and tKO mice.

3 days after B16 injection, mice were treated with monoclonal antibodies. (A) Tumour volume was measured at least twice weekly using callipers and the mean of three readings recorded for each mouse in each group; graph plots show median values (B) tumour weights at harvest on d21; each data point represents one mouse; bars show median values (C) representative excised tumours. Statistical analysis was performed using the Mann Whitney non parametric test. Data are representative of three independent experiments; n=6,4,6,5,6,4 respective to the groups in the order listed; * ,** indicate significance $p<0.05$ and $p<0.01$ respectively.

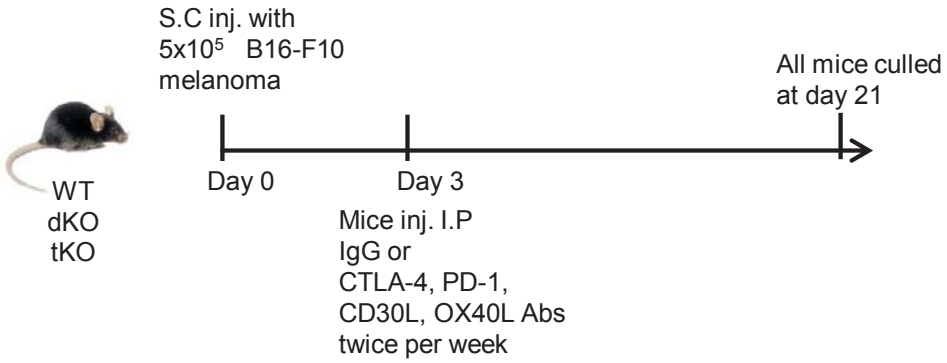
S.C inj. with
5x10^5 B16-F10
melanoma
All mice culled
at day 21
WT
dKO
tKO
Day 0
Day 3
Mice inj. I.P
IgG or
CTLA-4, PD-1,
CD30L, OX40L Abs
twice per week

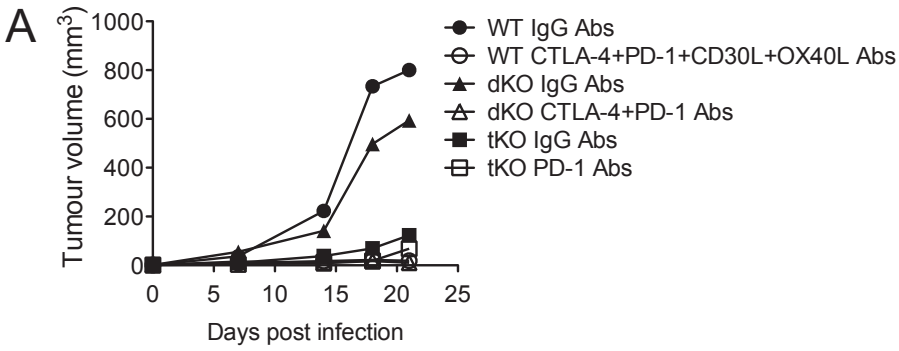
A
Tumour volume (mm3)
1000
800
600
400
200
0
0 5 10 15 20 25
Days post infection
WT IgG Abs
WT CTLA-4+PD-1+CD30L+OX40L Abs
dKO IgG Abs
dKO CTLA-4+PD-1 Abs
tKO IgG Abs
tKO PD-1 Abs

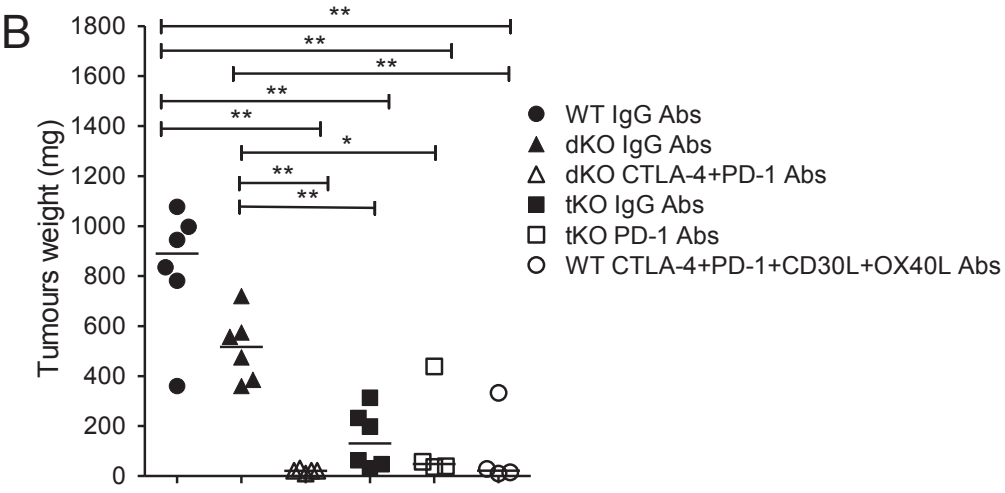
B
Tumours weight (mg)
1800
1600
1400
1200
1000
800
600
400
200
0
**
**
**
**
**
*
**
**
WT IgG Abs
dKO IgG Abs
dKO CTLA-4+PD-1 Abs
tKO IgG Abs
tKO PD-1 Abs
WT CTLA-4+PD-1+CD30L+OX40L Abs

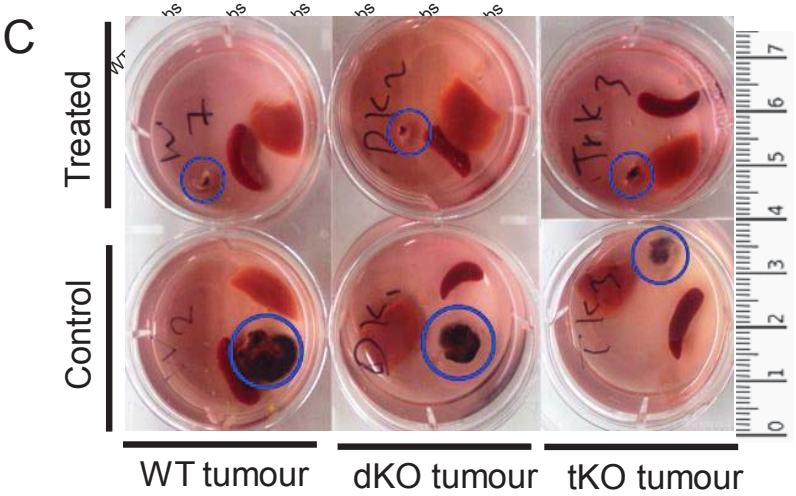
C
Treated
Control
WT tumour
dKO tumour
tKO tumour

3.2.3.4 The effect of blocking antibodies on the lymphocyte subsets infiltrating tumours

The effect of blocking antibodies on tumour-infiltrating T cells was investigated using flow cytometry for phenotype analysis and quantification (Figure 3.11). Compared with their anti-IgG mAbs treated controls, blocking mAbs treated WT mice showed a trend towards decreased $CD4^+$ T cells due to the absence of CD30 and OX40 signals, (Figure 3.11A,B). Adding anti-CTLA-4 mAbs to the treatment regimen of WT and dKO mice resulted in the depletion of tumour infiltrating $FoxP3^+$Tregs, as has been demonstrated in melanoma lesions (Simpson *et al.* 2013). The calculated Treg cells/g of WT and dKO treated tumours were significantly reduced compared with their controls, ($p<0.03$) and ($p<0.008$) respectively, but the reduction was greater ($p<0.004$) in treated dKO versus WT control (Figure 3.11A,D). Inhibition of PD-1, which is clearly expressed on tumour-infiltrating CD8 T cells, particularly in tKO mice, resulted in significantly increased CD8 infiltrates into tKO tumours in comparison with WT control ($p<0.009$), and that was also more pronounced than the difference between tKO and WT controls versus ($p<0.01$). Between tKO treated and control treated mice, however, the difference was marginal. As in the tKO mice, the anti-(CTLA-4,PD-1) combination in dKO and anti-(CTLA-4,PD-1,CD30L,OX40L) combination in WT both affected the migration of CD8 T cells into tumours significantly relative to their WT IgG treated counterparts (Figure 3.11C).

Figure 3.11: Flow cytometric analysis of the effect of monoclonal antibodies on tumour infiltrating cell populations in WT, dKO and tKO mice.

Tumours were harvested from all mice, digested and cell suspensions were surface stained, then fixed and permeabilised and FoxP3 stained (see Section 2.6) (A) Contour plots of lymphocytes gated on live $CD45^+CD3^+$ cells, showing expression of CD4, CD8, CD25 and FoxP3 expression on $CD4^+$ T cells and PD-1 expression on $CD8^+$ T cells; (B,C,D) Plots of infiltrating cell densities from individual tumours, bars show median values; (B) $CD4^+$ T cells, (C) $CD8^+$ T cells, (D) $FoxP3^+$ T cells. Statistical analysis was performed using the Mann Whitney non parametric test. Data are representative of three independent experiments, n=6,4,6,5,6,4 in respect of groups in order listed. * ,** indicate significance $p<0.05$ and $p<0.01$ respectively.

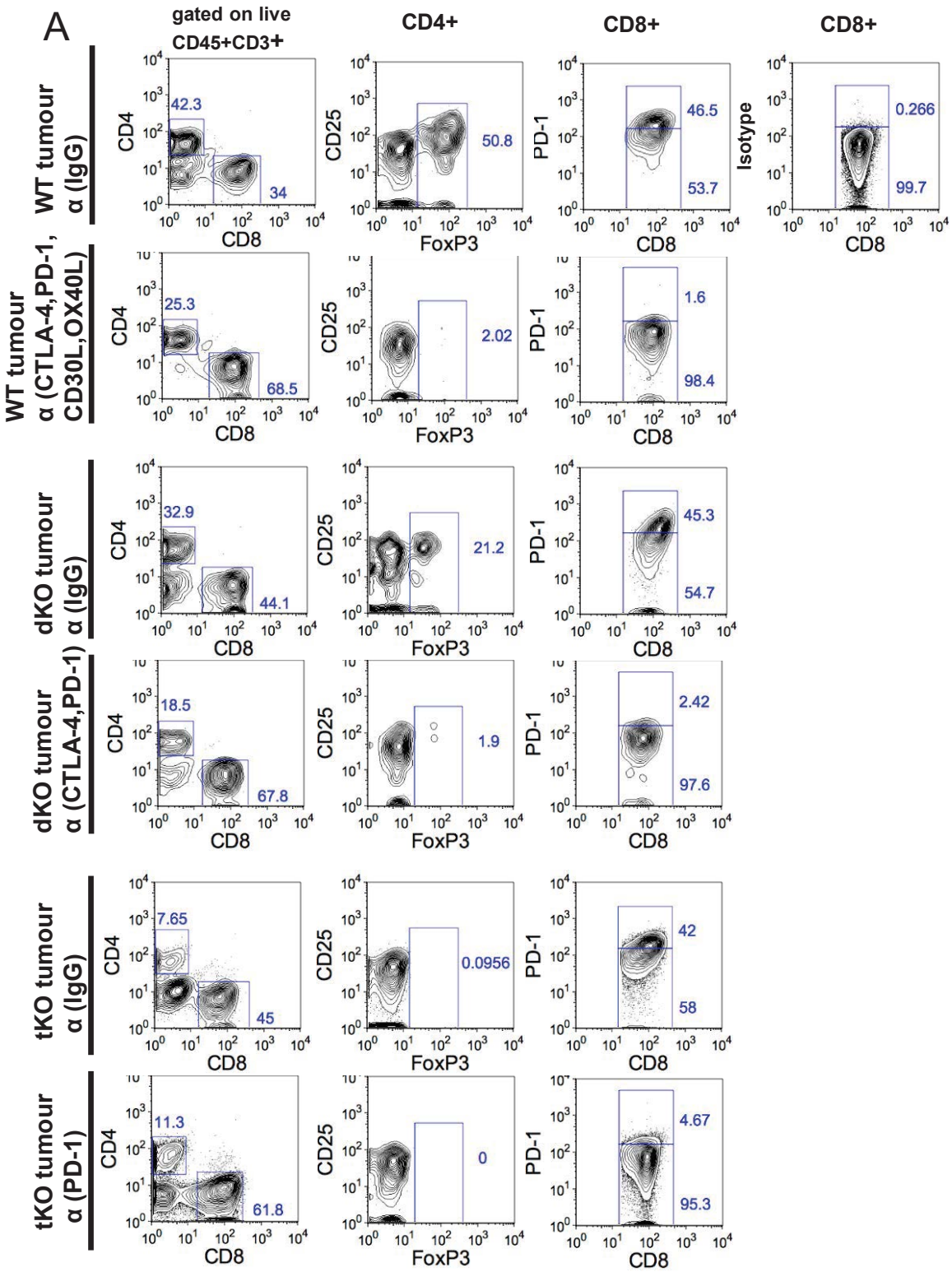
A
gated on live CD45+CD3+
CD4+
CD8+
CD8+
WT tumour α (IgG)
WT tumour α (CTLA-4,PD-1, CD30L,OX40L)
dKO tumour α (IgG)
dKO tumour α (CTLA-4,PD-1)
tKO tumour α (IgG)
tKO tumour α (PD-1)
CD4
CD8
CD25
FoxP3
PD-1
Isotype
42.3
34
50.8
46.5
53.7
0.266
99.7
25.3
68.5
2.02
1.6
98.4
32.9
44.1
21.2
45.3
54.7
18.5
67.8
1.9
2.42
97.6
7.65
45
0.0956
42
58
11.3
61.8
0
4.67
95.3

3.2.3.5 The effect of blocking antibodies on the secretion of IFNγ by CD8 T cells

The use of PD-1 blockade to restore function - IFNγ production - to PD-1^{high} CD8^{+} T cells has been documented (Barber *et al.* 2006), but due to the remarkably small size of the treated tumours, there were insufficient cells to examine cytokine production by tumour-infiltrating T cells. Lymphoid organs are the sites for T cell activation, so we used spleens to investigate the capacity of CD8 T cells to produce the effector cytokine IFNγ. For this, *in vitro* stimulated splenocytes for the treated and untreated mice were analysed for the expression of the activation marker CD44 and the production of IFNγ cytokine. Gating on CD8 T cells, IFNγ production in WT and dKO treated mice was two-fold greater than that in their anti-IgG controls, whereas in tKO anti-PD-1 treated mice it was three-fold higher than the WT and dKO controls and two-fold higher than the tKO control (Figure 3.12A). The frequency of CD8 T cells of CD44^{high}IFNγ^{high} phenotype in WT and dKO treated mice was around 20% and in tKO treated mice more than 30%, while the frequency for WT and dKO controls was approximately 8% and for the tKO control 20% (Figure 3.12B). As an indicator of activation and immune response, spleen weights were also recorded (Figure 3.12C). Generally, mice treated with blocking antibodies exhibited higher spleen weights (approximately 110mg) than their control mice (approximately 80mg).

Figure 3.12: The effect of monoclonal antibodies on IFNγ production by $CD8^+$ T cells in WT, dKO and tKO mice.

Splenocytes suspensions were stimulated *in vitro* on CD3 coated plates in the presence of CD28 and Golgi stop for 4hrs. After incubation, cells were surface stained, fixed, permeabilised and IFNγ stained (see Section 2.6). (A) FACS contour plots of splenocytes gated on $CD3^+CD8^+$ T cells and showing expression of CD44 and IFNγ on CD8 T cells in mAbs treated mice (right) and their controls (left). (B) Frequency of $CD44^+IFN\gamma^+$ CD8 T cells in spleens, (C) Spleen weights. Data points on scatter plots represent individual spleens, and bars show median values. Statistical analysis was performed using the Mann Whitney non parametric test. Data are representative of two independent experiments, n=3,4,4,5,3,4 respective to the groups in the order listed.

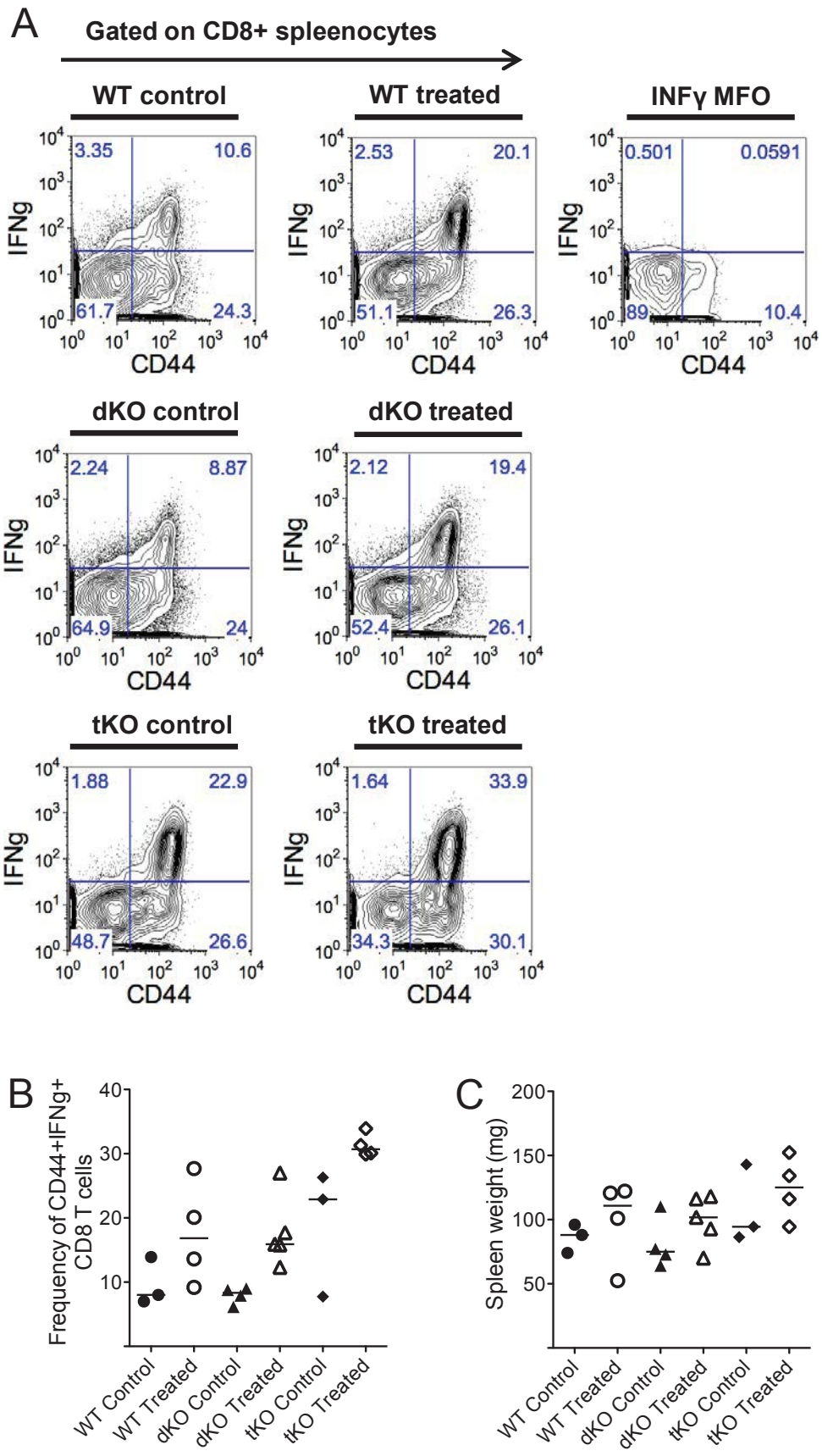
A
Gated on CD8+ spleenocytes
WT control
WT treated
INFγ MFO
dKO control
dKO treated
tKO control
tKO treated
IFNg
CD44
3.35
10.6
61.7
24.3
2.53
20.1
51.1
26.3
0.501
0.0591
89
10.4
2.24
8.87
64.9
24
2.12
19.4
52.4
26.1
1.88
22.9
48.7
26.6
1.64
33.9
34.3
30.1
B
Frequency of CD44+IFNg+ CD8 T cells
C
Spleen weight (mg)
WT Control
WT Treated
dKO Control
dKO Treated
tKO Control
tKO Treated

3.3 Discussion

3.3.1 Mice deficient in Foxp3 Tregs (tKO mice) are resistant to B16-F10-luc^{+} melanoma tumours and are highly infiltrated with CD8 T cells that express abundantly the inhibitor PD-1.

FoxP3 Treg deficient mice die as a result of severe multiorgan autoimmunity by the age of 6 weeks; therefore, we used our FoxP3^{KO}dKO (tKO) mice to investigate the immune response to B16-F10 melanoma model in a Treg deficient host. The tKO mice showed significant resistance to tumour growth, in agreement with the interpretation of numerous studies in various cancer types - melanoma (Klages *et al.* 2010, Jacobs *et al.* 2012), ovarian cancer (Curiel *et al.* 2004) breast cancer (Gobert *et al.* 2009) and hepatocellular carcinoma (Zhou *et al.* 2009) - that the suppression of cytotoxic T cells by Tregs contributes to tumour progression. However, other studies, for example on colon cancer and follicular lymphoma, have reported that a high frequency of Tregs in the tumour signals a favourable prognosis for the cancer outcome (Carreras *et al.* 2006, Salama *et al.* 2009). They propose that in some chronic inflammatory diseases, Tregs are essential to regulate inflammation triggered by microbial antigens, genetic instability and autoimmunity, and subsequently protect the body against tumour-associated inflammation, for example *H. pylori* bacteria and Th17 inflammation promoting cancers (Mantovani *et al.* 2008, Stewart *et al.* 2013). On the other hand, a recent study showed that Tregs promoted IL-17 driven toxigenic *Bacteroides fragilis* carcinogenesis in human by limiting IL-2 in the colon and thus initiating the development of Th17 cells which produce IL-17 in response to the bacterium (Geis *et al.* 2015). Current literature therefore points to no simple role for

Tregs as a prognostic factor for tumour progression (Shang *et al.* 2015), especially as confusion can arise when different markers are used for Treg identification or models used for Treg depletion are incomplete (deLeeuw et al. 2012). Our tKO model has the big advantage of providing healthy host mice with a normal life span in the absence of the Treg master regulator gene FoxP3, so that it addresses specifically the contribution of thymic nTregs to tumour prognosis.

The TNFR OX40 is constitutively expressed on Tregs and its contribution to the function of Tregs is controversial. Nonetheless, the kinetics of tumour growth observed in dKO ($CD30^{KO}OX40^{KO}$) mice was slower, and the numbers of infiltrating $CD4^{+}CD25^{+}FoxP3^{+}$ Tregs/g tumour and draining lymph nodes were significantly less than observed in WT mice, suggesting roles for OX40 and CD30 signals in $Foxp3^{+}$ Treg development, homing and suppressive functions. High levels of OX40 expression on thymus Treg progenitors have been shown, and found to contribute specifically to the strengthening of TCR signals that promote Treg development and shape its repertoire (Mahmud *et al.* 2014); synergy with CD30 signals may enhance the effect of OX40 not only on $CD4^{+}$ T cell effector functions but also on $FoxP3^{+}$ Treg development and suppressive function (Withers *et al.* 2011). We found that the absence of OX40 and CD30 resulted in a significant reduction in the number of Tregs infiltrating dKO tumours, suggesting that OX40 might be a signal for Tregs to home to tumours; this would fit with observations on human hepatitis cirrhotic or tumour lesions, where a highly suppressive $OX40^{+}FoxP3^{+}$ Treg phenotype was expanded, in comparison with non-suppressive $OX40^{-}FoxP3^{+}$ Tregs occurring in non-cirrhotic areas in the same liver tissue (Piconese *et al.* 2014). OX40 and CD30 signals are essential for CD4 T cell survival (Withers *et al.* 2009, Withers *et al.* 2012). Here we

have found in dKO and tKO tumours that CD4 T cells were significantly reduced in number, and while this difference was marginal in the inguinal draining lymph nodes, it confirms the dependence of CD4 effector/memory function on those TNFR signals. Further, in dKO lymph nodes, Treg numbers were also significantly decreased, possibly due to the impairment of the Treg priming phase and subsequent generation and expansion of tumour specific T cells in the dKO and tKO mice (Tanaka *et al.* 2002). It has also been found in a murine colitis model that $OX40^{-/-}$ Tregs were significantly under-represented in peripheral lymphoid organs as a consequence of induced cell death and inability to accumulate in the intestine and prevent disease, strong indication for a role for OX40 signals in Treg survival (Griseri *et al.* 2010). Taken together with these studies, the reduced numbers of Tregs that we saw in dKO and tKO tumours was associated with reduced tumour growth, is likely to have contributed the more successful anti-tumour to effect in the KO mice

CD8 T cells are the sharp end of the mammalian immune defence against viruses and tumours, and the density and location of those CD8 T cells in relation to $FoxP3^{+}$ Treg numbers have been found to be predictors for tumour prognosis because tumour reactive CD8 T cell immunity is dampened by immune tolerogenic Tregs (Chen *et al.* 2005, Galon *et al.* 2006). We show here that depletion of FoxP3 Tregs, as in tKO mice, or disruption of their suppressive function, as in dKO mice, increased significantly (tKO mice), or moderately (dKO mice), the number of CD8 T cells infiltrating the inner regions of tumours and correlated with limitation of tumour progression. Those CD8 T cells overcame the suppressive barriers of tumour associated Tregs to migrate deeper into tumour and attenuate tumour progression. The ratio of CD8 T cells to Tregs can be enhanced by vaccination (Klages *et al.*

2010) and potentiate tumour rejection. However, the infiltrating CD8 T cells are known to express PD-1 after activation and consistent exposure to melanoma antigens, a fact which has been found to be exploited by the B16 tumour through either intrinsic expression of the ligand PD-L1 (Dong *et al.* 2002) as we saw (section 3.2.3.2 above) or by induction of PD-L1 on tumour cells by CD8 T cells in an IFNγ dependent manner which subsequently deactivates tumour cytotoxic effects of CD8 T cells. (Spranger *et al.* 2013, Abiko *et al.* 2015)

3.3.2 Inhibition of melanoma growth in tKO mice is CD8 T cell dependent

Resistance to B16-F10 melanoma in our tKO mice was CD8 dependent because depletion of CD8 T cells in pre-established tKO tumours abrogated this resistance, and mice demonstrated a notable acceleration in tumour growth compared to the CD8 non-depleted tKO controls. Similar results have been shown in B7 transgenic melanoma where the elimination of Tregs permitted CD4 T cell independent tumour rejection (Townsend and Allison 1993, Nagai *et al.* 2004).

3.3.3 PD-1 blockade in Foxp3 Treg deficient (tKO) mice mimics the blockade combinations (CTLA-4,PD-1) in dKO mice and (CTLA-4,PD-1,OX40L,CD30L) in WT mice, to abrogate B16 melanoma growth

The anti-tumour immune response in tKO mice was augmented after targeting the highly infiltrated $CD8^{+}PD\text{-}1^{+}$ T cells with anti-PD-1 blocking mAbs, which resulted in the reduction of tumour volume and weight and enhancement of CD8 T cell

infiltrates, as well as activating CD8 T cells for the production of the effector cytokine INFγ. Restoring and augmenting the CD8 immune response has also been shown to be important in the resolution of chronic viral infection and tumours after PD-1 blockade (Iwai *et al.* 2002, Barber *et al.* 2006, Flies *et al.* 2011). However, the Treg deficiency in tKO mice obviates the effect of anti-PD-1 and anti-CTLA-4 mAb treatment; therapeutically therefore, the use of mAbs treatment in dKO and WT mice were of interest. CTLA-4 has been proven as the main functional effector for Tregs (Wing *et al.* 2008) and adding anti-CTLA-4 mAbs to anti-PD-1 mAbs for the treatment of dKO tumours showed a significant objective response compared to their counterpart controls. This was characterised by significant depletion of intra-tumour Tregs and considerable boosting of CD8 T cell infiltrates and IFNγ production, resulting in tumour rejection. The capacity of anti-CTLA-4 mAbs for selective depletion of Tregs (Simpson *et al.* 2013) and its broad synergetic effect with anti-PD-1 in melanoma rejection has been demonstrated in pre-clinical and clinical studies (Curran *et al.* 2010, Larkin *et al.* 2015). Strikingly, the fourfold combination of treatments anti-(CTLA-4,PD-1,CD30L and OX40L) mAbs in WT mimicked what we have seen in dKO and tKO treated mice.

3.3.4 Conclusion

In conclusion, our tKO model provides an excellent model for studying the role of nTregs in tumour immune responses. Our tKO mice model showed resistance to B16-F10 melanoma growth; tumour resistance was less pronounced in the dKO model, confirming the role of nTregs in tumour progression and the role of CD30 and OX40 in Treg function. The resistance of tKO mice to tumours is CD8 dependent and can be augmented by PD-1 blockade. It is of therapeutic relevance that this can be

imitated in dKO and WT by using (CTLA-4, PD-1) and (CTLA-4,PD-1,CD30L,OX40L) blockade combinations respectively.

Chapter Four Results

Concurrent administration of OX40L and CD30L blocking antibodies eliminates the CD4 driven autoimmune toxicity related to CTLA-4 and PD-1 blockades

4.1 Introduction

In the previous chapter, we showed that the tumour response observed in WT, dKO and tKO mice is mimicked if WT mice are treated with (CTLA-4,PD-1,OX40L and CD30L) blocking antibodies, but further examination is needed to dissect the efficacy of different combinations. Recent human clinical trials used anti-CTLA-4 and anti-PD-1 to target many types of tumours, including melanoma, with objective tumour remission and tumour-free survival being achieved, but with significant autoimmune side effects associated with the loss of the functions blocked by the antibodies, and exacerbated toxicity when used in combination (Hodi *et al.* 2010, Topalian *et al.* 2012, Wolchok *et al.* 2013, Larkin *et al.* 2015, Postow *et al.* 2015, Robert *et al.* 2015b). PD-1^{KO} mice develop late autoimmunity (Nishimura *et al.* 1999), but CTLA-4^{KO} mice suffer early fatal CD4 driven autoimmunity (Chambers *et al.* 1997), suggesting limitations on the blocking of those receptors for cancer immunotherapy. Human and murine models deficient in Foxp3 dependent Tregs show a similar fatal CD4 dependent lymphoproliferative autoimmunity to that found in CTLA-4 deficiency (Bennett *et al.* 2001, Brunkow *et al.* 2001, Wildin *et al.* 2001, Fontenot *et al.* 2003, Khattri *et al.* 2003). We previously showed that this CD4 driven autoimmunity was abrogated in our dKO Foxp3^{KO} mice, in which CD30 and OX40 signals are absent, while the functionality of CD8 T cells was entirely maintained (Gaspal *et al.* 2011). This result fitted neatly with the requirements for improving anti-CTLA-4/anti-PD-1

combination immunotherapy. We therefore aimed to investigate the effects of blocking OX40 and CD30 signals on treatment with anti-CTLA-4 and/or anti-PD-1 mAbs with regard to tumour growth and the possibility of limiting the treatment-associated autoimmune toxicity in WT and C57Bl/6 mice.

4.2 Results

4.2.1 The efficacy of combining OX40L and CD30L blocking antibodies with CTLA-4 and PD-1 treatments on tumour growth and CTLA-4 and PD-1 associated autoimmunity

4.2.1.1 Experimental protocol

In a double blind random study, a cohort of 6-8 week old female C57Bl/6 mice was randomly grouped as shown in (Figure 4.1). The mice were inoculated with $5x10^5$ B16-F10 melanoma cells on the right dorsal flank. Allowing 5 days for tumours to establish, the mice were injected I.P twice per week with anti-(CTLA-4,PD-1,OX40L and CD30L) single therapies or in combinations at doses (200µg, 250µg, 250µg and 250µg) respectively, or with the same equivalent doses of rat anti-IgG mAbs as control, for 42 days. As mentioned before (3.2.3.3), based on our previous studies in genes deficient mice and because of antibodies availability limitations we did not investigate all combinations such as anti-CD30L alone, anti-OX40L alone or in combinations; thus we chose the most relevant combinations for dissecting anti-tumour immune response and autoimmune toxicity associated with monoclonal antibodies therapy. The researcher was blind to which antibodies were injected into the tumour-transplanted groups and the tumour volumes were measured twice per

week using callipers. The mice were culled when the tumour diameter reached 12mm or underwent necrosis and bleeding. The experiment was terminated at day 42. Samples were collected for FACS, liver function tests, autoantibody titration and histopathology analysis (Figure 4.1).

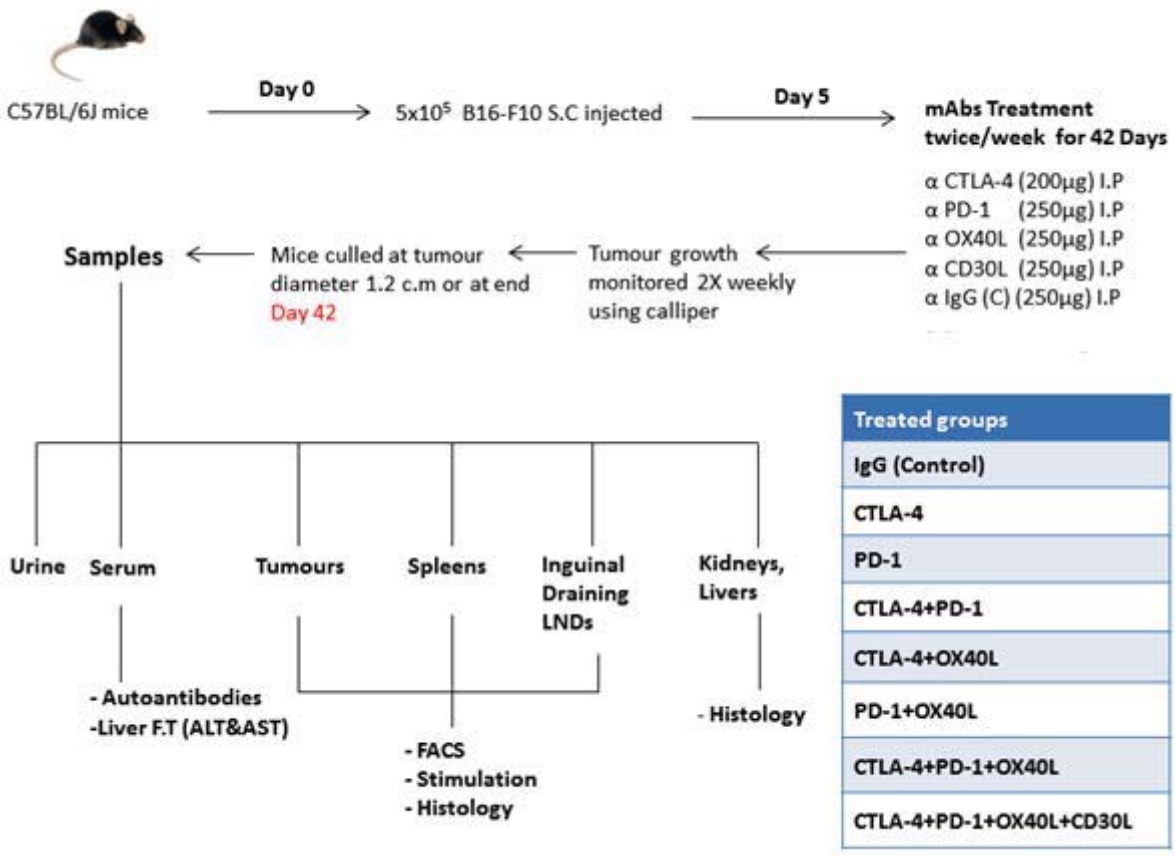

Figure 4.1: The experimental design of studying the efficacy of blocking antibodies on cancer immunotherapy and antibody associated toxicity.

4.2.1.2 B16 melanoma tumour volumes and weights in C57Bl/6 mice treated with OX40L and CD30L mAbs combined with anti-CTLA-4 and anti-PD-1 blockades in various combinations

Weekly calliper measurements of tumour sizes showed that anti-CTLA-4 administration decreased tumour growth compared to the rapid tumour growth in rat anti-IgG treated mice. Comparatively, this was further reduced with anti-PD-1 but with the combined anti-(CTLA-4,PD-1) treatments there was a substantial reduction in B16 melanoma growth (Figure 4.2). Adding anti-OX40L mAb to anti-CTLA-4 mAb slightly slowed down tumour growth relative to anti-CTLA-4 mAb alone, while there was no change when it was added to anti-PD-1. Interestingly, combining anti-OX40L and anti-CD30L with anti-CTLA-4 and anti-PD-1 mAbs showed significant reduction in tumour size, equal to that of (CTLA-4,PD-1) (Figure 4.2).

Tumour weights at harvest from the groups of mice were also assessed with respect to mAb treatments. The mice were sacrificed when their tumours reached the end point (12mm in diameter), or at termination on day 42. Consistent with the tumour sizes, the total tumour weight pooled from the anti-CTLA-4 mAb treated group was less compared to rat anti-IgG group but was not as significantly different as that from the anti-PD-1 mAb injected mice ($p<0.03$) or the anti-(CTLA-4,PD-1) combination therapy ($p<0.0025$) (Figure 4.3). In comparison to anti-CTLA-4 mAb on its own, adding OX40L blockade to anti-CTLA-4 improved its effectiveness markedly ($p<0.03$) while the efficacy of anti-(OX40L,PD-1) was the same as anti-PD-1. Lastly, combining anti-OX40L and anti-CD30L blockades with anti-CTLA-4 and anti-PD-1

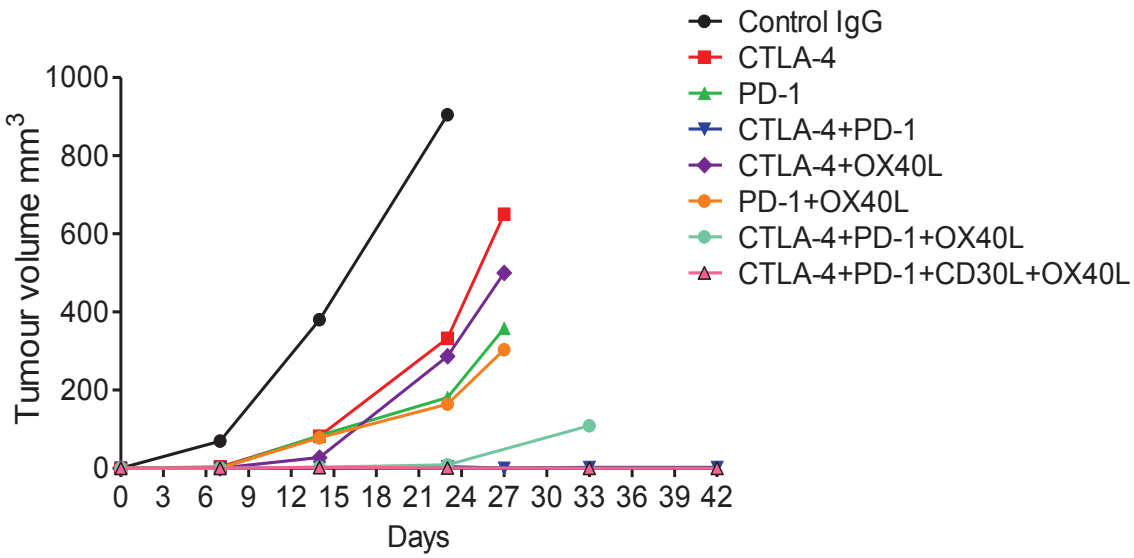

Figure 4.2: Tumour volumes for B16-F10 transfected C57BL/6 mice groups treated with monoclonal blocking antibodies.

Tumour volumes were measured weekly using callipers and the mean of three readings was recorded for each mouse in each group. Graph shows medians, and data are representative of three independent experiments, n=5,7,7,7,5,5,7,7 respective to each group in the order presented.

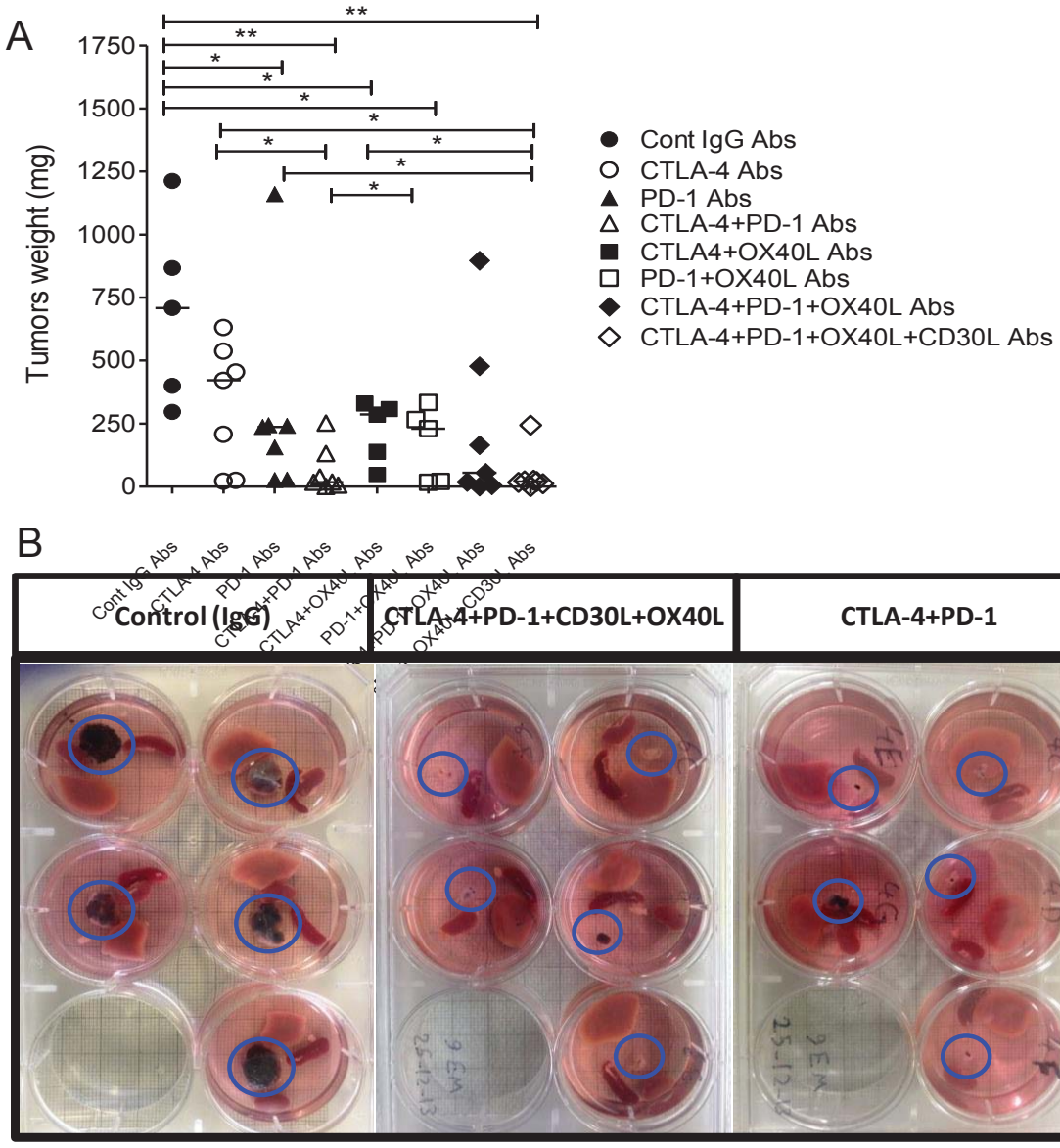
A
Tumors weight (mg)
1750
1500
1250
1000
750
500
250
0
**
**
*
*
*
*
*
*
*
*
*
Cont IgG Abs
CTLA-4 Abs
PD-1 Abs
CTLA-4+PD-1 Abs
CTLA4+OX40L Abs
PD-1+OX40L Abs
CTLA-4+PD-1+OX40L Abs
CTLA-4+PD-1+OX40L+CD30L Abs
B
Control (IgG)
CTLA-4+PD-1+CD30L+OX40L
CTLA-4+PD-1

4.2.1.3 The effect of monoclonal antibody blocking therapies on the survival rate of B16 implanted C57Bl/6 mice

All the mice injected with rat anti-IgG mAbs reached the humane endpoint of the experiment 3-4 weeks after B16-F10 melanoma implantation. Treatment with CTLA-4 or PD-1 blockade alone improved the survival percentage of B16 transplanted mice: 20% (1/5) for anti-CTLA-4 and 29% (2/7) for anti-PD-1 (Figure 4.4). It has been shown in other studies (Pardoll 2012, Robert *et al.* 2015b) that anti-PD-1 therapy confers a greater overall survival advantage than anti-CTLA-4. Including anti-OX40L with anti-CTLA-4 or anti-PD-1 improved the survival rate of the mice marginally: 29% (2/7) and 40% (2/5) respectively. A high survival rate was found in the anti-(CTLA-4,PD-1) group (71%, 5/7), which was enhanced by the addition of OX40L and CD30L blockades to CTLA-4 and PD-1 blockades combined therapy (86%, 6/7).

4.2.1.4 The effect of monoclonal antibody blocking therapies on liver immunopathology of B16 implanted C57Bl/6 mice

Adverse autoimmune side effects, particularly hepatitis and colitis, are associated with prolonged cancer immunotherapy using the combination of CTLA-4 and PD-1 blockades and to a milder degree with the use of anti-CTLA-4 or anti-PD-1 alone (Wolchok *et al.* 2013, Postow *et al.* 2015, Robert *et al.* 2015b). Previous work in our lab showed that blocking of CD30 and OX40 receptors prevented development of lethal liver pathology in our Foxp3 deficient mice (tKO) (Gaspal *et al.* 2011). Therefore, we investigated the effect of single or combined blockades on lymphocytic infiltration into the livers of the B16 transfected mice treated with the mAbs compared with anti-IgG controls.

Compared to the IgG group, all the other mouse groups treated with mAbs showed a degree of liver lymphocyte infiltration, but it was most significant in the mice treated with the anti-(CTLA-4,PD-1) combination ($p<0.002$ (Figure 4.5A,C). Importantly, the addition of OX40L blockade alone ($p<0.005$) or with CD30L blockade ($p<0.002$) resulted in a significant reduction of lymphocyte infiltration into liver tissues, to less than 6% of the grade found in the anti-(CTLA-4,PD-1) combination (Figure 4.5 B,C).

CD4 T cell mediated liver injury has been associated with abnormal levels of the liver biological and functional markers ALT and AST (Nishimura and Ohta 1999); here we found that ALT and AST were elevated in the serum of anti-(CTLA-4,PD-1) mAb treated mice (Figure 4.6A,B). OX40 was recognised as the main driver of CD4 mediated hepatic pathology in Foxp3 deficient mice (Gaspal *et al.* 2011) and here, concurrent blockade of OX40L and CD30L with CTLA-4 and PD-1 has maintained the serum amount of ALT and AST within the normal range (Figure 4.6A,B) (Schnell *et al.* 2002).

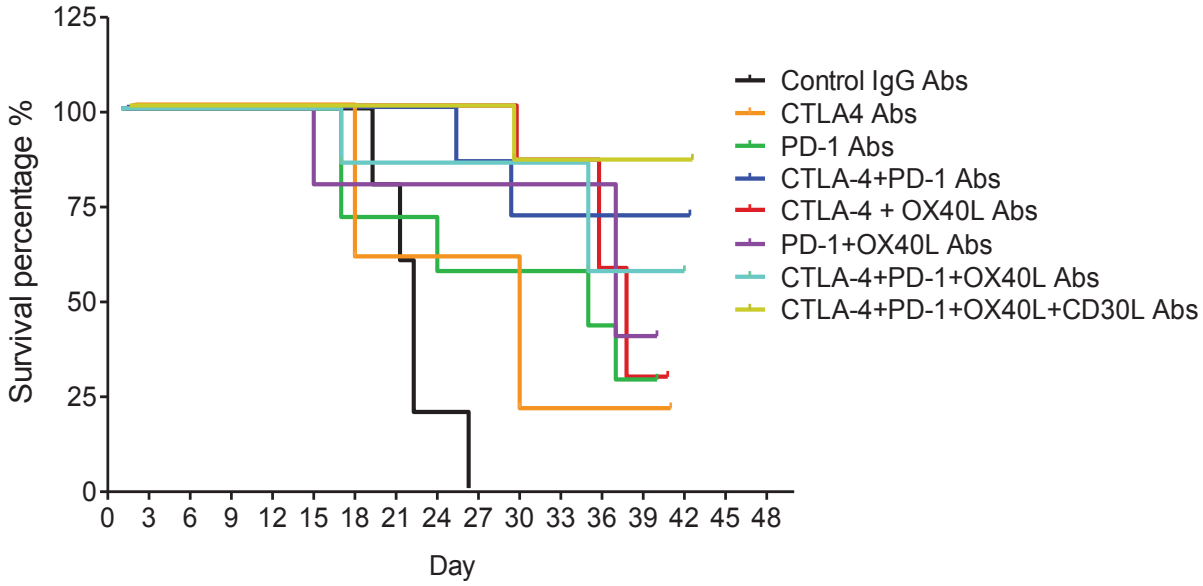

Figure 4.4: Kaplan Meier survival curves for B16-F10-luc^{+} transfected C57BL/6 mice groups treated with monoclonal blocking antibodies.

The survival percentage is recorded using Kaplan Meier graphs for 42 days for the C57BL/6 mice under various treatments. Mice were culled when tumour diameter reached 12 mm or tumours underwent necrosis and bleeding. Data are representative of three independent experiments, n=5,5,7,7,5,7,7 respective to each group in the order presented.

Figure 4.5: Number of lymphocyte aggregates per mm^2 of liver tissue x100

A,B Micrographs of formalin fixed liver tissue sections from B16-F10 injected C57Bl/6 mice stained for H&E, showing lymphocyte infiltration associated with immunotherapy using blocking antibodies to (A) anti-CTLA-4, anti-PD-1 in combination (B) anti-CTLA-4, anti-PD-1, anti-OX40L, anti-CD30L in combination. Scale bar = 100μm. (C) Quantification of lymphocyte infiltration into B16-F10 infected WT mouse livers treated with blocking antibodies in all combinations. Each data point represents one mouse, bars show medians values. Data are representative of three independent experiments, n=4,7,5,6,4,6,6, respective to each group in the order presented. Statistical analysis was performed using the Mann Whitney non parametric test; *,**,*** indicate significance $p<0.05$, $p<0.01$ and $p<0.005$ respectively.

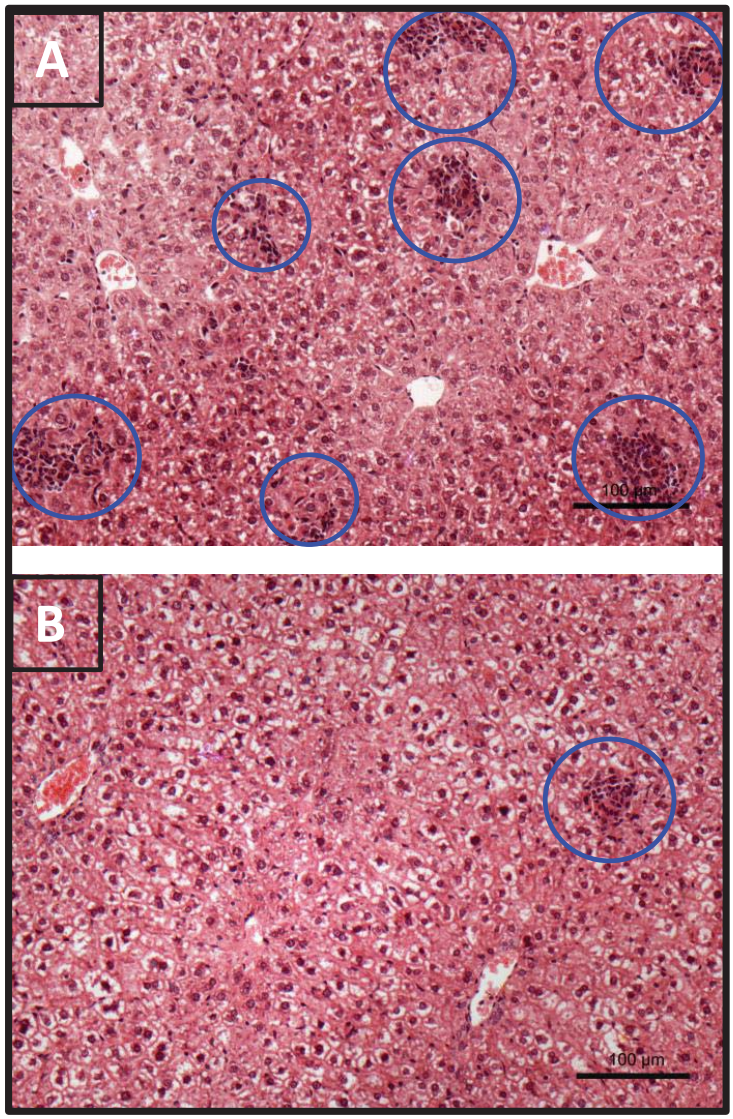

C No. of lymphocytes aggregated areas per mm^2 of liver tissue x100

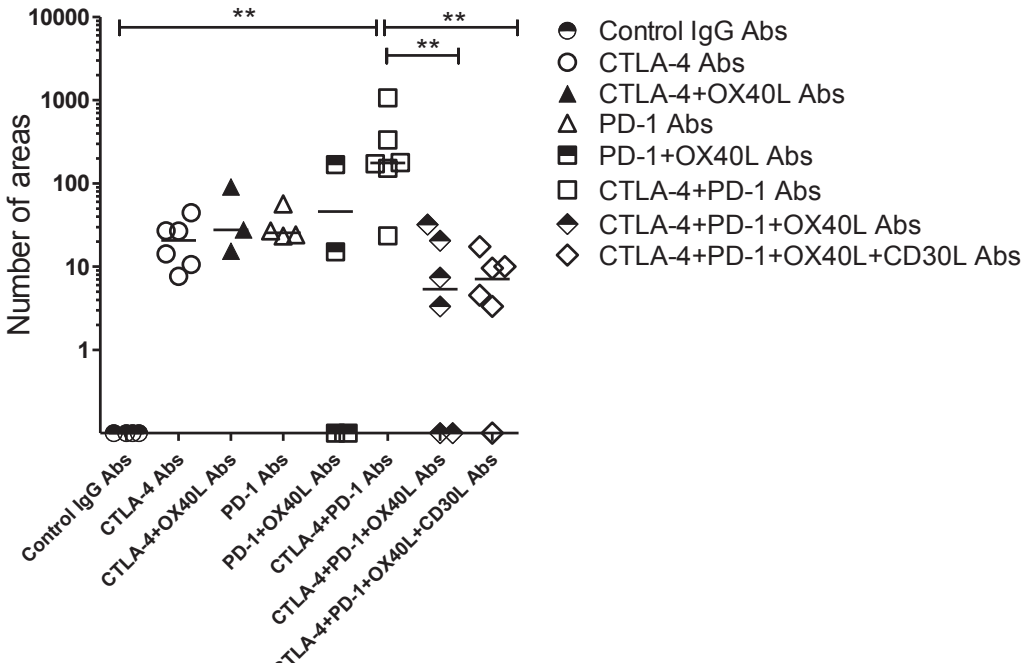

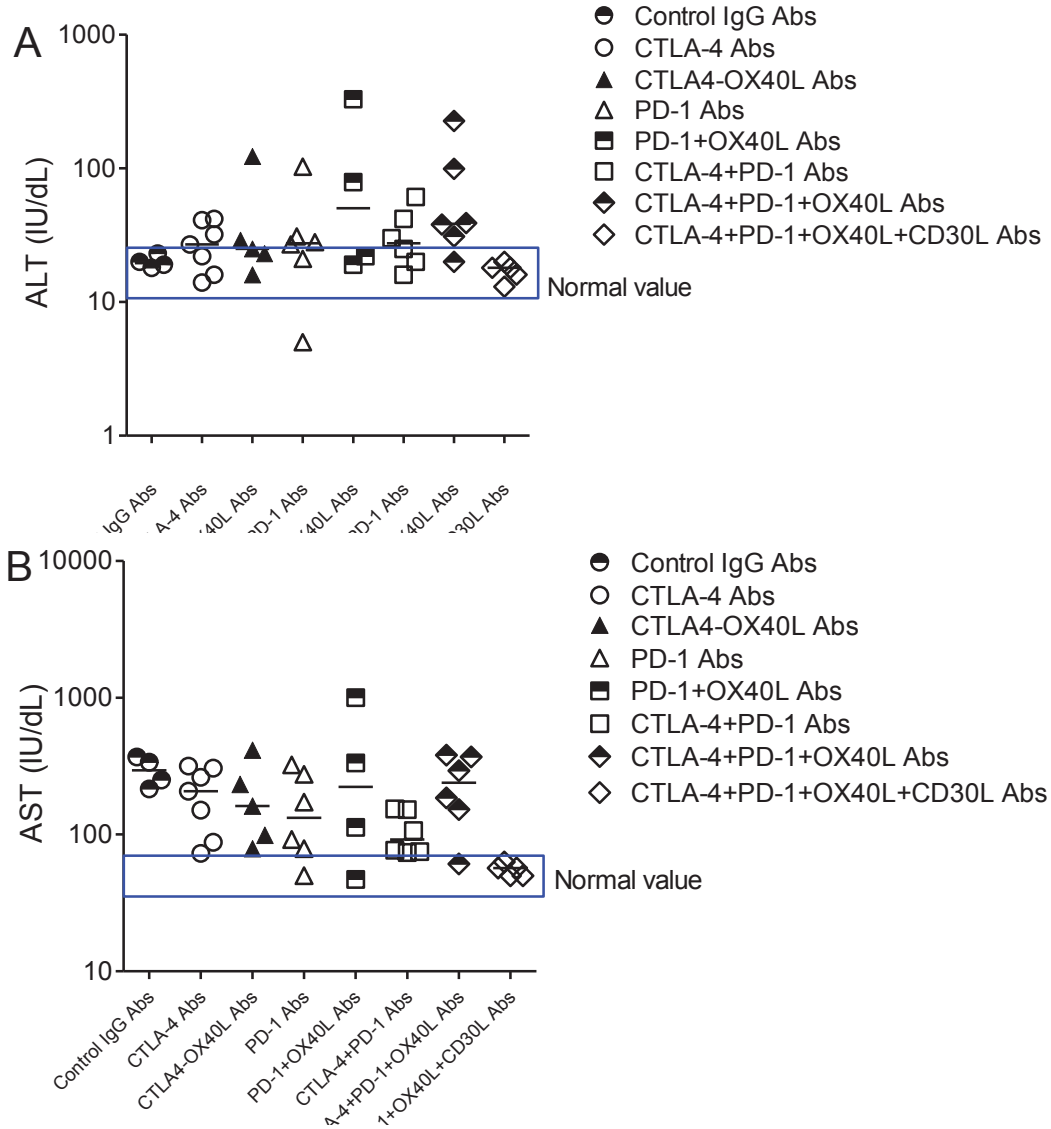

Figure 4.6: Liver function tests after injecting combinations of mAbs against CTLA-4, PD-1, OX40L and CD30L in B16-F10 injected C57Bl6 mice

Biomarkers of liver cellular injury in sera taken from treated C57Bl/6 mice: (A) alanine aminotransferase (ALT) (B) aspartate aminotransferase (AST). Each data point represents one mouse, bars show median values. Data represents duplicate tests for the sera, n= 4,7,5,6,4,6,6,6 respective to each group in the order presented. Blue rectangles show normal ranges of ALT serum values (24-42, median 33) and AST serum values (35-80, median 59).

4.2.1.5 The effect of monoclonal blocking antibody therapies on skin and hair depigmentation of B16 implanted C57Bl/6 mice

Vitiligo, or depigmentation, represents a sign of immune related adverse events associated with melanoma cases treated with anti-CTLA-4 and anti-PD-1 immunotherapy (van Elsas *et al.* 1999, Teulings *et al.* 2015). Unlike all the other mAb combinations, mice treated with anti-CTLA-4 mAbs (20%, 1/5) on its own or in combination with PD-1 blockades (42%, 3/7) developed skin and hair depigmentation, particularly at the site of B16 challenge or mAb injection and sometimes in distant areas (Figure 4.7). When OX40L blockade was included in the therapy regimen, it prohibited the development of vitiligo associated with anti-CTLA-4 and anti-PD-1. Similarly, addition of CD30L blockade to (CTLA-4,PD-1,OX40L) mAbs blockades prevented depigmentation (data not shown).

4.2.1.6 Serum autoantibody titre for anti-(CTLA-4,PD-1) and anti-(CTLA-4,PD-1,CD30L,OX40L) treatment groups

Production of high affinity autoantibodies at high titre is one of the fatal clinical features of autoimmunity which have been recognised in various non lymphoid tissues of scurfy mice, with a specific deficiency in $Foxp3^{+}$ Tregs, and $CTLA\text{-}4^{KO}$ and $PD\text{-}1^{KO}$ mice (Nishimura *et al.* 1999, Wing *et al.* 2008, Hadaschik *et al.* 2015). We previously showed that OX40 and CD30 are essential for the generation of high affinity antibodies (Gaspal *et al.* 2005) and abrogation of those TNFRs abolished autoantibody induction in $Foxp3^{KO}$ mice (Gaspal *et al.* 2011). Therefore, we examined sera from mice treated with antibodies to (CTLA-4, PD-1) and (CTLA-4, PD-1,OX40L,CD30L) by testing their reactivity on stomach, liver and kidney tissues

to investigate the possibility that OX40L and CD30L blockades can inhibit the autoantibody generation associated with CTLA-4 and PD-1 blockades, as seen in $Foxp3^{KO}$ mice.

Mouse sera were analysed for circulating autoantibodies as described in section 2.10. The threshold of background immunofluorescence intensity was set on negative controls and the grey intensity for a specified area was calculated for each serum sample. The median background immunofluorescence intensity obtained from anti-(CTLA-4,PD-1,CD30L,OX40L) group was notably less than that observed in anti-(CTLA-4,PD-1) group and in the positive control (Figure 4.8 A,B). As expected, the combination of anti-CTLA-4 and anti-PD-1 produced a significant autoimmune reaction, which was reduced when anti-OX40L and anti-CD30L mAbs were incorporated into the two combinations. Control (anti-IgG injected) mice showed no autoimmunity.

Figure 4.7: Depigmentation in B16-F10 injected C57Bl/6 mice treated with CTLA-4 mAbs.

Representative photograph of B16-F10 transfected C57Bl/6 mice after anti-CTLA-4 or anti-(CTLA-4,PD-1) blocking antibody treatment. Hair depigmentation (blue circles) occurred at the site of B16 challenge or mAb injection.

Figure 4.8: Fluorescence micrographs and serum autoantibody titres for anti-(CTLA-4,PD-1) and anti-(CTLA-4,PD-1,CD30L,OX40L) treatment groups on stomach, liver and kidney sections

Autoantibody titres were assessed using 1:20 dilutions of sera and indirect fluorescence staining on stomach, liver and kidney tissues (Nova kit). (A) Tissues were imaged by fluorescence on a Leica microscope, and acquired as tiff files. S, K, L symbols refers to stomach, kidney and liver tissues, respectively (B) The background fluorescence intensity was thresholded on negative controls and the grey intensity for a specified area was calculated for each serum sample. Each data point represents one mouse, bars show median values, n= 5,6,6,2 respective to each group in the order presented.

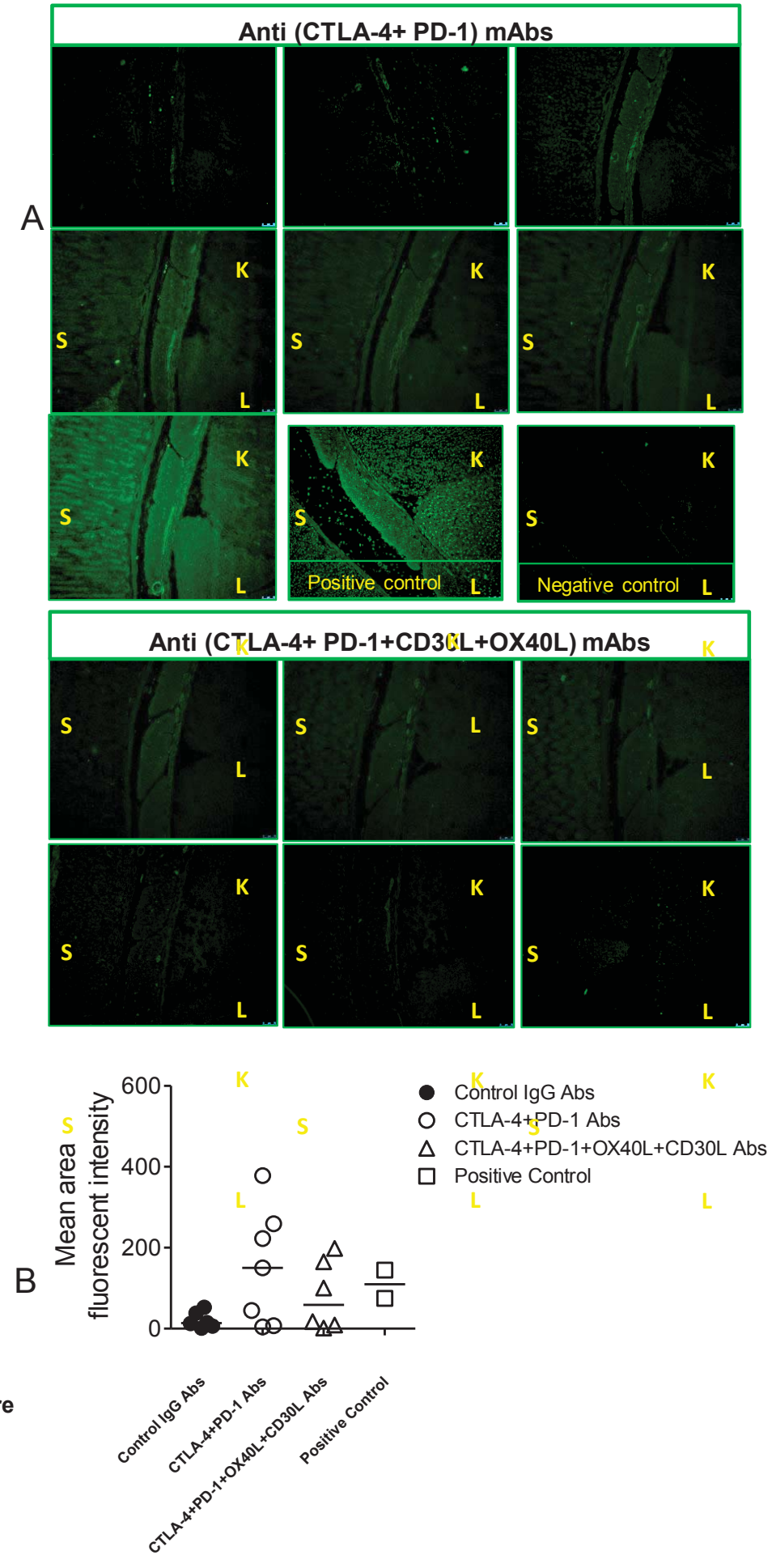
A
Anti (CTLA-4+ PD-1) mAbs
K
S
L
Positive control
Negative control
Anti (CTLA-4+ PD-1+CD30L+OX40L) mAbs
B
Mean area fluorescent intensity
600
400
200
0
Control IgG Abs
CTLA-4+PD-1 Abs
CTLA-4+PD-1+OX40L+CD30L Abs
Positive Control

Figure

4.2.2 The efficacy of monoclonal antibody immunotherapy for treating B16-F10 melanoma in CTLA-4 heterozygous mice

There is no obvious impact on the phenotype of mice heterozygous for CTLA-4, and it has been considered normal (Chambers *et al.* 1997). Others have reported that CTLA-4 genetic polymorphism carrier mice are sensitive to type one diabetes (T1D) (Ueda *et al.* 2003), and recently, heterozygous mutations in CTLA-4 have been identified in some patients who manifested clinical autoimmune symptoms (Kuehn *et al.* 2014, Schubert *et al.* 2014, Zeissig *et al.* 2015). In CTLA-4^{het} patients and carriers, there was a general elevation in the number of Tregs compared to healthy donors, but their Tregs showed reduction in CTLA-4 expression and dysfunctional suppressive activity, resulting from impairment of CTLA-4 binding to its ligands and malfunctioning transendocytosis, leading to a complicated immune dysregulation (Schubert *et al.* 2014). We wanted to investigate the efficacy of tumour immunotherapy by PD-1 blockades with partial inhibition of CTLA-4 using CTLA-4^{het} mice, as well as the effect of OX40 and CD30 deficiency using CTLA-$4^{het}OX40^{KO}CD30^{KO}$, mice which were generated in our lab by crossing CTLA-4^{het} with $OX40^{KO}CD30^{KO}$ mice.

4.2.2.1 Experimental protocol

6-8 week old female WT (BoyJ), CTLA-4^{het} and CTLA-$4^{het}OX40^{KO}CD30^{KO}$ mice were inoculated with $5x10^5$ B16-F10 melanoma cells on the right dorsal flank. 5 days later, the mice were injected I.P twice per week with anti-(PD-1) 250µg/dose or rat anti-IgG mAbs as control for 26 days (Figure 4.9). Tumour volumes were measured twice weekly using callipers. The mice were culled when the tumour diameter reached 12

mm or underwent necrosis and bleeding. Samples were collected for FACS analysis and quantification of infiltrates.

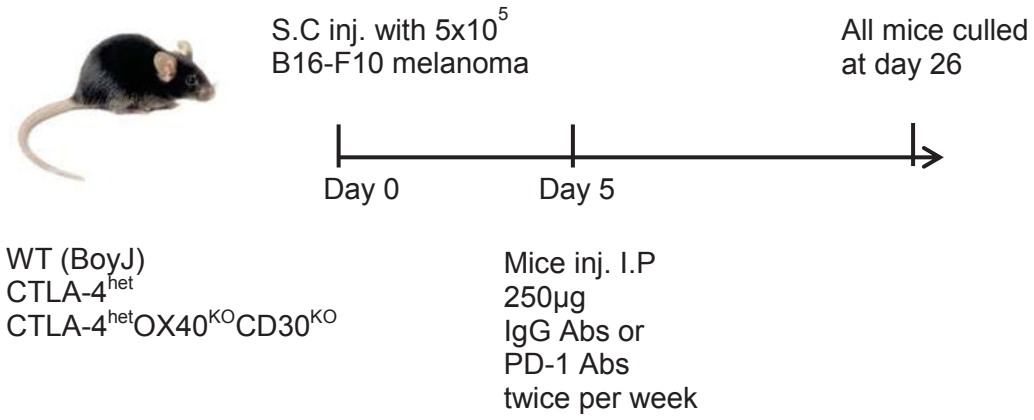

Figure 4.9: Experimental design to test the efficacy of immunotherapy in CTLA-4 heterozygous mice.

4.2.2.2 The dynamics of tumour growth in CTLA-4 heterozygous mice treated with anti-PD-1 mAbs

CTLA-4 heterozygous mice injected with B16 melanoma and treated with control IgG mAbs showed marginally slower tumour growth compared to their WT counterparts, and even slower growth was observed in the CTLA-4 control group (Figure 4.10 A). As seen before, relative to WT controls, WT mice treated with anti-PD-1 had markedly decreased tumour growth, which was also less than that seen in the CTLA-4^{het} and CTLA-$4^{het}CD30^{KO}OX40^{KO}$ control groups. Interestingly, there was no difference between WT and CTLA-4^{het} groups treated with anti-PD-1 blocking mAbs but the blockade showed better efficacy in the CTLA-$4^{het}CD30^{KO}OX40^{KO}$ mice. Finally, all CTLA-4^{het} phenotype mice treated with anti-PD-1 showed pronounced reduction in tumour growth compared to WT control mice.

Harvested tumour weights corresponded to the pattern found for tumour volumes. There was a minor difference between the tumour weights pooled from WT and CTLA-4^{het} control groups and a slightly bigger difference between WT and CTLA-$4^{het}CD30^{KO}OX40^{KO}$ anti-IgG group (Figure 4.10B), but neither of these was statistically significant. Although tumours were reduced in WT and CTLA-4^{het} mice treated with anti-PD-1 mAbs, ($p<0.53$) and ($p<0.47$) respectively, compared with the WT IgG group, no difference in the effectiveness of anti-PD-1 mAbs was found between them. The immunotherapeutic activity of anti-PD-1 in CTLA-$4^{het}CD30^{KO}OX40^{KO}$ mice was slightly better than in WT and CTLA-4^{het} treated mice, and using WT control mice as the reference, was statistically significant ($p<0.02$).

4.2.2.3 The effect of anti-PD-1 mAbs on Treg infiltration into established melanoma in CTLA-4 heterozygous mice

Phenotypic analysis of tumours and tumour infiltrates and quantification of $FoxP3^+$ Tregs showed that slightly fewer Tregs infiltrated the tumours of $CTLA\text{-}4^{het}$ control anti-IgG injected mice than of WT mice, and even fewer infiltrated the tumours of dKO $CTLA\text{-}4^{het}$ controls, but these differences were not statistically significant (Figure 4.11 A,B). Treatment of the mice with anti-PD-1 mAbs resulted in significant recruitment of Tregs into $CTLA\text{-}4^{het}$ tumours ($p<0.02$). Although the same effect was found in WT and dKO $CTLA\text{-}4^{het}$ mice, it was not significant statistically ($p<0.06$) and ($p<0.9$) respectively (Figure 4.11 A,B).

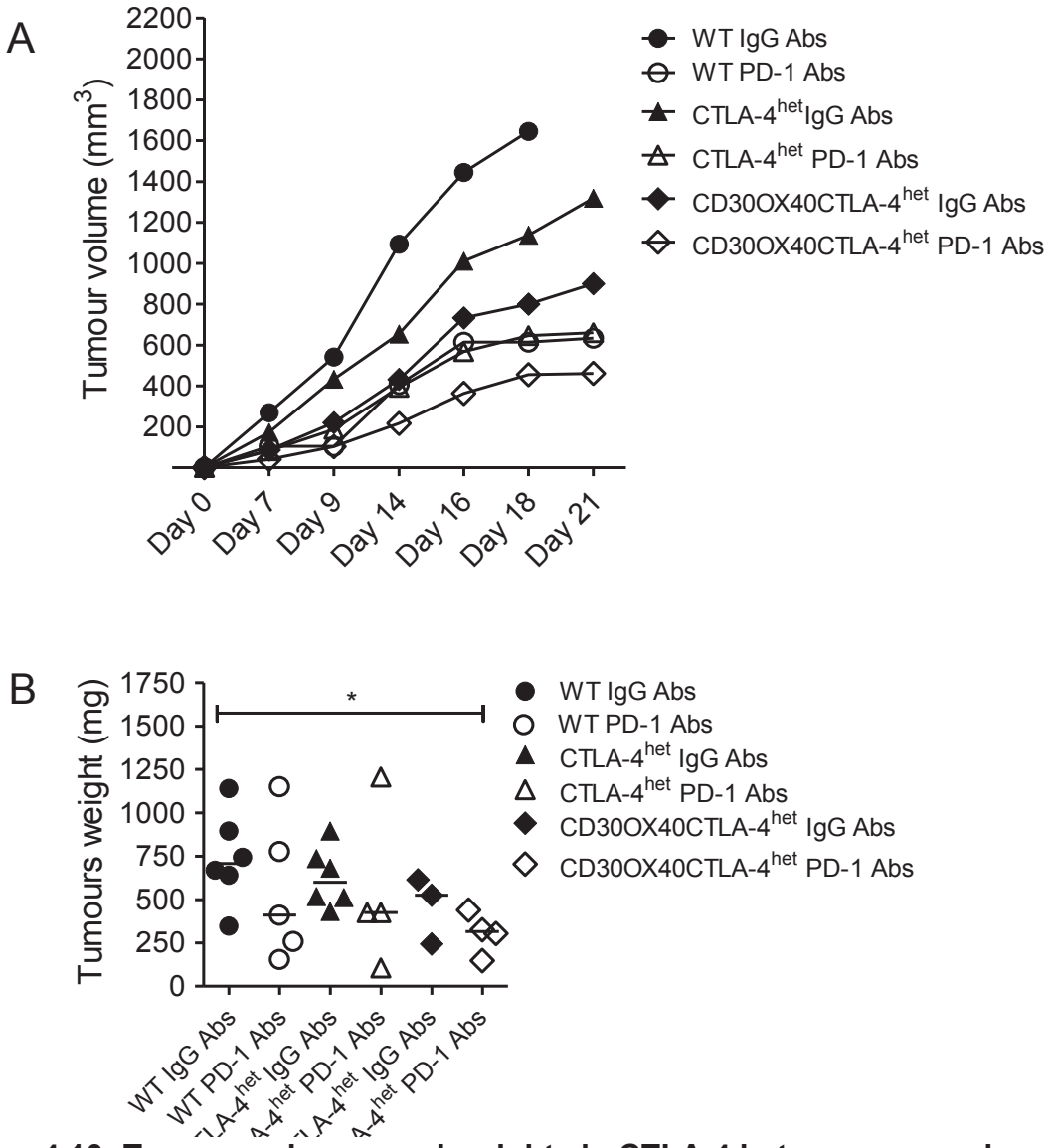

Figure 4.10: Tumour volumes and weights in CTLA-4 heterozygous mice treated with anti-PD-1 mAbs

(A). Tumour volumes were measured at least twice weekly using callipers, and the mean of three readings was recorded for each mouse. (B) Representative tumour weight at harvest. Data are representative of two independent experiments, n=6,5,6,4,3,4 respective to each group in the order presented. Statistical analysis was performed using the Mann Whitney non parametric test . * indicates significance at $p<0.02$.

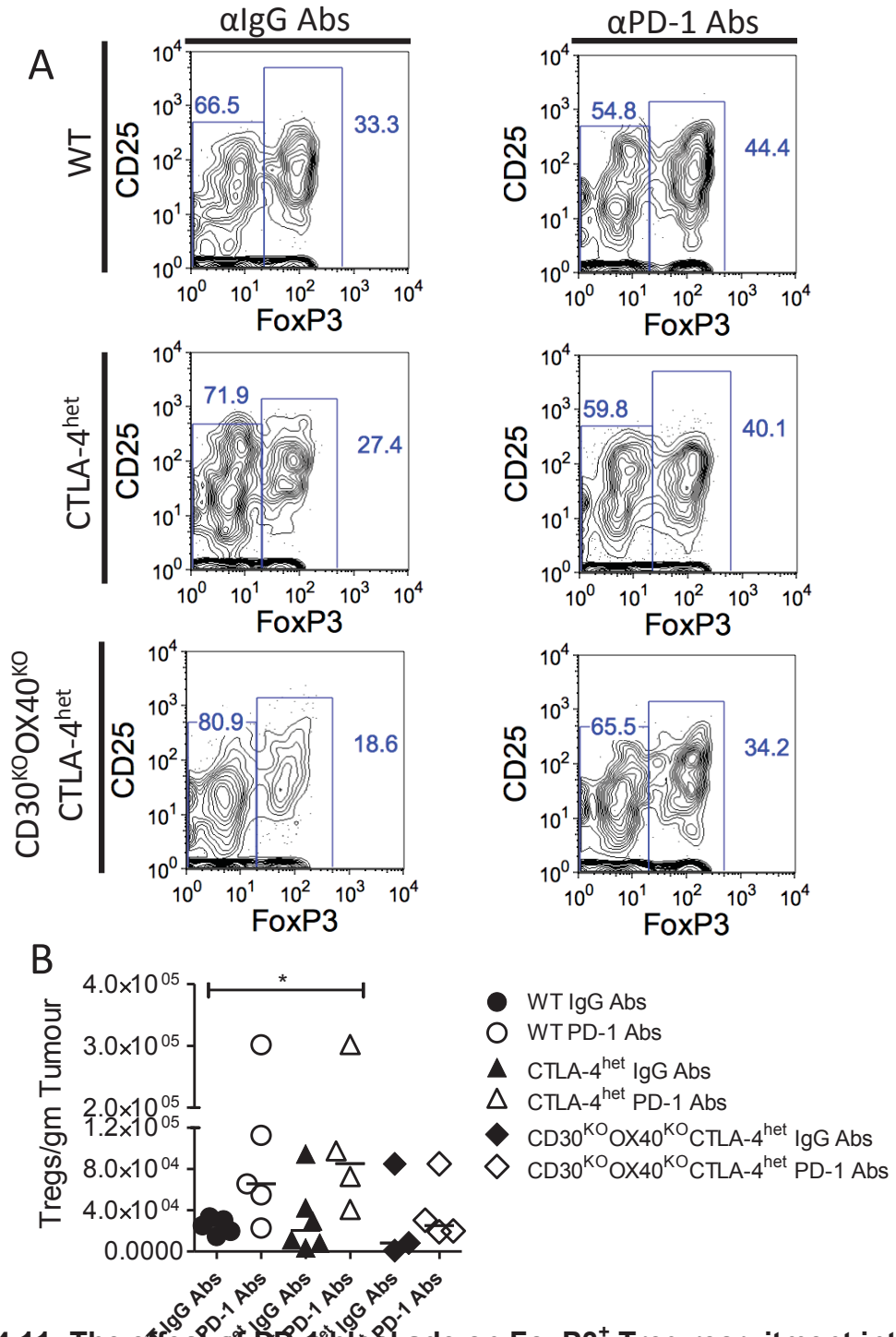

Figure 4.11: The effect of PD-1 blockade on FoxP3$^+$ Treg recruitment into WT and CTLA-4 heterozygous mice with established B16-F10 melanoma.

(A) Representative FACS contour plots of cellular infiltrates of tumours from mice treated with anti-IgG mAbs or anti-PD-1 mAbs, gated on live CD3$^+$CD4$^+$ and showing expression of CD25 and FoxP3 on CD4 T cells (B) Numbers of FoxP3$^+$ Tregs infiltrating tumours. Each data point represents one mouse, bar shows medians. Statistical analysis was performed using the Mann Whitney non parametric test. Data are representative of two independent experiments, n=6,5,6,4,3,4 respective to each group in the order presented. * indicates significance p<0.02.

4.3 Discussion

4.3.1 Simultaneous blockade of OX40L and CD30L does not interfere with the anti-tumour effect of CTLA-4 and PD-1 blocking antibodies used for the treatment of B16 melanoma in C57Bl/6 mice

Clinical trials using CTLA-4 (Hodi *et al.* 2010, Robert *et al.* 2011) and PD-1 blockades (Brahmer *et al.* 2012, Topalian *et al.* 2012, Robert *et al.* 2015a) have achieved objective anti-tumour responses and prolonged survival in a number of melanoma patients, and combined blockade of the two receptors had a more potent effect (Wolchok *et al.* 2013, Larkin *et al.* 2015, Postow *et al.* 2015). Antibody associated toxicity was found to be mainly autoimmune, and was dose dependent; consequently the efficacy of the therapy and dose escalation were limited. In agreement with previous studies (Leach *et al.* 1996, Peggs *et al.* 2009), we showed that anti-CTLA-4 mAbs therapy on its own reduced B16 tumour growth in WT mice, which probably works mainly through intra-tumour Treg depletion (Selby *et al.* 2013, Simpson *et al.* 2013). Adding anti-OX40L mAbs further reduced tumour growth, confirming that OX40L blockade does not interfere with anti-CTLA-4 mAb efficacy, and suggesting a role for OX40 in Treg function, as we have previously shown in dKO Foxp3^{KO} mice, or Treg homing, as has been found in hepatocellular carcinoma (Piconese *et al.* 2014). In spite of having its own effect on tumour growth, adding anti-OX40L blockade to anti-PD-1 blockade neither improved nor interfered with its efficacy. This can be interpreted to mean that the major effect of anti-PD-1 is in restoring exhausted CD8 tumour specific reactivity (Barber *et al.* 2006, Abiko *et al.* 2015),

which is less dependent on OX40 , and possibly independent of OX40, as CD8 T cell function was not affected in $CD30^{KO}OX40^{KO}Foxp3^{KO}$ mice and also in LTi ($RoR\gamma^{-/-}$) mice (Withers *et al.* 2009, Gaspal *et al.* 2011, Withers *et al.* 2012). We also found the significant therapeutic efficacy on B16 melanoma provided by anti-(CTLA-4,PD-1) blockade, as has been reported by others (Curran *et al.* 2010, Quezada and Peggs 2013). Our additional observation is that when blockade of OX40L alone or combined with CD30L is added to CTLA-4 and PD-1 blockades there is a slight increase in the therapeutic efficacy and total survival rate in C57Bl/6 mice with pre-established B16 melanoma, showing that blocking OX40L and CD30L does not interfere with anti-CTLA-4 and anti-PD-1 therapeutic efficacy. This is to be expected, as OX40 and CD30 share the same signalling pathway and act synergistically on CD4 T cell commitment and activation (Gaspal *et al.* 2005, Gaspal *et al.* 2008), whereas PD-1 and CTLA-4 have distinctive inhibitory T cell mechanisms of (Parry *et al.* 2005) which lead to Treg and MDSC depletion and expansion of CD8 effector cells (Curran *et al.* 2010).

4.3.2 Concurrent injection of antibodies to OX40L and CD30L abrogates the CD4 driven autoimmunity associated with CTLA-4 and PD-1 blocking antibodies

As anticipated, based on the precedent of the phenotype of $dKOFoxP3^{KO}$ mice, anti-CD30L and anti-OX40L blockades co-injected with anti-CTLA-4 and anti-PD-1 antibody combinations abrogated the CD4 driven autoimmunity associated with CTLA-4 and PD-1 blocking antibodies. The extensive lymphocyte infiltration into mouse livers treated with anti-(CTLA-4,PD-1) mAb combination was remarkably

ameliorated when anti-CD30L and anti-OX40L blockades were incorporated into the treatment, as has been observed previously in dKOFoxP3^{KO} livers compared with FoxP3^{KO} livers (Gaspal *et al.* 2011). FoxP3 Tregs suppress peripheral autoreactive T cells through the action of CTLA-4, and its blockade activates peripheral T cells and also depletes the Tregs that normally suppress autoreactive T cells and prevent them from infiltrating non-lymphoid organs (Wing *et al.* 2008, Selby *et al.* 2013). PD-1 also acts to maintain peripheral tolerance, but the accelerated fatal autoimmunity in CTLA-4^{KO} mice, compared to the mild chronic disease in PD-1^{KO} mice, demonstrates that CTLA-4 is more important for the suppression of CD4 autoimmunity. Anti-PD-1 blockade has been found to induce cytolytic genes in T cells, such as IFNγ, which is often the main driver of autoimmunity (Pollard *et al.* 2013), while anti-CTLA-4 blockade induces proliferative and homing genes in T cells (Das *et al.* 2015). Blocking of OX40 and CD30 signals can inhibit expansion and activation of self-reactive T cells and can abrogate cytokine production from pathogenic CD4 T cells, preventing liver and other tissue pathology, as we reported for the FoxP3 Treg deficient mice (Gaspal *et al.* 2011). Another indicator of liver cellular injury in the anti-CTLA-4 and anti-PD-1 treatment combination was the abnormal elevation of serum ALT and AST biomarkers, whose appearance is mainly IFNγ dependent (Nishimura and Ohta 1999, Jacobs *et al.* 2004). With the addition of combined anti-OX40L and anti-CD30L blockade, however, these serum enzymes were maintained within the normal range; that this is not the case with anti-OX40L alone is compatible with synergy between OX40 and CD30 signalling in reducing off-target toxicity. Persistent liver pathology results in liver failure, as shown in PD-1^{KO} treated with anti-CTLA-4 mAbs (Metushi *et al.* 2015), and this adverse outcome may be irreversible and lead

to death among cancer patients; for this reason treatment was discontinued in some clinical trials, such as those where melanoma patients were treated with Nivolumab and Iplimumab combined therapy (Larkin *et al.* 2015, Postow *et al.* 2015).

Treating mice with anti-CTLA-4 mAbs on their own or with anti-PD-1 resulted in hair depigmentation at the site of B16 challenge and at the site of mAb injection, a phenomenon that is regarded as an indicator of an objective anti-tumour response stimulated by tumour specific and autoreactive T cells, despite the fact that tumours progress in mice treated only with anti-CTLA-4 mAbs (van Elsas *et al.* 1999, Gubin *et al.* 2014, Snyder *et al.* 2014). Such autoreactive T cells not only cause destruction of tumour derived melanocytes but may also destroy skin pigment cells and melanin producing hair follicle cells, which is manifest as vitiligo in mice (van Elsas *et al.* 1999) and in melanoma patients treated with Ipilimumab or Nivolumab or both (Hodi *et al.* 2010, Topalian *et al.* 2012, Larkin *et al.* 2015, Postow *et al.* 2015). Vitiligo has been suggested to be a sign of tumour regression, tumour-free survival and low risk of tumour recurrence in metastatic melanoma patients targeted with immunotherapies (Teulings *et al.* 2015). Our double blockade of OX40L and CD30L prevented development of depigmentation in anti-CTLA-4 and anti-PD-1 treated mice without interfering with the efficacy of antibody treatment for tumour rejection, suggesting a use for blocking antibodies to OX40L and CD30L in ameliorating the toxicity of autoreactive T cells. Although autoreactive CD8 T cells have been implicated in autoimmunity (Liblau *et al.* 2002), they fail to produce autoimmune pathology in our $CD30^{KO}OX40^{KO}FoxP3^{KO}$ mice, suggesting that autoimmune damage is mainly CD4 T cell mediated, and/or CD8 T cells play only a minor role, which may

be dependent on OX40 and CD30 signals; that CD8 T cells contribute only minor autoimmunity has been confirmed previously in scurfy mice (Blair *et al.* 1994).

The other hallmark of autoimmune toxicity related to the double blockade of CTLA-4 and PD-1 is the high titre of high affinity autoantibodies (here measured against stomach, liver and kidney tissues); this, however, was mostly reduced in the four-antibody combination blocking CTLA-4, PD-1, OX4OL and CD30L all at once. Although PD-1 has been found to regulate GC $CD4^+$ T cells and participate in the generation of high affinity antibodies (Good-Jacobson *et al.* 2010), our findings suggest that OX40 and CD30 are the main signals contributing to the survival of CD4 effector/memory T cells and the generation of high affinity antibodies, as shown before (Gaspal *et al.* 2005), and by blocking those signals autoantibody formation can be abolished, as shown in dKOFoxP3^{KO} mice (Gaspal *et al.* 2011).

4.3.3 Partial impairment of CTLA-4 combined with anti-PD-1 is not as effective as double blockade of CTLA-4 and PD-1 in the treatment of B16 melanoma but the efficacy is improved with CD30 and OX40 blockade

We found that B16 melanoma grows at similar rates in WT and CTLA-4^{het} mice and treating tumours established in those mice with anti-PD-1 blocking mAbs reduced tumour growth in both strains of mice to a similar extent, in spite of the fact that some impairment of Treg suppressive function in CTLA-4^{het} mice has been reported (Schubert *et al.* 2014). Flow cytometric analysis and quantification of tumour infiltrates confirmed that tumours recruited $FoxP3^+$ Tregs as a replacement inhibitory mechanism for anti-PD-1 into WT tumours, to evade anti-tumour immunity, and to a

significant level into CTLA-4^{het} tumours. The importance of OX40 signalling to Treg mediated suppression of colitis (Griseri *et al.* 2010) and hepatocellular carcinoma (Piconese *et al.* 2014) has already been reported. In our dKO mice tumours, there was a clear influence of CD30 and OX40 signals on tumour growth in CTLA-4^{het} mice treated with anti-PD-1 compared to WT and CTLA-4^{het} controls, and in the numbers of Tregs recruited into tumours relative to those found in WT and CTLA-4^{het} controls or anti-PD-1 treated mice. PD-1 and CTLA-4 have been blocked at high doses to obtain objective tumour immunotherapy, especially for metastatic cases. We suggest that addition of anti-OX40L and anti-CD30L blockade to the regimen might address the significant limitation of the grade 3-4 immune adverse events and even death attributable to the CD4 driven autoimmunity associated with anti-CTLA-4 and anti-PD-1 blockades, which restrict their efficacy and dose escalation for cancer treatment (Topalian *et al.* 2012, Wolchok *et al.* 2013, Larkin *et al.* 2015, Postow *et al.* 2015).

Anti-OX40L blockade has been used in double blind trials to treat human asthma and found to be entirely safe, although not effective against asthma, in spite of resulting in the reduction of IgE and eosinophils (Gauvreau et al. 2014). While strategies are being patented for anti-CD30L blockade (WO2013163377A1), to our knowledge they have not been trialled in human.

4.4 Conclusion

We think that our approach using anti-OX40L and anti-CD30L blockades could be applied to immunotherapies to dissociate CD4 autoimmune toxicity from anti-tumour CD8 efficacy. This potential strategy could change cancer immunotherapy dramatically by providing highly efficacious combinations for treating a wide range of

cancer patients, particularly at early stages of tumour development, instead of being used as a last resort.

Chapter Five Results

Tumour immune response in a mouse model where T effectors are resistant to regulation

5.1 Introduction

In this part of the thesis, I have studied the anti-melanoma immune response in the Roquin mutant mouse model (sanroque). Roquin is an mRNA binding protein that regulates post-transcriptional mRNA of many genes (Di *et al.* 2007, Vogel *et al.* 2013), but the main point of interest here is that in a mutant mouse strain bearing a point mutation in Roquin (Vinuesa *et al.* 2005), overexpression of IFNγ confers resistance to T regulation (Lee *et al.* 2012). Work in our lab has shown that IFNγ activates macrophages, whose expression of inducible nitric oxide synthase (iNOS, *Nos2*) elicits strong expression of OX40L on effector T cells, enabling signalling through the regulator OX40, and conferring resistance to Tregs. Moreover, the presence of M1 type macrophages in tumours, which express iNOS and produce IL-12, was found to foster the promotion of strong immune responses against tumours (Mantovani *et al.* 2002, Movahedi *et al.* 2010, Heusinkveld *et al.* 2011, Mantovani and Allavena 2015). In previous chapters we have shown that robust CD8 driven immune responses occur if Treg function can be suppressed, particularly when used in combination with PD-1 blockade. We aimed here to investigate the immune response to B16-F10 melanoma in sanroque mice, to test whether mutant Roquin conferred resistance to regulation in CD8 T cells that control the tumour growth. Furthermore, because data from the lab has also shown that Treg function is impaired in the absence of OX40 and CD30 signals (dKO), we also studied sanroque dKO mice.

5.2 Results

5.2.1 Tumour immune response in Roq$^{san/san}$ and Roq$^{san/san}$dKO mice compared with WT and dKO mice

5.2.1.1 Experimental protocol

WT, dKO, Roquin$^{san/san}$ (Roq$^{san/san}$) and Roquin$^{san/san}$CD30^{KO}OX40^{KO} (Roq$^{san/san}$dKO) mice, aged 6-8 weeks, were injected subcutaneously with 5x10^{5} melanoma cells on the right flank and the dynamics of tumours growth were monitored using callipers for 3 weeks, after which all mice were culled, tumours were weighed and infiltrates analysed.

5.2.1.2 Pattern of tumour growth in Roq$^{san/san}$ and Roq$^{san/san}$dKO mice compared with WT and dKO mice

dKO and Roq$^{san/san}$ tumours grew at similar rates, slightly slower than in WT mice. Tumour growth was even slower in Roq$^{san/san}$dKO (Figure 5.1A). Similarly, weights of tumours excised from Roq$^{san/san}$dKO mice after 20 days of B16 injection were significantly less than those taken from WT mice ($p<0.01$), dKO and Roq$^{san/san}$ tumours (non-significant differences) (Figure 5.1B).

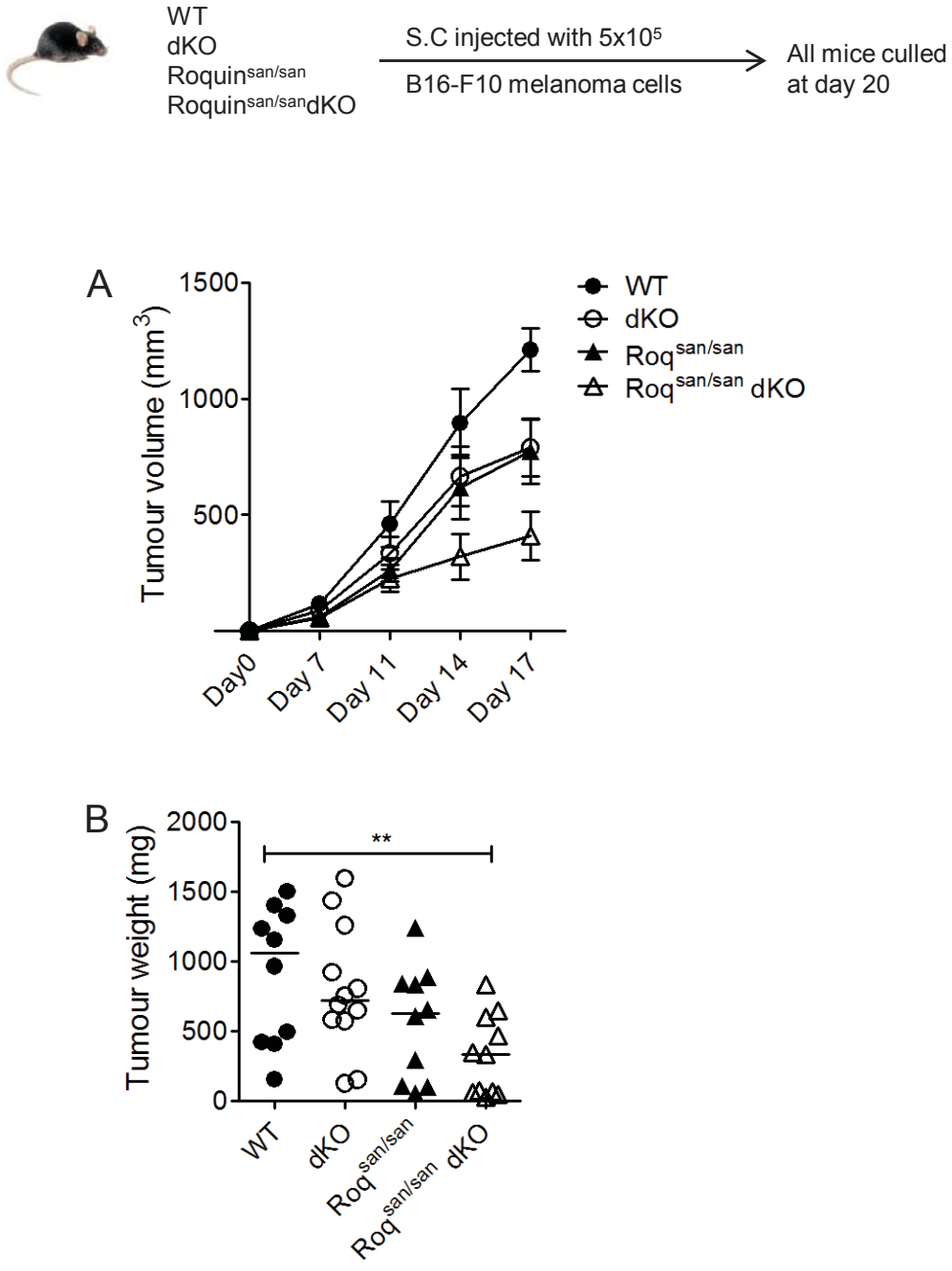

Figure 5.1: Pattern of tumour growth in WT, dKO, Roq$^{san/san}$, Roq$^{san/san}$dKO mice.

Tumour volumes were measured weekly using callipers, and tumours were harvested at 20d. (A) tumour volume measurements, medians ± standard error (B) tumour weight at harvest, each point represents one mouse, bars show medians. Statistical analysis was performed using the Mann Whitney non parametric test. Data are representative of three independent experiments, n=10,12,10,11 respective to each group in the order presented. ** indicates significance $p<0.01$.

5.2.1.3 FACS analysis of tumours and of tumour-infiltrating lymphocytes

Representative FACS data from tumours and tumour infiltrates are shown in Figure 5.2. The ratio of CD4:CD8 T cells infiltrating WT tumours – approximately 2:1 - was shifted in favour of CD8 in dKO (1:1.5), Roq$^{san/san}$ (1:2.5) and Roq$^{san/san}$dKO (1:8) tumours. Likewise, compared to WT, a trend of decreased Treg numbers in tumour infiltrates was seen in dKO, Roq$^{san/san}$ and Roq$^{san/san}$dKO mice (Figure 5.2F). Although Treg proportions were reduced in tumours, the situation was reversed in the draining lymph nodes; the frequencies of Tregs in the tumour-draining (inguinal) lymph nodes in Roq$^{san/san}$ and Roq$^{san/san}$dKO were 31% and 20% respectively, compared to 11% in WT and 7% in dKO (Figure 5.2B). Enumeration of T cell populations/g tumour showed significant increases in the TCRαβ ($p<0.01$) and CD4 ($p<0.05$) subsets in Roq$^{san/san}$ and Roq$^{san/san}$dKO relative to those from WT and dKO (Figure 5.2C,D). DKO mice showed an intermediate decrease in CD4 and Treg subsets compared to WT, but had more CD8 T cells (Figure 5.2D,E,F). In tumours, Treg numbers were most reduced compared to WT in Roq$^{san/san}$ mice and were intermediate in Roq$^{san/san}$dKO (Figure 5.2F). However this was not the case in the tumour draining lymph nodes. Treg numbers were significantly elevated in Roq$^{san/san}$ draining lymph nodes compared to dKO ($p<0.005$), WT ($p<0.01$) and Roq$^{san/san}$dKO ($p<0.05$) (Figure 5.2G) but in dKO mice were significantly reduced in comparison to both Roq$^{san/san}$ dKO and WT, ($p<0.01$ and $p<0.05$ respectively). CD8 T cell numbers in tumours were significantly increased in both Roq$^{san/san}$ and Roq$^{san/san}$dKO mice compared to WT mice ($p<0.005$), and in Roq$^{san/san}$dKO compared to dKO ($p<0.01$) and Roq$^{san/san}$ ($p<0.05$) (Figure 5.2E).

Figure 5.2: Flow cytometric analysis of tumours and tumour draining lymph nodes in WT, dKO, $Roq^{san/san}$, $Roq^{san/san}$dKO mice

Tumours and draining (inguinal) lymph nodes were digested and cell suspensions were surface stained, then fixed, permeabilised and FoxP3 stained. A,B: Contour plots of representative FACS analyses, (A) tumour digest gated on live $CD45^+TCR\alpha\beta^+$ cells and showing Treg populations (B) draining lymph nodes, Treg populations only.
C-G: Enumeration of infiltrating lymphocyte populations (C) Tumour $CD45^+TCR\alpha\beta^+$, (D) Tumour $CD4^+$, (E) Tumour $CD8^+$, (F) Tumour $FoxP3^+$, (G) Draining lymph node $FoxP3^+$; Each point represents one mouse, bars show median values. Statistical analysis was performed using the Mann Whitney non parametric test. Data are representative of three independent experiments, n = 10,12,10,11 respective to each group in the order presented. * ,**, *** indicate significance $p<0.05$, $p<0.01$ and $p<0.005$ respectively.

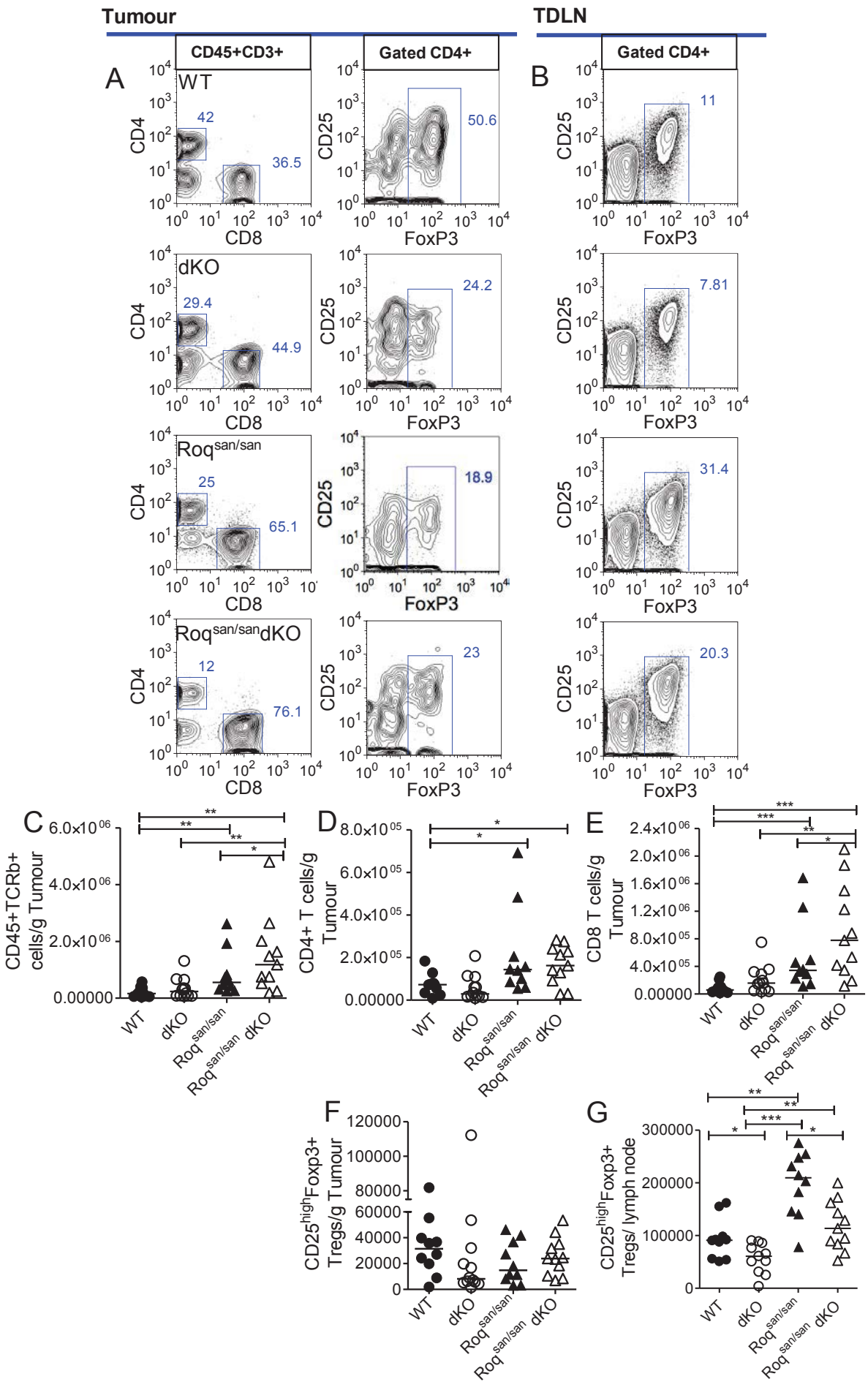
Tumour
TDLN
A
B
CD45+CD3+
Gated CD4+
WT
dKO
Roq san/san
Roq san/san dKO
CD4
CD8
CD25
FoxP3
42
36.5
50.6
29.4
44.9
24.2
25
65.1
18.9
12
76.1
23
11
7.81
31.4
20.3
C
D
E
F
G
CD45+TCRb+ cells/g Tumour
CD4+ T cells/g Tumour
CD8 T cells/g Tumour
CD25high Foxp3+ Tregs/g Tumour
CD25high Foxp3+ Tregs/ lymph node
WT
dKO
Roq san/san
Roq san/san dKO

5.2.1.4 Expression of PD-1 on $CD8^+$ T cells in tumour infiltrates.

Interestingly, the infiltrating CD8 T cells in $Roq^{san/san}$ tumours failed to express the inhibitory molecule PD-1 (Figure 5.3), significantly different from the populations taken from tumours in all other mice (Figure 5.3B).

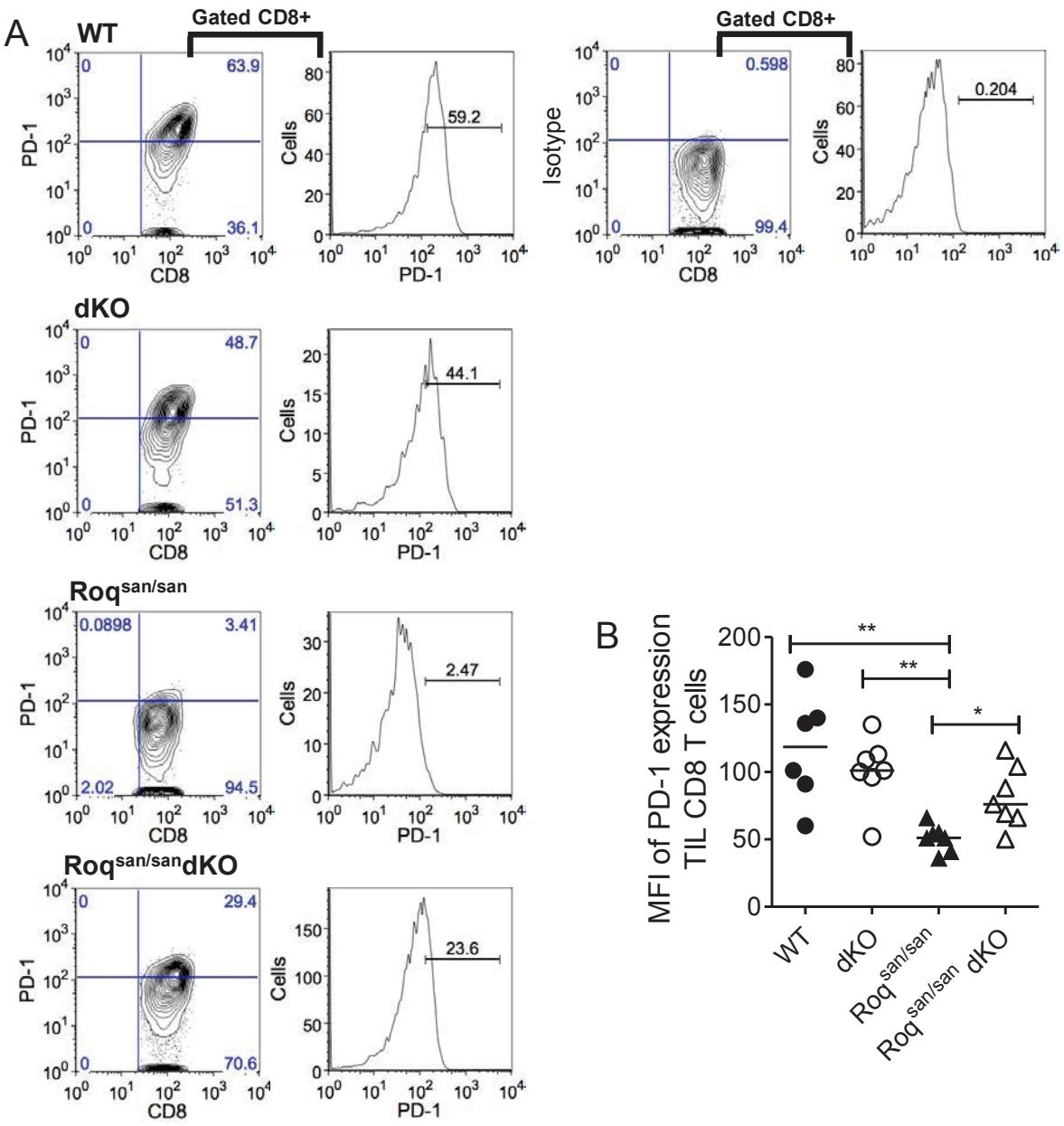
Tumour
A
WT
Gated CD8+
63.9
36.1
59.2
Isotype
0.598
99.4
0.204
dKO
48.7
51.3
44.1
Roq san/san
0.0898
3.41
2.02
94.5
2.47
Roq san/san dKO
29.4
70.6
23.6
PD-1
CD8
Cells
B
MFI of PD-1 expression
TIL CD8 T cells
WT
dKO
Roq san/san
Roq san/san dKO

5.2.2 The effect of αPD-1 immunotherapy on melanoma growth in Roq$^{san/san}$ and Roq$^{san/san}$ dKO mice compared to WT mice

CD8 T cells infiltrated significantly the tumours in both Roq$^{san/san}$ and Roq$^{san/san}$ dKO mice; however the expression of PD-1 on Roq$^{san/san}$ CD8 T cells was significantly reduced compared with that of the CD8 T cell infiltrate from tumours in WT mice. Anti-PD-1 has been shown to mediate an objective immune response in tumours characterised by the pre-existence of CD8^{+}PD-1^{high} T cells (Tumeh *et al.* 2014). Therefore we wanted to test the efficacy of anti-PD-1 blockade on tumour growth in Roq$^{san/san}$ mice.

5.2.2.1 Experimental protocol

WT, Roq$^{san/san}$ (Roquin$^{san/san}$) and Roq$^{san/san}$dKO (Roquin$^{san/san}$OX40^{KO}CD30^{KO}) female mice, aged 6-8 weeks, were injected with 5 x 10^5 B16-F10 melanoma cells and 5 days later mice were randomly grouped and treated with αPD-1 mAbs or rat anti-IgG 250μg/mouse, twice per week. Mice were culled when tumour diameter reached 12 mm and the Kaplan-Meier survival curve was used to represent the data.

5.2.2.2 Tumour volumes and weights after PD-1 treatment in WT, Roq$^{san/san}$ and Roq$^{san/san}$ dKO mice

After 5 days of B16 melanoma establishment, treating the mice with two doses of anti-PD-1 per week had no effect on tumour growth compared with the IgG treated group (Figure 5.4A). In contrast, WT tumours treated with anti-PD-1 grew more slowly than those in the WT control group. Interestingly, a significant remission in tumour volume was found in Roq$^{san/san}$ dKO treated with anti-PD-1 in comparison with

all treated and untreated groups. In keeping with the observed tumour growth rates, harvested tumour weights from Roq$^{san/san}$ treated and untreated groups were no different, whereas tumours from WT anti-PD-1 treated mice were reduced in weight compared to those from the IgG control mice (Figure 5.4B). Likewise, tumours from Roq$^{san/san}$ dKO anti-PD-1 treated mice were smaller than those from all other groups but this was only significant in comparison to the WT controls ($p<0.05$).

5.2.2.3 Survival rate and lymphocyte infiltration after anti-PD-1 treatment in WT, Roq$^{san/san}$ and Roq$^{san/san}$ dKO mice

Corresponding to the dynamics of tumour growth, Kaplan-Meier survival graphs showed only slight differences among Roq$^{san/san}$ anti-PD-1 and IgG mice, which all died within 27 days. The highest survival rate (80%) was recorded for the Roq$^{san/san}$ dKO anti-PD-1 group; these mice were the only ones surviving at 5 weeks post-tumour injection (Figure 5.4C). The humane endpoint for both WT anti-PD-1 and Roq$^{san/san}$ dKO anti-IgG was 4 weeks, one week longer than the WT controls (Figure 5.4C). In WT and Roq$^{san/san}$dKO mice treated with anti-PD-1 blockade, there was an increase in the infiltration of CD8$^+$ T cells into tumours, which was accompanied by a tendency to higher infiltration of Foxp3$^+$ Tregs, predominantly in WT mice, in comparison with their respective anti-IgG treated control groups (Figure 5.4E,F). There was no such increase, however, in the CD8$^+$ T cell infiltration into tumours in the Roq$^{san/san}$ anti-PD-1 treated group.

Figure 5.4: αPD-1 immunotherapy of melanoma in WT, Roq$^{san/san}$ and Roq$^{san/san}$ dKO mice

Tumour volumes were measured by callipers weekly, and mice were culled when tumours reached 12mm in diameter. Harvested tumours were weighed, digested and cells were stained and analysed by FACS. (A) tumour volumes, median of 3 measurements each (B) tumour weight at harvest, each point represents one mouse, bars show median values. (C) Kaplan-Meier survival graph D,E,F Tumour infiltrates (D) $CD4^+$ (E) $CD8^+$ (F) $FoxP3^+$. Statistical analysis was performed using the Mann Whitney non parametric test. Data are representative of two independent experiments, n=4,5,3,5,3,4 respective to each group in the order presented. * or ** indicates significance $p<0.05$ and $p<0.01$ respectively.

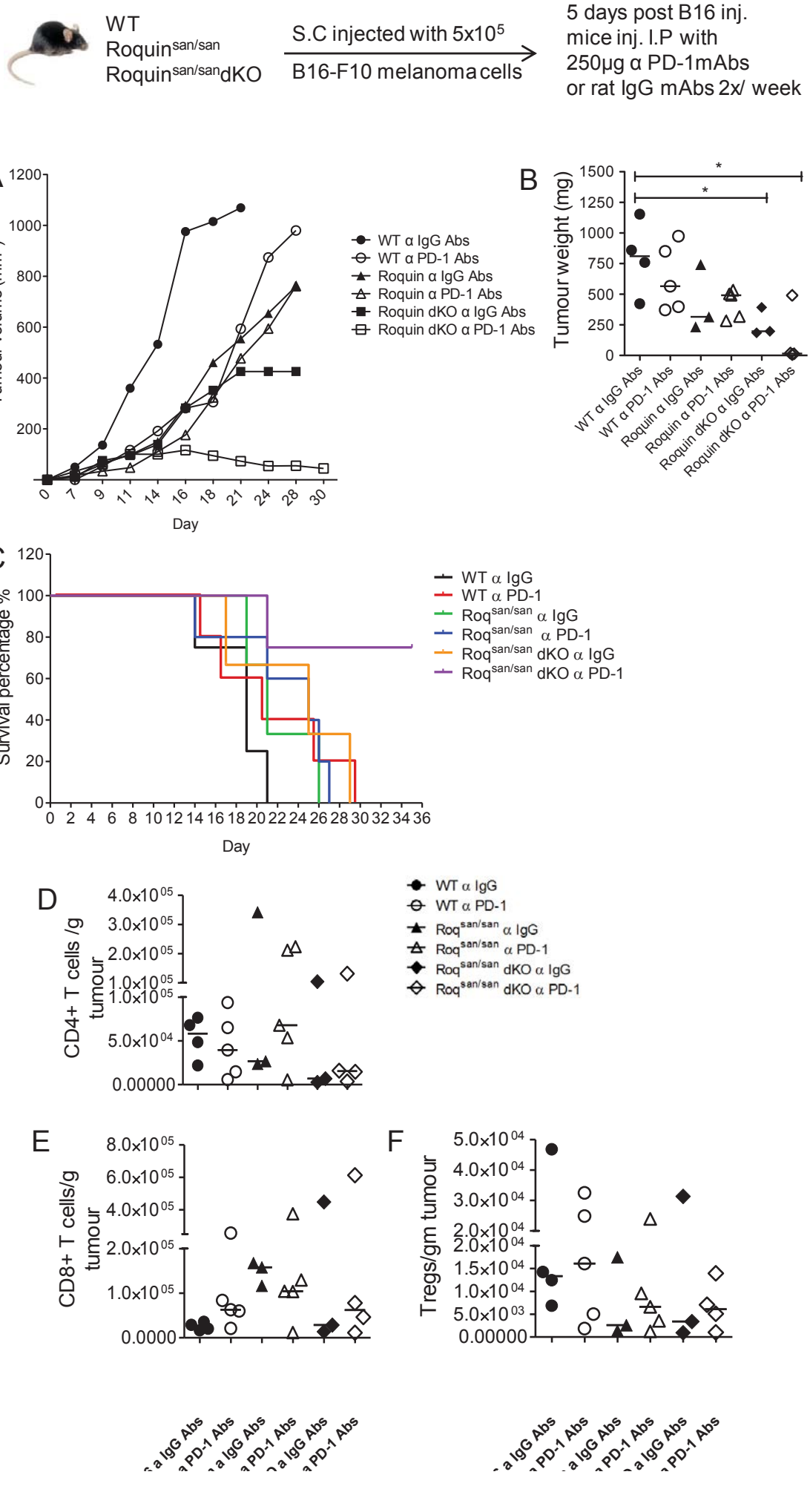
WT
Roquin san/san
Roquin san/san dKO
S.C injected with 5x10 5
B16-F10 melanoma cells
5 days post B16 inj.
mice inj. I.P with
250µg α PD-1mAbs
or rat IgG mAbs 2x/ week
A
Tumour volume (mm3)
Day
WT α IgG Abs
WT α PD-1 Abs
Roquin α IgG Abs
Roquin α PD-1 Abs
Roquin dKO α IgG Abs
Roquin dKO α PD-1 Abs
B
Tumour weight (mg)
C
Survival percentage %
Day
WT α IgG
WT α PD-1
Roq san/san α IgG
Roq san/san α PD-1
Roq san/san dKO α IgG
Roq san/san dKO α PD-1
D
CD4+ T cells /g tumour
E
CD8+ T cells/g tumour
F
Tregs/gm tumour

5.2.3 Experiment to test whether the lack of expression of PD-1 and increased CD8 infiltrate in Roq$^{san/san}$ mice was cell intrinsic or due to the environment in Roq$^{san/san}$ mice.

5.2.3.1 Experimental protocol

25X10^6 Roquin$^{san/san}$ (CD45.2) or WT (BoyJ, CD45.1) splenocytes were transferred alone or in a 1:1 mixture into T cell deficient hosts: Zap70 mice (Figure 5.5). 3 days post transfer 5x10^5 B16 cells were injected into the recipient mice. 14 days later tumour infiltrates were analysed. This experiment was conducted once but the results thus far clearly support our hypothesis that lack expression of PD-1 on Roq$^{san/san}$ CD8 T cells is cell intrinsic which leads to high infiltration of CD8 T cells into Roq$^{san/san}$ mice translated tumours .

5.2.3.2 FACS analysis and PD-1 expression on tumour infiltrating CD8 T cells

FACS analysis of tumours and enumeration of the infiltrating cells showed that the tumour infiltrate in chimeric mice was predominantly Roq$^{san/san}$ CD8 T cells, which were approximately 5 times as numerous as their WT counterparts (Figure 5.6B,D), and furthermore, Roq$^{san/san}$ CD8 T cells did not express PD-1, whereas the WT CD8 T cells expressed normal levels of PD-1 ($p<0.06$) (Figure 5.6F). The mean fluorescence intensity of PD-1 on CD8 T cells was not statistically significantly higher for WT than for Roq$^{san/san}$, but the consistency of the trend suggests that this would be the case if more mice were to be tested (Figure 5.6F). Moreover, WT Tregs could

neither inhibit Roq$^{san/san}$ CD8^{+} T cell infiltration into tumours nor increase tumour

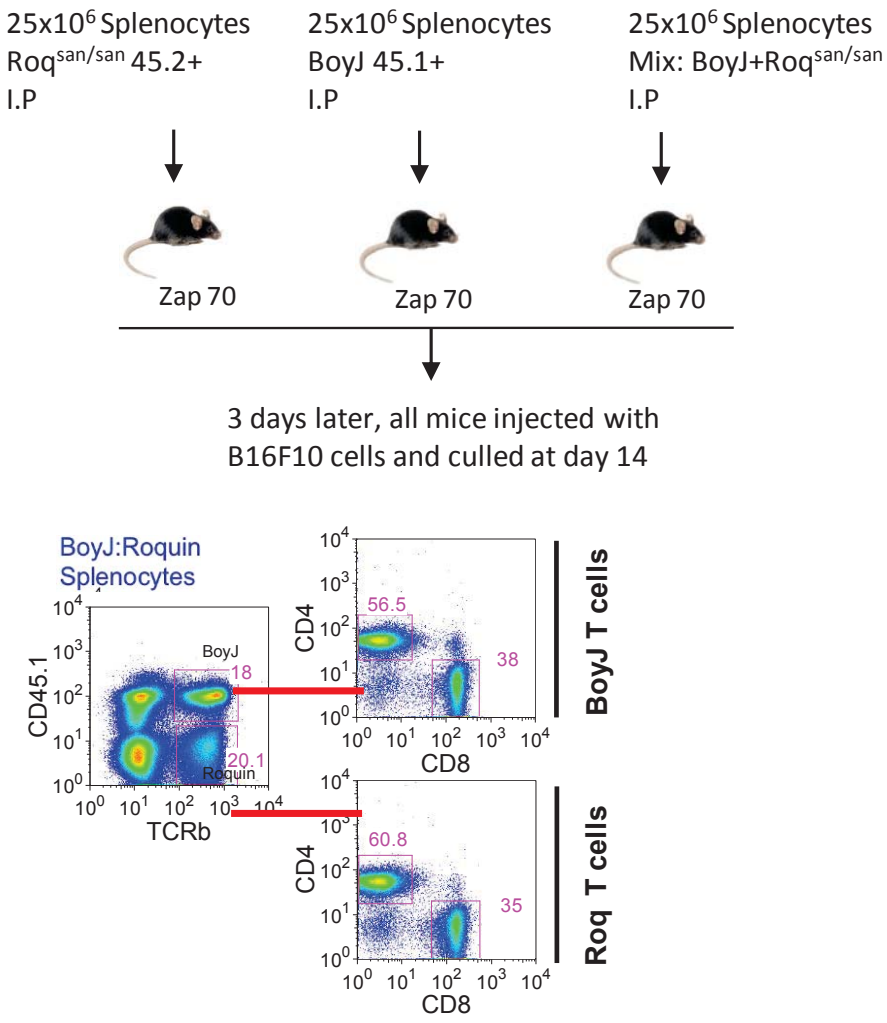

Figure 5.5: Experimental design to investigate whether the lack of expression of PD-1 on CD8 infiltrates in Roq$^{san/san}$ mice is cell intrinsic or cell extrinsic

FACS analysis of the BoyJ (CD45.1^{+}) and Roq$^{san/san}$ (CD45.2^{+}) splenocyte mixture before cells transfer into the T cell deficient recipient mice.

Figure 5.6: Adoptive transfer of WT (CD45.1^{+}) and Roq$^{san/san}$ (CD45.2^{+}) splenocytes mixtures into T cell deficient hosts transfected with B16 melanoma

(A) Tumour weights derived from T cell deficient host mice receiving BoyJ, Roq$^{san/san}$ and BoyJ:Roq$^{san/san}$ mixed splenocytes (B) Representative tumour FACS analysis C-E: cells/g tumour of lymphocyte infiltrates derived from BoyJ or Roq$^{san/san}$ donors (C) CD4^{+} T cells (D) CD8^{+} T cells (E) Tregs (F) PD-1 mean fluorescence intensity. Each data point represents one mouse, bars show median values. Data from a single experiment. Statistical analysis was performed using the Mann Whitney non parametric test, n=3,3,5 respective to each group in the order mentioned. * and ** indicate significance $p<0.05$ and $p<0.01$ respectively.

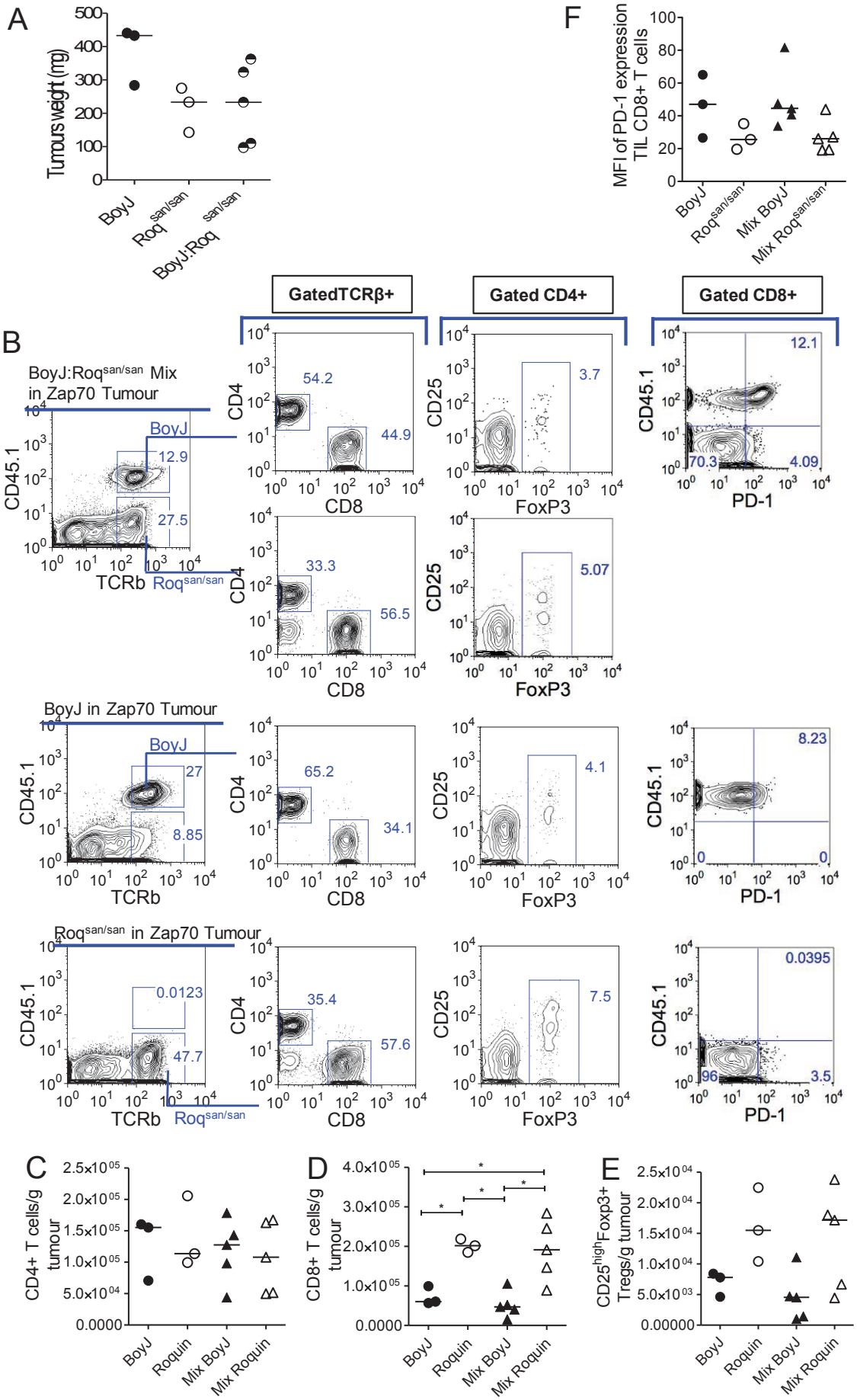
A
Tumour weight (mg)
BoyJ
Roq san/san
BoyJ:Roq san/san
F
MFI of PD-1 expression TIL CD8+ T cells
BoyJ
Roq san/san
Mix BoyJ
Mix Roq san/san
B
GatedTCRβ+
Gated CD4+
Gated CD8+
BoyJ:Roq san/san Mix in Zap70 Tumour
CD45.1
TCRb
BoyJ
Roq san/san
12.9
27.5
CD4
CD8
54.2
44.9
33.3
56.5
CD25
FoxP3
3.7
5.07
PD-1
12.1
70.3
4.09
BoyJ in Zap70 Tumour
27
8.85
65.2
34.1
4.1
8.23
0
0
Roq san/san in Zap70 Tumour
0.0123
47.7
35.4
57.6
7.5
0.0395
96
3.5
C
CD4+ T cells/g tumour
D
CD8+ T cells/g tumour
E
CD25high Foxp3+ Tregs/g tumour
BoyJ
Roquin
Mix BoyJ
Mix Roquin

5.2.4 The effect of anti-OX40 agonistic mAbs on PD-1 expression on T cells and melanoma response

We have shown that PD-1 expression is down regulated on T cells in $Roq^{san/san}$ mice, which overexpress OX40 in IFNγ dependent manner. We hypothesised that the effect of anti-OX40 agonistic Abs on melanoma response and the expression of PD-1 on T cells mimic that found in $Roq^{san/san}$ mice. Therefore, the following experiments were carried out.

5.2.4.1 Experimental protocol

WT (C57BL/6 Ly5.1) mice were injected with $5x10^5$ B16-F10 melanoma cells S.C on the right dorsal flank. After allowing 5 days for tumours to establish, WT mice were injected I.P with anti-OX40 agonistic Abs (clone OX86) or rat anti-IgG Abs, 100ug/mouse, twice per week.

5.2.4.2 The effect of OX40 agonist on WT tumour volume and weight

An antitumour effect of agonistic anti-OX40 antibodies has been reported (Weinberg *et al.* 2000); we wished to test this ourselves in WT mice, as well as in $Roq^{san/san}$ and $Roq^{san/san}$dKO mice, with a view to determining any effect on Treg behaviour and/or on tumour growth. To do this, anti-OX40 agonists were used to treat B16 melanoma in WT mice. Tumour volume measured over a three week period showed that anti-OX40 treatment slowed tumour growth and reduced the total tumour weight pooled from WT mice relative to that from WT controls, but the difference was not statistically significant (Figure 5.7A,B).

5.2.4.3 The effect of anti-OX40 agonist treatment on tumour lymphocyte phenotype and number

Cell phenotype analysis and enumeration by flow cytometry of infiltrates from the anti-OX40-treated WT tumours showed expansion, activation and infiltration of a $CD45^+CD3^+$ subset, both $CD4^+$ T cells and $CD8^+$ T cells (Figure 5.7C,D,E,F). Similar to $Roq^{san/san}$, the number of Tregs infiltrating the tumour somewhat less in anti-OX40 agonist treated group compared with anti-IgG treated tumours (Figure 5.7C,G).

5.2.4.4 The effect of anti-OX40 agonists on PD-1 expression on T cells

Treatment with anti-OX40 agonists led to the downregulation of PD-1 expression on tumour infiltrating $CD4^+$ and $CD8^+$ T cells (Figure 5.8A). Compared with the IgG treated group, $CD8^+$ T cells from tumours treated with the anti-OX40 agonist demonstrated a significant reduction of PD-1 expression ($p<0.05$). anti-OX40 may expand Tregs (Xiao *et al.* 2012), as occurred in $Roq^{san/san}$; the Tregs here were significantly expanded: their frequency was doubled from approximately 10% in IgG treated tumour draining lymph nodes to approximately 20% with OX86 treatment (Figure 5.7H).

Figure 5.7: The effect of anti-OX40 agonistic mAbs on melanoma response

WT mice were injected with 5 x 10^5 B16-F10 melanoma cells and 5 days later mice were treated with αOX40 agonistic mAbs or rat αIgG mAbs. Tumour volumes were measured using callipers weekly and mice were culled at 21d. Harvested tumours were weighed, digested and cells were stained for FACs analysis. (A) tumour volumes, medians of 3 measurements (B) tumour weights at harvest, each point represents one mouse, bars show median values (C) FACS tumour analysis gated on live cells D-G lymphocyte infiltrates (D) $CD45^+CD3^+$ population (E) $CD4^+$ T cells (F) $CD8^+$ T cells (G) Tregs (H) frequency of Tregs in tumour draining (inguinal) lymph node. Statistical analysis was performed using the Mann Whitney non parametric test. Data are representative of three independent experiments, n =7,12 for untreated and anti-OX40 agonist injected mice, respectively. ns indicates non-significant, ** significance $p<0.01$.

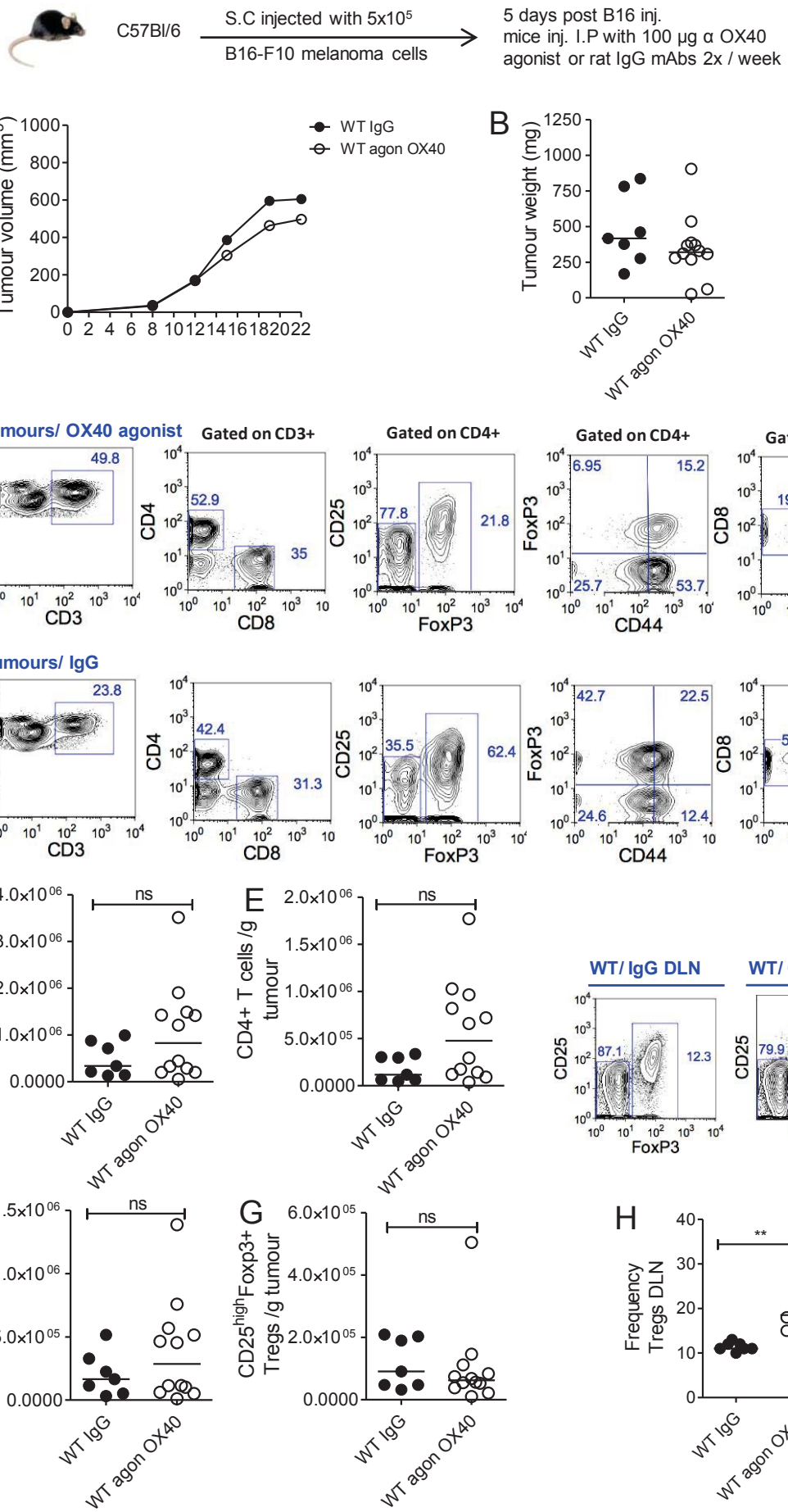
C57Bl/6
S.C injected with 5x10^5
B16-F10 melanoma cells
5 days post B16 inj.
mice inj. I.P with 100 µg α OX40
agonist or rat IgG mAbs 2x / week
A
Tumour volume (mm^3)
WT IgG
WT agon OX40
B
Tumour weight (mg)
WT IgG
WT agon OX40
C
WT tumours/ OX40 agonist
Gated on CD3+
Gated on CD4+
Gated on CD4+
Gated on CD8+
CD45
CD3
CD4
CD8
CD25
FoxP3
CD44
WT tumours/ IgG
D
CD45+CD3+ cells /g tumour
ns
E
CD4+ T cells /g tumour
WT/ IgG DLN
WT/ OX40 DLN
Gated on CD4+
F
CD8+ T cells /g tumour
G
CD25highFoxp3+ Tregs /g tumour
H
Frequency Tregs DLN
**

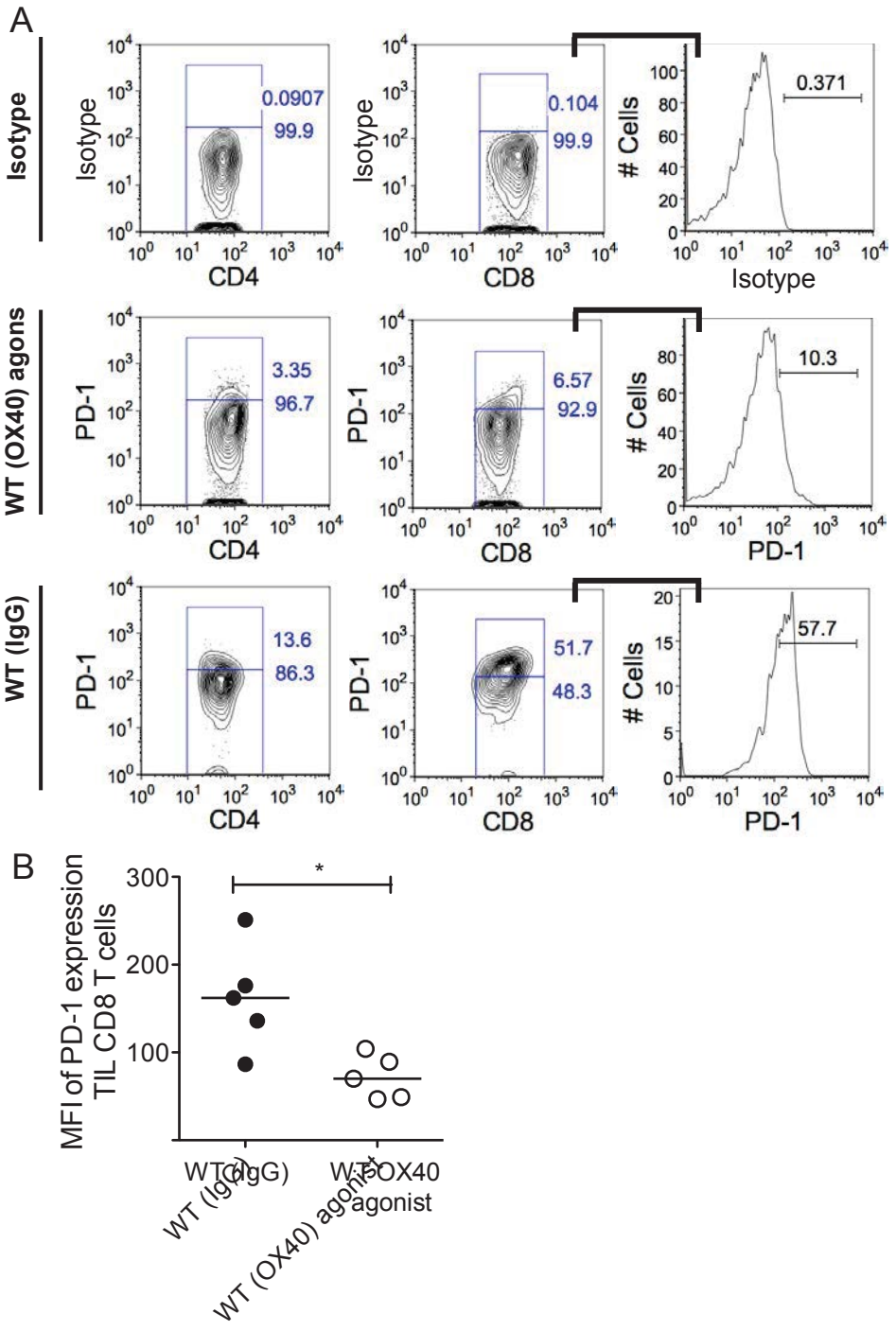
A
Isotype
WT (OX40) agons
WT (IgG)
Isotype
PD-1
CD4
CD8
Cells
0.0907
99.9
0.104
99.9
0.371
3.35
96.7
6.57
92.9
10.3
13.6
86.3
51.7
48.3
57.7
B
MFI of PD-1 expression TIL CD8 T cells
300
200
100
*
WT (IgG)
WT (OX40) agonist

5.3 Discussion

5.3.1 Tumours grow in Roq$^{san/san}$ and Roq $^{san/san}$dKO mice, but grow more slowly than in WT mice

The evidence provided by this part of the thesis shows that the tumour immune response in the Roq$^{san/san}$ model is similar to that in WT mice treated with anti-OX40 agonists. B16 transfected Roq$^{san/san}$ mice showed slower tumour growth compared with WT but this deceleration of tumour growth was more and was statistically significant in Roq$^{san/san}$dKO strain (Figure 5.1A,B). Fabrina Gaspal's work in our lab showed that Roquin mutant T cells produce IFNγ and GM-CSF, activating MØ to produce TNF and NO (via iNOS induction), which drive OX40L overexpression in T cells and render them resistant to extrinsic regulation mechanisms (Tregs) (Fabrina Gaspal, unpublished data). The significant tumour infiltration of CD8$^+$ T cells found in Roq$^{san/san}$ and Roq$^{san/san}$dKO mice suggests an intrinsic IFNγ-iNOS-OX40L dependent mechanism responsible for resistance to Treg suppression, not only in CD4$^+$ T cells but also in CD8$^+$ T cells, leading to their invasion of the tumour microenvironment and contributing to its rejection (Figure 5.2E). The high density of CD8$^+$ T cells and M1 MØ within tumours and abundance of IFNγ have been considered as strong favourable prognostic indicators in cancers (Mantovani *et al.* 2002, Pagès *et al.* 2005, Galon *et al.* 2006, Movahedi *et al.* 2010, Mantovani and Allavena 2015). In previous chapters, we showed significant CD8$^+$ infiltration in dKO tumours; here, deficiency of CD30 and OX40 further decreased tumour growth dynamics in Roq$^{san/san}$dKO mice compared with Roq$^{san/san}$, suggesting dysfunctionality of Tregs (Gaspal *et al.* 2011), likely to be responsible for the additional increase in CD8$^+$ infiltration of tumours.

Moreover, in the adoptive cell transfer model, our lab has shown that Roq$^{san/san}$ dKO Tregs are dysfunctional, since they fail to inhibit FoxP3 disease in T cell deficient mice while Roq$^{san/san}$ Tregs were functional and inhibited disease (Vinuesa *et al.* 2005). Tregs fail to inhibit the CD8^{+} T cell subset expansion in spite of the fact that in normal and tumour-bearing sanRoquin mice the Treg population in inguinal (draining) lymph nodes is about three times the size of that in WT mice (Figure 5.2H).

5.3.2 Impaired PD-1 expression is intrinsic to Roquin mutant mice but the phenotype is partial in Roq$^{san/san}$dKO

Interestingly, there was a variation in the expression of the inhibitory molecule PD-1 and its MFI on CD8^{+} T cells infiltrating WT, dKO, Roq$^{san/san}$ and Roq$^{san/san}$dKO tumours (Figure 5.3A-D,E). There was scant expression of PD-1 on Roq$^{san/san}$ CD8 T cells (approximately 3%) and intermediate expression on Roq$^{san/san}$dKO infiltrates, while it was abundantly expressed on WT and dKO CD8 infiltrates, suggesting an intrinsic pathway resultant from Roquin mutation and the dysregulation of IFNγ (Vinuesa *et al.* 2005). The latter study describes the IFNγ effect on CD4^{+} T cells, but in tumour models PD-1 is more pertinent to CD8 T cells. To our knowledge this is the first report of the effect of IFNγ on downregulating PD-1 on T cells; although IFNγ has been reported to drive the overexpression of PD-L1 on tumour cells, which leads to tumour progression (Blank *et al.* 2004, Abiko *et al.* 2015). It has also been reported that IFNα but not IFNγ results in upregulation of PD-1 on antigen derived CD8 T cells (Terawaki *et al.* 2011).

The intermediate phenotype of PD-1 in Roq$^{san/san}$dKO CD8^{+} T cells may be due to the intermediate expression of IFNγ on T cells and also the absence of CD30/CD30L and

OX40/OX40L signalling as feedback for augmenting IFNγ production. CD30 and OX40 deficiency has been found to downregulate IFNγ three-fold on $Roq^{san/san}$dKO $CD4^+$ T cells compared with $Roq^{san/san}$ (Fabrina Gaspal *et al*., unpublished data) and mostly abrogated IFNγ expression in CD4 T cells in FoxP3dKO mice (Gaspal *et al.* 2011); these reductions could restrict the IFNγ mediated upregulation of PD-1 on T cells in tumour microenvironments; however, this needs to be investigated. IFNγ can limit IL-2R expression, IL-2 signalling and Treg expansion (St. Rose *et al.* 2013) and PD-1 deficiency on conventional CD4 T cells plays a role in inhibition of peripheral Treg differentiation (Chen *et al.* 2014). This may suggest that the intrinsic overexpression of IFNγ in $Roq^{san/san}$ T cells, consequent upon NO from MØ, and downregulation of PD-1 have a role in reducing the number of Tregs infiltrating Roqsan and RoqsandKO tumours additional to the role of CD30 and OX40 (Figure 5.2F).

5.3.3 Anti-PD-1 slows tumour growth and increases survival rate in WT and $Roq^{san/san}$dKO mice but not in $Roq^{san/san}$ mice as a result of lack expression of PD-1 on $Roq^{san/san}$ T cells

Obtaining a tumour objective response by targeting with anti-PD-1 blockade has been proved experimentally in mice and clinically in human (Flies *et al.* 2011, Topalian *et al.* 2012, Robert *et al.* 2015a). We examined the efficacy of anti-PD-1 blockade on $Roq^{san/san}$ tumours in which $CD8^+$ T cells lack PD-1. Anti-PD-1 produced no additional benefit, as a result of lack of expression of PD-1 on CD8 T cells which was Tregs independent as shown in tKO, at targeting $Roq^{san/san}$ tumours compared with tumours in WT, where there was an objective response to anti-PD-1 treatment in

terms of tumour growth and individual survival rate (Figure 5.4A,B,C). This confirms that PD-1 inhibition is Roquin intrinsic. In comparison with WT and $Roq^{san/san}$, anti-PD-1 blockade of the partial expression of PD-1 on $Roq^{san/san}$ dKO $CD8^+$ T cells restored anti-tumour $CD8^+$ T cells (Barber *et al.* 2006, Sakuishi *et al.* 2010). In combination with the $Roq^{san/san}$ dKO Treg dysfunctionality (Gaspal *et al.* 2011) (Fabrina Gaspal *et al*., unpublished data) the overall effect was to enhance the tumour objective response and increase the survival rate in the $Roq^{san/san}$dKO treated group significantly and this was enhanced by further PD-1 blockade. Moreover, concurrent CD30 and OX40 deficiency attenuate sanRoquin CD4 driven autoimmunity (Fabrina Gaspal *et al*., upublished data), and, as we have shown in previous chapters, both molecules reduce anti-PD-1 toxicity. PD-1 blockade was accompanied by a tendency toward greater $CD8^+$ T cell infiltration into WT and $Roq^{san/san}$dKO treated tumours but not $Roq^{san/san}$ in comparison to their control groups. Infiltration of $CD8^+$ T cells, here seen accompanying PD-1 blockade (Figure 5.4F), may be counteracted by tumour-mediated recruitment of Tregs as a compensating inhibitory mechanism (Curiel *et al.* 2004). Our lab has also shown that $Roq^{san/san}$ and $Roq^{san/san}$dKO CD4 T cells produce GM-CSF, which has been found to synergise with anti-PD-1 in B16 tumour rejection and may represent another aspect of the anti-PD-1 tumour response in $Roq^{san/san}$dKO mice, but not in $Roq^{san/san}$ mice, which lack PD-1 (Li *et al.* 2009).

5.3.4 The suppressive expression of PD-1 is T cell intrinsic

The preliminary adoptive transfer experiments of WT (CD45.1) and $Roq^{san/san}$ (CD45.2) splenocyte mixtures showed substantial infiltration of $Roq^{san/san}$ $CD8^+$ T cells into T cell deficient host tumours. The immunosuppressive extrinsic

mechanisms of WT Tregs could not inhibit $Roq^{san/san}$ CD8 T cells, suggesting that the $OX40L^{high}$ T cells are intrinsically resistant to T regulation (Fabrina Gaspal *et al*., unpublished data). Moreover, the transfer of splenocyte mixtures also demonstrated downregulation of PD-1 on $Roq^{san/san}$ $CD8^+$ T cell infiltrates compared with their WT counterparts, confirming that their PD-1 impairment is not due to host stroma, but is a consequence of their Roquin mutation and the intrinsic IFNγ dysregulation associated with it.

5.3.5 Anti-OX40 agonists downregulate PD-1 expression on $CD4^+$ and $CD8^+$ T cells

The anti-melanoma effect in sanroque mice was mimicked when we used anti-OX40 agonists to target B16 melanoma in WT mice. We found that WT melanoma bearing mice treated with anti-OX40 agonists also downregulated PD-1 on WT $CD4^+$ and $CD8^+$ T cells. OX40 has been found to induce IFNγ production in CD8 T cells (De Smedt *et al.* 2002) and breaks tolerance (Bansal-Pakala *et al.* 2001). As we found in the Roquin IFNγ dependent phenotype, the results obtained with anti-OX40 agonists also may indicate that IFNγ plays a role in suppression of PD-1 on T cells, which needs to be confirmed in the future. The boosting of OX40 signals has been shown to slow tumour growth as a result of the activation of the anti-tumour effector and memory arm of the immune system and of breaking Treg tolerance (Bansal-Pakala *et al.* 2001, Valzasina *et al.* 2004, Piconese *et al.* 2008, Burocchi *et al.* 2011, Xiao *et al.* 2012). Others also reported similar results using OX40L-Ig to treat MCA 303 sarcoma, CT26 colon carcinoma, SM1 breast cancer and B16/F10 melanoma in mice (Weinberg *et al.* 2000). Our results further suggest that anti-OX40 agonists used in

tumour immunotherapy (Weinberg *et al.* 2011), are ineffective in combination with anti-PD-1, where there is also a high risk of lethal autoimmunity (Nishimura *et al.* 1999, Murata *et al.* 2002). To our knowledge, there is only one paper reporting that combined anti-OX40 agonist and anti-PD-1 blockade treatments promoted ovarian cancer rejection in mice compared to single treatments (Guo *et al.* 2014), in disagreement with our results. However, tumour response in this study was CD4 T cell mediated; whereas the B16 melanoma response is CD8 dependent (Townsend and Allison 1993, Saito *et al.* 2000, Overwijk *et al.* 2003, Ahmadzadeh *et al.* 2009, Fourcade *et al.* 2012, Tumeh *et al.* 2014).

5.3.6 Conclusion

This chapter concludes that the $Roq^{san/san}$ tumour immune response mimics that of anti-OX40 agonists. Intrinsic dysregulation of IFNγ in Roquin mutated mice contributes to the activation of the NO-producing MØ that induce overexpression of OX40L and CD30L, not only in $CD4^+$ T cells but also in $CD8^+$ T cells, rendering them resistant to regulation by Tregs. This ultimately contributed toward tumour rejection in $Roq^{san/san}$ mice, and in $Roq^{san/san}$dKO mice, where Tregs are also dysfunctional, survival was extended significantly. We also showed that there is intrinsic suppression of PD-1 expression on CD8 T cells in both Roquin mutant mice and in the tumours of anti- OX40 agonist-treated WT mice.

5.3.7 Future work

Our tumour studies on $Roq^{san/san}$ mice suggest two lines of investigation. The first one is the role of IFNγ in downregulation of PD-1 expression on tumour T cells infiltrates, which can be investigated by injecting αIFNγ into $Roq^{san/san}$ mice with established

B16 melanoma. The second line involves identifying the type of MØ infiltrating tumours in Roq$^{san/san}$ mice, and their role in promoting or inhibiting the anti-tumour response, with particular regard to our data showing that MØ overexpress iNOS and induce OX40L on T cells, which can lead to the breaking of Treg mediated tolerance (Fabrina Gaspal *et al*., unpublished data).

Chapter Six

General Discussion

Self-tolerance mechanisms including the action of nTregs and other T effector inhibitory pathways are exploited by tumours to dampen anti-tumour adaptive immunity (Dong *et al.* 2002, Iwai *et al.* 2002, Blank *et al.* 2004, Curiel *et al.* 2004, Chen *et al.* 2005, Ahmadzadeh *et al.* 2009). Recent anti-tumour trials targeting those mechanisms returned favourable objective outcomes, and led to FDA approval of CTLA-4 and PD-1 blocking antibodies for treating cancers. However, those blockades are associated with adverse autoimmune toxicity which restricts both viable dose and efficacy of the treatments (Hodi *et al.* 2010, Topalian *et al.* 2012, Wolchok *et al.* 2013, Postow *et al.* 2015). Therefore, the aim of this study was to dissociate anti-tumour immune responses from autoimmunity, using the autoimmunity-resistant $CD30^{KO}OX40^{KO}FoxP3^{KO}$ (tKO) mouse strain and various blocking antibody combinations, with the intention of developing a strategy to optimize tumour immunotherapy. As an additional tool in investigating tumour immune responses, we also applied our methods to the Sanroque mice, which harbor a mutation in the mRNA regulator, Roquin. These mice show intrinsic overexpression of IFNγ (Vinuesa *et al.* 2005) and MØ–iNOS dependent upregulation of OX40L on effector T cells, which consequently acquire resistance to regulation. The hypothesis was that blocking OX40 and CD30 signals would prevent CD4 driven autoimmunity while preserving excellent anti-tumour CD8 immune responses.

The prevalence of $FoxP3^{+}$ Tregs in tumours (Curiel *et al.* 2004) has been associated with a negative impact on melanoma patient survival (Shang *et al.* 2015) but their effect also been suggested to be positive in colon cancer (Salama *et al.* 2009). Our

data in chapter 3 defined the high frequency of FoxP3$^+$ Tregs relative to CD8$^+$ T effector cells in WT tumours, which correlated with accelerated tumour progression and viability, as assed by *in vivo* imaging. We could manipulate the regulator:effector balance in tumours by disruption of FoxP3$^+$ Treg suppressive function via the abrogation of CD30 and OX40 signals (dKO mice), and depletion of FoxP3$^+$ Tregs (tKO mice) (Chapter 3 and Figure 6.1), which shifted the lymphocyte balance in tumour infiltrates towards CD8 effector cells, and resulted in significant tumour shrinkage in tKO mice. CD8 T cells are critical for tumour rejection in B16 melanoma (Townsend and Allison 1993), and this was true for our tKO mice, whose B16 melanoma resistance was broken when CD8 T were cells depleted. FoxP3$^+$Treg depletion alone does not restore full tumour immunity, however, as tumours were not completely rejected in tKO mice, despite shifting the tumour infiltrates balance in favour of CD8$^+$ T cells; this is likely to be a consequence of the overexpression of the inhibitory receptor PD-L1 by tumours and PD-1 by CD8$^+$ T cells infiltrated into tKO tumour. This shows that PD-1 acts instead of Tregs by negating CD8 T cell action (Dong *et al.* 2002, Iwai *et al.* 2002, Blank *et al.* 2004, Ahmadzadeh *et al.* 2009, Fourcade *et al.* 2012). PD-1 blockade in tKO mice with established B16-F10 melanoma led to tumour rejection, and this outcome was mimicked in dKO and WT mice treated with the blocking antibody combinations anti-(CTLA-4,PD-1) and anti-(CTLA-4,PD-1,OX40L,CD30L) respectively (Chapter 3 and Figure 6.2). This effect is due to the ability of anti-PD-1 to restore CD8 functionality (Barber *et al.* 2006, Sakuishi *et al.* 2010) while anti-CTLA-4 depletes intra-tumour Tregs (Selby *et al.* 2013, Simpson *et al.* 2013). It is important to note that the anti-OX40L and anti-CD30L blockades did not interfere with CD8 anti-tumour response; rather they

abrogated the CD4 driven autoimmunity associated with CTLA-4 blockade, as we had already found in our FoxP3$^+$ deficient (tKO) mice (Gaspal *et al.* 2011).

It would be relevant to investigate the expression of other inhibitory molecules, such as TIM-3, on CD8 infiltrates in our tKO mice, and the efficacy of blocking those inhibitors alone or in combination with anti-PD-1 on tumour growth. Published studies have targeted tumours using anti-PD-1 and anti-TIM-3 blockades on their own or in combination, to restore exhausted CD8 anti-tumour immunity (Sakuishi *et al.* 2010), but not in the context of the absence of FoxP3$^+$ Tregs. We confirmed the negative impact of FoxP3$^+$ Tregs on melanoma outcomes; it would also be of great interest to conduct experiments on tKO mice using other tumour models, such as colon carcinoma, to explore the prognostic value of Tregs in various types of tumours, since recent meta-analytic studies suggested that this value could be affected by tumour location (Shang *et al.* 2015).

The latest immunotherapeutic approaches have experimented with the removal of autologous T cells from the tumour or periphery of a (human or mouse) host to be genetically engineered *in vitro* to express peptides and produce cytokines or stimulating growth factors. Transfer of the engineered cells back into their hosts has been reported to result in a dose dependent objective response in tumours in both mouse and human (Overwijk *et al.* 2003, Zhang *et al.* 2015). In the most recent of these studies (Overwijk *et al.* 2003, Zhang *et al.* 2015), however, the objective response rate of 63% was accompanied by both regression of the response and significant clinical toxicities of the treatment. In this regard, our tKO mice model is of strong interest for investigating adaptive cell therapeutic strategies, conferring

advantage in the assessment of any associated autoimmunity, as well as in the exploration of the reasons behind short term persistence of infused cells, in particular whether this might be Treg dependent or independent.

Human trials using cancer derived peptide vaccines have reported vaccine related autoimmunity (Phan *et al.* 2003), significant adverse toxicity and low treatment outcomes (Hodi *et al.* 2010). Vaccination with conditional Treg depletion, however, has been demonstrated to expand vaccine efficacy for tumour remission (Klages *et al.* 2010), another result that would justify the use of our tKO mouse model for vaccination based studies to disentangle toxicity and efficacy.

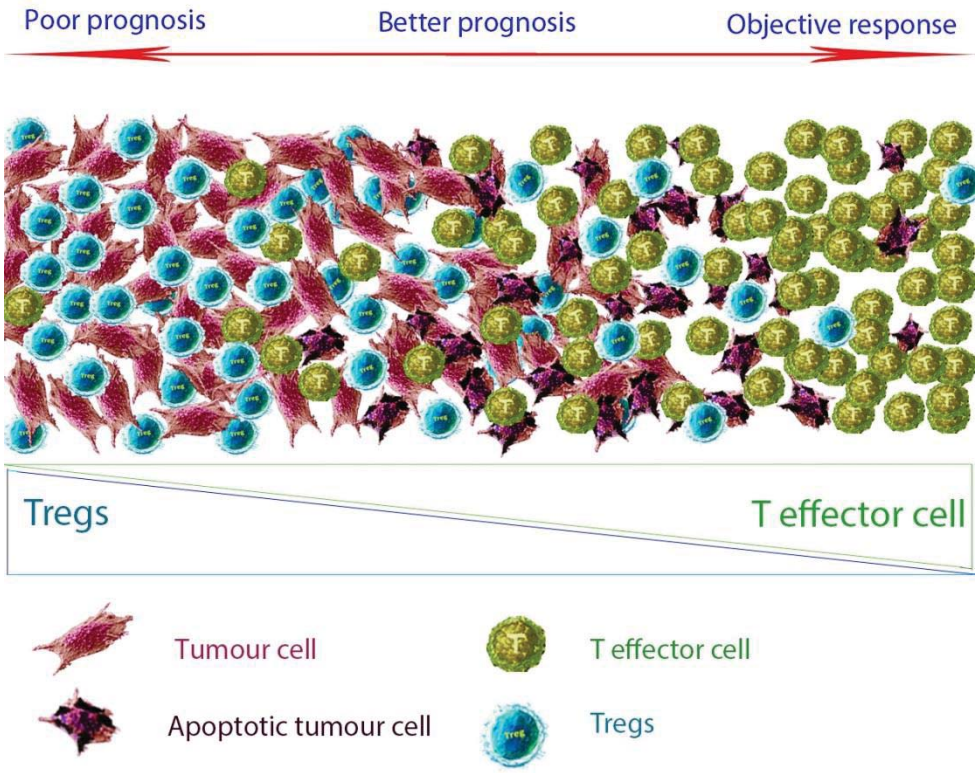

Figure 6.1: The balance between tumour associated Tregs and tumour specific effector cells.

The high frequency of self-specific Tregs (blue) in tumour microenvironments is associated with low frequency of anti-tumour effector T cells (green) and good viability of tumour cells (pink), and indicator of poor prognosis. CD30 and OX40 deficiency (dKO mice) shifted the balance towards effector T cells which correlated with better prognosis, while depletion of FoxP3$^+$ Tregs (tKO mice) further increased effector T cells and decreased tumour viability, increasing the numbers of apoptotic tumour cells (dark red) and leading to objective tumour shrinkage, particularly when treated with anti-PD-1 antibodies.

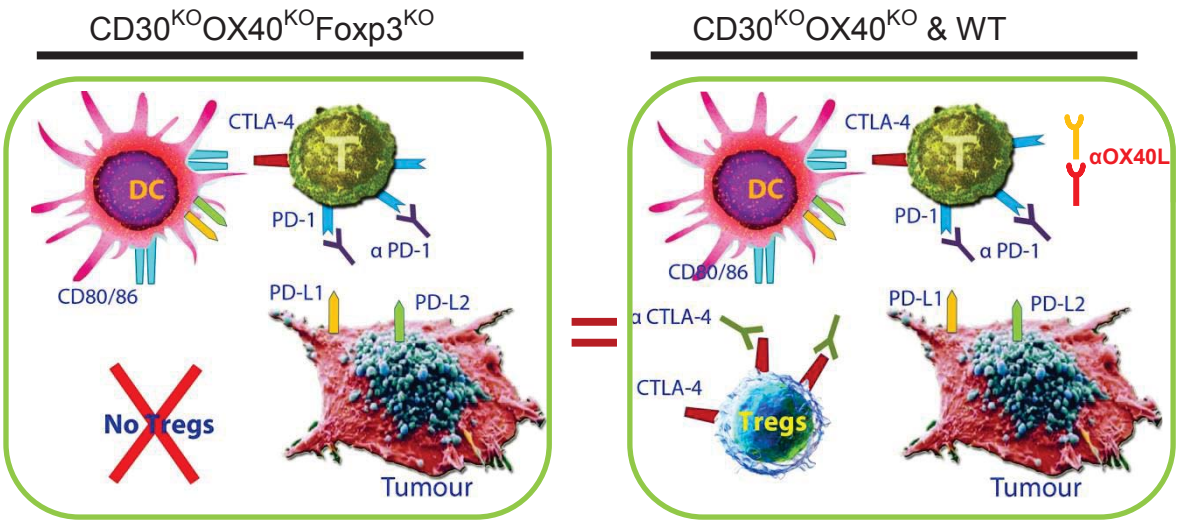

Figure 6.2: The beneficial effects of the gene deficiencies in $CD30^{KO}OX40^{KO}FoxP3^{KO}$ mice on tumour immune responses can be mimicked by the use of antibody blockade in WT and $CD30^{KO}OX40^{KO}$ mice.

Targeting pre-established B16-F10 melanoma in $CD30^{KO}OX40^{KO}Foxp3^{KO}$ mice with anti-PD-1 is similar to the treatment of $CD30^{KO}OX40^{KO}$ mice with anti-(CTLA-4,PD-1) and WT mice with anti-(CTLA-4,PD-1,OX40L,CD30L).

Importantly, our current study also confirmed that the excellent anti-tumour immune response of blocking antibodies in dKO and tKO mice could be preserved and replicated in normal (C57Bl/6) mice treated with a fourfold mAb combination anti-(CTLA-4,PD-1,OX40L,CD30L). Furthermore, we produced evidence that this approach could interfere with off-target autoimmune side effects by abrogating of OX40 and CD30 signals. The signs of CD4 driven autoimmunity associated with anti-CTLA-4 and anti-PD-1 blockades, including liver pathology, serum ALT and AST enzyme levels, autoantibody production and skin depigmentation, were remarkably attenuated or absent in C57Bl/6 mice treated concurrently with anti-OX40L and anti-CD30L, compared with the double blockade of anti-CTLA-4 and anti-PD-1 alone, for which mice showed severe autoimmune pathology. Clinically this adverse autoimmune toxicity is of great importance due to the limitations it places on dosage and efficacy of treatment, as has been reported in numerous clinical trials (Wolchok *et al.* 2013, Topalian *et al.* 2014, Larkin *et al.* 2015, Postow *et al.* 2015) The unique action of anti-OX40L and anti-CD30L blockades in abrogating CD4 driven autoimmunity, which is mainly cytokine mediated, delivers a strategy that would be highly advantageous not only in minimizing the toxicity associated with the inhibitory blockades but also in enhancing therapeutic outcomes in a wider spectrum of patients (Chapter 4 and Figure 6.3). A further dimension of this lies in the fact that Tregs constitutively express OX40 (Takeda *et al.* 2004), which has been shown to master the homing of nTregs to control colitis (Griseri *et al.* 2010) and recruitment of nTregs into the hepatocellular cancer site (Piconese *et al.* 2014), suggesting that the blocking of OX40 would inhibit nTreg infiltration into tumour microenvironments

and/or inhibit its suppressive function as we have shown in dKO and tKO mice (Chapter 4 and Figure 6.3).

In other studies, it was found that significant numbers of $CD3^{-}CD4^{+}ROR\gamma t^{+}CCR7^{+}$LTi cells were recruited into tumours in C57Bl/6 mice derived from either an engineered B16-F10 cell line expressing CCL21 at high levels ($B16CCL21^{high}$) or a normal B16 cell line that also secrets abundant CCL21, compared to their recruitment into tumours from a $CCL21^{low}$ B16-F10 source ($B16CCL21^{low}$) (Shields *et al.* 2010). Moreover, the LTi were found to induce lymphoid like stroma within the tumour, preparing an environment for the enrichment of Tregs and subsequent encouragement of tumour growth in $B16CCL21^{high}$ injected mice compared to $B16CCL21^{low}$ mice and mice with tumours treated with anti- CCR7 (Shields *et al.* 2010). OX40L and CD30L blockades could affect LTi (Figure 6.3), which express OX40L and CD30L (Kim *et al.* 2003, Kim *et al.* 2008), and may provide survival signals either to Tregs within the tumour microenvironment and lymphoid organs or to the memory autoreactive CD4 T cells that mediate autoimmunity (Gaspal *et al.* 2005, Withers *et al.* 2009, Diz *et al.* 2012). These are interesting possibilities that warrant investigation. Although the effect of anti-CD30L blockade alone on autoimmune toxicity associated with anti-CTLA-4 or anti-PD-1 alone or combined has not been examined in this study, we expected the role of OX40 to be dominant but cooperative with CD30 in supporting CD4 driven autoimmunity as was shown in $FoxP3^{+}$ deficient mice (Gaspal *et al.* 2011).

Investigation of the effect of our four-fold combination of blocking antibodies on metastatic forms of cancer and in long term therapeutic studies was beyond the

scope of the current project, but we believe that our results were sufficiently promising to encourage pursuit of this as a potentially successful cancer immunotherapy.

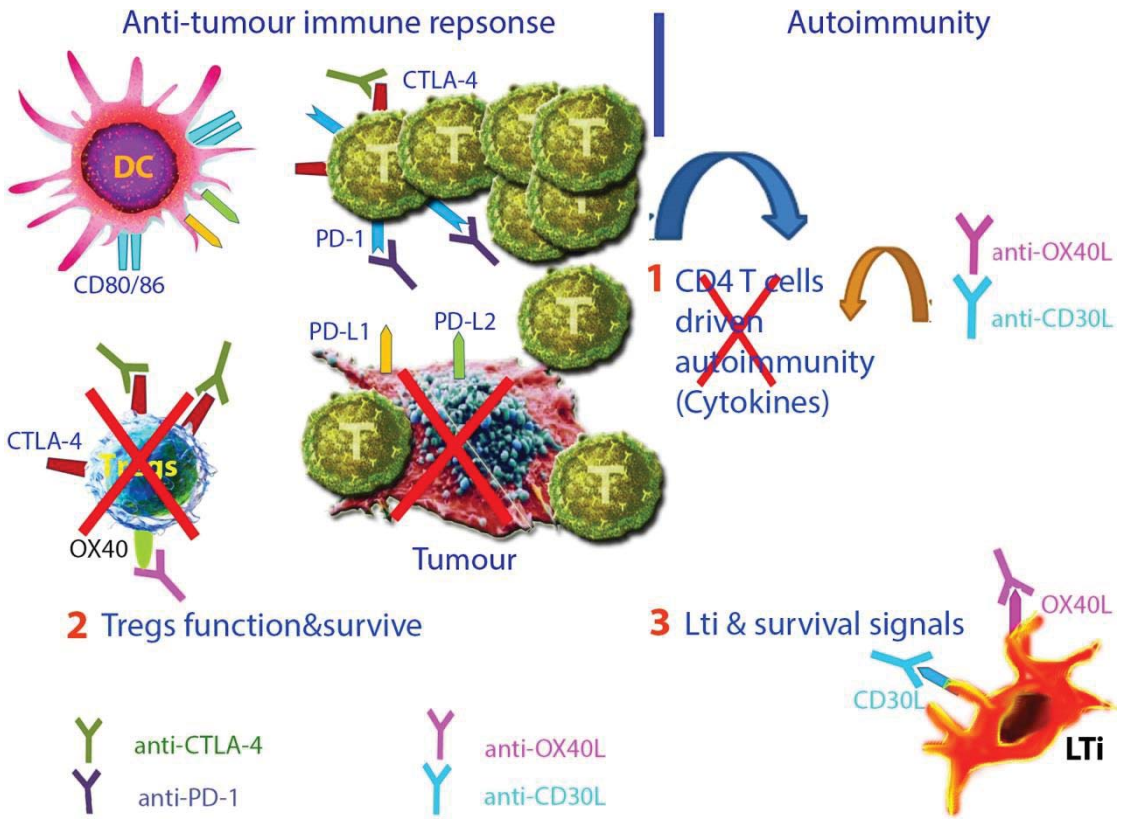

Figure 6.3: Strategy to dissociate tumour immunity from autoimmunity

Combining anti-OX40L and anti-CD30L blocking antibodies with anti-CTLA-4 and anti-PD-1 blockades may show three outputs: (1) abrogation of CD4 driven autoimmunity associated with anti-CTLA-4 and anti-PD-1 mAbs, (2) suppression of Treg function and homing into tumours, (3) suppression of tumour infiltration by LTi, which may provide survival signals to Tregs or auto-reactive memory T cells.

In the Roquin$^{san/san}$ mouse model, we observed the slowing down of tumour growth compared to WT mice; we showed that CD8 T cells infiltrated tumours in the Roquin$^{san/san}$ mice significantly more than WT mice, suggesting that those CD8 T cells were resistant to nTreg suppressive function, possibly in IFNγ-MØ-iNOS-OX40L dependent manner; however, the role of MØ remains to be investigated fully. Likewise, our lab also showed that this resistant mechanism extended to CD4 T cells in Roquin$^{san/san}$ models leading to SLE like autoimmunity, in spite of the fact that Treg function in those mice seems normal. Disturbing Treg function by depleting CD30 and OX40 further reduced tumour growth in dKORoquin$^{san/san}$ mice compared to both WT and Roquin$^{san/san}$ mice.

However, the IFNγ-MØ-iNOS-OX40L dependent mechanism significantly downregulated the expression of PD-1 on CD4 and CD8 tumour infiltrates in Roquin$^{san/san}$ mice in an intrinsic manner. CD30 and OX40 deficiency results in significant abrogation of CD4 T cell cytokine expression, including IFNγ (Gaspal *et al.* 2011); this led to over-expression of PD-1 on T cell populations infiltrating tumours in dKORoquin$^{san/san}$ mice. Treatment of those tumours with anti-PD-1 resulted in a significant therapeutic effect in dKORoquin$^{san/san}$ mice, while the same therapy made no difference to either Roquin$^{san/san}$ treated or untreated established tumours. Notably, we have also showed that anti-OX40 agonists reduce PD-1 expression on tumour T cells infiltrates as is observed in Roquin$^{san/san}$ mice, suggesting that approaches targeting tumours by combining OX40 agonists and anti-PD-1 may not work effectively as a general rule, although synergy between anti-OX40 agonist and anti-PD-1 has been reported to be effective in ovarian cancer (Guo *et al.* 2014). What is also interesting about this part of our study is that the literature reports that tumour-

associated macrophages are divided into two phenotypes; macrophage phenotype 1 (MØ1), associated with a good anti-tumour response via IL-12 production, while phenotype 2 (MØ2) suppresses anti-tumour immunity through IL-10 and TGF-β and CCL-22-CCR4 mediated recruitment of Tregs into the tumour microenvironment, which further strengthens the anti-inflammatory response (Curiel *et al.* 2004, Savage *et al.* 2008, Heusinkveld *et al.* 2011, Chanmee *et al.* 2014). This suggests that blocking OX40 would not interfere with the anti-tumour response if the tumour were enriched with MØ1, but rather would reduce off target autoimmunity (Figure 6.4). If the tumour were enriched with MØ2, OX40 blockade would repress the tumour infiltrating Tregs associated with MØ2, stimulate the anti-tumour response and also reduce off target autoimmunity (Figure 6.4). This concept and its mechanisms could be of great value and need to be investigated.

In conclusion, we propose a novel strategy using anti-OX40L and anti-CD30L blockades to attenuate autoimmunity associated with blocking antibodies used for treating cancer while preserving excellent anti-tumour immune response. This strategy would be suggested as the early choice for treating cancer patients rather than being a final treatment option, and could have the potential to be extended to a wide range of human cancer patients at high doses.

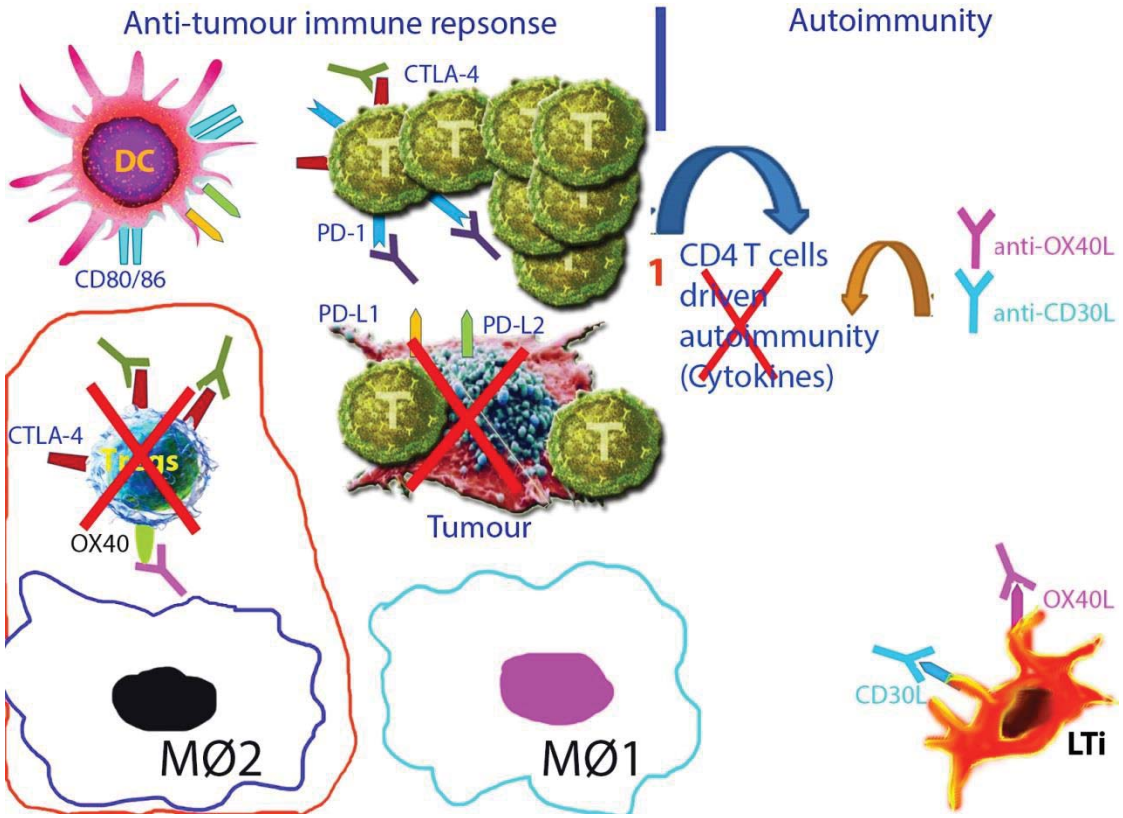

Figure 6.4: Blocking of OX40 in the presence of tumour-associated macrophages, type MØ1 or MØ2

The effect of blocking OX40 with anti-OX40 antibodies would be dependent on which type of tumour-associated macrophages was abundant in the tumour microenvironment. If MØ1 predominate, then OX40 blockade would not interfere with the anti-tumour effect of the MØ1 and would abrogate CD40 driven autoimmunity. But if MØ2 prevail, then anti-OX40 would interfere with tumour infiltration by Tregs and promote anti-tumour response, in addition to reducing CD4 driven autoimmunity.

Papers

- Lane, P. J., McConnell, F. M., Gaspal, F. M**., Nawaf, M.G.**, Withers, D. and Anderson, G. (**2014**) Evolving strategies for cancer and autoimmunity: back to the future. *Frontiers in Immunology, 5*.

- **Nawaf, M.G**., Ulvmar M., Withers, D., McConnell, F. M., Gaspal, F. M., Jones N. D., Yagita H., Allison J. P., Montalvo-Ortiz W., Lane, P. J. (2016) Concurrent OX40 and CD30-ligand blockade abrogates the CD4 T-cell driven autoimmunity associated with CTLA-4 and PD-1 blockade, while preserving CD8 T-cell mediated antitumor immunity. (**In Prep**).

- Fabrina M. Gaspal F.M., Nakamura K., Srivastava M., McConnell M.F., Jakhu P., **Nawaf M.G.**, Flores-Langarica A., De Santo C., Skinner J.P.J., Chong M.M.W., Wilson M.S., Vinuesa S.M., Lane P.J.L (2016) Macrophages confer T cell resistance to Tregs via OX40L and CD30L (**In Prep**).

References

Aaltonen, J., Bjorses, P., Perheentupa, J., Horelli Kuitunen, N., Palotie, A., Peltonen, L., Lee, Y. S., Francis, F., Henning, S., Thiel, C., Leharach, H. and Yaspo, M. L. (1997) An autoimmune disease, APECED, caused by mutations in a novel gene featuring two PHD-type zinc-finger domains. *Nat Genet, 17*(4), pp. 399-403.

Abbas, A. K., Benoist, C., Bluestone, J. A., Campbell, D. J., Ghosh, S., Hori, S., Jiang, S., Kuchroo, V. K., Mathis, D., Roncarolo, M. G., Rudensky, A., Sakaguchi, S., Shevach, E. M., Vignali, D. A. A. and Ziegler, S. F. (2013) Regulatory T cells: recommendations to simplify the nomenclature. *Nat Immunol, 14*(4), pp. 307-308.

Abiko, K., Matsumura, N., Hamanishi, J., Horikawa, N., Murakami, R., Yamaguchi, K., Yoshioka, Y., Baba, T., Konishi, I. and Mandai, M. (2015) IFN-γ from lymphocytes induces PD-L1 expression and promotes progression of ovarian cancer. *Br J Cancer, 112*(9), pp. 1501-1509.

Ahmadzadeh, M., Johnson, L. A., Heemskerk, B., Wunderlich, J. R., Dudley, M. E., White, D. E. and Rosenberg, S. A. (2009) Tumor antigen–specific CD8 T cells infiltrating the tumor express high levels of PD-1 and are functionally impaired. *Blood, 114*(8), pp. 1537-1544.

Akiyama, T., Shimo, Y., Yanai, H., Qin, J., Ohshima, D., Maruyama, Y., Asaumi, Y., Kitazawa, J., Takayanagi, H., Penninger, J. M., Matsumoto, M., Nitta, T., Takahama, Y. and Inoue, J.-i. (2008) The tumor necrosis factor family receptors RANK and CD40 cooperatively establish the thymic medullary microenvironment and self-tolerance. *Immunity, 29*(3), pp. 423-437.

Anderson, M. S., Venanzi, E. S., Klein, L., Chen, Z., Berzins, S. P., Turley, S. J., von Boehmer, H., Bronson, R., Dierich, A., Benoist, C. and Mathis, D. (2002) Projection of an immunological self shadow within the thymus by the Aire protein. *Science, 298*(5597), pp. 1395-1401.

Ansell, S. M., Hurvitz, S. A., Koenig, P. A., LaPlant, B. R., Kabat, B. F., Fernando, D., Habermann, T. M., Inwards, D. J., Verma, M., Yamada, R., Erlichman, C., Lowy, I. and Timmerman, J. M. (2009) Phase I study of ipilimumab, an anti–CTLA-4 monoclonal antibody, in patients with relapsed and refractory B-cell non–hodgkin lymphoma. *Clinical Cancer Research, 15*(20), pp. 6446-6453.

Ansell, S. M., Lesokhin, A. M., Borrello, I., Halwani, A., Scott, E. C., Gutierrez, M., Schuster, S. J., Millenson, M. M., Cattry, D., Freeman, G. J., Rodig, S. J., Chapuy, B., Ligon, A. H., Zhu, L., Grosso, J. F., Kim, S. Y., Timmerman, J. M., Shipp, M. A. and Armand, P. (2015) PD-1 blockade with nivolumab in relapsed or refractory Hodgkin's lymphoma. *New England Journal of Medicine, 372*(4), pp. 311-319.

Atkins, M. B., Lotze, M. T., Dutcher, J. P., Fisher, R. I., Weiss, G., Margolin, K., Abrams, J., Sznol, M., Parkinson, D., Hawkins, M., Paradise, C., Kunkel, L. and Rosenberg, S. A. (1999) High-dose recombinant interleukin 2 therapy for patients with metastatic melanoma: analysis of 270 patients treated between 1985 and 1993. *Journal of Clinical Oncology, 17*(7), pp. 2105.

Baecher-Allan, C., Brown, J. A., Freeman, G. J. and Hafler, D. A. (2001) $CD4^{+}CD25^{high}$ regulatory cells in human peripheral blood. *The Journal of Immunology, 167*(3), pp. 1245-1253.

Bajor, D. L., Mick, R., Riese, M. J., Richman, L. P., Xu, X., Torigian, D. A., Stelekati, E., Sweeney, M., Sullivan, B., Schuchter, L. M., Amaravadi, R., Wherry, E. J. and Vonderheide, R. H. (2015) Abstract CT137: Combination of agonistic CD40 monoclonal antibody CP-870,893 and anti-CTLA-4 antibody tremelimumab in patients with metastatic melanoma. *Cancer Research, 75*(15 Supplement), pp. CT137-CT137.

Balch, C. M., Soong, S. J., Gershenwald, J. E., Thompson, J. F., Reintgen, D. S., Cascinelli, N., Urist, M., McMasters, K. M., Ross, M. I., Kirkwood, J. M., Atkins, M. B., Thompson, J. A., Coit, D. G., Byrd, D., Desmond, R., Zhang, Y., Liu, P. Y., Lyman, G. H. and Morabito, A. (2001) Prognostic factors analysis of 17,600 melanoma patients: validation of the american joint committee on cancer melanoma staging system. *Journal of Clinical Oncology, 19*(16), pp. 3622-3634.

Banchereau, J., Dubois, B., Fayette, J., Burdin, N., Briere, F., Miossec, P., Rissoan, M.-C., Van Kooten, C. and Caux, C. (1995) Functional CD40 antigen on B cells, dendritic cells and fibroblasts. in *Dendritic cells in fundamental and clinical immunology*: Springer. pp. 79-83.

Bansal-Pakala, P., Gebre-Hiwot Jember, A. and Croft, M. (2001) Signaling through OX40 (CD134) breaks peripheral T-cell tolerance. *Nat Med, 7*(8), pp. 907-912.

Barber, D. L., Wherry, E. J., Masopust, D., Zhu, B., Allison, J. P., Sharpe, A. H., Freeman, G. J. and Ahmed, R. (2006) Restoring function in exhausted CD8 T cells during chronic viral infection. *Nature, 439*(7077), pp. 682-687.

Bashey, A., Medina, B., Corringham, S., Pasek, M., Carrier, E., Vrooman, L., Lowy, I., Solomon, S. R., Morris, L. E., Holland, H. K., Mason, J. R., Alyea, E. P., Soiffer, R. J. and Ball, E. D. (2008) CTLA4 blockade with ipilimumab to treat relapse of malignancy after allogeneic hematopoietic cell transplantation. *Blood, 113*(7), pp. 1581-1588.

Beatty, G. L., Chiorean, E. G., Fishman, M. P., Saboury, B., Teitelbaum, U. R., Sun, W., Huhn, R. D., Song, W., Li, D., Sharp, L. L., Torigian, D. A., O'Dwyer, P. J. and Vonderheide, R. H. (2011) CD40 agonists alter tumor stroma and show

efficacy against pancreatic carcinoma in mice and humans. *Science, 331*(6024), pp. 1612-1616.

Beck, K. E., Blansfield, J. A., Tran, K. Q., Feldman, A. L., Hughes, M. S., Royal, R. E., Kammula, U. S., Topalian, S. L., Sherry, R. M., Kleiner, D., Quezado, M., Lowy, I., Yellin, M., Rosenberg, S. A. and Yang, J. C. (2006) Enterocolitis in patients with cancer after antibody blockade of cytotoxic T-lymphocyte–associated antigen 4. *Journal of Clinical Oncology, 24*(15), pp. 2283-2289.

Bekiaris, V., Gaspal, F., Kim, M. Y., Withers, D. R., Sweet, C., Anderson, G. and Lane, P. J. L. (2009) Synergistic OX40 and CD30 signals sustain $CD8^+$ T cells during antigenic challenge. *European Journal of Immunology, 39*(8), pp. 2120-2125.

Bennett, C. L., Christie, J., Ramsdell, F., Brunkow, M. E., Ferguson, P. J., Whitesell, L., Kelly, T. E., Saulsbury, F. T., Chance, P. F. and Ochs, H. D. (2001) The immune dysregulation, polyendocrinopathy, enteropathy, X-linked syndrome (IPEX) is caused by mutations of FOXP3. *Nat Genet, 27*(1), pp. 20-21.

Benz, C. and Bleul, C. C. (2005) A multipotent precursor in the thymus maps to the branching point of the T versus B lineage decision. *The Journal of Experimental Medicine, 202*(1), pp. 21-31.

Berger, M. F., Hodis, E., Heffernan, T. P., Deribe, Y. L., Lawrence, M. S., Protopopov, A., Ivanova, E., Watson, I. R., Nickerson, E., Ghosh, P., Zhang, H., Zeid, R., Ren, X., Cibulskis, K., Sivachenko, A. Y., Wagle, N., Sucker, A., Sougnez, C., Onofrio, R., Ambrogio, L., Auclair, D., Fennell, T., Carter, S. L., Drier, Y., Stojanov, P., Singer, M. A., Voet, D., Jing, R., Saksena, G., Barretina, J., Ramos, A. H., Pugh, T. J., Stransky, N., Parkin, M., Winckler, W., Mahan, S., Ardlie, K., Baldwin, J., Wargo, J., Schadendorf, D., Meyerson, M., Gabriel, S. B., Golub, T. R., Wagner, S. N., Lander, E. S., Getz, G., Chin, L. and Garraway, L. A. (2012) Melanoma genome sequencing reveals frequent PREX2 mutations. *Nature, 485*(7399), pp. 502-506.

Bilate, A. M. and Lafaille, J. J. (2012) Induced $CD4^+Foxp3^+$ regulatory T cells in immune tolerance. *Annual Review of Immunology, 30*(1), pp. 733-758.

Blair, P. J., Bultman, S. J., Haas, J. C., Rouse, B. T., Wilkinson, J. E. and Godfrey, V. L. (1994) $CD4^+CD8^-$ T cells are the effector cells in disease pathogenesis in the scurfy (sf) mouse. *The Journal of Immunology, 153*(8), pp. 3764-74.

Blank, C., Brown, I., Peterson, A. C., Spiotto, M., Iwai, Y., Honjo, T. and Gajewski, T. F. (2004) PD-L1/B7H-1 inhibits the effector phase of tumor rejection by T cell receptor (TCR) transgenic $CD8^+$ T cells. *Cancer Research, 64*(3), pp. 1140-1145.

Borcherding, F., Nitschke, M., Hundorfean, G., Rupp, J., von Smolinski, D., Bieber, K., van Kooten, C., Lehnert, H., Fellermann, K. and Büning, J. (2010) The

CD40-CD40L pathway contributes to the proinflammatory function of intestinal epithelial cells in inflammatory bowel disease. *The American Journal of Pathology, 176*(4), pp. 1816-1827.

Bouillet, P., Purton, J. F., Godfrey, D. I., Zhang, L. C., Coultas, L., Puthalakath, H., Pellegrini, M., Cory, S., Adams, J. M. and Strasser, A. (2002) BH3-only Bcl-2 family member Bim is required for apoptosis of autoreactive thymocytes. *Nature, 415*(6874), pp. 922-926.

Brahmer, J. R., Tykodi, S. S., Chow, L. Q. M., Hwu, W.-J., Topalian, S. L., Hwu, P., Drake, C. G., Camacho, L. H., Kauh, J., Odunsi, K., Pitot, H. C., Hamid, O., Bhatia, S., Martins, R., Eaton, K., Chen, S., Salay, T. M., Alaparthy, S., Grosso, J. F., Korman, A. J., Parker, S. M., Agrawal, S., Goldberg, S. M., Pardoll, D. M., Gupta, A. and Wigginton, J. M. (2012) Safety and activity of anti–PD-L1 antibody in patients with advanced cancer. *New England Journal of Medicine, 366*(26), pp. 2455-2465.

Bruder, D., Probst-Kepper, M., Westendorf, A. M., Geffers, R., Beissert, S., Loser, K., von Boehmer, H., Buer, J. and Hansen, W. (2004) Frontline: neuropilin-1: a surface marker of regulatory T cells. *European Journal of Immunology, 34*(3), pp. 623-630.

Brunkow, M. E., Jeffery, E. W., Hjerrild, K. A., Paeper, B., Clark, L. B., Yasayko, S. A., Wilkinson, J. E., Galas, D., Ziegler, S. F. and Ramsdell, F. (2001) Disruption of a new forkhead/winged-helix protein, scurfin, results in the fatal lymphoproliferative disorder of the scurfy mouse. *Nat Genet, 27*(1), pp. 68-73.

Bulliard, Y., Jolicoeur, R., Windman, M., Rue, S. M., Ettenberg, S., Knee, D. A., Wilson, N. S., Dranoff, G. and Brogdon, J. L. (2013) Activating Fc γ receptors contribute to the antitumor activities of immunoregulatory receptor-targeting antibodies. *The Journal of Experimental Medicine, 210*(9), pp. 1685-1693.

Burocchi, A., Pittoni, P., Gorzanelli, A., Colombo, M. P. and Piconese, S. (2011) Intratumor OX40 stimulation inhibits IRF1 expression and IL-10 production by Treg cells while enhancing CD40L expression by effector memory T cells. *European Journal of Immunology, 41*(12), pp. 3615-3626.

Byun, M., Ma, C. S., Akcay, A., Pedergnana, V., Palendira, U., Myoung, J., Avery, D. T., Liu, Y., Abhyankar, A., Lorenzo, L., Schmidt, M., Lim, H. K., Cassar, O., Migaud, M., Rozenberg, F., Canpolat, N., Aydogan, G., Fleckenstein, B., Bustamante, J., Picard, C., Gessain, A., Jouanguy, E., Cesarman, E., Olivier, M., Gros, P., Abel, L., Croft, M., Tangye, S. G. and Casanova, J. L. (2013) Inherited human OX40 deficiency underlying classic Kaposi sarcoma of childhood. *J Exp Med*.

Camacho, L. H. (2015) CTLA-4 blockade with ipilimumab: biology, safety, efficacy, and future considerations. *Cancer Medicine, 4*(5), pp. 661-672.

Camacho, L. H., Antonia, S., Sosman, J., Kirkwood, J. M., Gajewski, T. F., Redman, B., Pavlov, D., Bulanhagui, C., Bozon, V. A., Gomez-Navarro, J. and Ribas, A. (2009) Phase I/II trial of tremelimumab in patients with metastatic melanoma. *Journal of Clinical Oncology, 27*(7), pp. 1075-1081.

CancerResearchUK (2014) *Skin cancer statistics* http://www.cancerresearchuk.org/cancer-info/cancerstats/keyfacts/skin-cancer/, Available: [Accessed 16.04 2015].

Cao, X., Cai, S. F., Fehniger, T. A., Song, J., Collins, L. I., Piwnica-Worms, D. R. and Ley, T. J. (2007) Granzyme B and perforin are important for regulatory T cell-mediated suppression of tumor clearance. *Immunity, 27*(4), pp. 635-646.

Carreras, J., Lopez-Guillermo, A., Fox, B. C., Colomo, L., Martinez, A., Roncador, G., Montserrat, E., Campo, E. and Banham, A. H. (2006) High numbers of tumor-infiltrating Foxp3-positive regulatory T cells are associated with improved overall survival in follicular lymphoma. *Blood, 108*(9), pp. 2957-2964.

Castelli, C., Rivoltini, L., Andreola, G., Carrabba, M., Renkvist, N. and Parmiani, G. (2000) T-cell recognition of melanoma-associated antigens. *Journal of Cellular Physiology, 182*(3), pp. 323-331.

Caux, C., Massacrier, C., Vanbervliet, B., Dubois, B., Van Kooten, C., Durand, I. and Banchereau, J. (1994) Activation of human dendritic cells through CD40 cross-linking. *The Journal of Experimental Medicine, 180*(4), pp. 1263-1272.

Chambers, C. A., Sullivan, T. J. and Allison, J. P. (1997) Lymphoproliferation in CTLA-4–deficient mice is mediated by costimulation-dependent activation of $CD4^+$ T cells. *Immunity, 7*(6), pp. 885-895.

Chanmee, T., Ontong, P., Konno, K. and Itano, N. (2014) Tumor-associated macrophages as major players in the tumor microenvironment. *Cancers, 6*(3), pp. 1670-1690.

Chaudhry, A., Samstein, R. M., Treuting, P., Liang, Y., Pils, M. C., Heinrich, J. M., Jack, R. S., Wunderlich, F. T., Brüning, J. C., Müller, W. and Rudensky, A. Y. (2011) Interleukin-10 signaling in regulatory T cells is required for suppression of Th17 cell-mediated inflammation. *Immunity, 34*(4), pp. 566-578.

Chen, L. and Flies, D. B. (2013) Molecular mechanisms of T cell co-stimulation and co-inhibition. *Nat Rev Immunol, 13*(4), pp. 227-242.

Chen, M. L., Pittet, M. J., Gorelik, L., Flavell, R. A., Weissleder, R., von Boehmer, H. and Khazaie, K. (2005) Regulatory T cells suppress tumor-specific CD8 T cell cytotoxicity through TGF-β signals in vivo. *Proceedings of the National Academy of Sciences of the United States of America, 102*(2), pp. 419-424.

Chen, S., Lee, L.-F., Fisher, T. S., Jessen, B., Elliott, M., Evering, W., Logronio, K., Tu, G. H., Tsaparikos, K., Li, X., Wang, H., Ying, C., Xiong, M., VanArsdale, T. and Lin, J. C. (2015) Combination of 4-1BB agonist and PD-1 antagonist promotes antitumor effector/memory CD8 T cells in a poorly immunogenic tumor model. *Cancer Immunology Research, 3*(2), pp. 149-160.

Chen, X., Fosco, D., Kline, D. E., Meng, L., Nishi, S., Savage, P. A. and Kline, J. (2014) PD-1 regulates extrathymic regulatory T-cell differentiation. *European Journal of Immunology, 44*(9), pp. 2603-2616.

Chin, L., Garraway, L. A. and Fisher, D. E. (2006) Malignant melanoma: genetics and therapeutics in the genomic era. *Genes & Development, 20*(16), pp. 2149-2182.

Clark Jr, W. H., Elder, D. E., Guerry Iv, D., Epstein, M. N., Greene, M. H. and Van Horn, M. (1984) A study of tumor progression: the precursor lesions of superficial spreading and nodular melanoma. *Human Pathology, 15*(12), pp. 1147-1165.

Cobbold, S. P., Jayasuriya, A., Nash, A., Prospero, T. D. and Waldmann, H. (1984) Therapy with monoclonal antibodies by elimination of T-cell subsets *in vivo*. *Nature, 312*(5994), pp. 548-551.

Collison, L. W., Chaturvedi, V., Henderson, A. L., Giacomin, P. R., Guy, C., Bankoti, J., Finkelstein, D., Forbes, K., Workman, C. J., Brown, S. A., Rehg, J. E., Jones, M. L., Ni, H. T., Artis, D., Turk, M. J. and Vignali, D. A. A. (2010) IL-35-mediated induction of a potent regulatory T cell population. *Nat Immunol, 11*(12), pp. 1093-1101.

Cooper, M. D. and Alder, M. N. (2006) The evolution of adaptive immune systems. *Cell, 124*(4), pp. 815-822.

Coulie, P. G., Van den Eynde, B. J., van der Bruggen, P. and Boon, T. (2014) Tumour antigens recognized by T lymphocytes: at the core of cancer immunotherapy. *Nat Rev Cancer, 14*(2), pp. 135-146.

Cowan, J. E., Parnell, S. M., Nakamura, K., Caamano, J. H., Lane, P. J. L., Jenkinson, E. J., Jenkinson, W. E. and Anderson, G. (2013) The thymic medulla is required for $Foxp3^+$ regulatory but not conventional $CD4^+$ thymocyte development. *The Journal of Experimental Medicine, 210*(4), pp. 675-681.

Croft, M. (2003) Co-stimulatory members of the TNFR family: keys to effective T-cell immunity? *Nat Rev Immunol, 3*(8), pp. 609-620.

Croft, M. (2009) The role of TNF superfamily members in T-cell function and diseases. *Nat Rev Immunol, 9*(4), pp. 271-285.

Croft, M. (2010) Control of immunity by the TNFR-related molecule OX40 (CD134). *Annual Review of Immunology, 28*(1), pp. 57-78.

Curiel, T. J., Coukos, G., Zou, L., Alvarez, X., Cheng, P., Mottram, P., Evdemon-Hogan, M., Conejo-Garcia, J. R., Zhang, L., Burow, M., Zhu, Y., Wei, S., Kryczek, I., Daniel, B., Gordon, A., Myers, L., Lackner, A., Disis, M. L., Knutson, K. L., Chen, L. and Zou, W. (2004) Specific recruitment of regulatory T cells in ovarian carcinoma fosters immune privilege and predicts reduced survival. *Nat Med, 10*(9), pp. 942-949.

Curran, M. A., Montalvo, W., Yagita, H. and Allison, J. P. (2010) PD-1 and CTLA-4 combination blockade expands infiltrating T cells and reduces regulatory T and myeloid cells within B16 melanoma tumors. *Proceedings of the National Academy of Sciences, 107*(9), pp. 4275-4280.

Damsky, W. E., Theodosakis, N. and Bosenberg, M. (2014) Melanoma metastasis: new concepts and evolving paradigms. *Oncogene, 33*(19), pp. 2413-2422.

Das, R., Verma, R., Sznol, M., Boddupalli, C. S., Gettinger, S. N., Kluger, H., Callahan, M., Wolchok, J. D., Halaban, R., Dhodapkar, M. V. and Dhodapkar, K. M. (2015) Combination therapy with anti–CTLA-4 and anti–PD-1 leads to distinct immunologic changes in vivo. *The Journal of Immunology, 194*(3), pp. 950-959.

de Heusch, M., Oldenhove, G., Urbain, J., Thielemans, K., Maliszewski, C., Leo, O. and Moser, M. (2004) Depending on their maturation state, splenic dendritic cells induce the differentiation of $CD4^+$ T lymphocytes into memory and/or effector cells *in vivo*. *European Journal of Immunology, 34*(7), pp. 1861-1869.

De Smedt, T., Smith, J., Baum, P., Fanslow, W., Butz, E. and Maliszewski, C. (2002) Ox40 costimulation enhances the development of T cell responses induced by dendritic cells *in vivo*. *The Journal of Immunology, 168*(2), pp. 661-670.

Deaglio, S., Dwyer, K. M., Gao, W., Friedman, D., Usheva, A., Erat, A., Chen, J.-F., Enjyoji, K., Linden, J., Oukka, M., Kuchroo, V. K., Strom, T. B. and Robson, S. C. (2007) Adenosine generation catalyzed by CD39 and CD73 expressed on regulatory T cells mediates immune suppression. *The Journal of Experimental Medicine, 204*(6), pp. 1257-1265.

Del Prete, G., De Carli, M., Almerigogna, F., Daniel, C. K., D'Elios, M. M., Zancuoghi, G., Vinante, F., Pizzolo, G. and Romagnani, S. (1995) Preferential expression of CD30 by human $CD4^+$ T cells producing Th2-type cytokines. *The FASEB Journal, 9*(1), pp. 81-6.

deLeeuw, R. J., Kost, S. E., Kakal, J. A. and Nelson, B. H. (2012) The prognostic value of $FoxP3^+$ tumor-infiltrating lymphocytes in cancer: a critical review of the literature. *Clinical Cancer Research, 18*(11), pp. 3022-3029.

Derbinski, J., Schulte, A., Kyewski, B. and Klein, L. (2001) Promiscuous gene expression in medullary thymic epithelial cells mirrors the peripheral self. *Nat Immunol, 2*(11), pp. 1032-1039.

Di, Y., Tan, A. H. M., Hu, X., Athanasopoulos, V., Simpson, N., Silva, D. G., Hutloff, A., Giles, K. M., Leedman, P. J., Lam, K. P., Goodnow, C. C. and Vinuesa, C. G. (2007) Roquin represses autoimmunity by limiting inducible T-cell co-stimulator messenger RNA. *Nature, 450*(7167), pp. 299-303.

Diz, R., Garland, A., Vincent, B. G., Johnson, M. C., Spidale, N., Wang, B. and Tisch, R. (2012) Autoreactive effector/memory $CD4^+$ and CD8 T cells infiltrating grafted and endogenous islets in diabetic NOD mice exhibit similar T cell receptor usage. *PLoS ONE, 7*(12), pp. e52054.

Dong, H., Strome, S. E., Salomao, D. R., Tamura, H., Hirano, F., Flies, D. B., Roche, P. C., Lu, J., Zhu, G., Tamada, K., Lennon, V. A., Celis, E. and Chen, L. (2002) Tumor-associated B7-H1 promotes T-cell apoptosis: a potential mechanism of immune evasion. *Nat Med, 8*(8), pp. 793-800.

Dong, H., Zhu, G., Tamada, K., Flies, D. B., van Deursen, J. M. A. and Chen, L. (2004) B7-H1 determines accumulation and deletion of intrahepatic $CD8^{+\ T}$ lymphocytes. *Immunity, 20*(3), pp. 327-336.

Dudley, E. C., Petrie, H. T., Shah, L. M., Owen, M. J. and Hayday, A. C. (1994) T cell receptor β chain gene rearrangement and selection during thymocyte development in adult mice. *Immunity, 1*(2), pp. 83-93.

Dudley, M. E., Wunderlich, J. R., Yang, J. C., Hwu, P., Schwartzentruber, D. J., Topalian, S. L., Sherry, R. M., Marincola, F. M., Leitman, S. F., Seipp, C. A., Rogers-Freezer, L., Morton, K. E., Nahvi, A., Mavroukakis, S. A., White, D. E. and Rosenberg, S. A. (2002) A phase I study of nonmyeloablative chemotherapy and adoptive transfer of autologous tumor antigen-specific T lymphocytes in patients with metastatic melanoma. *Journal of immunotherapy (Hagerstown, Md. : 1997), 25*(3), pp. 243-251.

Dunn, G. P., Bruce, A. T., Ikeda, H., Old, L. J. and Schreiber, R. D. (2002) Cancer immunoediting: from immunosurveillance to tumor escape. *Nat Immunol, 3*(11), pp. 991-998.

Dunn, G. P., Old, L. J. and Schreiber, R. D. (2004) The immunobiology of cancer immunosurveillance and immunoediting. *Immunity, 21*(2), pp. 137-148.

Ernst, P. B., Garrison, J. C. and Thompson, L. F. (2010) Much ado about adenosine: adenosine synthesis and function in regulatory T cell biology. *The Journal of Immunology, 185*(4), pp. 1993-1998.

Facciabene, A., Motz, G. T. and Coukos, G. (2012) T-regulatory cells: key players in tumor immune escape and angiogenesis. *Cancer Research, 72*(9), pp. 2162-2171.

Fallarino, F., Grohmann, U., Hwang, K. W., Orabona, C., Vacca, C., Bianchi, R., Belladonna, M. L., Fioretti, M. C., Alegre, M. L. and Puccetti, P. (2003) Modulation of tryptophan catabolism by regulatory T cells. *Nat Immunol, 4*(12), pp. 1206-1212.

Fang, L., Lee, V. C., Cha, E., Zhang, H. and Hwang, S. T. (2008) CCR7 regulates B16 murine melanoma cell tumorigenesis in skin. *Journal of Leukocyte Biology, 84*(4), pp. 965-972.

Fehling, H. J., Krotkova, A., Saint-Ruf, C. and von Boehmer, H. (1995) Crucial role of the pre-T-cell receptor alpha gene in development of alpha beta but not gamma delta T cells. *Nature, 375*(6534), pp. 795-798.

Fidler, I. J. (1974) Immune stimulation-inhibition of experimental cancer metastasis. *Cancer Research, 34*(3), pp. 491-498.

Fisher, G. H., Rosenberg, F. J., Straus, S. E., Dale, J. K., Middelton, L. A., Lin, A. Y., Strober, W., Lenardo, M. J. and Puck, J. M. (1995) Dominant interfering fas gene mutations impair apoptosis in a human autoimmune lymphoproliferative syndrome. *Cell, 81*(6), pp. 935-946.

Flaherty, K. T., Hodi, F. S. and Fisher, D. E. (2012) From genes to drugs: targeted strategies for melanoma. *Nat Rev Cancer, 12*(5), pp. 349-361.

Fletcher, A. L., Malhotra, D. and Turley, S. J. (2011) Lymph node stroma broaden the peripheral tolerance paradigm. *Trends in Immunology, 32*(1), pp. 12-18.

Flies, D. B., Sandler, B. J., Sznol, M. and Chen, L. (2011) Blockade of the B7-H1/PD-1 pathway for cancer immunotherapy. *The Yale Journal of Biology and Medicine, 84*(4), pp. 409-421.

Fontenot, J. D., Gavin, M. A. and Rudensky, A. Y. (2003) Foxp3 programs the development and function of $CD4^{+}CD25^{+}$ regulatory T cells. *Nat Immunol, 4*(4), pp. 330-336.

Fourcade, J., Sun, Z., Pagliano, O., Guillaume, P., Luescher, I. F., Sander, C., Kirkwood, J. M., Olive, D., Kuchroo, V. and Zarour, H. M. (2012) $CD8^{+}$ T cells specific for tumor antigens can be rendered dysfunctional by the tumor microenvironment through upregulation of the inhibitory receptors BTLA and PD-1. *Cancer Research, 72*(4), pp. 887-896.

Francisco, L. M., Sage, P. T. and Sharpe, A. H. (2010) The PD-1 pathway in tolerance and autoimmunity. *Immunological Reviews, 236*(1), pp. 219-242.

Francisco, L. M., Salinas, V. H., Brown, K. E., Vanguri, V. K., Freeman, G. J., Kuchroo, V. K. and Sharpe, A. H. (2009) PD-L1 regulates the development, maintenance, and function of induced regulatory T cells. *The Journal of Experimental Medicine, 206*(13), pp. 3015-3029.

French, R. R., Chan, H. T. C., Tutt, A. L. and Glennie, M. J. (1999) CD40 antibody evokes a cytotoxic T-cell response that eradicates lymphoma and bypasses T-cell help. *Nat Med, 5*(5), pp. 548-553.

Friedline, R. H., Brown, D. S., Nguyen, H., Kornfeld, H., Lee, J., Zhang, Y., Appleby, M., Der, S. D., Kang, J. and Chambers, C. A. (2009) $CD4^+$ regulatory T cells require CTLA-4 for the maintenance of systemic tolerance. *The Journal of Experimental Medicine, 206*(2), pp. 421-434.

Gabrilovich, D. I. and Nagaraj, S. (2009) Myeloid-derived-suppressor cells as regulators of the immune system. *Nature reviews. Immunology, 9*(3), pp. 162-174.

Gallegos, A. M. and Bevan, M. J. (2004) Central tolerance to tissue-specific antigens mediated by direct and indirect antigen presentation. *The Journal of Experimental Medicine, 200*(8), pp. 1039-1049.

Galon, J., Costes, A., Sanchez-Cabo, F., Kirilovsky, A., Mlecnik, B., Lagorce-Pagès, C., Tosolini, M., Camus, M., Berger, A., Wind, P., Zinzindohoué, F., Bruneval, P., Cugnenc, P. H., Trajanoski, Z., Fridman, W. H. and Pagès, F. (2006) Type, density, and location of immune cells within human colorectal tumors predict clinical outcome. *Science, 313*(5795), pp. 1960-1964.

Garon, E. B., Rizvi, N. A., Hui, R., Leighl, N., Balmanoukian, A. S., Eder, J. P., Patnaik, A., Aggarwal, C., Gubens, M., Horn, L., Carcereny, E., Ahn, M.-J., Felip, E., Lee, J.-S., Hellmann, M. D., Hamid, O., Goldman, J. W., Soria, J.-C., Dolled-Filhart, M., Rutledge, R. Z., Zhang, J., Lunceford, J. K., Rangwala, R., Lubiniecki, G. M., Roach, C., Emancipator, K. and Gandhi, L. (2015) Pembrolizumab for the treatment of non–small-cell lung cancer. *New England Journal of Medicine, 372*(21), pp. 2018-2028.

Gaspal, F., Bekiaris, V., Kim, M.-Y., Withers, D. R., Bobat, S., MacLennan, I. C. M., Anderson, G., Lane, P. J. and Cunningham, A. F. (2008) Critical synergy of CD30 and OX40 signals in CD4 T cell homeostasis and Th1 immunity to *Salmonella*. *The Journal of Immunology, 180*(5), pp. 2824-2829.

Gaspal, F. M. C., Kim, M. Y., McConnell, F. M., Raykundalia, C., Bekiaris, V. and Lane, P. J. L. (2005) Mice deficient in OX40 and CD30 signals lack memory antibody responses because of deficient CD4 T cell memory. *The Journal of Immunology, 174*(7), pp. 3891-3896.

Gaspal, F. M. C., Withers, D., Saini, M., Bekiaris, V., McConnell, F. M., White, A., Khan, M., Yagita, H., Walker, L. S. K., Anderson, G. and Lane, P. J. L. (2011)

Abrogation of CD30 and OX40 signals prevents autoimmune disease in FoxP3-deficient mice. *The Journal of Experimental Medicine, 208*(8), pp. 1579-1584.

Gauvreau, G. M., Boulet, L. P., Cockcroft, D. W., FitzGerald, J. M., Mayers, I., Carlsten, C., Laviolette, M., Killian, K. J., Davis, B. E., Larché, M., Kipling, C., Dua, B., Mosesova, S., Putnam, W., Zheng, Y., Scheerens, H., McClintock, D., Matthews, J. G. and O'Byrne, P. M. (2014) OX40L blockade and allergen-induced airway responses in subjects with mild asthma. *Clinical & Experimental Allergy, 44*(1), pp. 29-37.

Gavin, M. A., Torgerson, T. R., Houston, E., deRoos, P., Ho, W. Y., Stray-Pedersen, A., Ocheltree, E. L., Greenberg, P. D., Ochs, H. D. and Rudensky, A. Y. (2006) Single-cell analysis of normal and FOXP3-mutant human T cells: FOXP3 expression without regulatory T cell development. *Proceedings of the National Academy of Sciences, 103*(17), pp. 6659-6664.

Geis, A. L., Fan, H., Wu, X., Wu, S., Huso, D. L., Wolfe, J. L., Sears, C. L., Pardoll, D. M. and Housseau, F. (2015) Regulatory T-cell response to enterotoxigenic *Bacteroides fragilis* colonization triggers IL17-dependent colon carcinogenesis. *Cancer Discovery, 5*(10), pp. 1098-1109.

Gershon, R. K. and Kondo, K. (1970) Cell interactions in the induction of tolerance: the role of thymic lymphocytes. *Immunology, 18*(5), pp. 723-737.

Glasmacher, E., Hoefig, K. P., Vogel, K. U., Rath, N., Du, L., Wolf, C., Kremmer, E., Wang, X. and Heissmeyer, V. (2010) Roquin binds inducible costimulator mRNA and effectors of mRNA decay to induce microRNA-independent post-transcriptional repression. *Nat Immunol, 11*(8), pp. 725-733.

Glinka, Y. and Prud'homme, G. J. (2008) Neuropilin-1 is a receptor for transforming growth factor β-1, activates its latent form, and promotes regulatory T cell activity. *Journal of Leukocyte Biology, 84*(1), pp. 302-310.

Glinka, Y., Stoilova, S., Mohammed, N. and Prud'homme, G. J. (2011) Neuropilin-1 exerts co-receptor function for TGF-beta-1 on the membrane of cancer cells and enhances responses to both latent and active TGF-beta. *Carcinogenesis, 32*(4), pp. 613-621.

Gobert, M., Treilleux, I., Bendriss-Vermare, N., Bachelot, T., Goddard-Leon, S., Arfi, V., Biota, C., Doffin, A. C., Durand, I., Olive, D., Perez, S., Pasqual, N., Faure, C., Ray-Coquard, I., Puisieux, A., Caux, C., Blay, J.-Y. and Ménétrier-Caux, C. (2009) Regulatory T cells recruited through CCL22/CCR4 are selectively activated in lymphoid infiltrates surrounding primary breast tumors and lead to an adverse clinical outcome. *Cancer Research, 69*(5), pp. 2000-2009.

Godfrey, D. I., Kennedy, J., Suda, T. and Zlotnik, A. (1993) A developmental pathway involving four phenotypically and functionally distinct subsets of $CD3^-CD4^-CD8^-$

triple-negative adult mouse thymocytes defined by CD44 and CD25 expression. *The Journal of Immunology, 150*(10), pp. 4244-52.

Gogas, H., Ioannovich, J., Dafni, U., Stavropoulou-Giokas, C., Frangia, K., Tsoutsos, D., Panagiotou, P., Polyzos, A., Papadopoulos, O., Stratigos, A., Markopoulos, C., Bafaloukos, D., Pectasides, D., Fountzilas, G. and Kirkwood, J. M. (2006) Prognostic significance of autoimmunity during treatment of melanoma with interferon. *New England Journal of Medicine, 354*(7), pp. 709-718.

Gondek, D. C., Lu, L. F., Quezada, S. A., Sakaguchi, S. and Noelle, R. J. (2005) Cutting edge: contact-mediated suppression by $CD4^+CD25^+$ regulatory cells involves a granzyme B-dependent, perforin-independent mechanism. *The Journal of Immunology, 174*(4), pp. 1783-1786.

Good-Jacobson, K. L., Szumilas, C. G., Chen, L., Sharpe, A. H., Tomayko, M. M. and Shlomchik, M. J. (2010) PD-1 regulates germinal center B cell survival and the formation and affinity of long-lived plasma cells. *Nat Immunol, 11*(6), pp. 535-542.

Goodnow, C. C., Sprent, J., de St Groth, B. F. and Vinuesa, C. G. (2005) Cellular and genetic mechanisms of self tolerance and autoimmunity. *Nature, 435*(7042), pp. 590-597.

Gottschalk, R. A., Corse, E. and Allison, J. P. (2012) Expression of Helios in peripherally induced $Foxp3^+$ regulatory T cells. *The Journal of Immunology, 188*(3), pp. 976-980.

Gramaglia, I., Jember, A., Pippig, S. D., Weinberg, A. D., Killeen, N. and Croft, M. (2000) The OX40 costimulatory receptor determines the development of CD4 memory by regulating primary clonal expansion. *The Journal of Immunology, 165*(6), pp. 3043-3050.

Green, D. R., Droin, N. and Pinkoski, M. (2003) Activation-induced cell death in T cells. *Immunological Reviews, 193*(1), pp. 70-81.

Greenwald, R. J., Freeman, G. J. and Sharpe, A. H. (2005) The B7 family revisited. *Annual Review of Immunology, 23*(1), pp. 515-548.

Griseri, T., Asquith, M., Thompson, C. and Powrie, F. (2010) OX40 is required for regulatory T cell–mediated control of colitis. *The Journal of Experimental Medicine, 207*(4), pp. 699-709.

Gu, C., Rodriguez, E. R., Reimert, D. V., Shu, T., Fritzsch, B., Richards, L. J., Kolodkin, A. L. and Ginty, D. D. (2003) Neuropilin-1 conveys semaphorin and VEGF signaling during neural and cardiovascular development. *Developmental Cell, 5*(1), pp. 45-57.

Gubin, M. M., Zhang, X., Schuster, H., Caron, E., Ward, J. P., Noguchi, T., Ivanova, Y., Hundal, J., Arthur, C. D., Krebber, W. J., Mulder, G. E., Toebes, M., Vesely, M. D., Lam, S. S. K., Korman, A. J., Allison, J. P., Freeman, G. J., Sharpe, A. H., Pearce, E. L., Schumacher, T. N., Aebersold, R., Rammensee, H. G., Melief, C. J. M., Mardis, E. R., Gillanders, W. E., Artyomov, M. N. and Schreiber, R. D. (2014) Checkpoint blockade cancer immunotherapy targets tumour-specific mutant antigens. *Nature, 515*(7528), pp. 577-581.

Guldberg, P., Thor Straten, P., Birck, A., Ahrenkiel, V., Kirkin, A. F. and Zeuthen, J. (1997) Disruption of the MMAC1/PTEN gene by deletion or mutation is a frequent event in malignant melanoma. *Cancer Research, 57*(17), pp. 3660-3663.

Guo, Z., Wang, X., Cheng, D., Xia, Z., Luan, M. and Zhang, S. (2014) PD-1 blockade and OX40 triggering synergistically protects against tumor growth in a murine model of ovarian cancer. *PLoS ONE, 9*(2), pp. e89350.

Hadaschik, E. N., Wei, X., Leiss, H., Heckmann, B., Niederreiter, B., Steiner, G., Ulrich, W., Enk, A. H., Smolen, J. S. and Stummvoll, G. H. (2015) Regulatory T cell-deficient scurfy mice develop systemic autoimmune features resembling lupus-like disease. *Arthritis Research & Therapy, 17*(1), pp. 35.

Hamid, O., Robert, C., Daud, A., Hodi, F. S., Hwu, W. J., Kefford, R., Wolchok, J. D., Hersey, P., Joseph, R. W., Weber, J. S., Dronca, R., Gangadhar, T. C., Patnaik, A., Zarour, H., Joshua, A. M., Gergich, K., Elassaiss-Schaap, J., Algazi, A., Mateus, C., Boasberg, P., Tumeh, P. C., Chmielowski, B., Ebbinghaus, S. W., Li, X. N., Kang, S. P. and Ribas, A. (2013) Safety and tumor responses with lambrolizumab (anti–PD-1) in melanoma. *New England Journal of Medicine, 369*(2), pp. 134-144.

Hanahan, D. and Weinberg, Robert A. (2011) Hallmarks of cancer: the next generation. *Cell, 144*(5), pp. 646-674.

Hawiger, D., Inaba, K., Dorsett, Y., Guo, M., Mahnke, K., Rivera, M., Ravetch, J. V., Steinman, R. M. and Nussenzweig, M. C. (2001) Dendritic cells induce peripheral T cell unresponsiveness under steady state conditions in vivo. *The Journal of Experimental Medicine, 194*(6), pp. 769-780.

Herbst, R. S., Soria, J. C., Kowanetz, M., Fine, G. D., Hamid, O., Gordon, M. S., Sosman, J. A., McDermott, D. F., Powderly, J. D., Gettinger, S. N., Kohrt, H. E. K., Horn, L., Lawrence, D. P., Rost, S., Leabman, M., Xiao, Y., Mokatrin, A., Koeppen, H., Hegde, P. S., Mellman, I., Chen, D. S. and Hodi, F. S. (2014) Predictive correlates of response to the anti-PD-L1 antibody MPDL3280A in cancer patients. *Nature, 515*(7528), pp. 563-567.

Heusinkveld, M., de Vos van Steenwijk, P. J., Goedemans, R., Ramwadhdoebe, T. H., Gorter, A., Welters, M. J. P., van Hall, T. and van der Burg, S. H. (2011) M2 macrophages induced by prostaglandin E2 and IL-6 from cervical carcinoma

are switched to activated M1 macrophages by CD4+ Th1 cells. *The Journal of Immunology, 187*(3), pp. 1157-1165.

Hikosaka, Y., Nitta, T., Ohigashi, I., Yano, K., Ishimaru, N., Hayashi, Y., Matsumoto, M., Matsuo, K., Penninger, J. M., Takayanagi, H., Yokota, Y., Yamada, H., Yoshikai, Y., Inoue, J. I., Akiyama, T. and Takahama, Y. (2008) The cytokine RANKL produced by positively selected thymocytes fosters medullary thymic epithelial cells that express autoimmune regulator. *Immunity, 29*(3), pp. 438-450.

Hippen, K. L., Harker-Murray, P., Porter, S. B., Merkel, S. C., Londer, A., Taylor, D. K., Bina, M., Panoskaltsis-Mortari, A., Rubinstein, P., Van Rooijen, N., Golovina, T. N., Suhoski, M. M., Miller, J. S., Wagner, J. E., June, C. H., Riley, J. L. and Blazar, B. R. (2008) Umbilical cord blood regulatory T-cell expansion and functional effects of tumor necrosis factor receptor family members OX40 and 4-1BB expressed on artificial antigen-presenting cells. *Blood, 112*(7), pp. 2847-2857.

Hodi, F. S., Mihm, M. C., Soiffer, R. J., Haluska, F. G., Butler, M., Seiden, M. V., Davis, T., Henry-Spires, R., MacRae, S., Willman, A., Padera, R., Jaklitsch, M. T., Shankar, S., Chen, T. C., Korman, A., Allison, J. P. and Dranoff, G. (2003) Biologic activity of cytotoxic T lymphocyte-associated antigen 4 antibody blockade in previously vaccinated metastatic melanoma and ovarian carcinoma patients. *Proceedings of the National Academy of Sciences, 100*(8), pp. 4712-4717.

Hodi, F. S., O'Day, S. J., McDermott, D. F., Weber, R. W., Sosman, J. A., Haanen, J. B., Gonzalez, R., Robert, C., Schadendorf, D., Hassel, J. C., Akerley, W., van den Eertwegh, A. J. M., Lutzky, J., Lorigan, P., Vaubel, J. M., Linette, G. P., Hogg, D., Ottensmeier, C. H., Lebbé, C., Peschel, C., Quirt, I., Clark, J. I., Wolchok, J. D., Weber, J. S., Tian, J., Yellin, M. J., Nichol, G. M., Hoos, A. and Urba, W. J. (2010) Improved survival with ipilimumab in patients with metastatic melanoma. *New England Journal of Medicine, 363*(8), pp. 711-723.

Hodis, E., Watson, I. R., Kryukov, G. V., Arold, S. T., Imielinski, M., Theurillat, J. P., Nickerson, E., Auclair, D., Li, L., Place, C., DiCara, D., Ramos, A. H., Lawrence, M. S., Cibulskis, K., Sivachenko, A., Voet, D., Saksena, G., Stransky, N., Onofrio, R. C., Winckler, W., Ardlie, K., Wagle, N., Wargo, J., Chong, K., Morton, D. L., Stemke-Hale, K., Chen, G., Noble, M., Meyerson, M., Ladbury, J. E., Davies, M. A., Gershenwald, J. E., Wagner, S. N., Hoon, D. S. B., Schadendorf, D., Lander, E. S., Gabriel, S. B., Getz, G., Garraway, L. A. and Chin, L. (2012) A landscape of driver mutations in melanoma. *Cell, 150*(2), pp. 251-263.

Hofmann, U. B., Westphal, J. R., Van Kraats, A. A., Ruiter, D. J. and Van Muijen, G. N. P. (2000) Expression of integrin αvβ3 correlates with activation of membrane-type matrix metalloproteinase-1 (MT1-MMP) and matrix

metalloproteinase-2 (MMP-2) in human melanoma cells in vitro and in vivo. *International Journal of Cancer, 87*(1), pp. 12-19.

Hori, S., Nomura, T. and Sakaguchi, S. (2003) Control of regulatory T cell development by the transcription factor Foxp3. *Science, 299*(5609), pp. 1057-1061.

Houghton, A. N., Gold, J. S. and Blachere, N. E. (2001) Immunity against cancer: lessons learned from melanoma. *Current Opinion in Immunology, 13*(2), pp. 134-140.

Hsu, M., Andl, T., Li, G., Meinkoth, J. L. and Herlyn, M. (2000) Cadherin repertoire determines partner-specific gap junctional communication during melanoma progression. *Journal of Cell Science, 113*(9), pp. 1535-1542.

Huang, C. T., Workman, C. J., Flies, D., Pan, X., Marson, A. L., Zhou, G., Hipkiss, E. L., Ravi, S., Kowalski, J., Levitsky, H. I., Powell, J. D., Pardoll, D. M., Drake, C. G. and Vignali, D. A. A. (2004) Role of LAG-3 in regulatory T cells. *Immunity, 21*(4), pp. 503-513.

Hubert, F. X., Kinkel, S. A., Davey, G. M., Phipson, B., Mueller, S. N., Liston, A., Proietto, A. I., Cannon, P. Z. F., Forehan, S., Smyth, G. K., Wu, L., Goodnow, C. C., Carbone, F. R., Scott, H. S. and Heath, W. R. (2011) Aire regulates the transfer of antigen from mTECs to dendritic cells for induction of thymic tolerance. *Blood, 118*(9), pp. 2462-2472.

Iwai, Y., Ishida, M., Tanaka, Y., Okazaki, T., Honjo, T. and Minato, N. (2002) Involvement of PD-L1 on tumor cells in the escape from host immune system and tumor immunotherapy by PD-L1 blockade. *Proceedings of the National Academy of Sciences, 99*(19), pp. 12293-12297.

Jacobs, J. F. M., Nierkens, S., Figdor, C. G., de Vries, I. J. M. and Adema, G. J. (2012) Regulatory T cells in melanoma: the final hurdle towards effective immunotherapy? *The Lancet Oncology, 13*(1), pp. e32-e42.

Jacobs, T., Plate, T., Gaworski, I. and Fleischer, B. (2004) CTLA-4-dependent mechanisms prevent T cell induced-liver pathology during the erythrocyte stage of Plasmodium berghei malaria. *European Journal of Immunology, 34*(4), pp. 972-980.

Janas, M. L. and Turner, M. (2010) Stromal cell-derived factor 1α and CXCR4: newly defined requirements for efficient thymic β-selection. *Trends in Immunology, 31*(10), pp. 370-376.

Jin, H. T., Ahmed, R. and Okazaki, T. (2011) Role of PD-1 in regulating T-cell immunity. in Ahmed, R. and Honjo, T., (eds.) *Negative co-receptors and ligands*: Springer Berlin Heidelberg. pp. 17-37.

Josefowicz, S. Z., Lu, L. F. and Rudensky, A. Y. (2012) Regulatory T cells: mechanisms of differentiation and function. *Annual Review of Immunology, 30*(1), pp. 531-564.

Kawabe, T., Naka, T., Yoshida, K., Tanaka, T., Fujiwara, H., Suematsu, S., Yoshida, N., Kishimoto, T. and Kikutani, H. (1994) The immune responses in CD40-deficient mice: Impaired immunoglobulin class switching and germinal center formation. *Immunity, 1*(3), pp. 167-178.

Keir, M. E., Butte, M. J., Freeman, G. J. and Sharpe, A. H. (2008) PD-1 and its ligands in tolerance and immunity. *Annual Review of Immunology, 26*(1), pp. 677-704.

Kennedy, M. K., Willis, C. R. and Armitage, R. J. (2006) Deciphering CD30 ligand biology and its role in humoral immunity. *Immunology, 118*(2), pp. 143-152.

Khan, I. S., Mouchess, M. L., Zhu, M. L., Conley, B., Fasano, K. J., Hou, Y., Fong, L., Su, M. A. and Anderson, M. S. (2014) Enhancement of an anti-tumor immune response by transient blockade of central T cell tolerance. *The Journal of Experimental Medicine, 211*(5), pp. 761-768.

Khattri, R., Cox, T., Yasayko, S. A. and Ramsdell, F. (2003) An essential role for Scurfin in $CD4^{+}CD25^{+}$ T regulatory cells. *Nat Immunol, 4*(4), pp. 337-342.

Khong, H. T., Wang, Q. J. and Rosenberg, S. A. (2004) Identification of multiple antigens recognized by tumor-infiltrating lymphocytes from a single patient: tumor escape by antigen loss and loss of MHC expression. *Journal of immunotherapy, 27*(3), pp. 184-190.

Khor, B. and Sleckman, B. P. (2002) Allelic exclusion at the TCRβ locus. *Current Opinion in Immunology, 14*(2), pp. 230-234.

Kim, M.-Y., Rossi, S., Withers, D., McConnell, F., Toellner, K.-M., Gaspal, F., Jenkinson, E., Anderson, G. and Lane, P. J. L. (2008) Heterogeneity of lymphoid tissue inducer cell populations present in embryonic and adult mouse lymphoid tissues. *Immunology, 124*(2), pp. 166-174.

Kim, M. Y., Gaspal, F. M. C., Wiggett, H. E., McConnell, F. M., Gulbranson-Judge, A., Raykundalia, C., Walker, L. S. K., Goodall, M. D. and Lane, P. J. L. (2003) CD4(+)CD3(-) accessory cells costimulate primed CD4 T cells through OX40 and CD30 at sites where T cells collaborate with B cells. *Immunity, 18*(5), pp. 643-654.

Klages, K., Mayer, C. T., Lahl, K., Loddenkemper, C., Teng, M. W. L., Ngiow, S. F., Smyth, M. J., Hamann, A., Huehn, J. and Sparwasser, T. (2010) Selective Depletion of $Foxp3^{+}$ Regulatory T Cells Improves Effective Therapeutic Vaccination against Established Melanoma. *Cancer Research, 70*(20), pp. 7788-7799.

Klein, L., Hinterberger, M., Wirnsberger, G. and Kyewski, B. (2009) Antigen presentation in the thymus for positive selection and central tolerance induction. *Nat Rev Immunol, 9*(12), pp. 833-844.

Klein, L., Kyewski, B., Allen, P. M. and Hogquist, K. A. (2014) Positive and negative selection of the T cell repertoire: what thymocytes see (and don't see). *Nat Rev Immunol, 14*(6), pp. 377-391.

Ko, K., Yamazaki, S., Nakamura, K., Nishioka, T., Hirota, K., Yamaguchi, T., Shimizu, J., Nomura, T., Chiba, T. and Sakaguchi, S. (2005) Treatment of advanced tumors with agonistic anti-GITR mAb and its effects on tumor-infiltrating Foxp3+CD25+CD4+ regulatory T cells. *The Journal of Experimental Medicine, 202*(7), pp. 885-891.

Koch, M. A., Tucker-Heard, G. s., Perdue, N. R., Killebrew, J. R., Urdahl, K. B. and Campbell, D. J. (2009) The transcription factor T-bet controls regulatory T cell homeostasis and function during type 1 inflammation. *Nat Immunol, 10*(6), pp. 595-602.

Kuehn, H. S., Ouyang, W., Lo, B., Deenick, E. K., Niemela, J. E., Avery, D. T., Schickel, J. N., Tran, D. Q., Stoddard, J., Zhang, Y., Frucht, D. M., Dumitriu, B., Scheinberg, P., Folio, L. R., Frein, C. A., Price, S., Koh, C., Heller, T., Seroogy, C. M., Huttenlocher, A., Rao, V. K., Su, H. C., Kleiner, D., Notarangelo, L. D., Rampertaap, Y., Olivier, K. N., McElwee, J., Hughes, J., Pittaluga, S., Oliveira, J. B., Meffre, E., Fleisher, T. A., Holland, S. M., Lenardo, M. J., Tangye, S. G. and Uzel, G. (2014) Immune dysregulation in human subjects with heterozygous germline mutations in CTLA4. *Science, 345*(6204), pp. 1623-1627.

Kumar, R., Angelini, S., Snellman, E. and Hemminki, K. (2004) BRAF mutations are common somatic events in melanocytic nevi. *J Investig Dermatol, 122*(2), pp. 342-348.

Kwan Tat, S., Amiable, N., Pelletier, J.-P., Boileau, C., Lajeunesse, D., Duval, N. and Martel-Pelletier, J. (2009) Modulation of OPG, RANK and RANKL by human chondrocytes and their implication during osteoarthritis. *Rheumatology, 48*(12), pp. 1482-1490.

Kwon, E. D., Drake, C. G., Scher, H. I., Fizazi, K., Bossi, A., van den Eertwegh, A. J. M., Krainer, M., Houede, N., Santos, R., Mahammedi, H., Ng, S., Maio, M., Franke, F. A., Sundar, S., Agarwal, N., Bergman, A. M., Ciuleanu, T. E., Korbenfeld, E., Sengeløv, L., Hansen, S., Logothetis, C., Beer, T. M., McHenry, M. B., Gagnier, P., Liu, D. and Gerritsen, W. R. (2014) Ipilimumab versus placebo after radiotherapy in patients with metastatic castration-resistant prostate cancer that had progressed after docetaxel chemotherapy (CA184-043): a multicentre, randomised, double-blind, phase 3 trial. *The Lancet Oncology, 15*(7), pp. 700-712.

Kyewski, B. and Klein, L. (2006) A central role for central tolerance. *Annual Review of Immunology, 24*(1), pp. 571-606.

Larkin, J., Chiarion-Sileni, V., Gonzalez, R., Grob, J. J., Cowey, C. L., Lao, C. D., Schadendorf, D., Dummer, R., Smylie, M., Rutkowski, P., Ferrucci, P. F., Hill, A., Wagstaff, J., Carlino, M. S., Haanen, J. B., Maio, M., Marquez-Rodas, I., McArthur, G. A., Ascierto, P. A., Long, G. V., Callahan, M. K., Postow, M. A., Grossmann, K., Sznol, M., Dreno, B., Bastholt, L., Yang, A., Rollin, L. M., Horak, C., Hodi, F. S. and Wolchok, J. D. (2015) Combined nivolumab and ipilimumab or monotherapy in untreated melanoma. *New England Journal of Medicine, 373*(1), pp. 23-34.

Leach, D. R., Krummel, M. F. and Allison, J. P. (1996) Enhancement of antitumor immunity by CTLA-4 blockade. *Science, 271*(5256), pp. 1734-1736.

Lee, Sau K., Silva, Diego G., Martin, Jaime L., Pratama, A., Hu, X., Chang, P. P., Walters, G. and Vinuesa, Carola G. (2012) Interferon-γ excess leads to pathogenic accumulation of follicular helper T cells and germinal centers. *Immunity, 37*(5), pp. 880-892.

Leppek, K., Schott, J., Reitter, S., Poetz, F., Hammond, Ming C. and Stoecklin, G. (2013) Roquin promotes constitutive mRNA decay via a conserved class of stem-loop recognition motifs. *Cell, 153*(4), pp. 869-881.

Lesokhin, A. M., Callahan, M. K., Postow, M. A. and Wolchok, J. D. (2015) On being less tolerant: enhanced cancer immunosurveillance enabled by targeting checkpoints and agonists of T cell activation. *Science Translational Medicine, 7*(280), pp. 280sr1-280sr1.

Li, B., VanRoey, M., Wang, C., Chen, T. H. T., Korman, A. and Jooss, K. (2009) Anti–programmed death-1 synergizes with granulocyte macrophage colony-stimulating factor–secreting tumor cell immunotherapy providing therapeutic benefit to mice with established tumors. *Clinical Cancer Research, 15*(5), pp. 1623-1634.

Li, F. and Ravetch, J. V. (2011) Inhibitory Fcγ receptor engagement drives adjuvant and anti-tumor activities of agonistic CD40 antibodies. *Science, 333*(6045), pp. 1030-1034.

Li, S. and Liu, Y. (2013) Immunotherapy of melanoma with the immune costimulatory monoclonal antibodies targeting CD137. *Clin Pharmacol, 5*(Suppl 1), pp. 47-53.

Li, X., Kostareli, E., Suffner, J., Garbi, N. and Hämmerling, G. J. (2010) Efficient Treg depletion induces T-cell infiltration and rejection of large tumors. *European Journal of Immunology, 40*(12), pp. 3325-3335.

Liang, B., Workman, C., Lee, J., Chew, C., Dale, B. M., Colonna, L., Flores, M., Li, N., Schweighoffer, E., Greenberg, S., Tybulewicz, V., Vignali, D. and Clynes, R. (2008) Regulatory T cells inhibit dendritic cells by lymphocyte activation gene-3 engagement of MHC class II. *The Journal of Immunology, 180*(9), pp. 5916-5926.

Liblau, R. S., Wong, F. S., Mars, L. T. and Santamaria, P. (2002) Autoreactive CD8 T cells in organ-specific autoimmunity: emerging targets for therapeutic intervention. *Immunity, 17*(1), pp. 1-6.

Lind, E. F., Prockop, S. E., Porritt, H. E. and Petrie, H. T. (2001) Mapping precursor movement through the postnatal thymus reveals specific microenvironments supporting defined stages of early lymphoid development. *The Journal of Experimental Medicine, 194*(2), pp. 127-134.

Liu, W., Putnam, A. L., Xu-yu, Z., Szot, G. L., Lee, M. R., Zhu, S., Gottlieb, P. A., Kapranov, P., Gingeras, T. R., de St. Groth, B. F., Clayberger, C., Soper, D. M., Ziegler, S. F. and Bluestone, J. A. (2006) CD127 expression inversely correlates with FoxP3 and suppressive function of human $CD4^+$ T reg cells. *The Journal of Experimental Medicine, 203*(7), pp. 1701-1711.

Liyanage, U. K., Moore, T. T., Joo, H.-G., Tanaka, Y., Herrmann, V., Doherty, G., Drebin, J. A., Strasberg, S. M., Eberlein, T. J., Goedegebuure, P. S. and Linehan, D. C. (2002) Prevalence of regulatory T cells is increased in peripheral blood and tumor microenvironment of patients with pancreas or breast adenocarcinoma. *The Journal of Immunology, 169*(5), pp. 2756-2761.

Locksley, R. M., Killeen, N. and Lenardo, M. J. (2001) The TNF and TNF receptor superfamilies: integrating mammalian biology. *Cell, 104*(4), pp. 487-501.

Lopez-Bergami, P. (2011) The role of mitogen- and stress-activated protein kinase pathways in melanoma. *Pigment Cell & Melanoma Research, 24*(5), pp. 902-921.

Ma, D. Y. and Clark, E. A. (2009) The role of CD40 and CD154/CD40L in dendritic cells. *Seminars in Immunology, 21*(5), pp. 265-272.

MacKie, R. M., Hauschild, A. and Eggermont, A. M. M. (2009) Epidemiology of invasive cutaneous melanoma. *Annals of Oncology, 20*(suppl 6), pp. vi1-vi7.

MacKie, R. M., Reid, R. and Junor, B. (2003) Fatal melanoma transferred in a donated kidney 16 years after melanoma surgery. *New England Journal of Medicine, 348*(6), pp. 567-568.

Magis, C., van der Sloot, A. M., Serrano, L. and Notredame, C. (2012) An improved understanding of TNFL/TNFR interactions using structure-based classifications. *Trends in Biochemical Sciences, 37*(9), pp. 353-363.

Mahmud, S. A., Manlove, L. S., Schmitz, H. M., Xing, Y., Wang, Y., Owen, D. L., Schenkel, J. M., Boomer, J. S., Green, J. M., Yagita, H., Chi, H., Hogquist, K. A. and Farrar, M. A. (2014) Costimulation via the tumor-necrosis factor receptor superfamily couples TCR signal strength to the thymic differentiation of regulatory T cells. *Nat Immunol, 15*(5), pp. 473-481.

Maio, M. (2012) Melanoma as a model tumour for immuno-oncology. *Annals of Oncology, 23*(suppl 8), pp. viii10-viii14.

Maio, M., Grob, J. J., Aamdal, S., Bondarenko, I., Robert, C., Thomas, L., Garbe, C., Chiarion-Sileni, V., Testori, A., Chen, T. T., Tschaika, M. and Wolchok, J. D. (2015) Five-year survival rates for treatment-naive patients with advanced melanoma who received ipilimumab plus dacarbazine in a phase III trial. *Journal of Clinical Oncology, 33*(10), pp. 1191-1196.

Malchow, S., Leventhal, D. S., Nishi, S., Fischer, B. I., Shen, L., Paner, G. P., Amit, A. S., Kang, C., Geddes, J. E., Allison, J. P., Socci, N. D. and Savage, P. A. (2013) Aire-dependent thymic development of tumor-associated regulatory T cells. *Science, 339*(6124), pp. 1219-1224.

Mantovani, A. and Allavena, P. (2015) The interaction of anticancer therapies with tumor-associated macrophages. *The Journal of Experimental Medicine, 212*(4), pp. 435-445.

Mantovani, A., Allavena, P., Sica, A. and Balkwill, F. (2008) Cancer-related inflammation. *Nature, 454*(7203), pp. 436-444.

Mantovani, A., Sozzani, S., Locati, M., Allavena, P. and Sica, A. (2002) Macrophage polarization: tumor-associated macrophages as a paradigm for polarized M2 mononuclear phagocytes. *Trends in Immunology, 23*(11), pp. 549-555.

McCaughtry, T. M., Baldwin, T. A., Wilken, M. S. and Hogquist, K. A. (2008) Clonal deletion of thymocytes can occur in the cortex with no involvement of the medulla. *The Journal of Experimental Medicine, 205*(11), pp. 2575-2584.

McHugh, R. S., Whitters, M. J., Piccirillo, C. A., Young, D. A., Shevach, E. M., Collins, M. and Byrne, M. C. (2002) $CD4^{+}CD25^{+}$ immunoregulatory T cells: gene expression analysis reveals a functional role for the glucocorticoid-induced TNF receptor. *Immunity, 16*(2), pp. 311-323.

Melero, I., Shuford, W. W., Newby, S. A., Aruffo, A., Ledbetter, J. A., Hellstrom, K. E., Mittler, R. S. and Chen, L. (1997) Monoclonal antibodies against the 4-1BB T-cell activation molecule eradicate established tumors. *Nat Med, 3*(6), pp. 682-685.

Metushi, I. G., Hayes, M. A. and Uetrecht, J. (2015) Treatment of PD-1−/− mice with amodiaquine and anti-CTLA-4 leads to liver injury similar to idiosyncratic liver injury in patients. *Hepatology, 61*(4), pp. 1332-1342.

Metzger, T. C. and Anderson, M. S. (2011) Control of central and peripheral tolerance by Aire. *Immunological Reviews, 241*(1), pp. 89-103.

Miao, H.-Q., Lee, P., Lin, H., Soker, S. and Klagsburn, M. (2000) Neuropilin-1 expression by tumor cells promotes tumor angiogenesis and progression. *The FASEB Journal, 14*(15), pp. 2532-2539.

Miller, A. J. and Mihm, M. C. (2006) Melanoma: mechanisms of disease. *New England Journal of Medicine, 355*(1), pp. 51-65.

Mittal, D., Gubin, M. M., Schreiber, R. D. and Smyth, M. J. (2014) New insights into cancer immunoediting and its three component phases-elimination, equilibrium and escape. *Current Opinion in Immunology, 27*(0), pp. 16-25.

Moran, A. E., Kovacsovics-Bankowski, M. and Weinberg, A. D. (2013) The TNFRs OX40, 4-1BB, and CD40 as targets for cancer immunotherapy. *Current Opinion in Immunology, 25*(2), pp. 230-237.

Movahedi, K., Laoui, D., Gysemans, C., Baeten, M., Stangé, G., Van den Bossche, J., Mack, M., Pipeleers, D., In't Veld, P., De Baetselier, P. and Van Ginderachter, J. A. (2010) Different tumor microenvironments contain functionally distinct subsets of macrophages derived from $Ly6C^{(high)}$ monocytes. *Cancer Research, 70*(14), pp. 5728-5739.

Murata, K., Nose, M., Ndhlovu, L. C., Sato, T., Sugamura, K. and Ishii, N. (2002) Constitutive OX40/OX40 ligand interaction induces autoimmune-like diseases. *The Journal of Immunology, 169*(8), pp. 4628-4636.

Nagai, H., Horikawa, T., Hara, I., Fukunaga, A., Oniki, S., Oka, M., Nishigori, C. and Ichihashi, M. (2004) In vivo elimination of $CD25^+$ regulatory T cells leads to tumor rejection of B16F10 melanoma, when combined with interleukin-12 gene transfer. *Experimental Dermatology, 13*(10), pp. 613-620.

Nakamura, K., Kitani, A., Fuss, I., Pedersen, A., Harada, N., Nawata, H. and Strober, W. (2004) TGF-β1 plays an important role in the mechanism of $CD4^+CD25^+$ regulatory T cell Activity in both humans and mice. *The Journal of Immunology, 172*(2), pp. 834-842.

Nakamura, K., Kitani, A. and Strober, W. (2001) Cell contact–dependent immunosuppression by $CD4^+CD25^+$regulatory T cells is mediated by cell surface–bound transforming growth factor β. *The Journal of Experimental Medicine, 194*(5), pp. 629-644.

Negishi, I., Motoyama, N., Nakayama, K.-i., Nakayama, K., Senju, S., Hatakeyama, S., Zhang, Q., Chan, A. C. and Loh, D. Y. (1995) Essential role for ZAP-70 in both positive and negative selection of thymocytes. *Nature, 376*(6539), pp. 435-438.

Neufeld, G., Cohen, T., Gengrinovitch, S. and Poltorak, Z. (1999) Vascular endothelial growth factor (VEGF) and its receptors. *The FASEB Journal, 13*(1), pp. 9-22.

Nishikawa, H. and Sakaguchi, S. (2010) Regulatory T cells in tumor immunity. *International Journal of Cancer, 127*(4), pp. 759-767.

Nishimura, H., Nose, M., Hiai, H., Minato, N. and Honjo, T. (1999) Development of lupus-like autoimmune diseases by disruption of the PD-1 gene encoding an ITIM motif-carrying immunoreceptor. *Immunity, 11*(2), pp. 141-151.

Nishimura, T. and Ohta, A. (1999) A critical role for antigen-specific Th1 cells in acute liver injury in mice. *The Journal of Immunology, 162*(11), pp. 6503-6509.

Nishisho, I., Nakamura, Y., Miyoshi, Y., Miki, Y., Ando, H., Horii, A., Koyama, K., Utsunomiya, J., Baba, S. and Hedge, P. (1991) Mutations of chromosome 5q21 genes in FAP and colorectal cancer patients. *Science, 253*(5020), pp. 665-669.

Ochsenbein, A. F., Klenerman, P., Karrer, U., Ludewig, B., Pericin, M., Hengartner, H. and Zinkernagel, R. M. (1999) Immune surveillance against a solid tumor fails because of immunological ignorance. *Proceedings of the National Academy of Sciences, 96*(5), pp. 2233-2238.

Ohshima, Y., Yang, L. P., Uchiyama, T., Tanaka, Y., Baum, P., Sergerie, M., Hermann, P. and Delespesse, G. (1998) OX40 costimulation enhances interleukin-4 (IL-4) expression at priming and promotes the differentiation of naive human $CD4^+$ T cells into high IL-4–producing effectors. *Blood, 92*(9), pp. 3338-3345.

Overwijk, W. W., Theoret, M. R., Finkelstein, S. E., Surman, D. R., de Jong, L. A., Vyth-Dreese, F. A., Dellemijn, T. A., Antony, P. A., Spiess, P. J., Palmer, D. C., Heimann, D. M., Klebanoff, C. A., Yu, Z., Hwang, L. N., Feigenbaum, L., Kruisbeek, A. M., Rosenberg, S. A. and Restifo, N. P. (2003) Tumor regression and autoimmunity after reversal of a functionally tolerant state of self-reactive CD8+ T cells. *The Journal of Experimental Medicine, 198*(4), pp. 569-580.

Pagès, F., Berger, A., Camus, M., Sanchez-Cabo, F., Costes, A., Molidor, R., Mlecnik, B., Kirilovsky, A., Nilsson, M., Damotte, D., Meatchi, T., Bruneval, P., Cugnenc, P. H., Trajanoski, Z., Fridman, W. H. and Galon, J. (2005) Effector memory T cells, early metastasis, and survival in colorectal cancer. *New England Journal of Medicine, 353*(25), pp. 2654-2666.

Pardoll, D. M. (2012) The blockade of immune checkpoints in cancer immunotherapy. *Nat Rev Cancer, 12*(4), pp. 252-264.

Parry, R. V., Chemnitz, J. M., Frauwirth, K. A., Lanfranco, A. R., Braunstein, I., Kobayashi, S. V., Linsley, P. S., Thompson, C. B. and Riley, J. L. (2005) CTLA-4 and PD-1 receptors inhibit T-cell activation by distinct mechanisms. *Molecular and Cellular Biology, 25*(21), pp. 9543-9553.

Pauken, K. E. and Wherry, E. J. (2015) Overcoming T cell exhaustion in infection and cancer. *Trends in Immunology, 36*(4), pp. 265-276.

Pearse, G. (2006) Normal structure, function and histology of the thymus. *Toxicologic Pathology, 34*(5), pp. 504-514.

Peggs, K. S., Quezada, S. A., Chambers, C. A., Korman, A. J. and Allison, J. P. (2009) Blockade of CTLA-4 on both effector and regulatory T cell compartments contributes to the antitumor activity of anti–CTLA-4 antibodies. *The Journal of Experimental Medicine, 206*(8), pp. 1717-1725.

Pentcheva-Hoang, T., Corse, E. and Allison, J. P. (2009) Negative regulators of T-cell activation: potential targets for therapeutic intervention in cancer, autoimmune disease, and persistent infections. *Immunological Reviews, 229*(1), pp. 67-87.

Pérez-Sayáns, M., Somoza-Martín, J. M., Barros-Angueira, F., Rey, J. M. G. and García-García, A. (2010) RANK/RANKL/OPG role in distraction osteogenesis. *Oral Surgery, Oral Medicine, Oral Pathology, Oral Radiology, and Endodontology, 109*(5), pp. 679-686.

Perez, V. L., Van Parijs, L., Biuckians, A., Zheng, X. X., Strom, T. B. and Abbas, A. K. (1997) Induction of peripheral T cell tolerance *in vivo* requires CTLA-4 engagement. *Immunity, 6*(4), pp. 411-417.

Peters, A. L., Stunz, L. L. and Bishop, G. A. (2009) CD40 and autoimmunity: The dark side of a great activator. *Seminars in Immunology, 21*(5), pp. 293-300.

Petrie, H. T. and Zúñiga-Pflücker, J. C. (2007) Zoned out: functional mapping of stromal signaling microenvironments in the thymus. *Annual Review of Immunology, 25*(1), pp. 649-679.

Phan, G. Q., Yang, J. C., Sherry, R. M., Hwu, P., Topalian, S. L., Schwartzentruber, D. J., Restifo, N. P., Haworth, L. R., Seipp, C. A., Freezer, L. J., Morton, K. E., Mavroukakis, S. A., Duray, P. H., Steinberg, S. M., Allison, J. P., Davis, T. A. and Rosenberg, S. A. (2003) Cancer regression and autoimmunity induced by cytotoxic T lymphocyte-associated antigen 4 blockade in patients with metastatic melanoma. *Proceedings of the National Academy of Sciences, 100*(14), pp. 8372-8377.

Piccirillo, C. A., Letterio, J. J., Thornton, A. M., McHugh, R. S., Mamura, M., Mizuhara, H. and Shevach, E. M. (2002) $CD4^+CD25^+$ regulatory T cells can mediate suppressor function in the absence of transforming growth factor β1

production and responsiveness. *The Journal of Experimental Medicine, 196*(2), pp. 237-246.

Piconese, S., Pittoni, P., Burocchi, A., Gorzanelli, A., Carè, A., Tripodo, C. and Colombo, M. P. (2010) A non-redundant role for OX40 in the competitive fitness of Treg in response to IL-2. *European Journal of Immunology, 40*(10), pp. 2902-2913.

Piconese, S., Timperi, E., Pacella, I., Schinzari, V., Tripodo, C., Rossi, M., Guglielmo, N., Mennini, G., Grazi, G. L., Di Filippo, S., Brozzetti, S., Fazzi, K., Antonelli, G., Lozzi, M. A., Sanchez, M. and Barnaba, V. (2014) Human OX40 tunes the function of regulatory T cells in tumor and nontumor areas of hepatitis C virus–infected liver tissue. *Hepatology, 60*(5), pp. 1494-1507.

Piconese, S., Valzasina, B. and Colombo, M. P. (2008) OX40 triggering blocks suppression by regulatory T cells and facilitates tumor rejection. *The Journal of Experimental Medicine, 205*(4), pp. 825-839.

Pillai, V., Ortega, S. B., Wang, C. K. and Karandikar, N. J. (2007) Transient regulatory T-cells: a state attained by all activated human T-cells. *Clinical Immunology, 123*(1), pp. 18-29.

Pollard, K. M., Cauvi, D. M., Toomey, C. B., Morris, K. V. and Kono, D. H. (2013) Interferon-γ and systemic autoimmunity. *Discovery medicine, 16*(87), pp. 123-131.

Postow, M. A., Chesney, J., Pavlick, A. C., Robert, C., Grossmann, K., McDermott, D., Linette, G. P., Meyer, N., Giguere, J. K., Agarwala, S. S., Shaheen, M., Ernstoff, M. S., Minor, D., Salama, A. K., Taylor, M., Ott, P. A., Rollin, L. M., Horak, C., Gagnier, P., Wolchok, J. D. and Hodi, F. S. (2015) Nivolumab and ipilimumab versus ipilimumab in untreated melanoma. *New England Journal of Medicine, 372*(21), pp. 2006-2017.

Powles, T., Eder, J. P., Fine, G. D., Braiteh, F. S., Loriot, Y., Cruz, C., Bellmunt, J., Burris, H. A., Petrylak, D. P., Teng, S. L., Shen, X., Boyd, Z., Hegde, P. S., Chen, D. S. and Vogelzang, N. J. (2014) MPDL3280A (anti-PD-L1) treatment leads to clinical activity in metastatic bladder cancer. *Nature, 515*(7528), pp. 558-562.

Pratama, A., Ramiscal, Roybel R., Silva, Diego G., Das, Souvik K., Athanasopoulos, V., Fitch, J., Botelho, Natalia K., Chang, P. P., Hu, X., Hogan, Jennifer J., Maña, P., Bernal, D., Korner, H., Yu, D., Goodnow, Christopher C., Cook, Matthew C. and Vinuesa, Carola G. (2013) Roquin-2 shares functions with its paralog Roquin-1 in the repression of mRNAs controlling T follicular helper cells and systemic inflammation. *Immunity, 38*(4), pp. 669-680.

Probst, H. C., McCoy, K., Okazaki, T., Honjo, T. and van den Broek, M. (2005) Resting dendritic cells induce peripheral $CD8^+$ T cell tolerance through PD-1 and CTLA-4. *Nat Immunol, 6*(3), pp. 280-286.

Quezada, S. A. and Peggs, K. S. (2013) Exploiting CTLA-4, PD-1 and PD-L1 to reactivate the host immune response against cancer. *Br J Cancer, 108*(8), pp. 1560-1565.

Qureshi, O. S., Zheng, Y., Nakamura, K., Attridge, K., Manzotti, C., Schmidt, E. M., Baker, J., Jeffery, L. E., Kaur, S., Briggs, Z., Hou, T. Z., Futter, C. E., Anderson, G., Walker, L. S. K. and Sansom, D. M. (2011) Trans-endocytosis of CD80 and CD86: a molecular basis for the cell-extrinsic function of CTLA-4. *Science, 332*(6029), pp. 600-603.

Restifo, N. P., Dudley, M. E. and Rosenberg, S. A. (2012) Adoptive immunotherapy for cancer: harnessing the T cell response. *Nat Rev Immunol, 12*(4), pp. 269-281.

Ribas, A. (2012) Tumor immunotherapy directed at PD-1. *New England Journal of Medicine, 366*(26), pp. 2517-2519.

Ribas, A., Kefford, R., Marshall, M. A., Punt, C. J. A., Haanen, J. B., Marmol, M., Garbe, C., Gogas, H., Schachter, J., Linette, G., Lorigan, P., Kendra, K. L., Maio, M., Trefzer, U., Smylie, M., McArthur, G. A., Dreno, B., Nathan, P. D., Mackiewicz, J., Kirkwood, J. M., Gomez-Navarro, J., Huang, B., Pavlov, D. and Hauschild , A. (2013) Phase III randomized clinical trial comparing tremelimumab with standard-of-care chemotherapy in patients with advanced melanoma. *Journal of Clinical Oncology, 31*(5), pp. 616-622.

Riley, J. L. (2013) Combination checkpoint blockade - taking melanoma immunotherapy to the next level. *New England Journal of Medicine, 369*(2), pp. 187-189.

Robbins, P. F., Morgan, R. A., Feldman, S. A., Yang, J. C., Sherry, R. M., Dudley, M. E., Wunderlich, J. R., Nahvi, A. V., Helman, L. J., Mackall, C. L., Kammula, U. S., Hughes, M. S., Restifo, N. P., Raffeld, M., Lee, C.-C. R., Levy, C. L., Li, Y. F., El-Gamil, M., Schwarz, S. L., Laurencot, C. and Rosenberg, S. A. (2011) Tumor regression in patients with metastatic synovial cell sarcoma and melanoma using genetically engineered lymphocytes reactive with NY-ESO-1. *Journal of Clinical Oncology, 29*(7), pp. 917-924.

Robert, C., Long, G. V., Brady, B., Dutriaux, C., Maio, M., Mortier, L., Hassel, J. C., Rutkowski, P., McNeil, C., Kalinka-Warzocha, E., Savage, K. J., Hernberg, M. M., Lebbé, C., Charles, J., Mihalcioiu, C., Chiarion-Sileni, V., Mauch, C., Cognetti, F., Arance, A., Schmidt, H., Schadendorf, D., Gogas, H., Lundgren-Eriksson, L., Horak, C., Sharkey, B., Waxman, I. M., Atkinson, V. and Ascierto, P. A. (2015a) Nivolumab in previously untreated melanoma without BRAF mutation. *New England Journal of Medicine, 372*(4), pp. 320-330.

Robert, C., Schachter, J., Long, G. V., Arance, A., Grob, J. J., Mortier, L., Daud, A., Carlino, M. S., McNeil, C., Lotem, M., Larkin, J., Lorigan, P., Neyns, B., Blank, C. U., Hamid, O., Mateus, C., Shapira-Frommer, R., Kosh, M., Zhou, H., Ibrahim, N., Ebbinghaus, S. and Ribas, A. (2015b) Pembrolizumab versus ipilimumab in advanced melanoma. *New England Journal of Medicine, 372*(26), pp. 2521-2532.

Robert, C., Thomas, L., Bondarenko, I., O'Day, S., Weber, J., Garbe, C., Lebbe, C., Baurain, J. F., Testori, A., Grob, J. J., Davidson, N., Richards, J., Maio, M., Hauschild, A., Miller, W. H., Gascon, P., Lotem, M., Harmankaya, K., Ibrahim, R., Francis, S., Chen, T. T., Humphrey, R., Hoos, A. and Wolchok, J. D. (2011) Ipilimumab plus dacarbazine for previously untreated metastatic melanoma. *New England Journal of Medicine, 364*(26), pp. 2517-2526.

Roberts, Natalie A., White, Andrea J., Jenkinson, William E., Turchinovich, G., Nakamura, K., Withers, David R., McConnell, Fiona M., Desanti, Guillaume E., Benezech, C., Parnell, Sonia M., Cunningham, Adam F., Paolino, M., Penninger, J. M., Simon, A. K., Nitta, T., Ohigashi, I., Takahama, Y., Caamano, Jorge H., Hayday, Adrian C., Lane, Peter J. L., Jenkinson, Eric J. and Anderson, G. (2012) Rank signaling links the development of invariant γδ T cell progenitors and Aire+ medullary epithelium. *Immunity, 36*(3), pp. 427-437.

Rogers, P. R., Song, J., Gramaglia, I., Killeen, N. and Croft, M. (2001) OX40 promotes Bcl-xL and Bcl-2 expression and is essential for long-term survival of CD4 T cells. *Immunity, 15*(3), pp. 445-455.

Rowe, J. H., Ertelt, J. M., Xin, L. and Way, S. S. (2012) Pregnancy imprints regulatory memory that sustains anergy to fetal antigen. *Nature, 490*(7418), pp. 102-106.

Royal, R. E., Levy, C., Turner, K., Mathur, A., Hughes, M., Kammula, U. S., Sherry, R. M., Topalian, S. L., Yang, J. C., Lowy, I. and Rosenberg, S. A. (2010) Phase 2 trial of single agent ipilimumab (anti-CTLA-4) for locally advanced or metastatic pancreatic adenocarcinoma. *Journal of immunotherapy, 33*(8), pp. 828-833.

Rubtsov, Y. P., Rasmussen, J. P., Chi, E. Y., Fontenot, J., Castelli, L., Ye, X., Treuting, P., Siewe, L., Roers, A., Henderson Jr, W. R., Muller, W. and Rudensky, A. Y. (2008) Regulatory T cell-derived interleukin-10 limits inflammation at environmental interfaces. *Immunity, 28*(4), pp. 546-558.

Ruby, C. E., Yates, M. A., Hirschhorn-Cymerman, D., Chlebeck, P., Wolchok, J. D., Houghton, A. N., Offner, H. and Weinberg, A. D. (2009) Cutting edge: OX40 agonists can drive regulatory T cell expansion if the cytokine milieu is right. *The Journal of Immunology, 183*(8), pp. 4853-4857.

Rudd, C. E., Taylor, A. and Schneider, H. (2009) CD28 and CTLA-4 coreceptor expression and signal transduction. *Immunological Reviews, 229*(1), pp. 12-26.

Saint-Ruf, C., Ungewiss, K., Groettrup, M., Bruno, L., Fehling, H. and von Boehmer, H. (1994) Analysis and expression of a cloned pre-T cell receptor gene. *Science, 266*(5188), pp. 1208-1212.

Saito, T., Dworacki, G., Gooding, W., Lotze, M. T. and Whiteside, T. L. (2000) Spontaneous apoptosis of $CD8^+$ T lymphocytes in peripheral blood of patients with advanced melanoma. *Clinical Cancer Research, 6*(4), pp. 1351-1364.

Sakaguchi, S., Sakaguchi, N., Asano, M., Itoh, M. and Toda, M. (1995) Immunologic self-tolerance maintained by activated T cells expressing IL-2 receptor alpha-chains (CD25). Breakdown of a single mechanism of self-tolerance causes various autoimmune diseases. *The Journal of Immunology, 155*(3), pp. 1151-64.

Sakaguchi, S., Wing, K., Onishi, Y., Prieto-Martin, P. and Yamaguchi, T. (2009) Regulatory T cells: how do they suppress immune responses? *International Immunology, 21*(10), pp. 1105-1111.

Sakaguchi, S., Yamaguchi, T., Nomura, T. and Ono, M. (2008) Regulatory T cells and immune tolerance. *Cell, 133*(5), pp. 775-787.

Sakuishi, K., Apetoh, L., Sullivan, J. M., Blazar, B. R., Kuchroo, V. K. and Anderson, A. C. (2010) Targeting Tim-3 and PD-1 pathways to reverse T cell exhaustion and restore anti-tumor immunity. *The Journal of Experimental Medicine, 207*(10), pp. 2187-2194.

Salama, A. D., Chitnis, T., Imitola, J., Ansari, M. J. I., Akiba, H., Tushima, F., Azuma, M., Yagita, H., Sayegh, M. H. and Khoury, S. J. (2003) Critical role of the programmed death-1 (PD-1) pathway in regulation of experimental autoimmune encephalomyelitis. *The Journal of Experimental Medicine, 198*(1), pp. 71-78.

Salama, P., Phillips, M., Grieu, F., Morris, M., Zeps, N., Joseph, D., Platell, C. and Iacopetta, B. (2009) Tumor infiltrating $Foxp3^+$ T regulatory cells show strong prognostic significance in colorectal cancer. *Journal of Clinical Oncology, 27*(2), pp. 186-192.

Sarris, M., Andersen, K. G., Randow, F., Mayr, L. and Betz, A. G. (2008) Neuropilin-1 expression on regulatory T cells enhances their interactions with dendritic cells during antigen recognition. *Immunity, 28*(3), pp. 402-413.

Savage, N. D. L., de Boer, T., Walburg, K. V., Joosten, S. A., van Meijgaarden, K., Geluk, A. and Ottenhoff, T. H. M. (2008) Human anti-inflammatory macrophages induce $Foxp3^+GITR^+CD25^+$ regulatory T cells, which suppress

via membrane-bound TGFβ-1. *The Journal of Immunology, 181*(3), pp. 2220-2226.

Savage, P. A., Leventhal, D. S. and Malchow, S. (2014) Shaping the repertoire of tumor-infiltrating effector and regulatory T cells. *Immunological Reviews, 259*(1), pp. 245-258.

Schadendorf, D., Hodi, F. S., Robert, C., Weber, J. S., Margolin, K., Hamid, O., Patt, D., Chen, T. T., Berman, D. M. and Wolchok, J. D. (2015) Pooled analysis of long-term survival data from phase II and phase III trials of ipilimumab in unresectable or metastatic melanoma. *Journal of Clinical Oncology*.

Schmidt, A., Oberle, N. and Krammer, P. H. (2012) Molecular mechanisms of Treg-mediated T cell suppression. *Frontiers in Immunology, 3*.

Schmitt, E. G., Haribhai, D., Williams, J. B., Aggarwal, P., Jia, S., Charbonnier, L. M., Yan, K., Lorier, R., Turner, A., Ziegelbauer, J., Georgiev, P., Simpson, P., Salzman, N. H., Hessner, M. J., Broeckel, U., Chatila, T. A. and Williams, C. B. (2012) IL-10 produced by induced regulatory T cells (iTregs) controls colitis and pathogenic ex-iTregs during immunotherapy. *The Journal of Immunology, 189*(12), pp. 5638-5648.

Schnell, M. A., Hardy, C., Hawley, M., Propert, K. J. and Wilson, J. M. (2002) Effect of blood collection technique in mice on clinical pathology parameters. *Hum Gene Ther, 13*(1), pp. 155-61.

Schubert, D., Bode, C., Kenefeck, R., Hou, T. Z., Wing, J. B., Kennedy, A., Bulashevska, A., Petersen, B. S., Schaffer, A. A., Gruning, B. A., Unger, S., Frede, N., Baumann, U., Witte, T., Schmidt, R. E., Dueckers, G., Niehues, T., Seneviratne, S., Kanariou, M., Speckmann, C., Ehl, S., Rensing-Ehl, A., Warnatz, K., Rakhmanov, M., Thimme, R., Hasselblatt, P., Emmerich, F., Cathomen, T., Backofen, R., Fisch, P., Seidl, M., May, A., Schmitt-Graeff, A., Ikemizu, S., Salzer, U., Franke, A., Sakaguchi, S., Walker, L. S. K., Sansom, D. M. and Grimbacher, B. (2014) Autosomal dominant immune dysregulation syndrome in humans with CTLA4 mutations. *Nat Med, 20*(12), pp. 1410-1416.

Schwartz, J.-C. D., Zhang, X., Fedorov, A. A., Nathenson, S. G. and Almo, S. C. (2001) Structural basis for co-stimulation by the human CTLA-4/B7-2 complex. *Nature, 410*(6828), pp. 604-608.

Schwartz, R. H. (2003) T cell anergy. *Annual Review of Immunology, 21*(1), pp. 305-334.

Seddiki, N., Santner-Nanan, B., Martinson, J., Zaunders, J., Sasson, S., Landay, A., Solomon, M., Selby, W., Alexander, S. I., Nanan, R., Kelleher, A. and de St. Groth, B. F. (2006) Expression of interleukin IL-2 and IL-7 receptors discriminates between human regulatory and activated T cells. *The Journal of Experimental Medicine, 203*(7), pp. 1693-1700.

Selby, M. J., Engelhardt, J. J., Quigley, M., Henning, K. A., Chen, T., Srinivasan, M. and Korman, A. J. (2013) Anti-CTLA-4 antibodies of IgG2a isotype enhance antitumor activity through reduction of intratumoral regulatory T cells. *Cancer Immunology Research*.

Shang, B., Liu, Y., Jiang, S. J. and Liu, Y. (2015) Prognostic value of tumor-infiltrating $FoxP3^+$ regulatory T cells in cancers: a systematic review and meta-analysis. *Scientific Reports, 5*, pp. 15179.

Shankaran, V., Ikeda, H., Bruce, A. T., White, J. M., Swanson, P. E., Old, L. J. and Schreiber, R. D. (2001) IFN_γ and lymphocytes prevent primary tumour development and shape tumour immunogenicity. *Nature, 410*(6832), pp. 1107-1111.

Sheppard, K. A., Fitz, L. J., Lee, J. M., Benander, C., George, J. A., Wooters, J., Qiu, Y., Jussif, J. M., Carter, L. L., Wood, C. R. and Chaudhary, D. (2004) PD-1 inhibits T-cell receptor induced phosphorylation of the ZAP70/CD3ζ signalosome and downstream signaling to PKCθ. *FEBS Letters, 574*(1–3), pp. 37-41.

Shevach, E. M. and Stephens, G. L. (2006) The GITR-GITRL interaction: co-stimulation or contrasuppression of regulatory activity? *Nat Rev Immunol, 6*(8), pp. 613-618.

Shields, J. D., Kourtis, I. C., Tomei, A. A., Roberts, J. M. and Swartz, M. A. (2010) Induction of lymphoidlike stroma and immune escape by tumors that express the chemokine CCL21. *Science, 328*(5979), pp. 749-752.

Simpson, A. J. G., Caballero, O. L., Jungbluth, A., Chen, Y. T. and Old, L. J. (2005) Cancer/testis antigens, gametogenesis and cancer. *Nat Rev Cancer, 5*(8), pp. 615-625.

Simpson, T. R., Li, F., Montalvo-Ortiz, W., Sepulveda, M. A., Bergerhoff, K., Arce, F., Roddie, C., Henry, J. Y., Yagita, H., Wolchok, J. D., Peggs, K. S., Ravetch, J. V., Allison, J. P. and Quezada, S. A. (2013) Fc-dependent depletion of tumor-infiltrating regulatory T cells co-defines the efficacy of anti–CTLA-4 therapy against melanoma. *The Journal of Experimental Medicine, 210*(9), pp. 1695-1710.

Snyder, A., Makarov, V., Merghoub, T., Yuan, J., Zaretsky, J. M., Desrichard, A., Walsh, L. A., Postow, M. A., Wong, P., Ho, T. S., Hollmann, T. J., Bruggeman, C., Kannan, K., Li, Y., Elipenahli, C., Liu, C., Harbison, C. T., Wang, L., Ribas, A., Wolchok, J. D. and Chan, T. A. (2014) Genetic Basis for Clinical Response to CTLA-4 blockade in melanoma. *New England Journal of Medicine, 371*(23), pp. 2189-2199.

So, T., Song, J., Sugie, K., Altman, A. and Croft, M. (2006) Signals from OX40 regulate nuclear factor of activated T cells c1 and T cell helper 2 lineage commitment. *Proceedings of the National Academy of Sciences of the United States of America, 103*(10), pp. 3740-3745.

Song, J., So, T., Cheng, M., Tang, X. and Croft, M. (2005) Sustained survivin expression from OX40 costimulatory signals drives T cell clonal expansion. *Immunity, 22*(5), pp. 621-631.

Soroosh, P., Ine, S., Sugamura, K. and Ishii, N. (2006) OX40-OX40 ligand interaction through T cell-T cell contact contributes to CD4 T cell longevity. *The Journal of Immunology, 176*(10), pp. 5975-5987.

Speeckaert, R., van Geel, N., Vermaelen, K. V., Lambert, J., Van Gele, M., Speeckaert, M. M. and Brochez, L. (2011) Immune reactions in benign and malignant melanocytic lesions: lessons for immunotherapy. *Pigment Cell & Melanoma Research, 24*(2), pp. 334-344.

Spranger, S., Spaapen, R. M., Zha, Y., Williams, J., Meng, Y., Ha, T. T. and Gajewski, T. F. (2013) Up-regulation of PD-L1, IDO, and Tregs in the melanoma tumor microenvironment is driven by CD8+ T cells. *Science Translational Medicine, 5*(200), pp. 200ra116-200ra116.

St. Rose, M. C., Taylor, R. A., Bandyopadhyay, S., Qui, H. Z., Hagymasi, A. T., Vella, A. T. and Adler, A. J. (2013) CD134/CD137 dual costimulation-elicited IFN-γ maximizes effector T-cell function but limits Treg expansion. *Immunol Cell Biol, 91*(2), pp. 173-183.

Stewart, C. A., Metheny, H., Iida, N., Smith, L., Hanson, M., Steinhagen, F., Leighty, R. M., Roers, A., Karp, C. L., xFc, Iler, W. and Trinchieri, G. (2013) Interferon-dependent IL-10 production by Tregs limits tumor Th17 inflammation. *The Journal of Clinical Investigation, 123*(11), pp. 4859-4874.

Strome, S. E., Dong, H., Tamura, H., Voss, S. G., Flies, D. B., Tamada, K., Salomao, D., Cheville, J., Hirano, F., Lin, W., Kasperbauer, J. L., Ballman, K. V. and Chen, L. (2003) B7-H1 blockade augments adoptive T-cell immunotherapy for squamous cell carcinoma. *Cancer Research, 63*(19), pp. 6501-6505.

Sugiyama, D., Nishikawa, H., Maeda, Y., Nishioka, M., Tanemura, A., Katayama, I., Ezoe, S., Kanakura, Y., Sato, E., Fukumori, Y., Karbach, J., Jäger, E. and Sakaguchi, S. (2013) Anti-CCR4 mAb selectively depletes effector-type FoxP3^{+}CD4^{+} regulatory T cells, evoking antitumor immune responses in humans. *Proceedings of the National Academy of Sciences, 110*(44), pp. 17945-17950.

Sznol, M., Hodi, F., Margolin, K., McDermott, D., Ernstoff, M., Kirkwood, J., Wojtaszek, C., Feltquate, D. and Logan, T. (2008) Phase I study of BMS-663513, a fully human anti-CD137 agonist monoclonal antibody, in patients

(pts) with advanced cancer (CA). in *ASCO Annual Meeting Proceedings*. pp. 3007.

Tadokoro, C. E., Shakhar, G., Shen, S., Ding, Y., Lino, A. C., Maraver, A., Lafaille, J. J. and Dustin, M. L. (2006) Regulatory T cells inhibit stable contacts between CD4+ T cells and dendritic cells in vivo. *The Journal of Experimental Medicine, 203*(3), pp. 505-511.

Takeda, I., Ine, S., Killeen, N., Ndhlovu, L. C., Murata, K., Satomi, S., Sugamura, K. and Ishii, N. (2004) Distinct roles for the OX40-OX40 ligand interaction in regulatory and nonregulatory T cells. *The Journal of Immunology, 172*(6), pp. 3580-3589.

Tan, K. B., Harrop, J., Reddy, M., Young, P., Terrett, J., Emery, J., Moore, G. and Truneh, A. (1997) Characterization of a novel TNF-like ligand and recently described TNF ligand and TNF receptor superfamily genes and their constitutive and inducible expression in hematopoietic and non-hematopoietic cells1. *Gene, 204*(1–2), pp. 35-46.

Tanaka, H., Tanaka, J., Kjaergaard, J. and Shu, S. (2002) Depletion of $CD4^+CD25^+$ regulatory cells augments the generation of specific immune T cells in tumor-draining lymph nodes. *Journal of immunotherapy, 25*(3), pp. 207-217.

Terawaki, S., Chikuma, S., Shibayama, S., Hayashi, T., Yoshida, T., Okazaki, T. and Honjo, T. (2011) IFN-α directly promotes programmed cell death-1 transcription and limits the duration of T cell-mediated immunity. *The Journal of Immunology, 186*(5), pp. 2772-2779.

Teulings, H. E., Limpens, J., Jansen, S. N., Zwinderman, A. H., Reitsma, J. B., Spuls, P. I. and Luiten, R. M. (2015) Vitiligo-like depigmentation in patients with stage III-IV melanoma receiving immunotherapy and its association with survival: a systematic review and meta-analysis. *Journal of Clinical Oncology, 33*(7), pp. 773-781.

Thornton, A. M., Korty, P. E., Tran, D. Q., Wohlfert, E. A., Murray, P. E., Belkaid, Y. and Shevach, E. M. (2010) Expression of helios, an Ikaros transcription factor family member, differentiates thymic-derived from peripherally induced Foxp3+ T regulatory cells. *The Journal of Immunology, 184*(7), pp. 3433-3441.

Tivol, E. A., Borriello, F., Schweitzer, A. N., Lynch, W. P., Bluestone, J. A. and Sharpe, A. H. (1995) Loss of CTLA-4 leads to massive lymphoproliferation and fatal multiorgan tissue destruction, revealing a critical negative regulatory role of CTLA-4. *Immunity, 3*(5), pp. 541-547.

Toennies, H. M., Green, J. M. and Arch, R. H. (2004) Expression of CD30 and Ox40 on T lymphocyte subsets is controlled by distinct regulatory mechanisms. *Journal of Leukocyte Biology, 75*(2), pp. 350-357.

Tomasini, P., Khobta, N., Greillier, L. and Barlesi, F. (2012) Ipilimumab: its potential in non-small cell lung cancer. *Therapeutic Advances in Medical Oncology, 4*(2), pp. 43-50.

Tone, M., Tone, Y., Adams, E., Yates, S. F., Frewin, M. R., Cobbold, S. P. and Waldmann, H. (2003) Mouse glucocorticoid-induced tumor necrosis factor receptor ligand is costimulatory for T cells. *Proceedings of the National Academy of Sciences, 100*(25), pp. 15059-15064.

Topalian, S. L., Hodi, F. S., Brahmer, J. R., Gettinger, S. N., Smith, D. C., McDermott, D. F., Powderly, J. D., Carvajal, R. D., Sosman, J. A., Atkins, M. B., Leming, P. D., Spigel, D. R., Antonia, S. J., Horn, L., Drake, C. G., Pardoll, D. M., Chen, L., Sharfman, W. H., Anders, R. A., Taube, J. M., McMiller, T. L., Xu, H., Korman, A. J., Jure-Kunkel, M., Agrawal, S., McDonald, D., Kollia, G. D., Gupta, A., Wigginton, J. M. and Sznol, M. (2012) Safety, activity, and immune correlates of anti–PD-1 antibody in cancer. *New England Journal of Medicine, 366*(26), pp. 2443-2454.

Topalian, S. L., Sznol, M., McDermott, D. F., Kluger, H. M., Carvajal, R. D., Sharfman, W. H., Brahmer, J. R., Lawrence, D. P., Atkins, M. B., Powderly, J. D., Leming, P. D., Lipson, E. J., Puzanov, I., Smith, D. C., Taube, J. M., Wigginton, J. M., Kollia, G. D., Gupta, A., Pardoll, D. M., Sosman, J. A. and Hodi, F. S. (2014) Survival, durable tumor remission, and long-term safety in patients with advanced melanoma receiving nivolumab. *Journal of Clinical Oncology, 32*(10), pp. 1020-1030.

Townsend, S. and Allison, J. (1993) Tumor rejection after direct costimulation of CD8+ T cells by B7-transfected melanoma cells. *Science, 259*(5093), pp. 368-370.

Träger, U., Sierro, S., Djordjevic, G., Bouzo, B., Khandwala, S., Meloni, A., Mortensen, M. and Simon, A. K. (2012) The immune response to melanoma is limited by thymic selection of self-antigens. *PLoS ONE, 7*(4), pp. e35005.

Travis, M. A., Reizis, B., Melton, A. C., Masteller, E., Tang, Q., Proctor, J. M., Wang, Y., Bernstein, X., Huang, X., Reichardt, L. F., Bluestone, J. A. and Sheppard, D. (2007) Loss of integrin alpha (v) beta 8 on dendritic cells causes autoimmunity and colitis in mice. *Nature, 449*(7160), pp. 361-365.

Tumeh, P. C., Harview, C. L., Yearley, J. H., Shintaku, I. P., Taylor, E. J. M., Robert, L., Chmielowski, B., Spasic, M., Henry, G., Ciobanu, V., West, A. N., Carmona, M., Kivork, C., Seja, E., Cherry, G., Gutierrez, A. J., Grogan, T. R., Mateus, C., Tomasic, G., Glaspy, J. A., Emerson, R. O., Robins, H., Pierce, R. H., Elashoff, D. A., Robert, C. and Ribas, A. (2014) PD-1 blockade induces responses by inhibiting adaptive immune resistance. *Nature, 515*(7528), pp. 568-571.

Ueda, H., Howson, J. M. M., Esposito, L., Heward, J., Snook, Chamberlain, G., Rainbow, D. B., Hunter, K. M. D., Smith, A. N., Di Genova, G., Herr, M. H.,

Dahlman, I., Payne, F., Smyth, D., Lowe, C., Twells, R. C. J., Howlett, S., Healy, B., Nutland, S., Rance, H. E., Everett, V., Smink, L. J., Lam, A. C., Cordell, H. J., Walker, N. M., Bordin, C., Hulme, J., Motzo, C., Cucca, F., Hess, J. F., Metzker, M. L., Rogers, J., Gregory, S., Allahabadia, A., Nithiyananthan, R., Tuomilehto-Wolf, E., Tuomilehto, J., Bingley, P., Gillespie, K. M., Undlien, D. E., Ronningen, K. S., Guja, C., Ionescu-Tirgoviste, C., Savage, D. A., Maxwell, A. P., Carson, D. J., Patterson, C. C., Franklyn, J. A., Clayton, D. G., Peterson, L. B., Wicker, L. S., Todd, J. A. and Gough, S. C. L. (2003) Association of the T-cell regulatory gene CTLA4 with susceptibility to autoimmune disease. *Nature, 423*(6939), pp. 506-511.

Uyttenhove, C., Pilotte, L., Theate, I., Stroobant, V., Colau, D., Parmentier, N., Boon, T. and Van den Eynde, B. J. (2003) Evidence for a tumoral immune resistance mechanism based on tryptophan degradation by indoleamine 2,3-dioxygenase. *Nat Med, 9*(10), pp. 1269-1274.

Valzasina, B., Guiducci, C., Dislich, H., Killeen, N., Weinberg, A. D. and Colombo, M. P. (2004) Triggering of OX40 (CD134) on $CD4^+CD25^+$ T cells blocks their inhibitory activity: a novel regulatory role for OX40 and its comparison with GITR. *Blood, 105*(7), pp. 2845-2851.

Valzasina, B., Piconese, S., Guiducci, C. and Colombo, M. P. (2006) Tumor-induced expansion of regulatory T cells by conversion of $CD4^+CD25^-$ lymphocytes is thymus and proliferation independent. *Cancer Research, 66*(8), pp. 4488-4495.

van Elsas, A., Hurwitz, A. A. and Allison, J. P. (1999) Combination immunotherapy of B16 melanoma using anti–cytotoxic T lymphocyte–associated antigen 4 (Ctla-4) and granulocyte/macrophage colony-stimulating factor (Gm-Csf)-producing vaccines induces rejection of subcutaneous and metastatic tumors accompanied by autoimmune depigmentation. *The Journal of Experimental Medicine, 190*(3), pp. 355-366.

van Kooten, C. and Banchereau, J. (2000) CD40-CD40 ligand. *Journal of Leukocyte Biology, 67*(1), pp. 2-17.

Vesely, M. D., Kershaw, M. H., Schreiber, R. D. and Smyth, M. J. (2011) Natural innate and adaptive immunity to cancer. *Annual Review of Immunology, 29*(1), pp. 235-271.

Vieira, P. L., Christensen, J. R., Minaee, S., O'Neill, E. J., Barrat, F. J., Boonstra, A., Barthlott, T., Stockinger, B., Wraith, D. C. and O'Garra, A. (2004) IL-10-secreting regulatory T cells do not express Foxp3 but have comparable regulatory function to naturally occurring $CD4^+CD25^+$ regulatory T cells. *The Journal of Immunology, 172*(10), pp. 5986-5993.

Viguier, M., Lemaître, F., Verola, O., Cho, M. S., Gorochov, G., Dubertret, L., Bachelez, H., Kourilsky, P. and Ferradini, L. (2004) Foxp3 expressing

$CD4^{+}CD25^{high}$ regulatory T cells are overrepresented in human metastatic melanoma lymph nodes and inhibit the function of infiltrating T cells. *The Journal of Immunology, 173*(2), pp. 1444-1453.

Villablanca, E. J., Raccosta, L., Zhou, D., Fontana, R., Maggioni, D., Negro, A., Sanvito, F., Ponzoni, M., Valentinis, B., Bregni, M., Prinetti, A., Steffensen, K. R., Sonnino, S., Gustafsson, J. A., Doglioni, C., Bordignon, C., Traversari, C. and Russo, V. (2010) Tumor-mediated liver X receptor-alpha activation inhibits CC chemokine receptor-7 expression on dendritic cells and dampens antitumor responses. *Nat Med, 16*(1), pp. 98-105.

Vinuesa, C. G., Cook, M. C., Angelucci, C., Athanasopoulos, V., Rui, L., Hill, K. M., Yu, D., Domaschenz, H., Whittle, B., Lambe, T., Roberts, I. S., Copley, R. R., Bell, J. I., Cornall, R. J. and Goodnow, C. C. (2005) A RING-type ubiquitin ligase family member required to repress follicular helper T cells and autoimmunity. *Nature, 435*(7041), pp. 452-458.

Vogel, Katharina U., Edelmann, Stephanie L., Jeltsch, Katharina M., Bertossi, A., Heger, K., Heinz, Gitta A., Zöller, J., Warth, Sebastian C., Hoefig, Kai P., Lohs, C., Neff, F., Kremmer, E., Schick, J., Repsilber, D., Geerlof, A., Blum, H., Wurst, W., Heikenwälder, M., Schmidt-Supprian, M. and Heissmeyer, V. (2013) Roquin paralogs 1 and 2 redundantly repress the ICOS and OX40 costimulator mRNAs and control follicular helper T cell differentiation. *Immunity, 38*(4), pp. 655-668.

Vogelstein, B. and Kinzler, K. W. (2004) Cancer genes and pathways they control. *Nature Medicine, 10*, pp. 789-799.

Vogelstein, B., Papadopoulos, N., Velculescu, V. E., Zhou, S., Diaz, L. A. and Kinzler, K. W. (2013) Cancer genome landscapes. *Science, 339*(6127), pp. 1546-1558.

von Boehmer, H. (2005) Mechanisms of suppression by suppressor T cells. *Nat Immunol, 6*(4), pp. 338-344.

Vonderheide, R. H., Dutcher, J. P., Anderson, J. E., Eckhardt, S. G., Stephans, K. F., Razvillas, B., Garl, S., Butine, M. D., Perry, V. P., Armitage, R. J., Ghalie, R., Caron, D. A. and Gribben, J. G. (2001) Phase I study of recombinant human CD40 ligand in cancer patients. *Journal of Clinical Oncology, 19*(13), pp. 3280-3287.

Vonderheide, R. H. and Glennie, M. J. (2013) Agonistic CD40 antibodies and cancer therapy. *American Association for Cancer Research, 19*(5), pp. 1035-1043.

Vu, M. D., Xiao, X., Gao, W., Degauque, N., Chen, M., Kroemer, A., Killeen, N., Ishii, N. and Chang Li, X. (2007) OX40 costimulation turns off $Foxp3^{+}$ Tregs. *Blood, 110*(7), pp. 2501-2510.

Watanabe-Fukunaga, R., Brannan, C. I., Copeland, N. G., Jenkins, N. A. and Nagata, S. (1992) Lymphoproliferation disorder in mice explained by defects in Fas antigen that mediates apoptosis. *Nature, 356*(6367), pp. 314-317.

Watson, I. R., Takahashi, K., Futreal, P. A. and Chin, L. (2013) Emerging patterns of somatic mutations in cancer. *Nat Rev Genet, 14*(10), pp. 703-718.

Watts, T. H. (2005) TNF/TNFR family members in costimulation of T cell responses. *Annual Review of Immunology, 23*(1), pp. 23-68.

Weber, J. S., Dummer, R., de Pril, V., Lebbé, C., Hodi, F. S. and for the, M. D. X. I. (2013) Patterns of onset and resolution of immune-related adverse events of special interest with ipilimumab. *Cancer, 119*(9), pp. 1675-1682.

Weber, J. S., Kähler, K. C. and Hauschild, A. (2012) Management of immune-related adverse events and kinetics of response with ipilimumab. *Journal of Clinical Oncology, 30*(21), pp. 2691-2697.

Weinberg, A. D., Morris, N. P., Kovacsovics-Bankowski, M., Urba, W. J. and Curti, B. D. (2011) Science gone translational: the OX40 agonist story. *Immunological Reviews, 244*(1), pp. 218-231.

Weinberg, A. D., Rivera, M. M., Prell, R., Morris, A., Ramstad, T., Vetto, J. T., Urba, W. J., Alvord, G., Bunce, C. and Shields, J. (2000) Engagement of the OX-40 receptor *in vivo* enhances antitumor immunity. *The Journal of Immunology, 164*(4), pp. 2160-2169.

Weiner, H. L. (2001) Induction and mechanism of action of transforming growth factor-β-secreting Th3 regulatory cells. *Immunological Reviews, 182*(1), pp. 207-214.

Weiss, J. M., Bilate, A. M., Gobert, M., Ding, Y., Curotto de Lafaille, M. A., Parkhurst, C. N., Xiong, H., Dolpady, J., Frey, A. B., Ruocco, M. G., Yang, Y., Floess, S., Huehn, J., Oh, S., Li, M. O., Niec, R. E., Rudensky, A. Y., Dustin, M. L., Littman, D. R. and Lafaille, J. J. (2012) Neuropilin 1 is expressed on thymus-derived natural regulatory T cells, but not mucosa-generated induced Foxp3^{+} T reg cells. *The Journal of Experimental Medicine, 209*(10), pp. 1723-1742.

Whiteside, T. L. (2012) What are regulatory T cells (Treg) regulating in cancer and why? *Seminars in Cancer Biology, 22*(4), pp. 327-334.

Wildin, R. S., Ramsdell, F., Peake, J., Faravelli, F., Casanova, J. L., Buist, N., Levy-Lahad, E., Mazzella, M., Goulet, O., Perroni, L., Dagna Bricarelli, F., Byrne, G., McEuen, M., Proll, S., Appleby, M. and Brunkow, M. E. (2001) X-linked neonatal diabetes mellitus, enteropathy and endocrinopathy syndrome is the human equivalent of mouse scurfy. *Nat Genet, 27*(1), pp. 18-20.

Williams, C. A., Murray, S. E., Weinberg, A. D. and Parker, D. C. (2007) OX40-mediated derentiation to effector function requires IL-2 receptor signaling but not CD28, CD40, IL-12Rβ2, or T-bet. *The Journal of Immunology, 178*(12), pp. 7694-7702.

Wing, K., Onishi, Y., Prieto-Martin, P., Yamaguchi, T., Miyara, M., Fehervari, Z., Nomura, T. and Sakaguchi, S. (2008) CTLA-4 control over $Foxp3^+$ regulatory T cell function. *Science, 322*(5899), pp. 271-275.

Wing, K., Yamaguchi, T. and Sakaguchi, S. (2011) Cell-autonomous and -non-autonomous roles of CTLA-4 in immune regulation. *Trends in Immunology, 32*(9), pp. 428-433.

Withers, D. R., Gaspal, F. M., Bekiaris, V., McConnell, F. M., Kim, M., Anderson, G. and Lane, P. J. L. (2011) OX40 and CD30 signals in $CD4^+$ T-cell effector and memory function: a distinct role for lymphoid tissue inducer cells in maintaining $CD4^+$ T-cell memory but not effector function. *Immunological Reviews, 244*(1), pp. 134-148.

Withers, D. R., Gaspal, F. M., Mackley, E. C., Marriott, C. L., Ross, E. A., Desanti, G. E., Roberts, N. A., White, A. J., Flores-Langarica, A., McConnell, F. M., Anderson, G. and Lane, P. J. L. (2012) Cutting edge: lymphoid tissue inducer cells maintain memory CD4 T cells within secondary lymphoid tissue. *The Journal of Immunology, 189*(5), pp. 2094-2098.

Withers, D. R., Jaensson, E., Gaspal, F., McConnell, F. M., Eksteen, B., Anderson, G., Agace, W. W. and Lane, P. J. L. (2009) The survival of memory $CD4^+$ T cells within the gut lamina propria requires OX40 and CD30 signals. *The Journal of Immunology, 183*(8), pp. 5079-5084.

Wodarz, D. and Zauber, A. G. (2015) Cancer: risk factors and random chances. *Nature, 517*(7536), pp. 563-564.

Wolchok, J. D., Kluger, H., Callahan, M. K., Postow, M. A., Rizvi, N. A., Lesokhin, A. M., Segal, N. H., Ariyan, C. E., Gordon, R. A., Reed, K., Burke, M. M., Caldwell, A., Kronenberg, S. A., Agunwamba, B. U., Zhang, X., Lowy, I., Inzunza, H. D., Feely, W., Horak, C. E., Hong, Q., Korman, A. J., Wigginton, J. M., Gupta, A. and Sznol, M. (2013) Nivolumab plus ipilimumab in advanced melanoma. *New England Journal of Medicine, 369*(2), pp. 122-133.

Wolchok, J. D., Neyns, B., Linette, G., Negrier, S., Lutzky, J., Thomas, L., Waterfield, W., Schadendorf, D., Smylie, M., Guthrie Jr, T., Grob, J.-J., Chesney, J., Chin, K., Chen, K., Hoos, A., O'Day, S. J. and Lebbé, C. (2010) Ipilimumab monotherapy in patients with pretreated advanced melanoma: a randomised, double-blind, multicentre, phase 2, dose-ranging study. *The Lancet Oncology, 11*(2), pp. 155-164.

Woo, E. Y., Chu, C. S., Goletz, T. J., Schlienger, K., Yeh, H., Coukos, G., Rubin, S. C., Kaiser, L. R. and June, C. H. (2001) Regulatory $CD4^+CD25^+$ T cells in tumors from patients with early-stage non-small cell lung cancer and late-stage ovarian cancer. *Cancer Research, 61*(12), pp. 4766-4772.

Wu, H. and Hymowitz, S. G. (2009) *Structure and function of tumor necrosis factor (TNF) at the cell surface, Handbook of cell signalling,* Uniteed States of America: Academic Press Elsevier.

Xiao, X., Gong, W., Demirci, G., Liu, W., Spoerl, S., Chu, X., Bishop, D. K., Turka, L. A. and Li, X. C. (2012) New insights on OX40 in the control of T cell immunity and immune tolerance in vivo. *The Journal of Immunology, 188*(2), pp. 892-901.

Xiao, X., Kroemer, A., Gao, W., Ishii, N., Demirci, G. and Li, X. C. (2008) OX40/OX40L costimulation affects induction of $Foxp3^+$ regulatory T cells in part by expanding memory T cells in vivo. *The Journal of Immunology, 181*(5), pp. 3193-3201.

Xing, Y. and Hogquist, K. A. (2012) T-cell tolerance: central and peripheral. *Cold Spring Harbor Perspectives in Biology, 4*(6), pp. 1-16.

Yadav, M., Louvet, C., Davini, D., Gardner, J. M., Martinez-Llordella, M., Bailey-Bucktrout, S., Anthony, B. A., Sverdrup, F. M., Head, R., Kuster, D. J., Ruminski, P., Weiss, D., Von Schack, D. and Bluestone, J. A. (2012) Neuropilin-1 distinguishes natural and inducible regulatory T cells among regulatory T cell subsets in vivo. *The Journal of Experimental Medicine, 209*(10), pp. 1713-1722.

Yang, J. C., Hughes, M., Kammula, U., Royal, R., Sherry, R. M., Topalian, S. L., Suri, K. B., Levy, C., Allen, T., Mavroukakis, S., Lowy, I., White, D. E. and Rosenberg, S. A. (2007) Ipilimumab (anti-CTLA-4 antibody) causes regression of metastatic renal cell cancer associated with enteritis and hypophysitis. *Journal of immunotherapy, 30*(8), pp. 825-830.

Yeh, S., Karne, N. K., Kerkar, S. P., Heller, C. K., Palmer, D. C., Johnson, L. A., Li, Z., Bishop, R. J., Wong, W. T., Sherry, R. M., Yang, J. C., Dudley, M. E., Restifo, N. P., Rosenberg, S. A. and Nussenblatt, R. B. (2009) Ocular and systemic autoimmunity after successful tumor-infiltrating lymphocyte immunotherapy for recurrent, metastatic melanoma. *Ophthalmology, 116*(5), pp. 981-989.e1.

Yokosuka, T., Takamatsu, M., Kobayashi-Imanishi, W., Hashimoto-Tane, A., Azuma, M. and Saito, T. (2012) Programmed cell death 1 forms negative costimulatory microclusters that directly inhibit T cell receptor signaling by recruiting phosphatase SHP2. *The Journal of Experimental Medicine, 209*(6), pp. 1201-1217.

Yu, X., Harden, K., C Gonzalez, L., Francesco, M., Chiang, E., Irving, B., Tom, I., Ivelja, S., Refino, C. J., Clark, H., Eaton, D. and Grogan, J. L. (2009) The surface protein TIGIT suppresses T cell activation by promoting the generation of mature immunoregulatory dendritic cells. *Nat Immunol, 10*(1), pp. 48-57.

Zaks, T. Z., Chappell, D. B., Rosenberg, S. A. and Restifo, N. P. (1999) Fas-mediated suicide of tumor-reactive T cells following activation by specific tumor: selective rescue by caspase inhibition. *The Journal of Immunology, 162*(6), pp. 3273-3279.

Zeissig, S., Petersen, B. S., Tomczak, M., Melum, E., Huc-Claustre, E., Dougan, S. K., Laerdahl, J. K., Stade, B., Forster, M., Schreiber, S., Weir, D., Leichtner, A. M., Franke, A. and Blumberg, R. S. (2015) Early-onset Crohn's disease and autoimmunity associated with a variant in CTLA-4. *Gut, 64*(12), pp. 1889-1897.

Zhang, L., Morgan, R. A., Beane, J. D., Zheng, Z., Dudley, M. E., Kassim, S. H., Nahvi, A. V., Ngo, L. T., Sherry, R. M., Phan, G. Q., Hughes, M. S., Kammula, U. S., Feldman, S. A., Toomey, M. A., Kerkar, S. P., Restifo, N. P., Yang, J. C. and Rosenberg, S. A. (2015) Tumor-infiltrating lymphocytes genetically engineered with an inducible gene encoding interleukin-12 for the immunotherapy of metastatic melanoma. *Clinical Cancer Research, 21*(10), pp. 2278-2288.

Zhou, G. and Levitsky, H. I. (2007) Natural regulatory T cells and de novo-induced regulatory T cells contribute independently to tumor-specific tolerance. *The Journal of Immunology, 178*(4), pp. 2155-2162.

Zhou, J., Ding, T., Pan, W., Zhu, L. Y., Li, L. and Zheng, L. (2009) Increased intratumoral regulatory T cells are related to intratumoral macrophages and poor prognosis in hepatocellular carcinoma patients. *International Journal of Cancer, 125*(7), pp. 1640-1648.

Zhou, T., Cheng, J., Yang, P., Wang, Z., Liu, C., Su, X., Bluethmann, H. and Mountz, J. D. (1996) Inhibition of Nur77/Nurr1 leads to inefficient clonal deletion of self-reactive T cells. *The Journal of Experimental Medicine, 183*(4), pp. 1879-1892.

Zou, W. (2006) Regulatory T cells, tumour immunity and immunotherapy. *Nat Rev Immunol, 6*(4), pp. 295-307.